STEREOSELECTIVE TRANSFORMATIONS OF VINYL CYCLIC CARBONATES AND APPLICATIONS IN NATURAL PRODUCT SYNTHESIS

Àlex Cristòfol Martínez

UNIVERSITAT ROVIRA i VIRGILI

Stereoselective Transformations of Vinyl Cyclic Carbonates and Applications in Natural Product Synthesis

ÀLEX CRISTÒFOL MARTÍNEZ

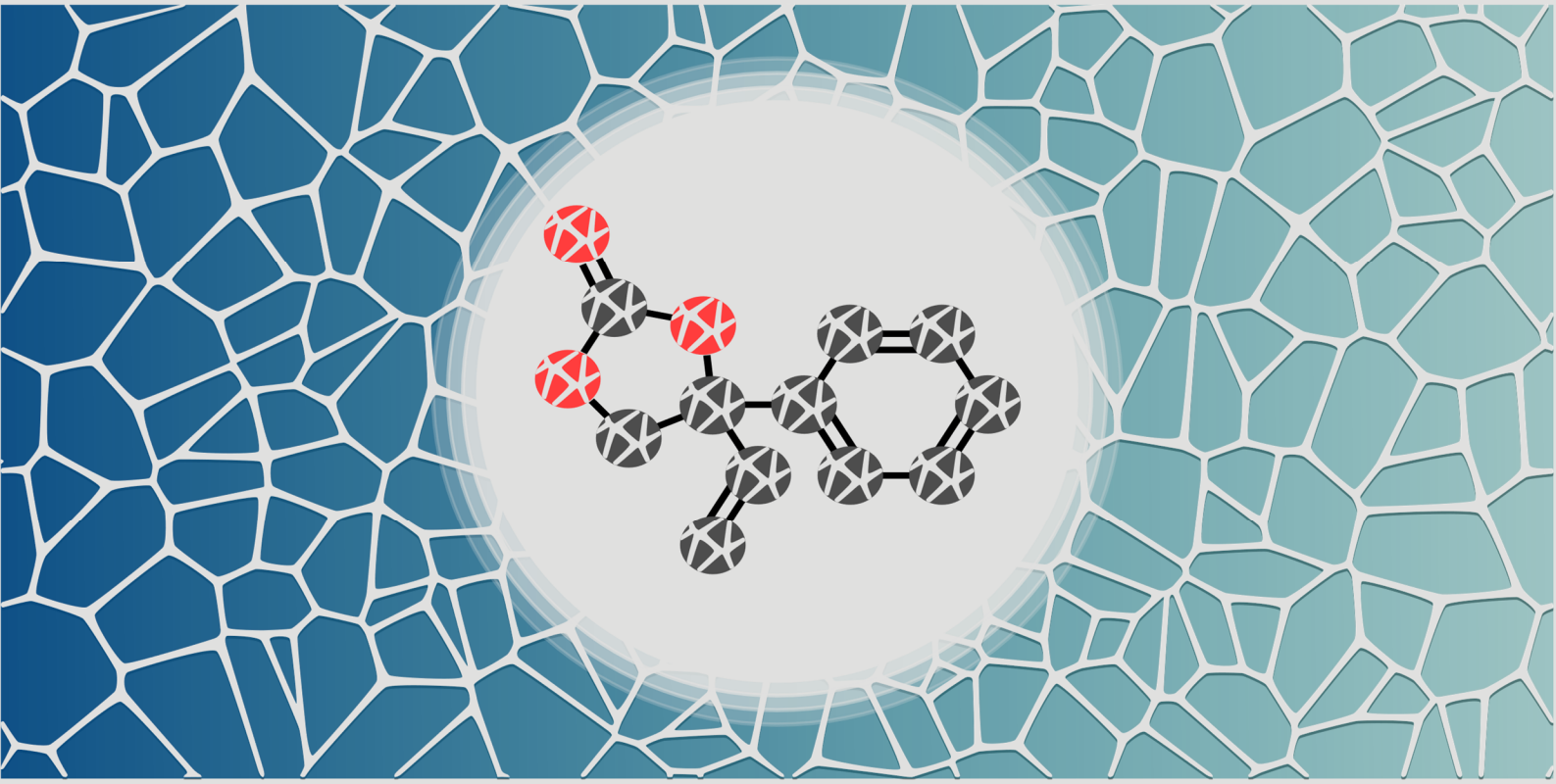

DOCTORAL THESIS

2021

UNIVERSITAT ROVIRA I VIRGILI
STEREOSELECTIVE TRANSFORMATIONS OF VINYL CYCLIC CARBONATES AND APPLICATIONS IN NATURAL PRODUCT SYNTHESIS
Àlex Cristòfol Martínez

UNIVERSITAT ROVIRA I VIRGILI
STEREOSELECTIVE TRANSFORMATIONS OF VINYL CYCLIC CARBONATES AND APPLICATIONS IN NATURAL PRODUCT SYNTHESIS
Àlex Cristòfol Martínez

UNIVERSITAT ROVIRA I VIRGILI
STEREOSELECTIVE TRANSFORMATIONS OF VINYL CYCLIC CARBONATES AND APPLICATIONS IN NATURAL PRODUCT SYNTHESIS
Àlex Cristòfol Martínez

PhD Thesis

Stereoselective Transformations of Vinyl Cyclic Carbonates and Applications in Natural Product Synthesis

Àlex Cristòfol Martínez

Supervised by Prof. Dr. Arjan W. Kleij

Tarragona

September 2021

UNIVERSITAT ROVIRA I VIRGILI
STEREOSELECTIVE TRANSFORMATIONS OF VINYL CYCLIC CARBONATES AND APPLICATIONS IN NATURAL PRODUCT SYNTHESIS
Àlex Cristòfol Martínez

Prof. Dr. Arjan W. Kleij, Group Leader at the Institute of Chemical Research of Catalonia (ICIQ) and Research Professor at the Catalan Institution for Research and Advanced Studies (ICREA),

I STATE that the present Doctoral Thesis, entitled "**Stereoselective Transformations of Vinyl Cyclic Carbonates and Applications in Natural Product Synthesis**" presented by Àlex Cristòfol Martínez to receive the degree of Doctor, has been carried out under my supervision at the Institute of Chemical Research of Catalonia (ICIQ).

Tarragona, August 2021

Doctoral Thesis Supervisor

Prof. Dr. Arjan W. Kleij

UNIVERSITAT ROVIRA I VIRGILI
STEREOSELECTIVE TRANSFORMATIONS OF VINYL CYCLIC CARBONATES AND APPLICATIONS IN NATURAL PRODUCT SYNTHESIS
Àlex Cristòfol Martínez

Aquest treball està completament dedicat als meus respectuosos pares i germana, i a la meva estimada parella, sense el suport constant dels quals aquesta tesi doctoral no seria possible.

UNIVERSITAT ROVIRA I VIRGILI
STEREOSELECTIVE TRANSFORMATIONS OF VINYL CYCLIC CARBONATES AND APPLICATIONS IN NATURAL PRODUCT SYNTHESIS
Àlex Cristòfol Martínez

ACKNOWLEDGMENTS

Ohana means family. Family
means nobody gets left behind,
or forgotten. — Lilo & Stitch

Since I arrived at ICIQ to pursue my doctoral studies (and before), I owe my most sincere gratitude to many people for all their support and all the enjoyable times they have shared with me. All of them mean *Ohana* to me for different reasons.

On a professional level, I would like to start by thanking **Arjan Kleij** for the experience of working in his research group and for supporting me throughout the entire PhD period. I really appreciate your confidence in me since my period as a summer fellow, and your willingness to support me throughout my master's degree and PhD studies. Thank you for allowing me to take a proactive approach towards discovering new reactions and managing research projects. It might not have been the most time-efficient process, but those are the most valuable skills I could have honed here that will certainly help me in the rest of my career. Lastly, thank you for your great effort and proactive approach towards publication of the scientific work, as I believe it has enormously helped me build a competitive CV right from the start.

Secondly, I would like to express my warmest gratitude to former and current members of the Kleij group, with whom I have shared all these years: **Tharun Jose**, **Víctor Laserna**, **Sergio Sopeña**, **Jeroen Rintjema**, **Luís Rodríguez**, **Claudia Miceli**, **Silvia Gaspa**, **Mariachiara Cozzolino**, **Huang Rui**, **Vicente Dorado**, **Antonella Pizzolante**, **Michela Marchese**, **Sarah Dechent**, **Josefine Sprachmann**, **Aijie Cai**, **Cristina Maquilón**, **Alèria García**, **Kun Guo**, **Chang Qiao**, **Alba Villar**, **Nicola Zanda**, **Xuetong Li**, **Qian Zeng** and **Arianna Brandolese**. In addition, I would especially like to credit the people with whom I collaborated with different projects, whose chemistry insights and fruitful discussions have greatly benefited my career: **Nicole Kindermann**, **Leticia Peña**, **Wusheng Guo**, **Christian Böhmer**, **José Enrique Gómez** (Kike), **Jianing Xie**, **Bart Limburg**, **Sijing Xie**, **Francesco Della Monica**, **Debasish Ghorai**, and **Jixiang Ni**.

Apart from them, I want to acknowledge DAAD to finance my doctoral stay with Prof. **Lutz Ackermann** in Göttingen (Germany). I was impressed when I stepped down the train and saw a sign where it said: *Göttingen, die Stadt die Wissen shafft* (Göttingen, the town that creates knowledge). I learned many things in this inspiring town and had a great time thanks to the Ackermann group members. I will especially remember the moments I shared with **Leonardo Massignan**, **Nate Ang**, **Alexej Scheremetjew**, and **Fabio Pesciaioli**.

On a more personal level, I wish to dedicate some words to certain people that I will keep close to my heart forever. **David Nieto**, we both started at ICIQ during the 2016 Summer Fellowship program, and you have been a good friend throughout the years. I will always remember the multitude of *padel* matches that we played. **Cristina Maquilón**, you have been like my second sister throughout my PhD and have greatly eased my day-to-day life at work. I thank you for your awesome birthday decorations and writings on the sash of my fumehood and computer desk. **Kike**, you were always eager to help me and have always been a trustworthy person. **Francesco Della Monica**, you were always open to hear me and share your experience with me. I will especially remember the evening shifts during COVID-19 and the countless snacks you shared with me. **Bart Limburg**, you have been game-changing in the mid-to-late stage of my PhD and I truly had such a magnificent time here working on photochemistry with you. I appreciate all our conversations and *whatsapping* we had, the unconditional support, and all the informal gatherings to drink some beers together with Francesco.

A més a més, m'agradaria agrair també el suport al llarg d'aquest temps dels meus excel·lents amics d'escola, **Marc Ruiz** i **Cristina Aljama**, sempre he pogut confiar plenament en vosaltres i he pogut gaudir de molts moments únics i irrepetibles.

Per últim, i més important, volia agrair el suport que he rebut en tot moment de part de la meva família i parella. **Bea**, des d'un bon principi em vas transmetre el teu encant i la teva gran capacitat per ajudar als altres a resoldre qualsevol problema. Sempre m'has donat el teu 100% a l'hora d'afrontar qualsevol dificultat i gaudir molts moments d'alegria i felicitat. La convivència amb tu durant la major part d'aquest doctorat ha estat molt fàcil i reconfortant. T'he d'agrair la teva voluntat d'adaptació i de superació que vas mostrar molt aviat al voler-te quedar a Catalunya amb mi. Em demostres cada dia que aixecar-se del llit i afrontar aquesta vida val la pena. També volia agrair el suport rebut de la teva família de Saragossa, que sempre m'han rebut com un membre més de la família. Als meus pares i germana, **Ramon**, **Piedad** i **Lídia**, us agraeixo eternament que m'hàgiu deixat estudiar sempre el que he volgut i d'haver-me educat amb els millors valors del món. Malgrat entendre poc sobre el meu treball diari, heu sabut confiar sempre en mi i acceptar que prengui les meves pròpies decisions. Sou els tres uns referents dels quals he après moltes coses per afrontar aquesta vida amb seguretat i optimisme, i que s'han vist reflectits en la realització d'aquesta tesi doctoral.

I love you all, / Os quiero a todos, / Us estimo a tots,

Àlex Cristòfol Martínez, 2021

CURRICULUM VITAE

Àlex Cristòfol Martínez was born on the 22nd of May **1994** in Reus (Spain). He studied Chemistry at the Universitat Rovira i Virgili (URV) in Tarragona and obtained his degree in June **2016**. During his undergraduate studies, he joined the group of Prof. Sergio Castillón during summer **2015** and worked on the synthesis of trifluoromethylated sugars. Then, he pursued his curricular internship at the technology transfer unit CSOL, at ICIQ, under the supervision of Dr. Fernando Bravo, where he was involved in the development and scale-up of the synthesis of an amino acid organocatalyst. He was awarded the best URV BSc final project in Chemistry by the Catalan Chemical Society. Hereafter, he was awarded a summer fellowship at ICIQ to work as a summer student (**2016**) in the research group of Prof. Dr. Arjan W. Kleij. During this period, he was involved in the synthesis of cyclic carbonates and polycarbonates from biorenewable sources. In October **2016**, he enrolled at the master's degree *Synthesis, Catalysis and Molecular Design* offered by the URV and ICIQ, and presented his master's thesis in June **2017** under the supervision of Prof. Dr. Arjan W. Kleij. Shortly after that, he started his PhD studies in October **2017** at ICIQ in the same group, where he performed the research described within this PhD thesis. His research was financially supported with an ICIQ PhD Fellowship. During his PhD studies, he received a 6-month funded research grant by DAAD to work on novel C–H activation methodologies in the laboratories of Prof. Lutz Ackermann in Göttingen, Germany. Part of his PhD results have been communicated orally at the 43rd International Conference on Coordination Chemistry (ICCC2018) in Sendai, Japan (**2018**), and at the 2nd ICIQ PhD Day (**2019**). In addition, he was part of the local organizing committee of the 4th EuChemMS Conference on Green and Sustainable Chemistry (**2019**) in Tarragona.

UNIVERSITAT ROVIRA I VIRGILI
STEREOSELECTIVE TRANSFORMATIONS OF VINYL CYCLIC CARBONATES AND APPLICATIONS IN NATURAL PRODUCT SYNTHESIS
Àlex Cristòfol Martínez

PUBLICATIONS

This doctoral thesis is based on the following original publications:

- Guo, W.; Gómez, J. E.; Cristòfol, À.; Xie, J.; Kleij, A. W. Catalytic Transformations of Functionalized Cyclic Organic Carbonates. *Angew. Chem. Int. Ed.* **2018**, *57*, 13735–13747. (Review Article)
- Cristòfol, À.; Escudero-Adán, E. C.; Kleij, A. W. Palladium-Catalyzed (Z)-Selective Allylation of Nitroalkanes: Access to Highly Functionalized Homoallylic Scaffolds. *J. Org. Chem.* **2018**, *83*, 9978–9990.
- Cristòfol, À.; Böhmer, C.; Kleij, A. W. Formal Synthesis of Indolizidine and Quinolizidine Alkaloids from Vinyl Cyclic Carbonates. *Chem. Eur. J.* **2019**, *25*, 15055–15058.
- Cristòfol, À.; Limburg, B.; Kleij, A. W. Expedient Dual Co/Organophotoredox Catalyzed Stereoselective Synthesis of All-Carbon Quaternary Centers. *Angew. Chem. Int. Ed.* **2021**, *60*, 15266–15270.

The following publications relate to other activities during and before the thesis:

- Kindermann, N.; Cristòfol, À.; Kleij, A. W. Access to Biorenewable Polycarbonates with Unusual Glass-Transition Temperature (*Tg*) Modulation. *ACS Catal.* **2017**, *7*, 3860–3863.
- Carrodeguas, L. P.; Cristòfol, À.; Fraile, J. M.; Mayoral, J. A.; Dorado, V.; Herrerías, C. I.; Kleij, A. W. Fatty acid based biocarbonates: Al-mediated stereoselective preparation of mono-, di- and tricarbonates under mild and solvent-less conditions. *Green Chem.* **2017**, *19*, 3535–3541.
- Gómez, J. E.; Cristòfol, À.; Kleij, A. W. Copper-Catalyzed Enantioselective Construction of Tertiary Propargylic Sulfones. *Angew. Chem. Int. Ed.* **2019**, *58*, 3903–3907.
- Limburg, B.; Cristòfol, À.; Della Monica, F.; Kleij, A. W. Unlocking the Potential of Substrate-Directed CO_2 Activation and Conversion: Pushing the Boundaries of Catalytic Cyclic Carbonate and Carbamate Formation. *ChemSusChem* **2020**, *13*, 6056–6065. (Concept Article)
- Aomchad, V.; Cristòfol, À.; Della Monica, F.; Limburg, B.; D'Elia, V.; Kleij, A. W. Recent progress in the catalytic transformation of carbon dioxide into biosourced organic carbonates. *Green Chem.* **2021**, *23*, 1077–1113. (Review Article)
- Ni, J.; Cristòfol, À.; Kleij, A. W. Formation of β-cyano-ketones through cyanide-promoted ring-opening of cyclic organic carbonates. *Org. Chem. Front.* **2021**, 8, 4520-4526.

UNIVERSITAT ROVIRA I VIRGILI
STEREOSELECTIVE TRANSFORMATIONS OF VINYL CYCLIC CARBONATES AND APPLICATIONS IN NATURAL PRODUCT SYNTHESIS
Àlex Cristòfol Martínez

TABLE OF CONTENTS

UNIVERSITAT ROVIRA I VIRGILI
STEREOSELECTIVE TRANSFORMATIONS OF VINYL CYCLIC CARBONATES AND APPLICATIONS IN NATURAL PRODUCT SYNTHESIS
Àlex Cristòfol Martínez

LIST OF ABBREVIATIONS

3DPAFIPN	2,4,6-Tris(diphenylamino)-5-fluoroisophthalonitrile
4CzIPN	2,4,5,6-Tetrakis(9*H*-carbazol-9-yl) isophthalonitrile
4CzTPN	2,3,5,6-Tetrakis(carbazol-9-yl)-1,4-dicyanobenzene
9-BBN	9-Borabicyclo[3.3.1]nonane
Ac	Acetate
acac	Acetylacetonate
Ad	Adamantyl
ADDM	Azodicarboxylic Dimorpholide
ADDP	1,1′-(Azodicarbonyl)dipiperidine
Ar	Aromatic
BHT	3,5-Di-*tert*-4-butylhydroxytoluene
BINAP	2,2′-Bis(diphenylphosphino)-1,1′-binaphthyl
Bn	Benzyl
BNAH	1-Benzyl-1,4-dihydronicotinamide
Boc	*tert*-Butoxycarbonyl
bpy	2,2'-Bipyridine
brsm	Based on Recovered Starting Material
Bu	Butyl
Bz	Benzoate
cat.	Catalytic
Cbz	Carboxybenzyl
COD	1,5-Cyclooctadiene
conv.	Conversion
COSY	Correlation Spectroscopy
Cp	Cyclopentadienyl
Cy	Cyclohexyl
dba	Dibenzylideneacetone
DBU	1,8-Diazabicyclo[5.4.0]undec-7-ene
DCE	1,2-Dichloroethane
DEAD	Diethyl azodicarboxylate
DEPT	Distortionless Enhancement by Polarization Transfer
DFT	Density Functional Theory
DG	Directing Group

DIBAL-H	Diisobutylaluminium Hydride
DIPEA	*N*,*N*-Diisopropiletilamina
DMF	*N*,*N*-Dimethylformamide
DMSO	Dimethylsulfoxide
DPEPhos	Bis(2-diphenylphosphinophenyl)ether
dppb	1,4-Bis(diphenylphosphino)butane
DPPBA	Diphenylphosphino Benzoic Acid
dppe	1,2-Bis(diphenylphosphino)ethane
dppf	1,1'-Bis(diphenylphosphino)ferrocene
dppp	1,3-Bis(diphenylphosphino)propane
dr	Diastereomeric Ratio
dtbbpy	4,4′-Di-*t*ert-butyl-2,2′-bipyridine
DTBMP	2,6-Di-*tert*-butyl-4-methylpyridine
ee	Enantiomeric Excess
es	Enantioespecificity
ESI/TOF	Electrospray Ionization/Time-Of-Flight
Et	Ethyl
EWG	Electron-Withdrawing Group
FG	Functional Group
FID	Flame Ionization Detector
FTIR	Fourier Transform Infrared
GC	Gas Chromatography
HAT	Hydrogen Atom Transfer
HE	Hantzsch Ester
HMBC	Heteronuclear Multiple Bond Correlation
HMQC	Heteronuclear Multiple-Quantum Correlation
HRMS	High Resolution Mass Spectrometry
HWE	Horner-Wadsworth-Emmons
IBX	2-Iodoxybenzoic Acid
IUPAC	International Union of Pure and Applied Chemistry
LA	Lewis Acid
LDA	Lithium Diisopropylamide
LED	Light-Emitting Diode
LG	Leaving Group
m-CPBA	*meta*-Chloroperbenzoic Acid

Me	Methyl
Mes	Mesityl
MOM	Methoxymethyl
Ms	Mesylate
MS	Molecular Sieves
NBS	*N*- Bromosuccinimide
NHC	*N*-Heterocyclic Carbene
NMO	4-Methylmorpholine *N*-Oxide
NMP	*N*-Methyl-2-Pyrrolidone
NMR	Nuclear Magnetic Resonance
Ns	Nosyl
Nuc	Nucleophile
PC	Photocatalyst
PF	Prompt Fluorescence
Ph	Phenyl
phen	1,10-Phenantroline
PHOX	Phosphino-Oxazoline
pin	Pinacolato
Piv	Pivalate
pmdba	bis(*p*-Methoxybenzylidene)acetone
PMP	*Para*-Methoxyphenyl
Pr	Propyl
rr	Regioisomeric Ratio
SAR	Structure-Activity Relationship
SET	Single Electron Transfer
S_N1	Unimolecular Nucleophilic Substitution
S_N2	Bimolecular Nucleophilic Substitution
TADF	Thermally Activated Delayed Fluorescence
TBAF	Tetra-*n*-Butylammonium Fluoride
TBD	1,5,7-Triazabicyclo[4.4.0]dec-5-ene
TBDMS	*tert*-Butyldimethylsilyl
TBDPS	*tert*-Butyldiphenylsilyl
TCSPC	Time-Correlated Single-Photon Counting
TEMPO	2,2,6,6-Tetramethylpiperidine 1-Oxyl
Tf	Triflate

TFA	Trifluoroacetic Acid
TFP	Tri(2-furyl)phosphine
THF	Tetrahydrofuran
TIPS	Triisopropylsilyl
TLC	Thin Layer Chromatography
TM	Transition Metal
TMAD	*N*,*N*,*N*′,*N*′-Tetramethylazodicarboxamide
TMM	Trimethylenemethane
TMP	Tetramethylpiperidine
TMS	Trimethylsilyl
TPGS-750-M	DL-α-Tocopherol methoxypolyethylene Glycol Succinate
Ts	Tosylate
TS	Transition state
UV	Ultraviolet
VCC	Vinyl Cyclic Carbonate
Vis	Visible
XantPhos	4,5-Bis(diphenylphosphino)-9,9-dimethylxanthene

SUMMARY

Finding new strategies to forge carbon-carbon bonds has become fundamental to synthesize complex molecules rapidly and efficiently. This doctoral thesis aims to devise novel catalytic and stereoselective methods for the construction of such carbon-carbon bonds using vinyl cyclic carbonates to build more elaborate molecules with potential application for the synthesis of natural products and pharmaceuticals The doctoral thesis is composed of four chapters:

- **Chapter 1** is introductory and reviews the main aspects and methods utilizing metal-catalyzed allylation reactions, as well as the state-of-the-art in the use of vinyl cyclic carbonates as allylic surrogates.
- **Chapter 2** presents a stereoselective method for the allylation of nitroalkanes using vinyl cyclic carbonates, giving rise to homoallylic nitroalkanes featuring stereodefined tri- and tetrasubstituted olefins. A preliminary study towards the application of this method towards the synthesis of more elaborated molecular scaffolds is also described.
- **Chapter 3** describes the synthesis of biologically active indolizidine and quinolizidine natural products. The main strategy relies on the application of the allylation of nitroalkanes using vinyl cyclic carbonates presented in Chapter 2.
- **Chapter 4** concentrates on the generation of nucleophilic allyl species from vinyl cyclic carbonates using a newly developed dual cobalt-organophotoredox catalyzed reaction. The method generates a wide scope of *syn*-1,3-diols featuring quaternary carbon stereocenters with high diastereoselectivity without relying on precious transition metals. Moreover, a preliminary study to produce *anti*-configured homoallylic alcohols from the same vinyl cyclic carbonates is also outlined.

The general conclusions are drawn at the end of the thesis. The combined experimental results from this thesis showcase how vinyl cyclic carbonates can be effectively reacted under the influence of a transition metal catalyst to forge strategic carbon-carbon bonds that allow the synthesis of more elaborated intermediates and natural products. The extent of this work will help revitalize the use of such scaffolds in modern synthetic campaigns and method development.

UNIVERSITAT ROVIRA I VIRGILI
STEREOSELECTIVE TRANSFORMATIONS OF VINYL CYCLIC CARBONATES AND APPLICATIONS IN NATURAL PRODUCT SYNTHESIS
Àlex Cristòfol Martínez

The greatest challenge to any thinker is stating the problem in a way that will allow a solution. — Bertrand Russell

CHAPTER 1

General Introduction

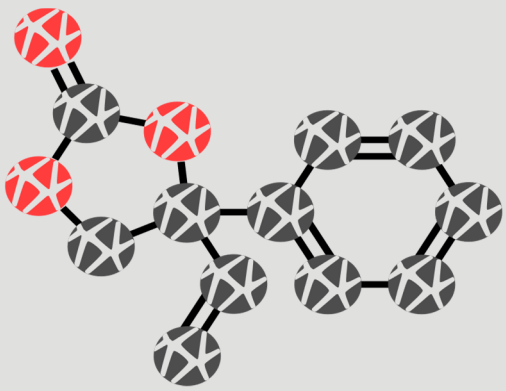

Parts of this chapter have been adapted from:

Guo, W.; Gómez, J. E.; Cristòfol, À.; Xie, J.; Kleij, A. W. *Angew. Chem. Int. Ed.* **2018**, *57*, 13735-13747

1.1 The Allyl Group in Organic Synthesis

Among the wide diversity of chemical reactions, the formation of C–C bonds undoubtedly represents a privileged one to organic chemists being of high importance to build complex organic molecules in the most efficient and atom-economical way.[1] The challenge in making these bonds primarily relates to the generation of each synthon, as the carbon atom is neither as electronegative to efficiently stabilize negative charge (*cf.*, formation of carbanions), as compared to halogens, oxygen, or sulfur, nor as electropositive to stabilize positive charge (*cf.*, formation of carbocations), when compared to alkali or alkaline-earth metals.

Despite these intrinsic difficulties, the presence of additional functional groups near the carbon atom has been key to efficiently promote C–C bond-forming reactions. The most classical examples in this regard are carbonyl compounds, which can efficiently stabilize carbanions at the α-position, thus providing versatile synthetic methods such as the Aldol or Michael reactions. The additional stabilization comes from the delocalization of the negative charge to the more electronegative oxygen atom (resonance effect). On the other hand, the presence of other non-polar π-unsaturated derivatives, such as olefins, which are present in many organic molecules, constitute an alternative functionality that can be used to forge new C–C bonds. An allylic fragment can thus be considered as a double bond adjacent to a carbon center. Compared to carbonyl compounds, allyl groups can stabilize carbocations more efficiently via resonance effect, while carbanions are less stabilized. Therefore, this group has been frequently used to accelerate substitution reactions of organic halides by nucleophiles, either through S_N1 or S_N2 mechanisms. In addition, this group can readily stabilize radicals via resonance effect, so examples of radical reactions are often encountered, including the allylic bromination of olefins, and the allylic oxidation of olefins to α,β-unsaturated ketones.

While the general accessibility of many olefins makes it attractive to utilize this functional group as an activator of the α (allylic) position, the utility of this group for structural elaboration suffers from the inability to functionalize chemo- and regioselectively at the allylic position. This lack of selectivity is, for instance, illustrated in the allylic bromination of non-symmetrical olefins, which is difficult towards the formation of one regioisomer, and also competitive bromination of the double bond occurs.[2] In contrast to the well-known behavior of carbonyl compounds for which α-substitutions are relatively simple to perform through the intermediacy of enols or enolates, an analogous chemo- and regioselective process for alkenes is much more challenging (**SCHEME 1.1**).

[1] Trost, B. M.; Fleming, I., *Comprehensive Organic Synthesis: Carbon–Carbon σ-Bond Formation*. Elsevier Ltd: Oxford, 1991; Vol. 3.
[2] McMurry, J., *Organic Chemistry*. 7th ed.; Cengage Learning: Belmont, 2008.

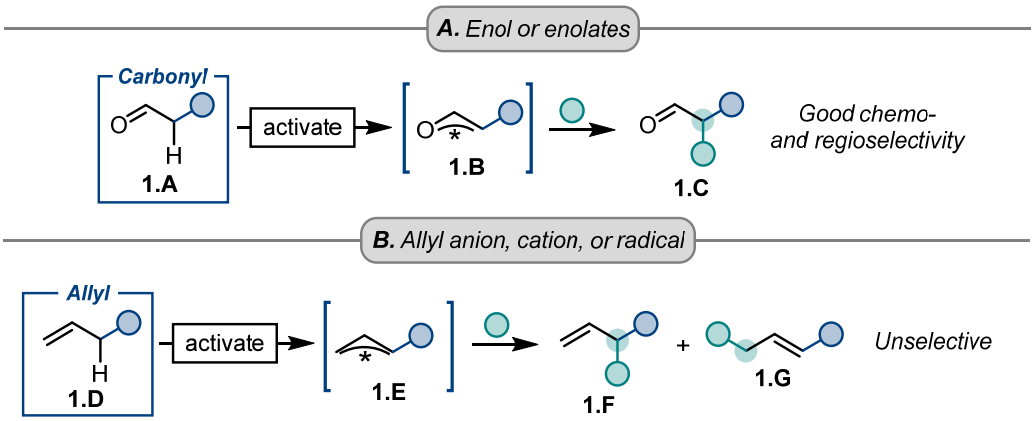

SCHEME 1.1. Comparison of the α-functionalization of carbonyl compounds and alkenes.

The transformations of the olefin unit in the allyl group into other functionalities are complementary to the transformations of carbonyl groups, thus widening the available synthetic strategies to make complex organic molecules (**SCHEME 1.2**). For example, the olefin group can be readily reduced into alkanes through catalytic hydrogenation. Additionally, it can be oxidized to epoxides, transformed into alcohols, methyl ketones, aldehydes, and even be transformed into other olefins via ruthenium-catalyzed olefin metathesis. Lastly, they may also be transformed into carbonyl groups using either a reductive ozonolysis reaction, or a dihydroxylation-oxidative cleavage sequence.

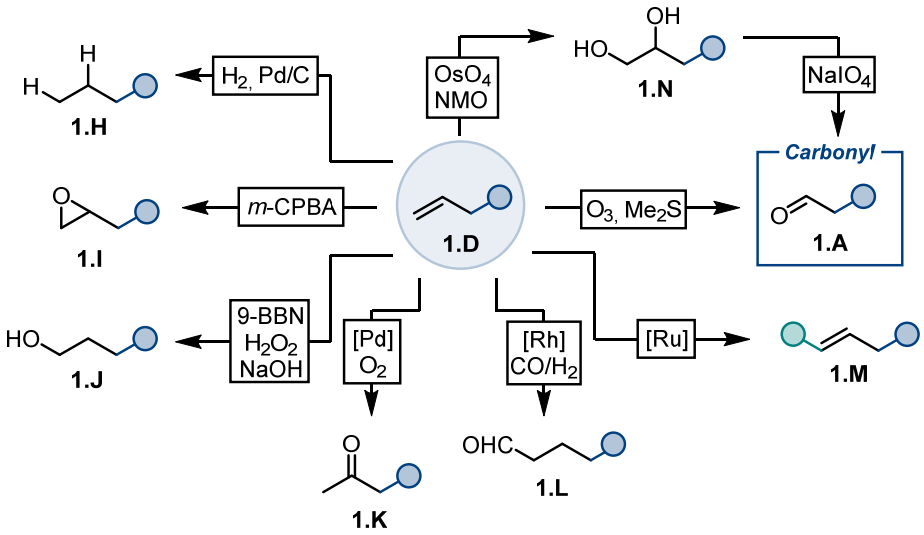

SCHEME 1.2. Representative transformations of the double bond in allylic compounds.

1.2 Metal-Catalyzed Allylic Substitutions with Nucleophiles

One of the most utilized methods to introduce allyl groups in organic molecules is the metal-catalyzed allylic substitution in the presence of nucleophiles. We can distinguish between two distinct scenarios (**SCHEME 1.3**). The first one relates to oxidative C–H functionalizations of unactivated allylic substrates, which requires the addition of a stoichiometric oxidant to regenerate the active catalytic species. While no pre-functionalization of the substrate is needed, these reactions usually suffer from chemo- and regioselectivity issues in the activation of the (desired) C–H bond.[3] Although the area has significantly advanced over the years,[4] it will not be a topic of discussion in the subsequent chapters of the thesis.

The second scenario relates to the direct allylation of nucleophiles with *activated* allylic substrates (*i.e.,* having a leaving group at the allylic position). Compared to oxidative allylic substitutions processes, these reactions start and finish with the same active low-valent metal catalyst, which simplifies the overall catalytic cycle. While the direct allylation of nucleophiles may be achieved without a metal catalyst, strong nucleophiles or highly activated allylic surrogates are often necessary. The addition of a metal catalyst increases the reaction rate and allows the utilization of other, less activated allylic surrogates. In addition, a metal catalyst can provide control over the regio-, diastereo-, and enantioselectivity of the process when non-symmetrical allyl groups are involved.[5]

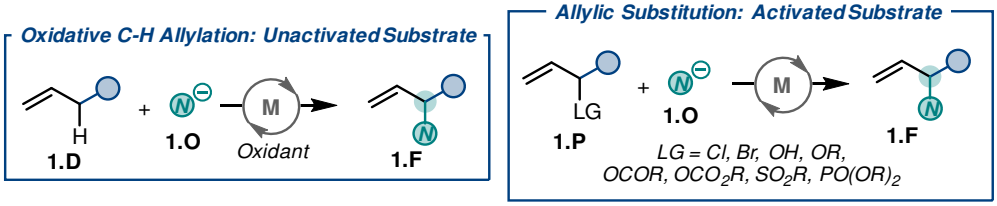

SCHEME 1.3. Comparison between oxidative C–H and direct allylations of activated substrates.

[3] For selected reviews on C–H activations, see: a) Planas, O.; Chirila, P. G.; Whiteoak, C. J.; Ribas, X. Current Mechanistic Understanding of Cobalt-Catalyzed C–H Functionalization. In *Advances in Organometallic Chemistry*, Vol. 69; Elsevier Ltd, 2018; pp 209-282. b) Murali, K.; Machado, L. A.; Carvalho, R. L.; Pedrosa, L. F.; Mukherjee, R.; Da Silva Júnior, E. N.; Maiti, D. *Chem. Eur. J.* **2021**, *27*, DOI: 10.1002/chem.202101004. c) Rogge, T.; Kaplaneris, N.; Chatani, N.; Kim, J.; Chang, S.; Punji, B.; Schafer, L. L.; Musaev, D. G.; Wencel-Delord, J.; Roberts, C. A.; Sarpong, R.; Wilson, Z. E.; Brimble, M. A.; Johansson, M. J.; Ackermann, L. *Nat Rev Methods Primers* **2021**, *1*, 43-73.

[4] For selected reviews on oxidative C–H allylations, see: a) Kazerouni, A. M.; McKoy, Q. A.; Blakey, S. B. *Chem. Commun.* **2020**, *56*, 13287-13300. b) Manoharan, R.; Jeganmohan, M. *Eur. J. Org. Chem.* **2020**, 7304-7319.

[5] For selected reviews on allylic substitution reactions, see: a) Trost, B. M.; Van Vranken, D. L. *Chem. Rev.* **1996**, *96*, 395-422. b) Weaver, J. D.; Recio, A.; Grenning, A. J.; Tunge, J. A. *Chem. Rev.* **2011**, *111*, 1846-1913. c) Sundararaju, B.; Achard, M.; Bruneau, C. *Chem. Soc. Rev.* **2012**, *41*. d) Butt, N. A.; Zhang, W. *Chem. Soc. Rev.* **2015**, *44*, 7929-7967.

1.2.1 Metal-Catalyzed Allylic Substitutions of Activated Substrates

Palladium catalysts have tremendously revolutionized the field of allylic substitution reactions since they were initially discovered by Tsuji in 1965.[6] In this seminal work, the stoichiometric reaction of π-allylpalladium chloride (II) with ethyl malonate and acetoacetate is described. Although the initial discovery is attributed to Tsuji, the reaction was largely developed by Trost.[7] To credit this discovery, the palladium-catalyzed version of the allylic substitution reaction is usually called the *Tsuji-Trost* reaction. Whilst the most employed substrates for palladium-catalyzed allylic substitutions are allylic acetates, a variety of leaving groups also function effectively. These include halides, sulfonates, carbonates, carbamates, epoxides, and phosphates, but also alcohols or ethers are applicable under certain conditions. Suitable nucleophiles are stabilized carbon nucleophiles, such as malonates, but it is important to mention that a wide variety of heteroatom-based nucleophiles (*e.g.*, *N*-, *O*-, and *S*-based nucleophiles) also represent excellent coupling partners in the *Tsuji-Trost* reaction.

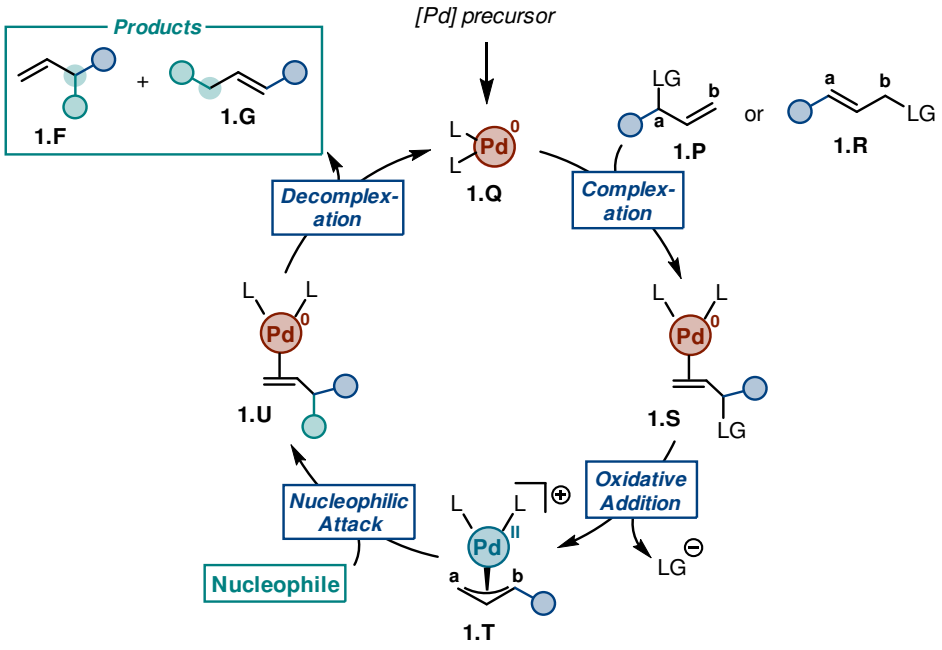

SCHEME 1.4. Simplified catalytic cycle of the *Tsuji-Trost* allylic substitution process.

[6] Tsuji, J.; Takahashi, H.; Morikawa, M. *Tetrahedron Lett.* **1965**, *6*, 4387-4388.
[7] Trost, B. M. *Tetrahedron* **2015**, *71*, 5708-5733.

The mechanism of this transformation consists of the initial activation of the allylic substrate to form a π-allylPd^{II} complex and the subsequent substitution stage to convert this complex to the final product (**SCHEME 1.4**). The reaction commences with a reactive 14-electron Pd^0 complex **1.Q**, which can coordinate the allylic substrate to afford palladium complex **1.S**. Hereafter, the orientation of the leaving group (LG)[8] *anti* to the palladium atom and a high electron density of the palladium promotes oxidative addition to generate a cationic π-allylPd^{II} intermediate **1.T**.[9] At this point, the original positional information of the leaving group at C_a (branched) or C_b (linear) is lost. Thus, in many instances, the choice of the initial substrate (*i.e.,* leaving group at C_a or C_b) depends upon the availability of these precursors. At the substitution stage, the nucleophile normally attacks the face of the allyl unit that is opposite to palladium. The inversion during the initial ionization (oxidative addition) and a second inversion during the displacement step (nucleophilic attack) lead to net retention in this substitution reaction, which complements the normal displacements that involve overall inversion of configuration. Attack of the nucleophile at C_a or at C_b depends upon the nature of the nucleophile, the nature of the substitution in the π-allyl unit, and the nature of the ligands coordinated to the palladium center.[10] The ability to manipulate these factors and, therefore, the regioselectivity of the allylic substitution (*cf.*, products **1.F** and **1.G**) is essentially achieved through transition metal templates. Thus, the Pd^0 species serves initially as a nucleophile but evolves into a leaving group and reflects the first demonstration of a metalated species acting as an electrophile. This discovery counterbalanced decades of research that suggested that such entities only behave as nucleophiles.

[8] The choice of leaving group has also important consequences in the reactivity, see: Krapcho, P.; Agenet, N.; Amatore, C.; Gamez, S.; Gérardin, H.; Jutand, A.; Meyer, G.; Orthwein, C. *Arkivoc (Gainesville, FL, U. S.)* **2002**, 92-101.

[9] Mechanistic studies regarding the elementary steps to generate cationic π-allylPd^{II} species have been reported, see: a) Amatore, C.; Jutand, A.; Meyer, G.; Mottier, L. *Chem. Eur. J.* **1999**, *5*, 466-473. b) Amatore, C.; Gamez, S.; Jutand, A.; Meyer, G.; Moreno-Mañas, M.; Morral, L.; Pleixats, R. *Chem. Eur. J.* **2000**, *6*, 3372-3376. c) Amatore, C. *Electrochim. Acta* **2001**, *46*, 3237-3244. d) Amatore, C.; Gamez, S.; Jutand, A. *Chem. Eur. J.* **2001**, *7*, 1273-1280. e) Amatore, C.; Jutand, A.; M'Barki, Mohamed A.; Meyer, G.; Mottier, L. *Eur. J. Inorg. Chem.* **2001**, 873-880. f) Amatore, C.; Bahsoun, A. A.; Jutand, A.; Mensah, L.; Meyer, G.; Ricard, L. *Organometallics* **2005**, *24*, 1569-1577.

[10] As a general rule, linear regioselectivity is observed for palladium-catalyzed allylic substitutions, which is also the case when using nickel. On the other hand, iridium, rhodium, cobalt, and molybdenum tend to give branch regioselectivity.

1.2.2 Hard and Soft Nucleophiles

Concerning the nucleophilic attack onto the π-allyl group, two modes of nucleophilic attack are possible. On one hand, the nucleophile can attack directly the π-allyl moiety (outer-sphere pathway), which is characteristic of *soft* nucleophiles. On the other hand, *hard* nucleophiles can attack the metal center (inner-sphere pathway) prior to C–Nu bond formation (transmetalation-reductive elimination). A classification to distinguish between the two modes of attack is based on the pK_a of the pronucleophile. If its pK_a is lower than 25, it is considered a *soft* nucleophile, whereas a pK_a higher than 25 is assigned to a *hard* nucleophile. However, this classification has some exceptions that raised the pK_a limit of *soft* nucleophiles. This is, for instance, the case for 2-picoline-derived nucleophiles,[11] polynitrogen-containing heterocycles,[12] chromium-stabilized toluene derivatives[13], and diarylmethane derivatives.[14] The consequences of both attacks can be observed by analyzing the stereochemical outcome of the reaction. Whereas *soft* nucleophiles give rise to retention of the configuration of the carbon center attached to the leaving group (**SCHEME 1.5**, path a), *hard* nucleophiles induce a net inversion of configuration (**SCHEME 1.5**, path b) because the nucleophile attacks the allyl moiety at the same face where the metal center resides.

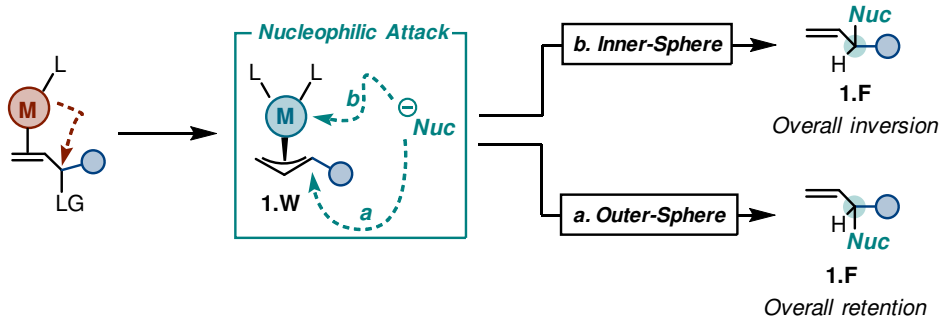

SCHEME 1.5. Stereochemical outcome when using *soft* and *hard* nucleophiles.

1.2.3 Dynamic Processes of Allyl Groups

One of the most interesting features of allyl groups bound to metals is that they are involved in multiple dynamic equilibria. On the time scale of the catalytic cycle, the fluxional behavior of these complexes involves processes such as ligand exchange, dimerization, or isomerization.

[11] Trost, B. M.; Thaisrivongs, D. A. *J. Am. Chem. Soc.* **2009**, *131*, 12056-12057.
[12] Trost, B. M.; Thaisrivongs, D. A.; Hartwig, J. *J. Am. Chem. Soc.* **2011**, *133*, 12439-12441.
[13] Zhang, J.; Stanciu, C.; Wang, B.; Hussain, M. M.; Da, C.-S.; Carroll, P. J.; Dreher, S. D.; Walsh, P. J. *J. Am. Chem. Soc.* **2011**, *133*, 20552-20560.
[14] Sha, S.-C.; Zhang, J.; Carroll, P. J.; Walsh, P. J. *J. Am. Chem. Soc.* **2013**, *135*, 17602-17609.

- **Ligand exchange:** In solution, it is possible to exchange one or both ligands L in the η^3-allyl metal complex. This exchange can proceed through a dissociative or an associative mechanism (**SCHEME 1.6**).

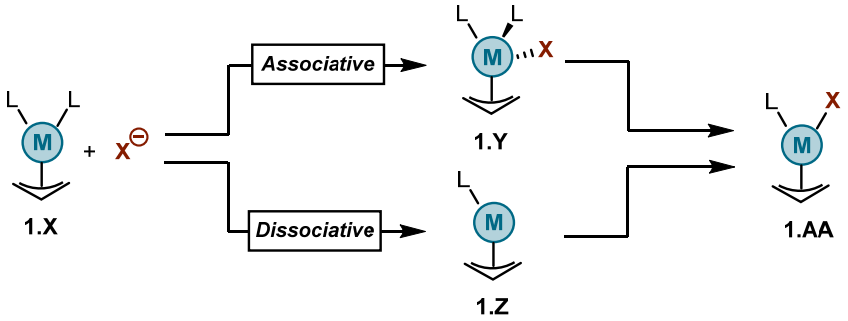

SCHEME 1.6. Mechanism of ligand exchange in π-allyl complexes.

- **Dimerization:** If one of the ligands in the η^3-allyl metal complex dissociates, the resulting complex can dimerize towards the formation of $[(\eta^3\text{-allyl})MX]_2$ (**SCHEME 1.7**). This is often observed when X is Cl, Br, OAc, or $OCOCF_3$. The dimeric species is often unreactive, and thus can be considered an *off*-cycle species.

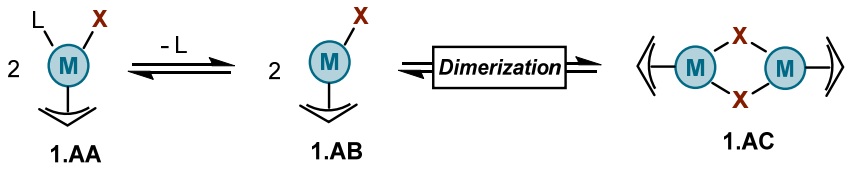

SCHEME 1.7. Dimerization of π-allyl complexes.

- **π-σ-π Isomerization (*syn-anti* isomerization):** Substituents on allylic ligands are traditionally named according to their configuration relative to the *central* substituent of the allyl moiety. The groups which are on the same side of the central substituent are designated as *syn*, whereas the groups on the opposite side, are labeled as *anti*. On the time scale of a typical substitution reaction, the *syn/anti* substituents in a π-allyl metal complex can usually exchange positions tens or hundreds of times faster than the actual substitution process, although the rate depends on multiple factors, such as the type of ligand coordinated to Pd, the solvent, additives, among others.[15] The isomerization occurs via a change in the coordination of the allyl group to palladium from η^3 to η^1 and *vice versa*. The C–C bond in the η^1-complex can rotate freely and

[15] a) Fagnou, K.; Lautens, M. *Angew. Chem. Int. Ed.* **2002**, *41*, 26-47. b) Ogasawara, M.; Takizawa, K.-i.; Hayashi, T. *Organometallics* **2002**, *21*, 4853-4861.

hereafter the η^3-allyl complex is reformed with either *syn* or *anti* stereochemistry. The latter is the result of a *syn-anti* isomerization and an inversion at C_1 (**SCHEME 1.8**). These pair of isomers are thus diastereomers when the allyl group is substituted.

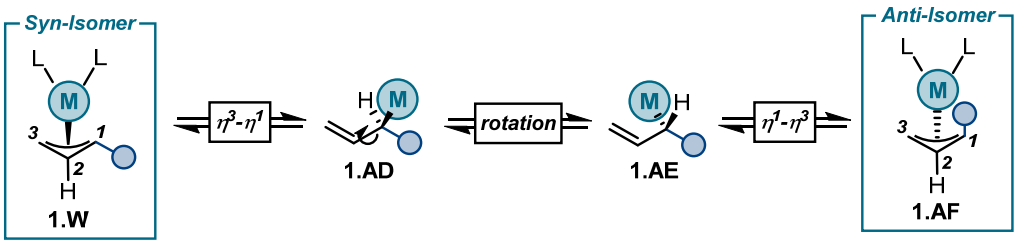

SCHEME 1.8. Mechanism of *syn-anti* isomerization in π-allyl groups.

Owing to the slight tilt of the allyl ligand from being perpendicular, *anti*-substituents are pointing towards the coordination sphere of the metal and have thus a destabilizing effect. Consequently, monosubstituted or 1,3-disubstituted allyl complexes nearly exclusively possess a *syn* geometry (**SCHEME 1.9A**). However, within certain 1,2-disubstituted or 1,2,3-trisubstituted allyl-Pd complexes, steric repulsion between vicinal *syn* substituents may lead to a larger proportion of the *anti*-isomer. Moreover, it has been reported that by using 2,9-disubstituted phenanthroline ligands, the *anti*-isomer is the most stable one and was even isolated (**SCHEME 1.9B**).[16]

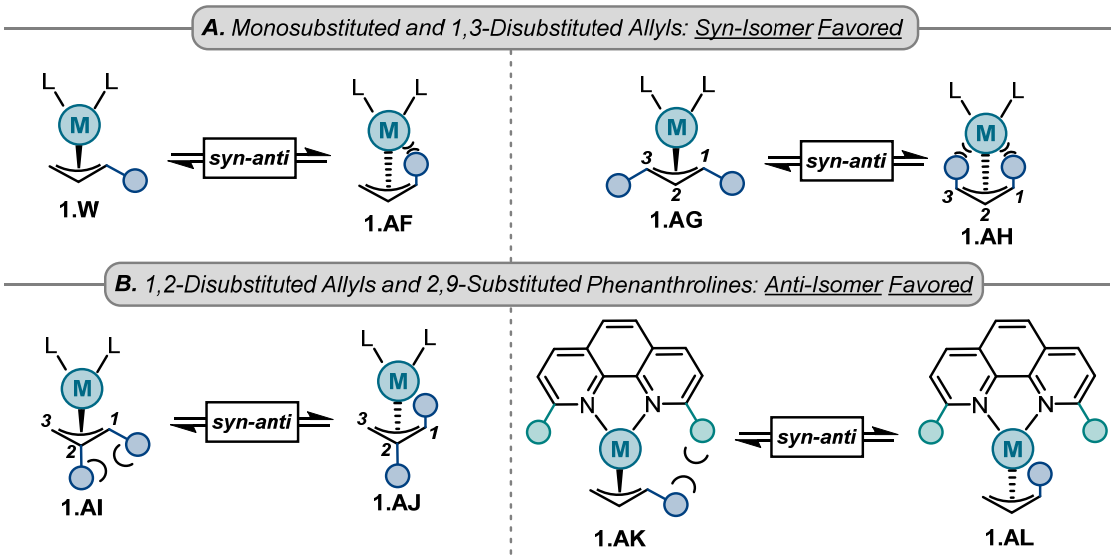

SCHEME 1.9. Relative stability of *syn-anti* isomers in: **(A)** Monosubstituted and 1,3-disubstituted allyl groups; **(B)** 1,2-disubstituted allyl groups and 2,9-disubstituted phenanthroline ligands influencing *syn*/*anti* isomerism.

[16] Sjoegren, M.; Hansson, S.; Norrby, P. O.; Aakermark, B.; Cucciolito, M. E.; Vitagliano, A. *Organometallics* **1992**, *11*, 3954-3964.

The attack of the nucleophile on the *syn* or *anti* complexes has consequences for the double bond geometry in the final product. Considering a monosubstituted allyl group and the nucleophilic attack occurring at the terminal carbon, the *syn*-complex will lead to the (*E*)-configured product, while the *anti*-complex will lead to the (*Z*)-configured product (**SCHEME 1.10**). Therefore, considering a Curtin-Hammett scenario, apart from the relative rates (k_{syn} vs. k_{anti}) leading to each diastereomeric product, the relative concentrations of each species, namely [*syn*] and [*anti*] will also play an important role in the observed overall diastereoselectivity. Other factors affecting the diastereoselectivity are the rate of *syn-anti* isomerization, which affects the concentration of the *syn*- and *anti*-isomers over time, and whether the substrate has a stereodefined double bond configuration.

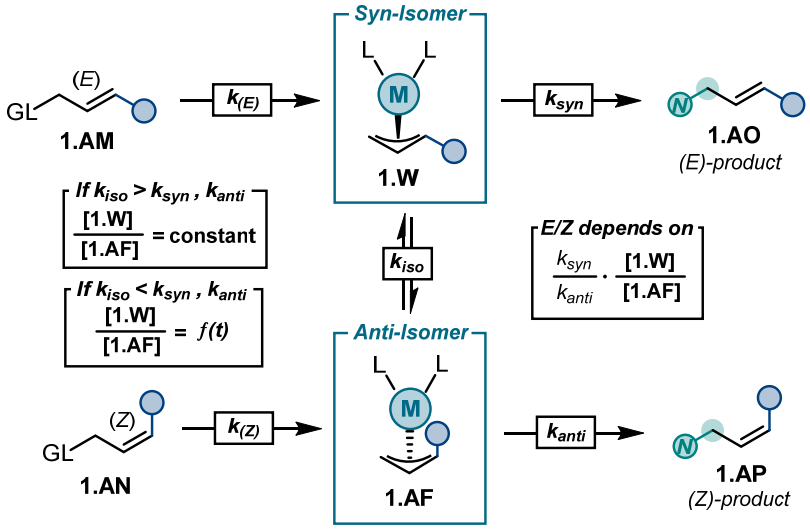

SCHEME 1.10. Rationale of the observed diastereoselectivity in common allylic substitution reactions.

- **π-Rotation:** Ligands in π-allyl metal complexes can exchange positions relative to the allyl moiety with the palladium bonded to the same face of the allyl group. Two different mechanisms have been suggested, an associative *pseudo*-rotation[17] and a dissociative mechanism[18] (**SCHEME 1.11**). If the allyl group points "up", the isomer is called *endo*, whereas if the allyl group points "down", the isomer is denoted as *exo*. Note that these compounds are diastereomers if the bidentate ligand has C_1 symmetry, but can become the same compound if the bidentate ligand has C_2 symmetry.

[17] Hansson, S.; Norrby, P. O.; Soegren, M. P. T.; Aakermark, B.; Cucciolito, M. E.; Giordano, F.; Vitagliano, A. *Organometallics* **1993**, *12*, 4940-4948.

[18] a) Gogoll, A.; Örnebro, J.; Grennberg, H.; Bäckvall, J.-E. *J. Am. Chem. Soc.* **1994**, *116*, 3631-3632. b) Faller, J. W.; Stokes-Huby, H. L.; Albrizzio, M. A. *Helv. Chim. Acta* **2001**, *84*, 3031-3042.

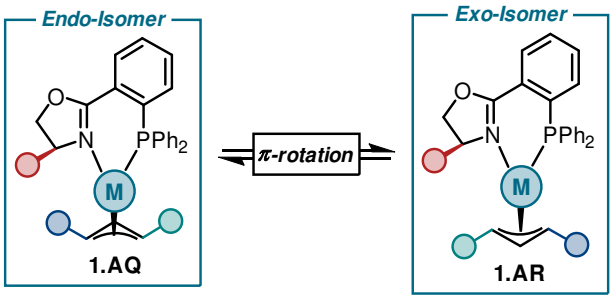

SCHEME 1.11. Representation of *exo*- and *endo*-isomers of allyl-metal complexes.

1.2.4 Representative Examples

Most of the breakthroughs in the area of allylic substitution reactions have been realized through extensive ligand development and engineering. The application of ligands in the allylic alkylation reaction has a dual purpose, the activation of the η^3-allyl for nucleophilic attack and the control over the selectivity of the reaction. Before discussing ligand design, it is paramount to first comment on the difference in reactivity between the terminal and internal positions of the allyl group.

In general, the terminal position is less sterically hindered, and thus regioselectivity is best achieved by steric factors within the ligand, substrate, and nucleophile. On the other hand, the internal position is preferred through electronic effects, as the transient transition state of the reaction leaves a positive charge on the allyl moiety which is more efficiently stabilized at the more substituted (internal) carbon atom. Consequently, π-accepting ligands and relatively non-bulky substrates/nucleophiles may give rise to branched products. To support this idea, Åkermark and Vitagliano carried out a detailed study by ^{13}C NMR.[19] In allyl complexes, the internal carbon center is always observed downfield from the terminal carbons. With a better π-accepting ligand, the chemical shift difference between the internal and the terminal carbon centers is increased, and the internal carbon becomes more positively charged and susceptible to nucleophilic attack.

[19] Åkermark, B.; Krakenberger, B.; Hansson, S.; Vitagliano, A. *Organometallics* **1987**, *6*, 620-628.

The bite angle (in the case of bidentate ligands) is also an important factor and detailed studies have been carried out on the influence on the selectivity and rate of catalytic allylic substitution reactions.[20] In palladium-catalyzed allylic substitution, it was shown that the steric hindrance at the palladium center (that increases with wider bite angle ligands) induced selectivity towards the linear product. However, with an extremely large bite angle, deterioration of the reactivity of the π-allylpalladium complex was observed. These observations were explained by the increasing embracing effect of the allylic fragment by the ligand, which inhibits the formation of the branched product.

Despite all these considerations, there is no straightforward rationale when it comes to choosing the right combination of metal and ligand, as it has been shown to be extremely substrate-specific, and to some extent, nucleophile-dependent. Therefore, much empirical experimentation is needed to find the right combination when developing methods for specific new substrate-nucleophile combinations. In most cases though, bidentate ligands display better results than monodentate ligands (except for phosphoramidites), and diphosphine ligands are often reported to be effective.

o Trost Ligands

As can be anticipated, the most prominent examples of allylic substitution reaction employ chiral ligands to induce enantio-discrimination at the branch position. Regarding palladium-based catalysts, the most remarkable and seminal examples were introduced early on by Trost using newly developed and easy-to-prepare C_2-symmetric ligands composed of two diphenylphosphino benzoic acid motifs linked to a chiral diamine scaffold (also known as DPPBA-based ligands). These ligands exhibit good reactivity, excellent branch-selectivity, and high asymmetric induction for several cyclic and acyclic substrates with a wide range of *C*-, *N*-, *S*-, and *O*-nucleophiles, and are equally applied to intra- and intermolecular reactions (**SCHEME 1.12**). Their success in the high asymmetric induction lies in the confined chiral pocket created by the ligand, in which two phenyl groups bound to the phosphine (denoted as *walls*) are approximately perpendicular to the plane of the allyl unit and the other two phenyl groups (denoted as *flaps*) that sit parallel to the plane. As illustrated in the molecular model (**SCHEME 1.12**), these ligands create a chiral environment where the back right and front left quadrants are effectively blocked, thus creating a steric differentiation between the two front quadrants.[21] On the other hand, the tight confinement created by the ligand is counterproductive when bulkier allylic substrates are used, especially when creating sterically congested quaternary carbon stereocenters, as the initial Pd^0 complex is often not able to ionize the substrate.

[20] van Leeuwen, P. W. N. M.; Kamer, P. C. J.; Reek, J. N. H.; Dierkes, P. *Chem. Rev.* **2000**, *100*, 2741-2770.
[21] Trost, B. M.; Machacek, M. R.; Aponick, A. *Acc. Chem. Res.* **2006**, *39*, 747-760.

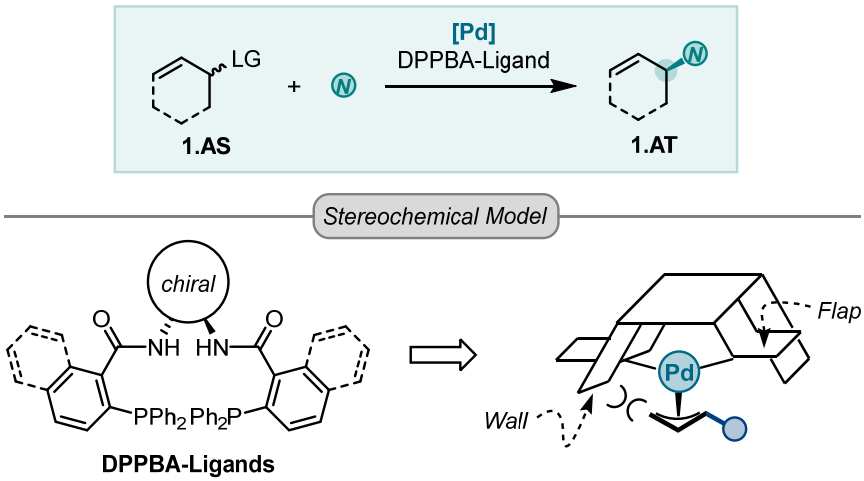

SCHEME 1.12. Palladium-catalyzed allylic substitution reactions with DPPBA-based ligands.

o PHOX Ligands

Other successful chiral ligands for palladium-catalyzed allylic substitution reactions have been developed by Helmchen, Pfaltz, and Williams, which introduced phosphine-oxazoline ligands (PHOX ligands) able to achieve high asymmetric induction with mostly symmetrical 1,3-disubstituted allylic substrates having relatively bulky groups (**SCHEME 1.13**).[22] As these ligands do not possess C_2-symmetry, the asymmetric induction is mainly achieved by the electronic differentiation between the phosphine and the oxazoline groups, and therefore the nucleophilic addition onto the allyl group is predominantly occurring at the carbon *trans* to the P-atom (*trans* effect). Apart from that, the relative concentrations of the *endo*- and *exo*-isomers must also be carefully controlled for high asymmetric induction. X-ray crystal structures of allyl-Pd(PHOX) complexes demonstrated that the dominant interaction between the ligand and the allylic moiety originates from the equatorial P-aryl group (colored blue in **SCHEME 1.13**) which repels the substituent at C_1 of the allyl group.[23] This repulsive interaction is smaller for the *exo*- than the *endo*-diastereomer, thus favoring a higher concentration of the *exo* species. In addition, NMR studies proved that the *trans* effect in the *exo* isomer is weaker, thus explaining its lower reactivity compared to the *endo* isomer, which is in line with the observed enantioselectivities that usually exceed the *endo*/*exo* ratios observed in reaction mixtures.[24] On the other hand, less bulky substituents on the allyl moiety were less prone to be converted with high enantioinduction, but this challenge could be conveniently addressed by increasing the steric properties of the oxazolidinone substituent, which led to an enhanced bending of the chelate ring with the consequence that the

[22] Helmchen, G.; Pfatz, A. *Acc. Chem. Res.* **2000**, *33*, 336-345.
[23] a) Sprinz, J.; Kiefer, M.; Helmchen, G.; Reggelin, M.; Huttner, G.; Walter, O.; Zsolnai, L. *Tetrahedron Lett.* **1994**, *35*, 1523-1526. b) Schaffner, S.; Müller, J. F. K.; Neuburger, M.; Zehnder, M. *Helv. Chim. Acta* **1998**, *81*, 1223-1232.
[24] Armstrong, P. B.; Dembicer, E. A.; DesBois, A. J.; Fitzgerald, J. T.; Gehrmann, J. K.; Nelson, N. C.; Noble, A. L.; Bunt, R. C. *Organometallics* **2012**, *31*, 6933-6946.

crucial equatorial P-phenyl group is pushed nearer to the allyl group, leading to destabilization of the *endo* isomer. Finally, the development of Pd complexes of PHOX-derived ligands having a biaryl phosphite (instead of the phosphine group) proved to be very effective catalysts for reactions of both hindered, unhindered, and even cyclic substrates.[25]

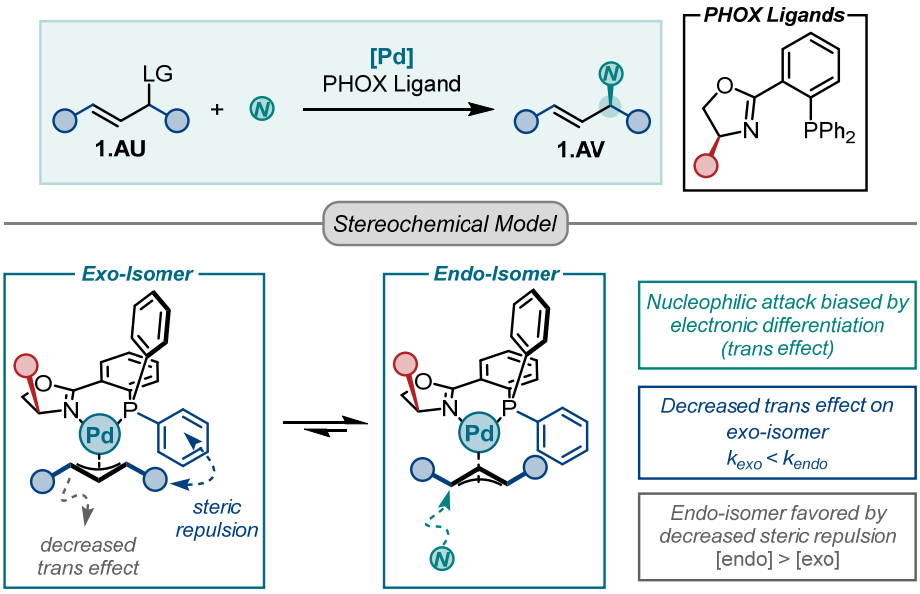

SCHEME 1.13. Palladium-catalyzed allylic substitution reactions with PHOX ligands.

The application of Pd-PHOX catalysts to generate quaternary carbon stereocenters and tetrasubstituted tertiary centers with high asymmetric induction and yields has been reported by Stoltz.[26] Building on previous studies by Tsuji[27] on allylic alkylation of silyl enol ethers, enol carbonates, and β-ketoesters derived from non-symmetrical, non-stabilized ketones, which provided an elegant solution to circumvent position-selective enolate generation and subsequent alkylation, the Stoltz group developed various enantioselective methods to introduce allyl groups into a wide range of cyclic carbonyl substrates (**SCHEME 1.14**). The method is tolerant to the use of different allylic electrophiles, such as allylic carbonates, acetates, sulfonates, and in some instances, halides. In contrast to the work reported by Helmchen, Pfaltz, and Williams, the asymmetric induction is exerted on the prochiral enolate, rather than on the prochiral allylic substrate, which suggests a different stereochemical model. Empirical and computational evidence suggested that the nucleophilic addition onto the allyl group happens through an inner-sphere pathway involving an *O*-bound enolate

[25] a) Pàmies, O.; Diéguez, M.; Claver, C. *J. Am. Chem. Soc.* **2005**, *127*, 3646-3647. b) Bellini, R.; Magre, M.; Biosca, M.; Norrby, P.-O.; Pàmies, O.; Diéguez, M.; Moberg, C. *ACS Catal.* **2016**, *6*, 1701-1712. c) Biosca, M.; Saltó, J.; Magre, M.; Norrby, P.-O.; Pàmies, O.; Diéguez, M. *ACS Catal.* **2019**, *9*, 6033-6048.

[26] Liu, Y.; Han, S.-J.; Liu, W.-B.; Stoltz, B. M. *Acc. Chem. Res.* **2015**, *48*, 740-751.

[27] a) Shimizu, I.; Yamada, T.; Tsuji, J. *Tetrahedron Lett.* **1980**, *21*, 3199-3202. b) Tsuji, J.; Minami, I.; Shimizu, I. *Tetrahedron Lett.* **1983**, *24*, 1793-1796.

and a η^1-allyl group via a cyclic seven-membered reductive elimination that resembles a pericyclic transition state found in sigmatropic rearrangements.[28] Importantly, situating the carbocyclic ring of the enolate fragment away from the bulky *t*-Bu group of the oxazoline provides a plausible predictive model for the observed enantiofacial selectivity. The reaction is limited mostly to non-stabilized cyclic enolates and simple allyl groups, although the scope could be extended to acyclic stabilized enolates and more functionalized allyl groups by using an Ir-phosphoramidite catalyst.[29]

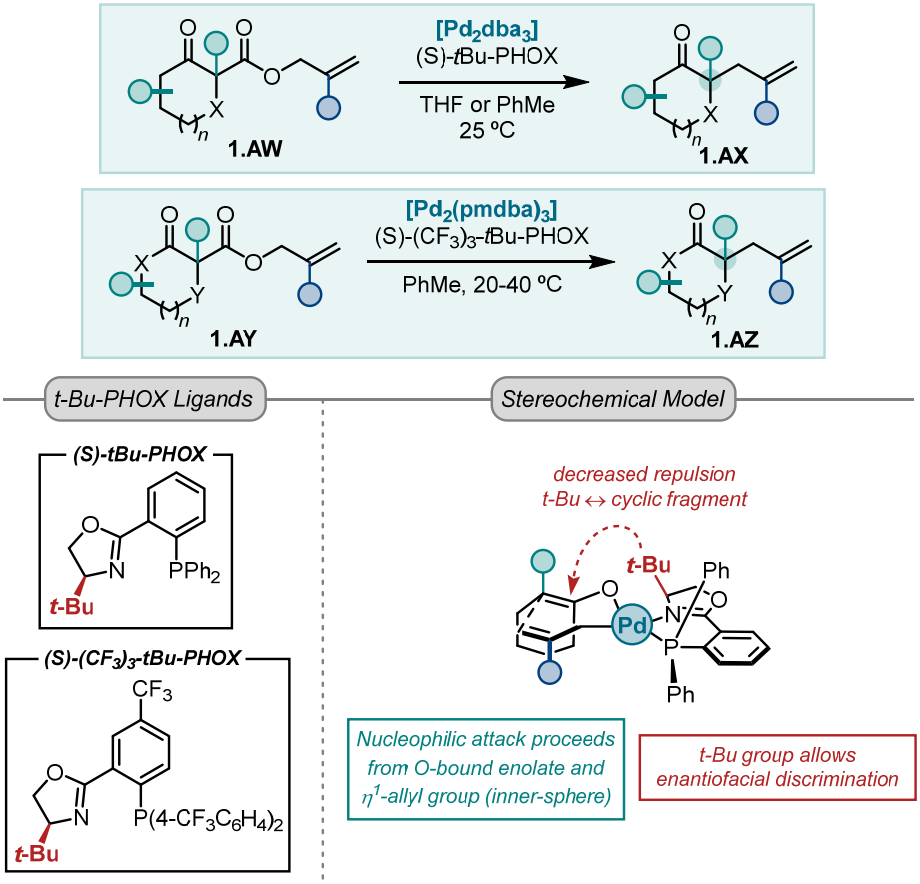

SCHEME 1.14. Enantioselective allylic alkylation of enolates with PHOX ligands.

[28] a) Keith, J. A.; Behenna, D. C.; Mohr, J. T.; Ma, S.; Marinescu, S. C.; Oxgaard, J.; Stoltz, B. M.; Goddard, W. A. *J. Am. Chem. Soc.* **2007**, *129*, 11876-11877. b) Behenna, D. C.; Mohr, J. T.; Sherden, N. H.; Marinescu, S. C.; Harned, A. M.; Tani, K.; Seto, M.; Ma, S.; Novák, Z.; Krout, M. R.; McFadden, R. M.; Roizen, J. L.; Enquist, J. A.; White, D. E.; Levine, S. R.; Petrova, K. V.; Iwashita, A.; Virgil, S. C.; Stoltz, B. M. *Chem. Eur. J.* **2011**, *17*, 14199-14223.

[29] Liu, W.-B.; Reeves, C. M.; Stoltz, B. M. *J. Am. Chem. Soc.* **2013**, *135*, 17298-17301.

o Phosphoramidite Ligands

Another class of privileged ligands that have revolutionized allylic substitution reactions promoted by palladium and iridium are phosphoramidite ligands. Since the introduction of the phosphoramidite ligands by Feringa,[30] the most illustrative application of these ligands is probably the asymmetric version of the palladium-catalyzed TMM cycloaddition to forge odd-membered rings (**SCHEME 1.15**). The development of pyrrolidine-based phosphoramidite and diamidophosphite ligands by Trost has been the key to unlock the asymmetric variant of this transformation and extent the method to a wide variety of TMM donors and unsaturated acceptor molecules.[31] Despite apparently being monodentate ligands, X-ray structures of palladium-phosphoramidite complexes show that the phosphoramidite can bind the palladium atom through a bidentate coordination mode (in the solid state), with one of the aromatic groups acting as a donor through a η^2-coordination.[32] The enantio-determining step is likely the initial nucleophilic addition of the TMM onto the prochiral unsaturated acceptor molecule, and, therefore, enantiofacial discrimination is achieved by steric interactions between the ligand backbone and the prochiral acceptor molecule. However, the exact origin of these steric interactions has not been elucidated yet.

[30] Teichert, J. F.; Feringa, B. L. *Angew. Chem. Int. Ed.* **2010**, *49*, 2486-2528.
[31] Trost, B. M.; Mata, G. *Acc. Chem. Res.* **2020**, *53*, 1293-1305.
[32] Mikhel, I. S.; Rüegger, H.; Butti, P.; Camponovo, F.; Huber, D.; Mezzetti, A. *Organometallics* **2008**, *27*, 2937-2948.

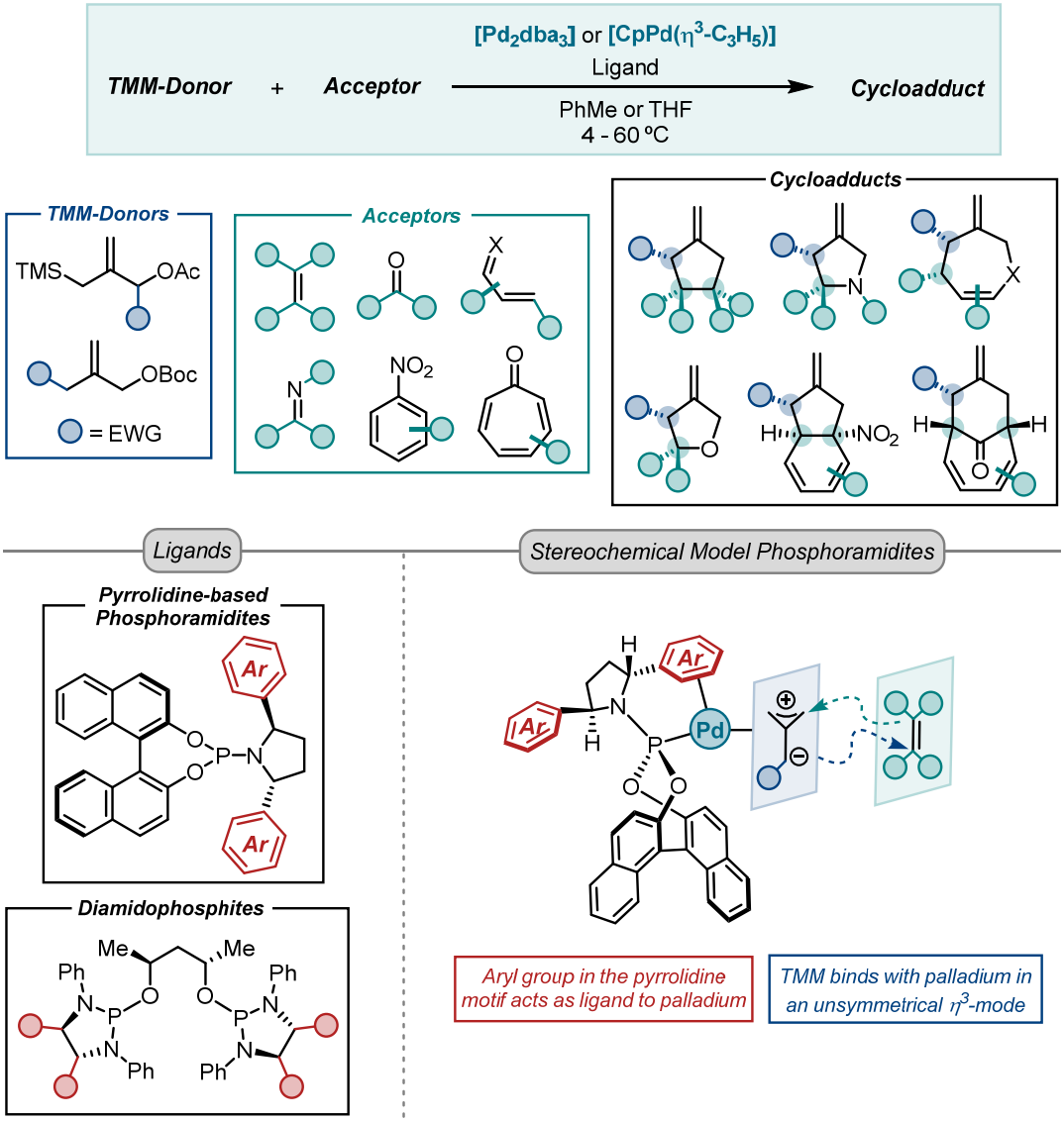

SCHEME 1.15. Asymmetric Pd-catalyzed TMM cycloadditions with phosphoramidite and diamidophosphite ligands.

Regarding iridium-catalyzed allylic substitutions, a landmark contribution to the field was made by the Hartwig group in 2003 when studying the allylic amination using the Feringa or the Alexakis phosphoramidite ligands.[33] They found that active *cyclometalated* iridium catalysts were formed by base-assisted C(sp^3)–H activation of the C–H bond on one of the Me groups in the phosphoramidite ligands, with this step being reversible in the presence of acid. Apart from increasing the reactivity of the catalyst towards oxidative addition, the second point of binding significantly decreases the number of degrees of freedom of the ligand, thus providing a more effective way to generate enantioinduction. In addition, the group of You greatly contributed to the development of new methods for iridium-catalyzed asymmetric allylic dearomatization reactions.[34] Compared with Hartwig's work, they used phosphoramidite ligands bearing more rigid

[33] Hartwig, J. F.; Stanley, L. M. *Acc. Chem. Res.* **2010**, *43*, 1461-1475.
[34] Zhuo, C.-X.; Zheng, C.; You, S.-L. *Acc. Chem. Res.* **2014**, *47*, 2558-2573.

tetrahydroquinoline (THQphos) or benzhydrylaniline (BHPphos) motifs. Analogously, the second point of binding is generated by base-assisted C(sp^2)–H activation of an aromatic C–H bond. The enantio-determining step in these transformations is usually the oxidative addition of the allylic substrate. Enantio-discrimination is provided by repulsive steric interactions exerted by the chiral binaphthol unit and the 1,5-cyclooctadiene molecule onto the allyl fragment. Both types of cationic iridium complexes feature exceptional reactivity and high asymmetric induction, being tolerant to several stabilized nucleophiles. Some limitations include the requirement of linear allylic substrates, instead of the branch allylic substrate, to provide higher enantioselectivities, and the requirement for basic reaction conditions to promote the generation of the cyclometalated iridium catalyst.

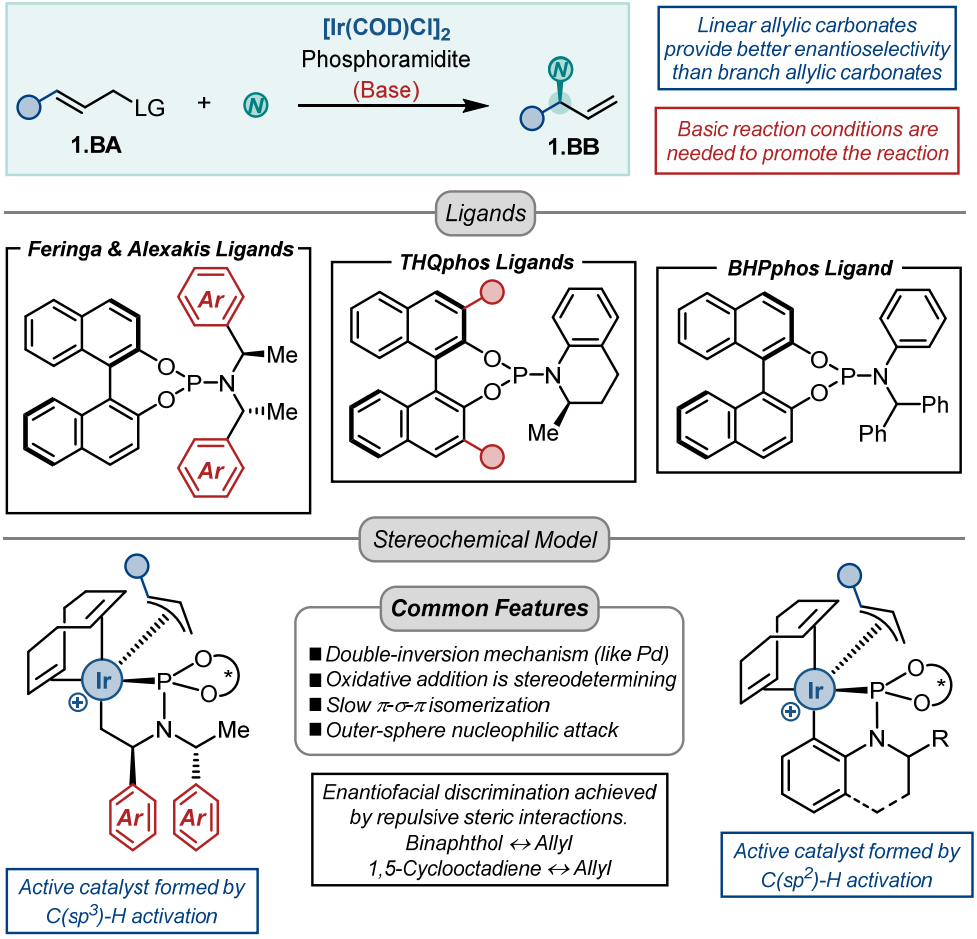

SCHEME 1.16. Enantioselective iridium-catalyzed allylic substitutions using cationic cyclometalated iridium-phosphoramidite complexes.

The last set of representative examples were introduced by the group of Carreira using hybrid (phosphoramidite-olefin) ligands.[35] Importantly, better results were obtained when mixing [Ir(COD)Cl]$_2$ with

[35] Rössler, S. L.; Petrone, D. A.; Carreira, E. M. *Acc. Chem. Res.* **2019**, *52*, 2657-2672.

this ligand in a 1:2 ratio, respectively. Indeed, mechanistic studies revealed that the resulting iridium complexes throughout the catalytic cycle contained one phosphoramidite ligand coordinated in a bidentate (η^2-κP) fashion, and a second phosphoramidite ligand is bound solely through phosphorus (**SCHEME 1.17**).[36] Compared with the iridium-catalyzed allylic substitution reactions reported by Hartwig and You, these complexes are oxygen, moisture, and acid-tolerant, and thus the allylic substitutions can be directly conducted from more abundant and atom-economical allylic alcohols. Additionally, a wide range of carbon nucleophiles can be used, which is not typical for most of the well-established palladium and iridium-catalyzed allylic substitution reactions. Moreover, even weakly nucleophilic compounds, such as 1,1-disubstituted olefins can be used as nucleophiles. To date, the nature of the nucleophilic attack (outer- vs. inner-sphere) is not completely understood, but NMR studies showed the existence of a rapid equilibrating mixture of *endo*- and *exo*-isomers after oxidative addition. This suggests that the enantioselectivity is not greatly influenced by the ratio of these isomers, but more likely by the difference of kinetic rates of the nucleophilic attack onto each of the isomers.

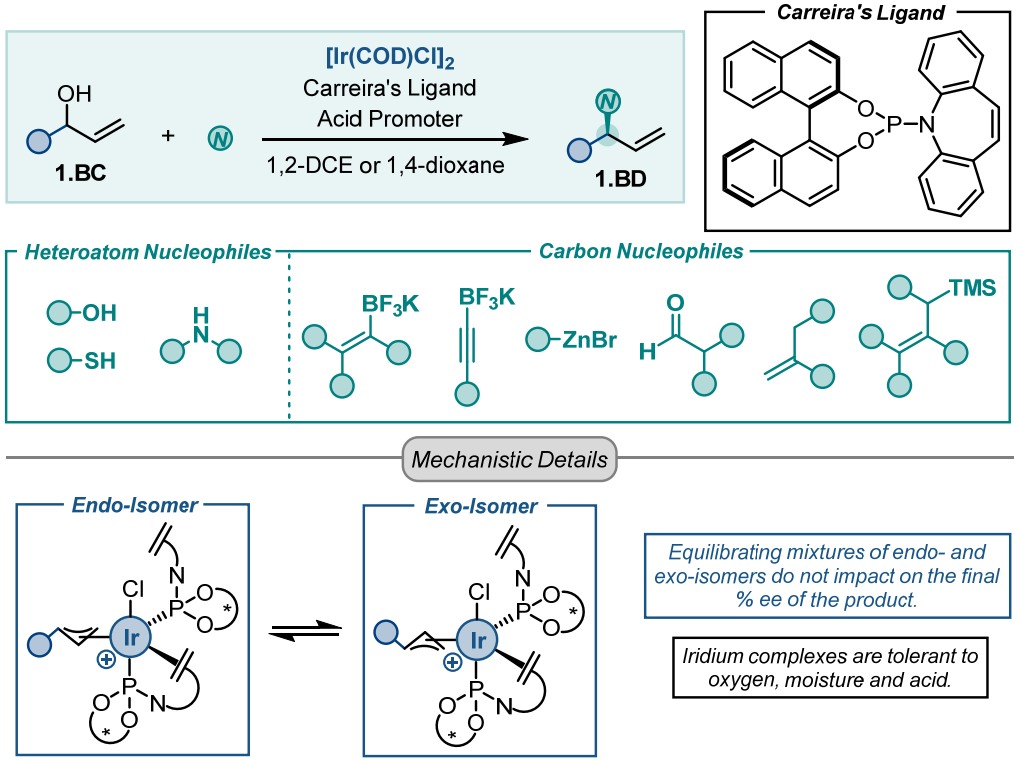

SCHEME 1.17. Enantioselective iridium-catalyzed allylic substitution of branch allylic alcohols using Carreira's (P,olefin) ligand.

[36] Rössler, S. L.; Krautwald, S.; Carreira, E. M. *J. Am. Chem. Soc.* **2017**, *139*, 3603-3606.

1.3 Metal-Catalyzed Substitutions with Electrophiles

A complementary strategy to introduce allyl groups in organic molecules is through metal-catalyzed allylic substitution reactions using *electrophiles*. Due to their electrophilic nature and importance in target-oriented synthesis, numerous methods rely on the allylation of carbonyl compounds, namely aldehydes, imines, and ketones, to generate synthetically useful homoallylic alcohols and amines.

For many years, carbonyl additions mediated by pre-metalated reagents have played a central role in synthetic organic chemistry (**SCHEME 1.18A**). This chemistry has been well developed by several research groups and has led to some important named reactions that are still used nowadays in complex natural product synthesis. These reactions include, for example, the Brown allylation, the Keck allylation, the Hosomi-Sakurai reaction, and the Nozaki-Hiyama-Kishi reaction.[37] Despite affording the desired homoallylic molecules in high yields, the requisite use of organometallic reagents poses issues in terms of safety, requires multistep approaches, and generates stoichiometric quantities of metal-containing byproducts.

A more elegant and atom-economical way to generate these important homoallylic alcohols and amines scaffolds involve the catalytic generation of allyl-metal reagents from abundant chemical feedstocks (**SCHEME 1.18B**). In this context, two important methods will be discussed in subsection 1.3.2. On one hand, the methods developed by Krische involve the catalytic generation of nucleophilic iridium or ruthenium allyl species via hydrogen transfer between alcohols and π-unsaturated reactants, while the methods developed by Buchwald (and others) rely on the catalytic generation of nucleophilic copper-allyl species by insertion of a Cu–H into allenes or 1,3-dienes.

[37] a) Abdul Fattah, T.; Saeed, A. *New J. Chem.* **2017**, *41*, 14804-14821. b) Gil, A.; Albericio, F.; Álvarez, M. *Chem. Rev.* **2017**, *117*, 8420-8446. c) Lee, J. H. *Tetrahedron* **2020**, *76*, 131351-131371. d) Boiarska, Z.; Braga, T.; Silvani, A.; Passarella, D. *Eur. J. Org. Chem.* **2021**, 3214-3222.

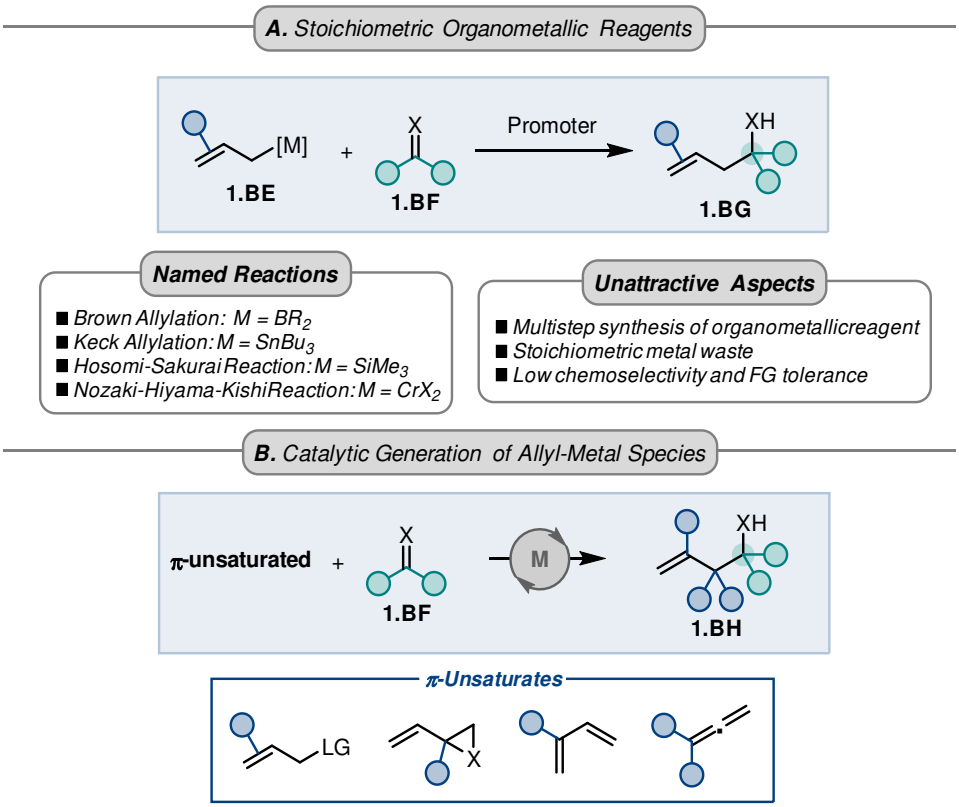

SCHEME 1.18. Comparison between stoichiometric and catalytic allylation methods.

1.3.1 Nucleophilic vs. Electrophilic Allyl Species

Before explaining the main intricacies of the metal-catalyzed allylations developed by Krische and Buchwald, it is worth explaining the reasons why some allyl-metal complexes behave as electrophiles (as in section 1.2) or as nucleophiles.

As discussed in subsection 1.2.3, the allyl group has a fluxional behavior when coordinated to transition metals, such that it can coordinate in an η^3-form (π-allyl) or an η^1-form (σ-allyl). These two coordination modes often result in distinct reactivity. If the molecular orbitals of the π-allyl are analyzed, one can note that the Ψ_1 and Ψ_2 orbitals usually engage in ligand to metal σ–donation, with Ψ_1 involving in a covalent X-type bonding with metal d_σ-orbitals and Ψ_2 participating in a dative L-type bonding with the metal d_π-orbitals (**SCHEME 1.19A**). As in other metal-olefin complexes, this flow of electrons to the metal center leaves the allyl fragment with an electrophilic character. On the other hand, the π-electrons of the olefin group in the σ-allyl do not interact with the metal center, and therefore the classical nucleophilic character of the olefin is preserved (**SCHEME 1.19B**). The ability to favor predominantly a π-allyl or σ-allyl species depends on the availability of metal *d*-orbitals. If an additional empty *d*-orbital can accept the additional electron density

from the allyl π-electrons, the allyl group will exist predominantly in the η^3-form. However, if all the remaining *d*-orbitals are occupied by other ligands, it will exist predominantly in the η^1-form.

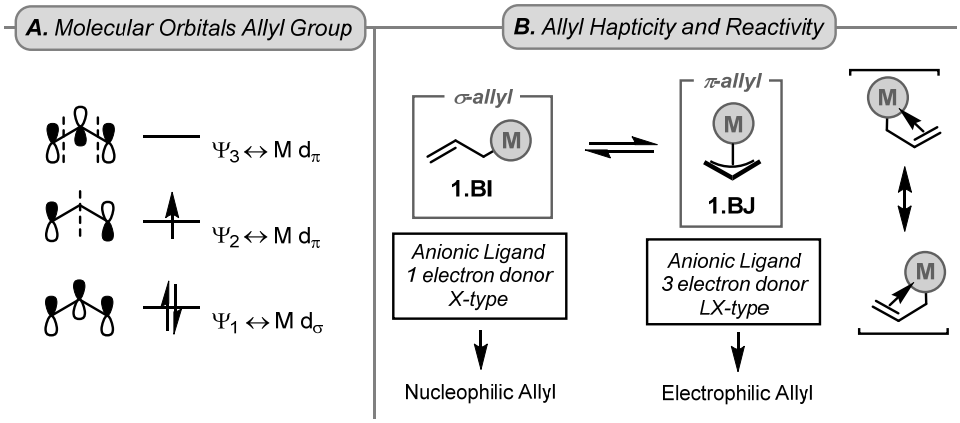

SCHEME 1.19. **(A)** Molecular orbitals of the allyl group; **(B)** Correlation between allyl hapticity and reactivity.

Apart from the above, σ-allyl species display improved nucleophilicity compared to simple olefins, which can be explained by increased hyperconjugation of the M–C σ-bond with the π-system of the C=C bond. In other words, if a Markovnikov addition of a given electrophile to the C=C bond is considered, the positive charge left on the β-carbon would be stabilized by hyperconjugation of the M–C σ-bond (β-effect). Therefore, these nucleophilic σ-allyl species also feature a more pronounced reactivity at the γ-position (**SCHEME 1.20**). This effect has been quantified by Mayr for a range of allyl silanes, allyl stannanes, allyl boronic esters, allyl trifluoroborates, allyl boronates, allyl germanes, and allyl iron reagents.[38]

[38] a) Mayr, H.; Bug, T.; Gotta, M. F.; Hering, N.; Irrgang, B.; Janker, B.; Kempf, B.; Loos, R.; Ofial, A. R.; Remennikov, G.; Schimmel, H. *J. Am. Chem. Soc.* **2001**, *123*, 9500-9512. b) Mayr, H.; Kempf, B.; Ofial, A. R. *Acc. Chem. Res.* **2003**, *36*, 66-77. c) Dulich, F.; Müller, K.-H.; Ofial, A. R.; Mayr, H. *Helv. Chim. Acta* **2005**, *88*, 1754-1768. d) Ammer, J.; Nolte, C.; Mayr, H. *J. Am. Chem. Soc.* **2012**, *134*, 13902-13911. e) García-Ruiz, C.; Chen, J. L. Y.; Sandford, C.; Feeney, K.; Lorenzo, P.; Berionni, G.; Mayr, H.; Aggarwal, V. K. *J. Am. Chem. Soc.* **2017**, *139*, 15324-15327.

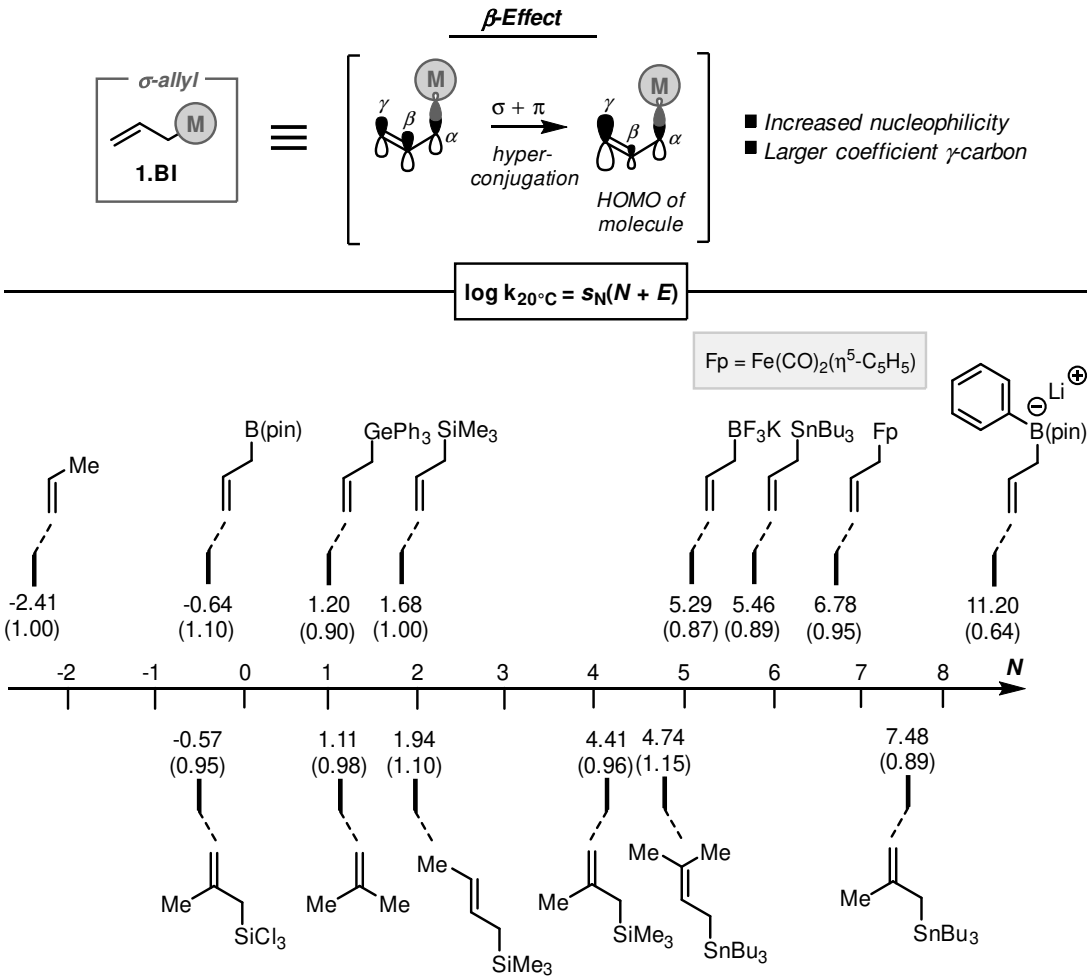

SCHEME 1.20. Comparison of nucleophilicity parameters N (susceptibility parameters s_N in parentheses) of allylmetal reagents.

1.3.2 Representative Examples

In analogy to the methods reported by the groups of Hartwig and You, the most widely applied method for the enantioselective allylation of carbonyl compounds came from the introduction of neutral cyclometalated iridium catalysts, which were exclusively developed by Krische.[39] These π-allyliridium (C,O)-benzoate catalysts contain a chiral diphosphine ligand with axial chirality, which belongs to the binaphthyl or biphenyl ligand families. These π-allyliridium (C,O)-benzoate complexes are chromatographically stable and are readily prepared through the combination of $[Ir(COD)Cl]_2$, allyl acetate, 4-substituted 3-nitrobenzoic acids, and a range of axially chiral chelating phosphine ligands. These catalysts can oxidize primary alcohols to aldehydes *in situ*, and therefore, these methods are often classified as redox-triggered C=O couplings via H_2 transfer. In terms of scope, a wide range of allylic surrogates are tolerated, such as allylic acetates, benzoates,

[39] Kim, S. W.; Zhang, W.; Krische, M. J. *Acc. Chem. Res.* **2017**, *50*, 2371-2380.

chlorides, carbonates, and vinyl epoxides, aziridines, and activated cyclopropanes (**SCHEME 1.21**). All these reported methods yield the desired homoallylic alcohols in high yields and excellent *anti*-diastereoselectivity, branch selectivity, and enantioselectivity. However, these methods are mostly limited to the use of the more reactive aldehydes as carbonyl compounds and require prolonged reaction times under heating. Mechanistic studies corroborate with a catalytic cycle wherein carbonyl addition represents the turnover-limiting event.[40] The initial steps leading to a nucleophilic allyl-Ir^{III} species include alcohol oxidation, deprotonation of the resulting Ir^{III}–H, and oxidative addition.

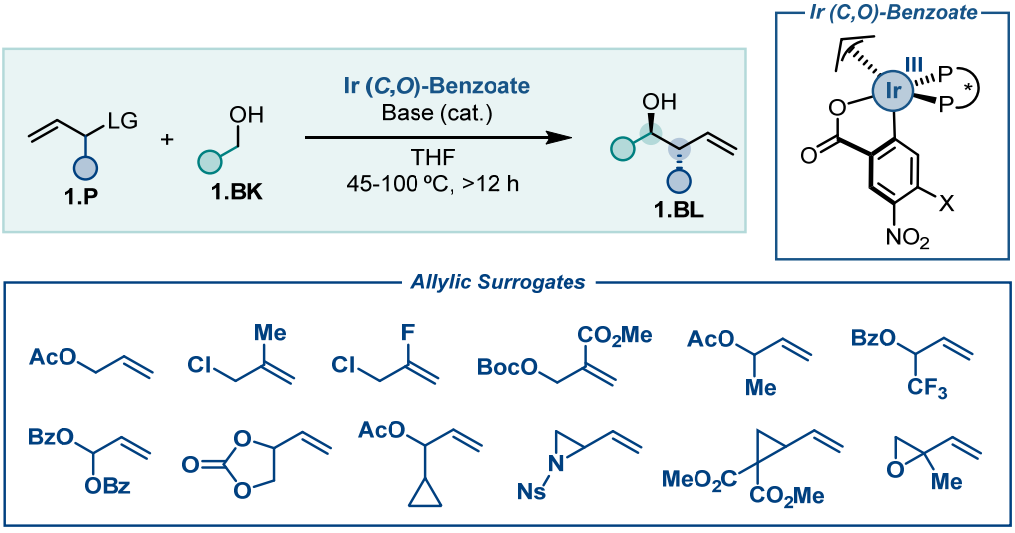

SCHEME 1.21. Enantioselective iridium-catalyzed allylation of aldehydes using cyclometalated Ir (*C,O*)-benzoate catalysts.

Other catalytic methods that generate nucleophilic allyl species start from 1,3-dienes or allenes by migratory insertion of a metal-hydride species. This has been exemplified by Krische using iridium and ruthenium complexes, but also by Buchwald and others using copper complexes (**SCHEME 1.22**).[41] Regarding the ruthenium-based catalysts, the combination of $H_2Ru(CO)(PPh_3)_3$ with a diphosphine ligand leads to a catalytically active Ru^{II}–H species which can insert into allenes and 1,3-dienes, and generate as such the necessary nucleophilic Ru^{II}-allyl species. Enantioselective variants have been achieved by using chiral diphosphines or chiral phosphoric acids. Alternatively, kinetically competent allyl-Ir^{III} species have been generated from the combination of $[Ir(COD)Cl]_2$ and (*R*)-PhanePhos as ligand. The resulting catalyst is also a cyclometalated iridium species, which can generate the active Ir^{III}–H species by oxidation of *i*-PrOH in the absence of a base. Conversely, the methods relating to copper complexes directly utilize a stoichiometric

[40] Kim, I. S.; Ngai, M.-Y.; Krische, M. J. *J. Am. Chem. Soc.* **2008**, *130*, 14891-14899.
[41] a) Liu, R. Y.; Buchwald, S. L. *Acc. Chem. Res.* **2020**, *53*, 1229-1243. b) Xiang, M.; Pfaffinger, D.; Krische, M. J. *Chem. Eur. J.* **2021**, *27*, DOI: 10.1002/chem.202101890.

silane reagent to generate the active copper(I)-hydride species. Combining the latter with a chiral diphosphine ligand provides a catalytic system that enables high asymmetric induction. Contrary to the iridium- and ruthenium-based methods by Krische, in the case of using 1,3-dienes as substrates, the migratory insertion of a Cu(I)–H species occurs at the less substituted C=C bond, and therefore produces predominantly the other regioisomeric product. Importantly, less electrophilic imines and ketones also react well with these *in situ* generated allyl-Cu(I) species. Therefore, these copper-hydride catalyzed transformations truly provide an orthogonal strategy to access allylated products which are so far unattainable through the Krische allylation.

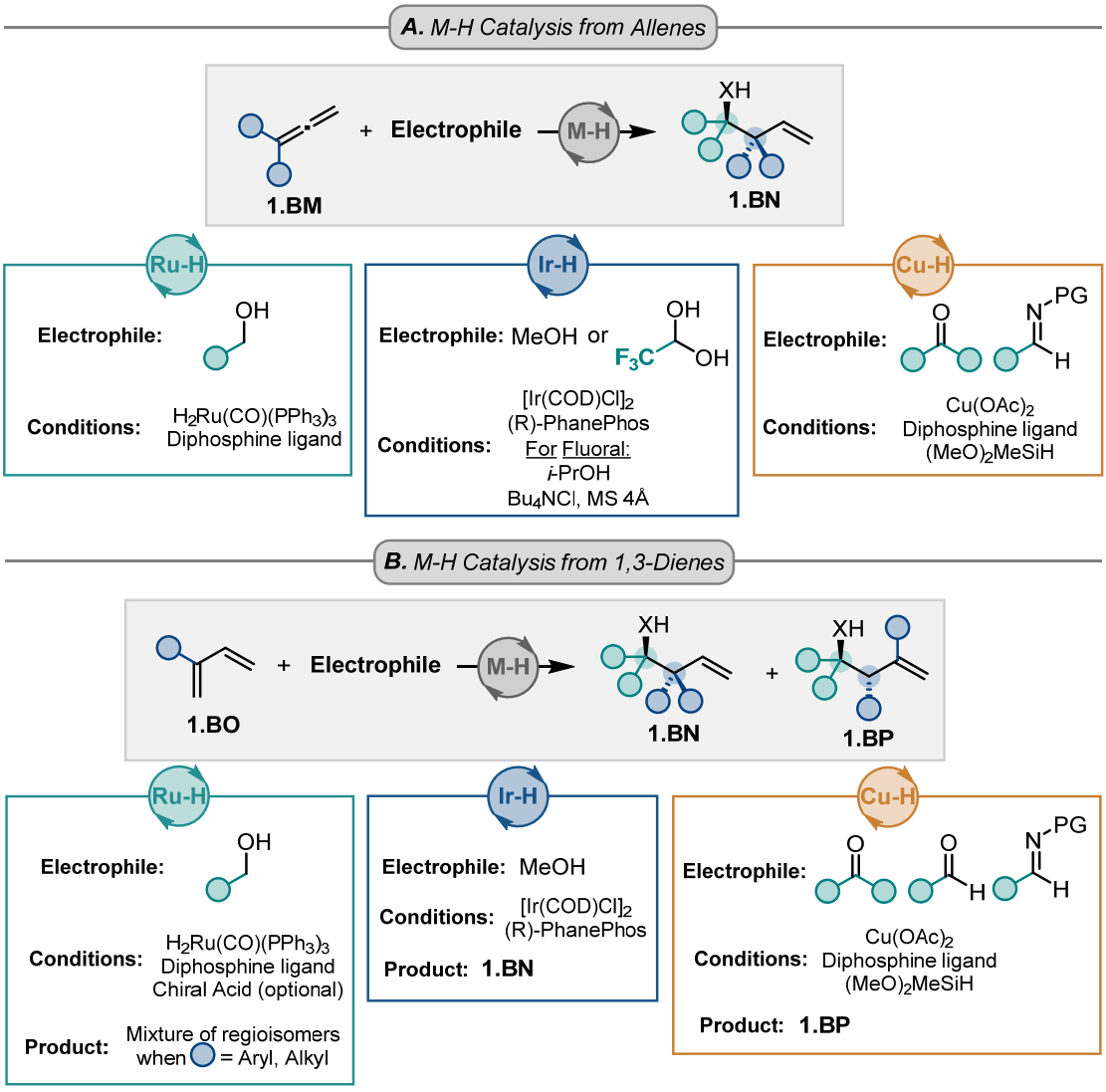

SCHEME 1.22. Catalytic allylation of carbonyl compounds using metal-hydride catalysis.

1.4 Vinyl Cyclic Carbonates

The synthesis of cyclic carbonates from CO_2 and epoxides has been a widely investigated topic in the last decade.[42] In some cases, cyclic carbonates are of importance to industry, such as ethylene carbonate (EC), propylene carbonate (PC), and glycerol carbonate (GC), as they have excellent properties as additives in lithium-ion batteries, or as polar aprotic solvents.[43] Despite being quite stable molecules, our research group has focused on exploring the reactivity of (functional) cyclic carbonates and has developed methods to transform them into more complex and useful molecular scaffolds.

In this regard, one of our main research areas has been the development of stereoselective methods that use vinyl cyclic carbonates (VCCs) as allylic surrogates in transition-metal catalyzed allylic substitutions reactions. Note that the term VCC (or VCCs) is used to refer to vinyl cyclic carbonates throughout the thesis as a more practical way to the IUPAC nomenclature (*i.e.*, 4-vinyl-1,3-dioxolan-2-one), but other authors have preferred to use other terms, such as vinyl ethylene carbonates (VECs) to refer to the same molecules (**FIGURE 1.1**).

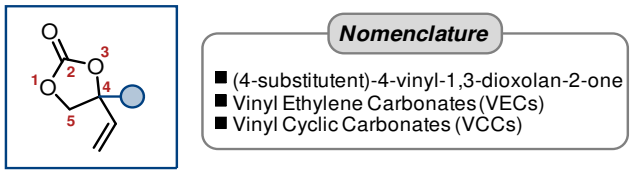

FIGURE 1.1. Nomenclature of vinyl cyclic carbonates.

1.4.1 Synthesis of Vinyl Cyclic Carbonates

Apart from the parent 4-vinyl-1,3-dioxolan-2-one, which can be purchased from common chemical suppliers, the synthesis of VCCs can be easily accomplished in 2-to-3 steps from α-hydroxyketones (**SCHEME 1.23**). Commercially available α-hydroxyketones include the ones having a Ph and a Me group, and the others can be prepared in one step from commercially available aldehydes and formaldehyde, or by alternative methods. With these latter starting materials in hand, the vinyl group (or other alkenyl groups) can be introduced through a Grignard reaction using 2 equivalents of vinylmagnesium bromide. The resulting 1,2-diol (after work-up) is conveniently converted to the cyclic carbonate using triphosgene and pyridine. This

[42] For selected reviews, see: a) Bobbink, F. D.; Gruszka, W.; Hulla, M.; Das, S.; Dyson, P. J. *Chem. Commun.* **2016**, *52*, 10787-10790. b) Della Monica, F.; Kleij, A. W. *Catal. Sci. Technol.* **2020**, *10*, 3483-3501. c) Aomchad, V.; Cristòfol, À.; Della Monica, F.; Limburg, B.; D'Elia, V.; Kleij, A. W. *Green Chem.* **2021**, *23*, 1077-1113.

[43] For selected examples, see: a) Scrosati, B.; Hassoun, J.; Sun, Y.-K. *Energy Environ. Sci.* **2011**, *4*, 3287–3295. b) Parker, H. L.; Sherwood, J.; Hunt, A. J.; Clark, J. H. *ACS Sustainable Chem. Eng.* **2014**, *2*, 1739-1742.

synthetic sequence allows to access a relatively large scope of VCCs having either alkyl or (hetero)aryl groups. Additionally, these molecules are in most cases bench-stable and easy to handle reagents.

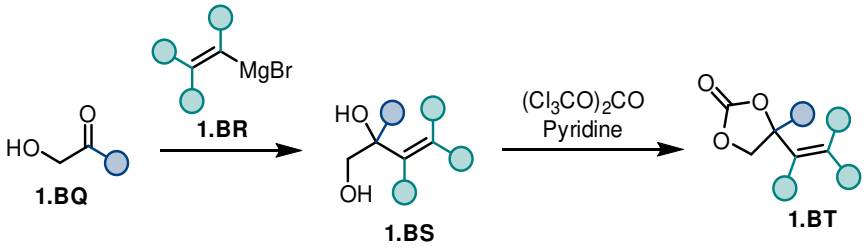

SCHEME 1.23. General sequence towards VCCs from α-hydroxyketones.

1.4.2 Reactivity of Vinyl Cyclic Carbonates

Since an early report by Trost in 1991, in which VCCs were employed as alternative reagents to the more commonly used vinyl epoxides,[44] these reagents have attracted increased attention from many research groups in recent years (**FIGURE 1.2**).[45] Over 123 research articles have been published using VCCs as allylating reagents, of which 84% were published between 2016 and 2021.[46] Among the possible reactivity modes, VCCs have been extensively used to generate zwitterionic intermediates (dipoles), which can be matched with a wide range of dipolarophiles to generate annulated products. The second most studied reactivity mode of VCCs has been as an electrophilic allyl source to generate allylic products when combined with suitable (pro)nucleophiles. The utilization of VCCs as nucleophilic allyl sources has only been studied on one occasion, while other publications reported other ring-opening reactions of VCCs with nucleophiles, among other miscellaneous reactivity.

[44] Trost, B. M.; Granja, J. R. *Tetrahedron Lett.* **1991**, *32*, 2193-2196.

[45] The area of VCCs has been reviewed on three occasions and includes the most relevant developments until mid-2019, see: a) Zhang, Y. J.; Khan, A. *Synlett* **2015**, *26*, 853-860. b) Guo, W.; Gómez, J. E.; Cristòfol, À.; Xie, J.; Kleij, A. W. *Angew. Chem. Int. Ed.* **2018**, *57*, 13735-13747. c) Zuo, L.; Liu, T.; Chang, X.; Guo, W. *Molecules* **2019**, *24*, 3930-3945.

[46] The collected papers refer to the period before the 31st of July 2021, as found in the SciFinder database.

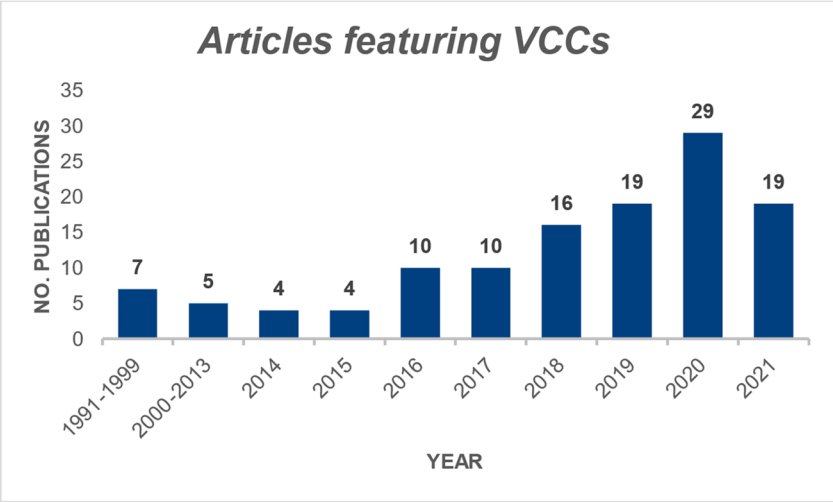

FIGURE 1.2. Number of research articles since 1991 using VCCs as allylating reagents.

o VCCs as Electrophilic Allyl Sources

The generation of electrophilic allyl species from VCCs has been a major focus since the early report by Trost,[44] and the initial development by Kang (**SCHEME 1.24**).[47] Apart from those early reports, an asymmetric version using 1,2-divinylethylene carbonate has been reported by Trost in 2006, in which their well-established Trost ligands allowed the selective formation of a branch allylic product with high enantioselectivity.[48] In line with Trost's research, most of the breakthrough results in this area originate from using palladium catalysts, although ruthenium, rhodium, nickel, copper, and iridium-based systems have also been reported.[49]

[47] a) Kang, S.-K.; Kim, S.-G.; Lee, J.-S. *Tetrahedron: Asymmetry* **1992**, *3*, 1139-1140. b) Kang, S.-K.; Park, D.-C.; Rho, H.-S.; Yu, C.-M.; Hong, J.-H. *Synth. Commun.* **1995**, *25*, 203-214. c) Kang, S.-K.; Kim, D.-Y.; Hong, R.-K.; Ho, P.-S. *Synth. Commun.* **1996**, *26*, 3225-3235. d) Kang, S.-K.; Kim, D.-Y.; Rho, H.-S.; Yoon, S.-H.; Ho, P.-S. *Synth. Commun.* **1996**, *26*, 1485-1492.

[48] Trost, B. M.; Aponick, A. *J. Am. Chem. Soc.* **2006**, *128*, 3931-3933.

[49] a) Mizojiri, R.; Kobayashi, Y. *J. Chem. Soc., Perkin Trans. 1* **1995**, 2073-2075. b) Lee, J. H.; Lee, S.-g. *Chem. Sci.* **2013**, *4*, 2922-2927. c) Bayer, A.; Kazmaier, U. *J. Org. Chem.* **2014**, *79*, 8498-8504. d) Li, C.; Breit, B. *Chem. Eur. J.* **2016**, *22*, 14655-14663. e) Miralles, N.; Gómez, J. E.; Kleij, A. W.; Fernández, E. *Org. Lett.* **2017**, *19*, 6096-6099. f) Huang, W.-Y.; Lu, C.-H.; Ghorai, S.; Li, B.; Li, C. *J. Am. Chem. Soc.* **2020**, *142*, 15276-15281. g) Huang, Y.; Ma, C.; Liu, S.; Yang, L.-C.; Lan, Y.; Zhao, Y. *Chem* **2021**, *7*, 812-826. h) Lin, Z.; Jin, Y.; Hu, W.; Wang, C. *Chem. Sci.* **2021**, *12*, 6712-6718.

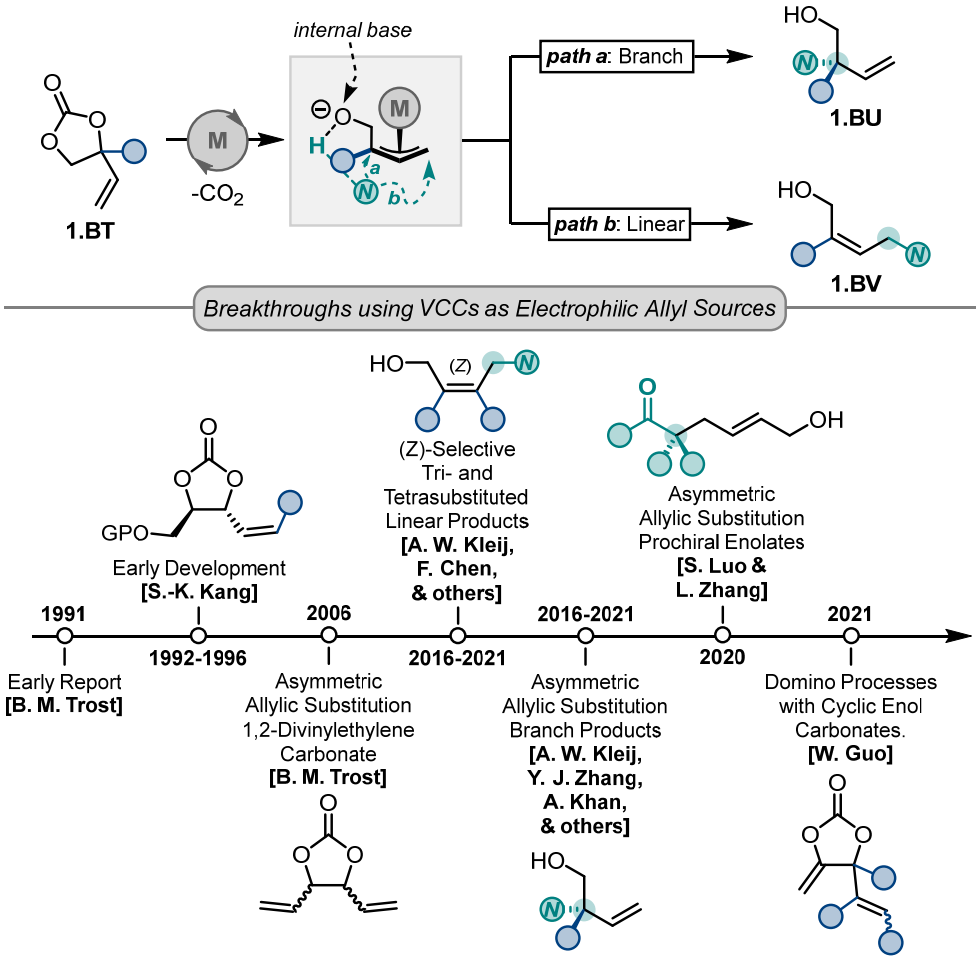

SCHEME 1.24. Generation of electrophilic allyl species using VCCs as precursors, and selected milestones.

This decarboxylative strategy relies on using the pendent alkoxide (produced *in situ*) as an internal base to deprotonate the pronucleophile such that the addition of an exogenous base is not required. The control over the regioselectivity to obtain linear or branch products has been studied in detail by our group. The chiral branch product featuring elusive acyclic quaternary carbon stereocenters can be achieved by a palladium catalyst containing a phosphoramidite ligand,[50] or a Trost ligand when using alkyl-substituted VCCs.[51] Mechanistic studies on this Pd(phosphoramidite)-catalyzed process point towards a favorable inner-sphere nucleophilic attack through η^2-aryl coordination of the aromatic group of the aniline pronucleophile to the Pd center.[52] On the other hand, linear products containing stereodefined tri- and tetrasubstituted olefins are obtained with excellent (*Z*)-selectivity using a palladium catalyst containing the DPEPhos ligand (or similar

[50] a) Cai, A.; Guo, W.; Martínez-Rodríguez, L.; Kleij, A. W. *J. Am. Chem. Soc.* **2016**, *138*, 14194-14197. b) Khan, A.; Khan, S.; Khan, I.; Zhao, C.; Mao, Y.; Chen, Y.; Zhang, Y. J. *J. Am. Chem. Soc.* **2017**, *139*, 10733-10741. c) Xie, J.; Guo, W.; Cai, A.; Escudero-Adán, E. C.; Kleij, A. W. *Org. Lett.* **2017**, *19*, 6388-6391. d) Khan, S.; Li, H.; Zhao, C.; Wu, X.; Zhang, Y. J. *Org. Lett.* **2019**, *21*, 9457-9462.
[51] Khan, A.; Zhao, H.; Zhang, M.; Khan, S.; Zhao, D. *Angew. Chem. Int. Ed.* **2019**, *59*, 1340-1345.
[52] Hu, L.; Cai, A.; Wu, Z.; Kleij, A. W.; Huang, G. *Angew. Chem. Int. Ed.* **2019**, *58*, 14694-14702.

diphosphine ligands).[50c,53] Mechanistic studies by DFT revealed a kinetically faster decarboxylation from the *anti*-allylPd^{II} diastereomer, resulting in a relatively stable palladacyclic intermediate.[53c] Subsequent nucleophilic attack has been calculated to proceed with a lower energy barrier than π-σ-π isomerization (*syn-anti* isomerization). In addition, Luo and Zhang have disclosed in 2020 an elegant approach to combine allyl groups derived from VCCs with prochiral enolates in an enantioselective manner with the mediation of a chiral primary amine.[54] Finally, Guo and coworkers have recently expanded the scope of VCCs and products by developing two domino processes using cyclic enol carbonates to obtain pyrroles and furans.[55]

o VCCs as Nucleophilic Allyl Sources

Contrary to the more widely investigated use of VCCs as electrophilic allyl sources, the generation of nucleophilic allyl species from VCCs has only been reported on one occasion by Krische.[56] Using their well-established cyclometalated iridium complexes, a range of *anti*-1,3-diols can be synthesized in good yields, good diastereoselectivity, and excellent enantioselectivity (**SCHEME 1.25**). However, the scope of VCCs used in this case was limited to the simplest 4-vinyl-1,3-dioxolan-2-one.

[53] a) Mao, Y.; Zhai, X.; Khan, A.; Cheng, J.; Wu, X.; Zhang, Y. J. *Tetrahedron Lett.* **2016**, *57*, 3268-3271. b) Guo, W.; Martínez-Rodríguez, L.; Martin, E.; Escudero-Adán, E. C.; Kleij, A. W. *Angew. Chem. Int. Ed.* **2016**, *55*, 11037-11040. c) Guo, W.; Martínez-Rodríguez, L.; Kuniyil, R.; Martin, E.; Escudero-Adán, E. C.; Maseras, F.; Kleij, A. W. *J. Am. Chem. Soc.* **2016**, *138*, 11970-11978. d) Gómez, J. E.; Guo, W.; Kleij, A. W. *Org. Lett.* **2016**, *18*, 6042-6045. e) Cristòfol, À.; Escudero-Adán, E. C.; Kleij, A. W. *J. Org. Chem.* **2018**, *83*, 9978-9990. f) Deng, L.; Kleij, A. W.; Yang, W. *Chem. Eur. J.* **2018**, *24*, 19156-19161. g) Shi, L.; He, Y.; Gong, J.; Yang, Z. *Asian J. Org. Chem.* **2019**, *8*, 823-827. h) Ke, M.; Huang, G.; Ding, L.; Fang, J.; Chen, F. *ChemCatChem* **2019**, *11*, 4720-4724. i) Ke, M.; Liu, Z.; Huang, G.; Wang, J.; Tao, Y.; Chen, F. *Org. Lett.* **2020**, *22*, 4135-4140. j) Khan, A.; Zhang, J.; Khan, S. *Green Chem.* **2020**, *22*, 4116-4120. k) Zhang, M.-N.; Khan, S.; Zhang, J.; Khan, A. *RSC Adv.* **2020**, *10*, 31022-31026. l) Liu, Z.; Ke, M.; Zhang, K.; Wang, Z.; Ye, B.; Chen, F. *ChemCatChem* **2021**, *13*, 1753-1762.

[54] Wang, Y.; Chai, J.; You, C.; Zhang, J.; Mi, X.; Zhang, L.; Luo, S. *J. Am. Chem. Soc.* **2020**, *142*, 3184-3195.

[55] a) Yang, Y.; Zuo, L.; Wei, K.; Guo, W. *Org. Lett.* **2021**, *23*, 3195-3200. b) Zuo, L.; Yang, Y.; Guo, W. *Org. Lett.* **2021**, *23*, 2013-2018.

[56] Zhang, Y. J.; Yang, J. H.; Kim, S. H.; Krische, M. J. *J. Am. Chem. Soc.* **2010**, *132*, 4562-4563.

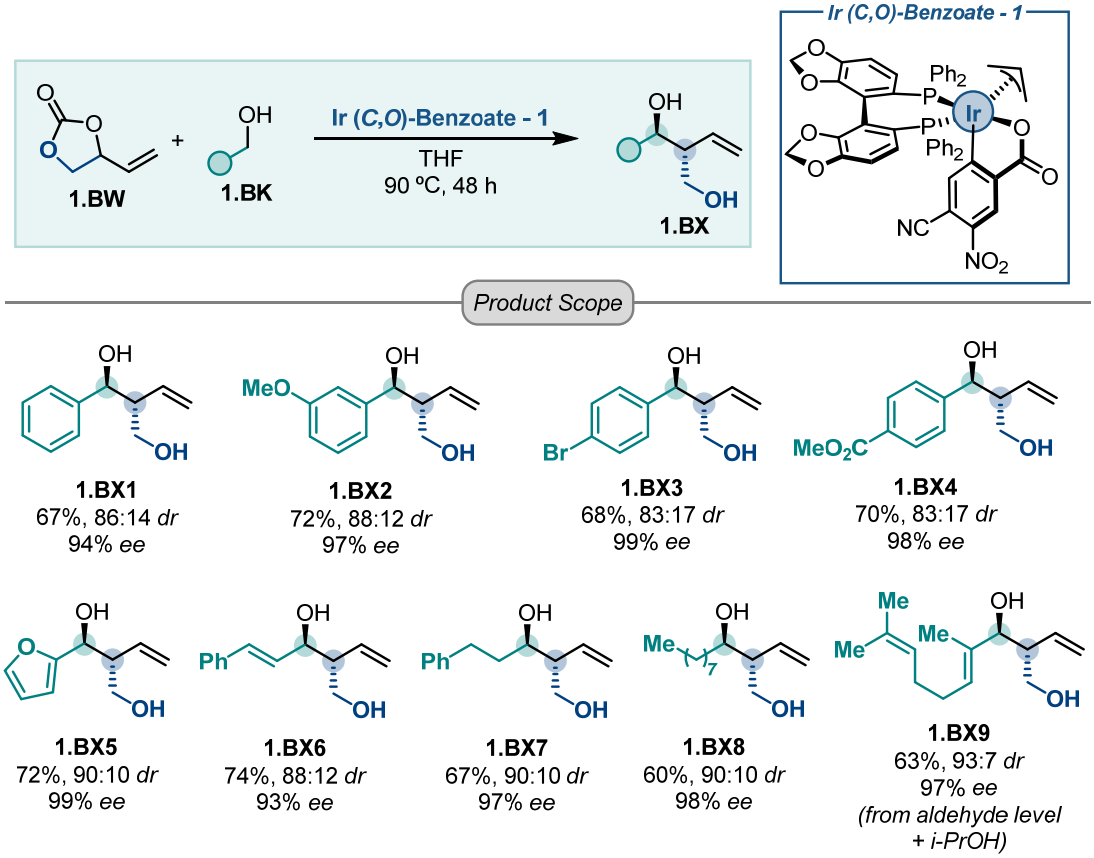

SCHEME 1.25. Generation of nucleophilic allyl species from VCCs reported by Krische.

o Cycloaddition reactions using VCCs as dipoles

Beyond utilizing VCCs as purely electrophilic or nucleophilic allyl sources, Zhang and coworkers introduced in 2014 an enantioselective formal [3+2] cycloaddition reaction using VCCs as dipoles and formaldehyde as dipolarophile (**SCHEME 1.26**).[57] This different reactivity mode makes use of the zwitterionic nature of the metal-allyl species produced *in situ*, in which the pendent alkoxide group is used as a nucleophilic (rather than a basic) site reacting with the dipolarophile, and the resulting cationic π-allyl fragment is subsequently intercepted by the *in situ* generated nucleophile in an asynchronous manner. Another milestone came from introducing prochiral dipolarophiles to forge two or three carbon stereocenters enantioselectively. In this respect, Zhang subsequently reported a formal [3+2] cycloaddition reaction using prochiral imines as dipolarophiles to forge two carbon stereocenters,[58] and this report was followed by other similar transformations.[59] These precedents encouraged other research groups to study related [3+2] cycloaddition

[57] Khan, A.; Zheng, R.; Kan, Y.; Ye, J.; Xing, J.; Zhang, Y. J. *Angew. Chem. Int. Ed.* **2014**, *53*, 6439-6442.
[58] Yang, L.; Khan, A.; Zheng, R.; Jin, L. Y.; Zhang, Y. J. *Org. Lett.* **2015**, *17*, 6230-6233.
[59] a) Khan, A.; Xing, J.; Zhao, J.; Kan, Y.; Zhang, W.; Zhang, Y. J. *Chem. Eur. J.* **2015**, *21*, 120-124. b) Khan, I.; Zhao, C.; Zhang, Y. J. *Chem. Commun.* **2018**, *54*, 4708-4711. c) Liu, K.; Khan, I.; Cheng, J.; Hsueh, Y. J.; Zhang, Y. J. *ACS Catal.* **2018**, *8*, 11600-11604. d) Zhao, C.; Khan, I.; Zhang, Y. J. *Chem. Commun.* **2020**, *56*, 12431-12434. e) Zhao, C.; Shah, B. H.; Li, H.; Wu, X.; Zhang, Y. J. *Asian J. Org. Chem.* **2021**, *10*, 545-548.

reactions with other dipolarophiles.[60] One noteworthy example of a [3+2] cycloaddition process was reported by Glorius, who achieved the diastereodivergent synthesis of enantioenriched α,β-disubstituted γ-butyrolactones with access to all four stereodyads.[61]

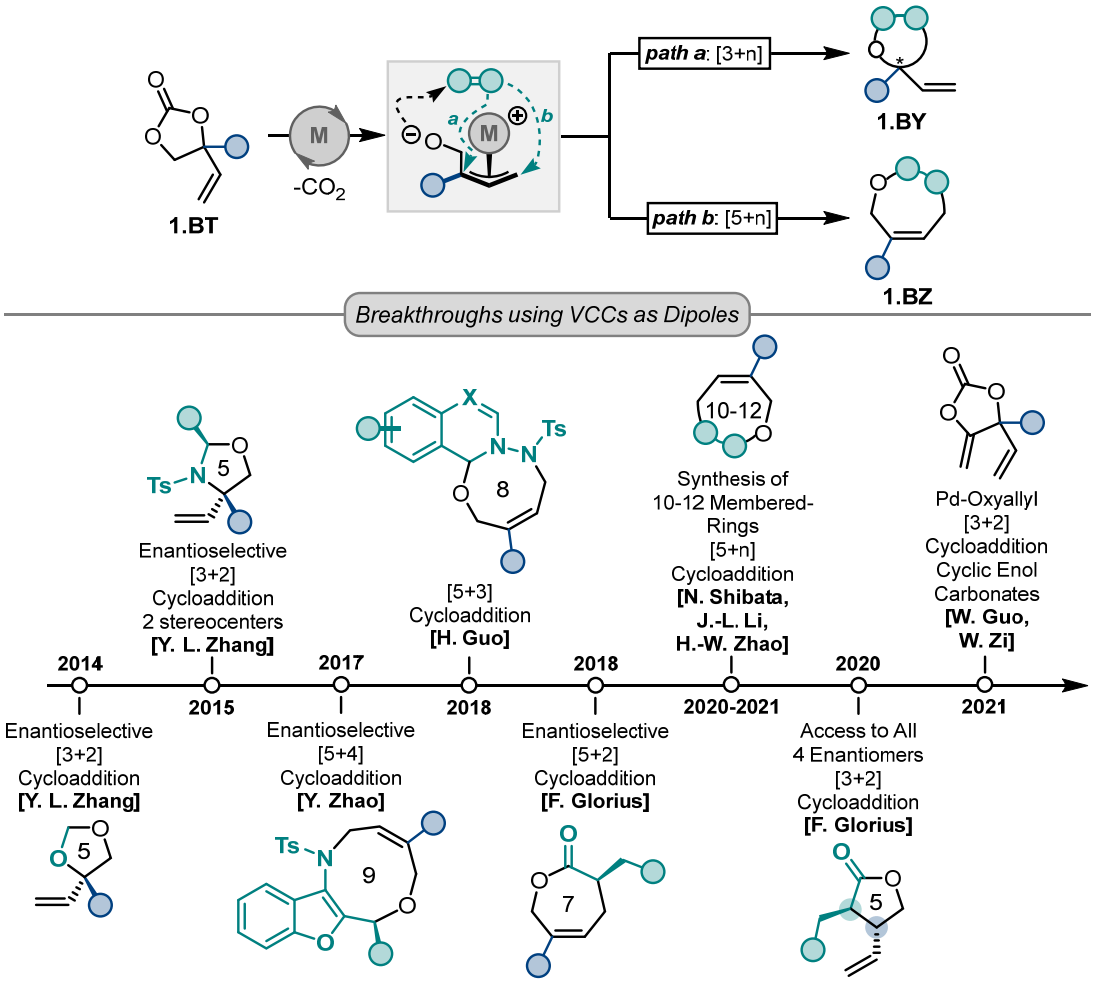

SCHEME 1.26. Formal cycloaddition reactions using VCCs as dipoles, and selected milestones.

[60] a) Yang, Y.; Yang, W. *Chem. Commun.* **2018**, *54*, 12182-12185. b) Gao, X.; Xia, M.; Yuan, C.; Zhou, L.; Sun, W.; Li, C.; Wu, B.; Zhu, D.; Zhang, C.; Zheng, B.; Wang, D.; Guo, H. *ACS Catal.* **2019**, *9*, 1645-1654. c) Liu, Q.; Liu, T.-X.; Ru, Y.; Zhu, X.; Zhang, G. *Chem. Commun.* **2019**, *55*, 14498-14501. d) Liu, Y.; Huang, Q.-W.; Li, Q.-Z.; Leng, H.-J.; Dai, Q.-S.; Zeng, R.; Liu, Y.-Q.; Zhang, X.; Han, B.; Li, J.-L. *Org. Lett.* **2019**, *21*, 7478-7483. e) Xia, Y.; Bao, Q.-F.; Li, Y.; Wang, L.-J.; Zhang, B.-S.; Liu, H.-C.; Liang, Y.-M. *Chem. Commun.* **2019**, *55*, 4675-4678. f) Park, J. U.; Ahn, H. I.; Cho, H. J.; Xuan, Z.; Kim, J. H. *Adv. Synth. Catal.* **2020**, *362*, 1836-1840. g) Taily, I. M.; Saha, D.; Banerjee, P. *Org. Biomol. Chem.* **2020**, *18*, 6564-6570. h) Wang, J.; Zhao, L.; Rong, Q.; Lv, C.; Lu, Y.; Pan, X.; Zhao, L.; Hu, L. *Org. Lett.* **2020**, *22*, 5833-5838. i) Xiong, W.; Zhang, S.; Li, H.; Zhang, Z.; Xu, T. *J. Org. Chem.* **2020**, *85*, 8773-8779. j) Zhang, H.; Gao, X.; Jiang, F.; Shi, W.; Wang, W.; Wu, Y.; Zhang, C.; Shi, X.; Guo, H. *Eur. J. Org. Chem.* **2020**, 4801-4804. k) Gao, X.; Zhu, D.; Jiang, F.; Liao, J.; Wang, W.; Wu, Y.; Zheng, L.; Guo, H. *Org. Biomol. Chem.* **2021**, *19*, 4877-4881. l) Lv, H.-P.; Yang, X.-P.; Wang, B.-L.; Yang, H.-D.; Wang, X.-W.; Wang, Z. *Org. Lett.* **2021**, *23*, 4715-4720. m) Ming, S.; Qurban, S.; Du, Y.; Su, W. *Chem. Eur. J.* **2021**, *27*, DOI: 10.1002/chem.202102024.

[61] Singha, S.; Serrano, E.; Mondal, S.; Daniliuc, C. G.; Glorius, F. *Nat. Catal.* **2020**, *3*, 48-54.

Beyond [3+2] cycloadditions, the synthesis of larger rings with dipolarophiles having extended π-systems has become a major topic of interest. In 2017, Zhao and coworkers achieved the synthesis of 9-membered rings using *N*-tosyl azadienes as dipolarophiles,[62] which served as an inspiring example for other research groups to achieve the synthesis of other heterocycles featuring 8-, 9-, 10-, 11-, and 12-membered rings.[63] Apart from these larger membered rings, Glorius and coworkers reported a highly enantioselective approach to 7-membered lactones using α,β-unsaturated aldehydes as dipolarophiles and a chiral NHC catalyst,[64]whereas access to other 7-membered rings by formal [5+2] cycloadditions were reported by other research groups.[65] Finally, the groups of Guo and Zi independently published methods involving the cycloaddition of palladium-oxyallyl species generated from newly introduced cyclic enol carbonates, thus opening new avenues for other dipoles that can be generated from VCCs.[66]

[62] a) Yang, L.-C.; Rong, Z.-Q.; Wang, Y.-N.; Tan, Z. Y.; Wang, M.; Zhao, Y. *Angew. Chem. Int. Ed.* **2017**, *56*, 2927-2931. b) Rong, Z.-Q.; Yang, L.-C.; Liu, S.; Yu, Z.; Wang, Y.-N.; Tan, Z. Y.; Huang, R.-Z.; Lan, Y.; Zhao, Y. *J. Am. Chem. Soc.* **2017**, *139*, 15304-15307.

[63] a) Das, P.; Gondo, S.; Nagender, P.; Uno, H.; Tokunaga, E.; Shibata, N. *Chem. Sci.* **2018**, *9*, 3276-3281. b) Yuan, C.; Wu, Y.; Wang, D.; Zhang, Z.; Wang, C.; Zhou, L.; Zhang, C.; Song, B.; Guo, H. *Adv. Synth. Catal.* **2018**, *360*, 652-658. c) Niu, B.; Wu, X.-Y.; Wei, Y.; Shi, M. *Org. Lett.* **2019**, *21*, 4859-4863. d) Zhao, H. W.; Wang, L. R.; Guo, J. M.; Ding, W. Q.; Song, X. Q.; Wu, H. H.; Tang, Z.; Fan, X. Z.; Bi, X. F. *Adv. Synth. Catal.* **2019**, *361*, 4761-4771. e) An, X. T.; Du, J. Y.; Jia, Z. L.; Zhang, Q.; Yu, K. Y.; Zhang, Y. Z.; Zhao, X. H.; Fang, R.; Fan, C. A. *Chem. Eur. J.* **2020**, *26*, 3803-3809. f) Dai, Q.-S.; Tao, Y.-M.; Zhang, X.; Leng, H.-J.; Huang, H.; Xiang, P.; Li, Q.-Z.; Wang, Q.-W.; Li, J.-L. *Chem. Commun.* **2020**, *56*, 12439-12442. g) Uno, H.; Kawai, K.; Shiro, M.; Shibata, N. *ACS Catal.* **2020**, *10*, 14117-14126. h) Uno, H.; Punna, N.; Tokunaga, E.; Shiro, M.; Shibata, N. *Angew. Chem. Int. Ed.* **2020**, *59*, 8187-8194. i) Xia, C.; Wang, D.-C.; Qu, G.-R.; Guo, H.-M. *Org. Chem. Front.* **2020**, *7*, 1474-1480. j) Zhang, X.; Li, X.; Li, J.-L.; Wang, Q.-W.; Zou, W.-L.; Liu, Y.-Q.; Jia, Z.-Q.; Peng, F.; Han, B. *Chem. Sci.* **2020**, *11*, 2888-2894. k) Wu, H.-H.; Fan, X.-Z.; Tang, Z.; Zhang, H.; Cai, L.-Y.; Bi, X.-F.; Zhao, H.-W. *Org. Lett.* **2021**, *23*, 2802-2806. l) Yang, G.; Ke, Y. M.; Zhao, Y. *Angew. Chem. Int. Ed.* **2021**, *60*, 12775-12780.

[64] Singha, S.; Patra, T.; Daniliuc, C. G.; Glorius, F. *J. Am. Chem. Soc.* **2018**, *140*, 3551-3554.

[65] a) Zhao, H.-W.; Du, J.; Guo, J.-M.; Feng, N.-N.; Wang, L.-R.; Ding, W.-Q.; Song, X.-Q. *Chem. Commun.* **2018**, *54*, 9178-9181. b) Wei, Y.; Liu, S.; Li, M.-M.; Li, Y.; Lan, Y.; Lu, L.-Q.; Xiao, W.-J. *J. Am. Chem. Soc.* **2019**, *141*, 133-137. c) Ahn, H.-I.; Park, J.-U.; Xuan, Z.; Kim, J. H. *Org. Biomol. Chem.* **2020**, *18*, 9826-9830. d) Gao, X.; Zhu, D.; Chen, Y.; Deng, H.; Jiang, F.; Wang, W.; Wu, Y.; Guo, H. *Org. Lett.* **2020**, *22*, 7158-7163.

[66] a) Yan, B.; Zuo, L.; Chang, X.; Liu, T.; Cui, M.; Liu, Y.; Sun, H.; Chen, W.; Guo, W. *Org. Lett.* **2021**, *23*, 351-357. b) Zheng, Y.; Qin, T.; Zi, W. *J. Am. Chem. Soc.* **2021**, *143*, 1038-1045. c) Liu, T.; Fang, Y.; Zuo, L.; Yang, Y.; Liu, Y.; Chen, W.; Dang, L.; Guo, W. *Org. Chem. Front.* **2021**, *8*, 1902-1909.

o VCCs in C–H Activation Reactions

Beyond the ubiquitous nature of metal-allyl species in synthetic chemistry, allyl intermediates produced from VCCs can also be transferred through migratory insertion of an organometallic species to an alkene group, followed by β-*O*-elimination/decarboxylation. This strategy has been frequently employed in C–H activation reactions, where the metal catalyst is unable to activate the VCC through an oxidative addition pathway. Predominantly, these methods have used nitrogen-containing directing groups in combination with noble metals, such as Rh or Ru, to activate aromatic or olefinic C–H bonds (**SCHEME 1.27**, **1.CB1**-**1.CB4**),[67] although an example of a weak directing group (carbamate) was reported by Kim (**SCHEME 1.27**, **1.CB5**).[68] The groups of Ackermann, Glorius, and Yu expanded these methods using strong directing groups that combine well with 3d transition metals, such as Co and Mn (**SCHEME 1.27**, **1.CB6**-**1.CB9**).[69] An interesting application of C–H allylation using VCCs was reported by Shi and coworkers, in which an atroposelective C–H allylation protocol was developed to generate a wide scope of axially chiral biaryl compounds (**SCHEME 1.27**, **1.CB10**).[70] Nonetheless, the scope of VCCs was mostly limited to the simplest 4-vinyl-1,3-dioxolan-2-one until the group of Yang developed a solvent-less protocol using a diversity of aryl-substituted VCCs (**SCHEME 1.27**, **1.CB11**).[71] Importantly, the (*Z*)-selectivity remained excellent across the scope of products, which enabled the preparation of several macrolides of importance to the development of P-glycoprotein inhibitors.

[67] a) Zhang, S.-S.; Wu, J.-Q.; Lao, Y.-X.; Liu, X.-G.; Liu, Y.; Lv, W.-X.; Tan, D.-H.; Zeng, Y.-F.; Wang, H. *Org. Lett.* **2014**, *16*, 6412-6415. b) Zhang, S.-S.; Wu, J.-Q.; Liu, X.; Wang, H. *ACS Catal.* **2015**, *5*, 210-214. c) Jo, H.; Han, S.; Park, J.; Choi, M.; Han, S. H.; Jeong, T.; Lee, S.-Y.; Kwak, J. H.; Jung, Y. H.; Kim, I. S. *Tetrahedron* **2016**, *72*, 571-578. d) Liu, S.; Jiang, H.; Liu, W.; Zhu, X.; Hao, X.-Q.; Song, M.-P. *J. Org. Chem.* **2020**, *85*, 15167-15182.

[68] Sharma, S.; Han, S. H.; Oh, Y.; Mishra, N. K.; Han, S.; Kwak, J. H.; Lee, S.-Y.; Jung, Y. H.; Kim, I. S. *J. Org. Chem.* **2016**, *81*, 2243-2251.

[69] a) Jiang, X.; Chen, J.; Zhu, W.; Cheng, K.; Liu, Y.; Su, W.-K.; Yu, C. *J. Org. Chem.* **2017**, *82*, 10665-10672. b) Lu, Q.; Klauck, F. J. R.; Glorius, F. *Chem. Sci.* **2017**, *8*, 3379-3383. c) Wang, H.; Lorion, M. M.; Ackermann, L. *Angew. Chem. Int. Ed.* **2017**, *56*, 6339-6342. d) Wang, H.; Lorion, M. M.; Ackermann, L. *ACS Catal.* **2017**, *7*, 3430-3433.

[70] Liao, G.; Li, B.; Chen, H. M.; Yao, Q. J.; Xia, Y. N.; Luo, J.; Shi, B. F. *Angew. Chem. Int. Ed.* **2018**, *57*, 17151-17155.

[71] Chen, L.; Quan, H.; Xu, Z.; Wang, H.; Xia, Y.; Lou, L.; Yang, W. *Nat. Commun.* **2020**, *11*, 2151-2158.

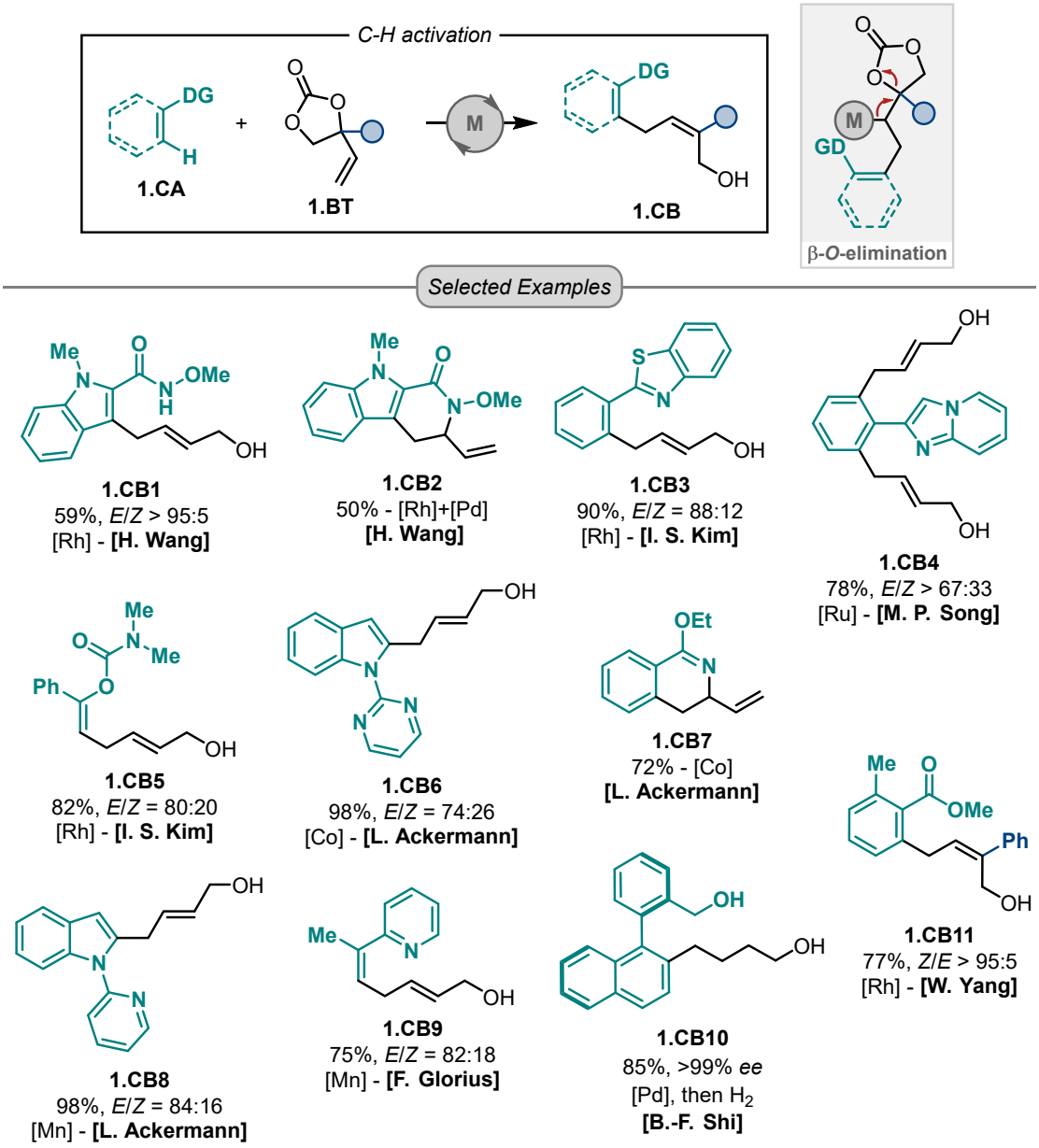

SCHEME 1.27. C–H activation reactions using VCCs as allylating reagents.

o Ring-opening Reactions of VCCs with Nucleophiles

Apart from the transition metal-catalyzed methods discussed above, VCCs can also react with nucleophiles at higher temperatures or with the help of a basic additive. Although ring-opening reactions have been mainly studied with cyclic carbonates not incorporating a vinyl group, some reported methods feature 1-to-3 VCCs in their product scope. An interesting feature is the site-selectivity of the nucleophilic attack. It has been observed that aliphatic and aromatic amines (in the presence of a catalyst)[72] prefer to react at the carbonyl carbon (path a, **SCHEME 1.28**), while cyanide[73] and phthalimide[74] react preferentially at the methylene carbon (path b, **SCHEME 1.28**).

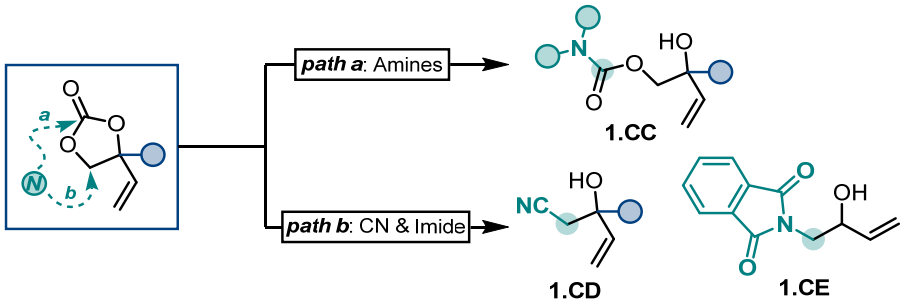

SCHEME 1.28. Ring-opening of VCCs with nucleophiles.

o Miscellaneous Examples

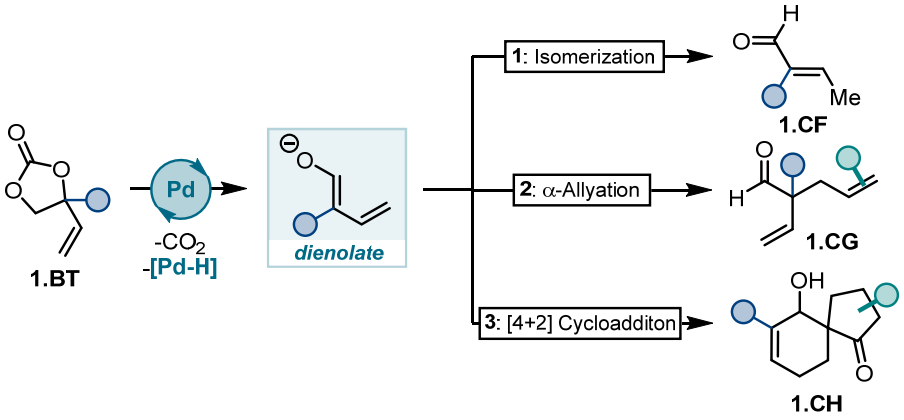

SCHEME 1.29. Generation of dienolate intermediates from VCCs, and their applications.

[72] a) Guo, W.; Gónzalez-Fabra, J.; Bandeira, N. A. G.; Bo, C.; Kleij, A. W. *Angew. Chem. Int. Ed.* **2015**, *54*, 11686-11690. b) Sopeña, S.; Laserna, V.; Guo, W.; Martin, E.; Escudero-Adán, E. C.; Kleij, A. W. *Adv. Synth. Catal.* **2016**, *358*, 2172-2178. c) Olsén, P.; Oschmann, M.; Johnston, E. V.; Åkermark, B. *Green Chem.* **2018**, *20*, 469-475.
[73] Ni, J.; Cristòfol, À.; Kleij, A. W. *Org. Chem. Front.* **2021**, *8*, 4520-4526.
[74] Wuts, P. G. M. *J. Iran. Chem. Soc.* **2008**, *5*, 306-308.

Another interesting phenomenon occurs when VCCs and a low-valent palladium catalyst are combined. A dienolate intermediate can be slowly formed from a zwitterionic allyl-Pd^{II} species through a β-*H*-elimination process (**SCHEME 1.29**).[75] From this dienolate intermediate, three distinct reaction pathways have been reported: (**1**) isomerization to α,β-unsaturated aldehydes **1.CF**, a process driven by thermodynamics; (**2**) α-allylation with another molecule of an allyl-Pd^{II} intermediate, and (**3**) [4+2] cycloaddition using a suitable dipolarophile.

The last application of VCCs discussed here is the synthesis of highly substituted cyclopentenones that was reported by the group of Yamada, who developed a stereospecific Nazarov cyclization starting from cyclic enol carbonates **1.CI** (**SCHEME 1.30**).[76] Importantly, chirality present in the VCC substrate could also be transferred to the final cyclopentenone product. These reactions require the addition of a Lewis acid catalyst or heating.

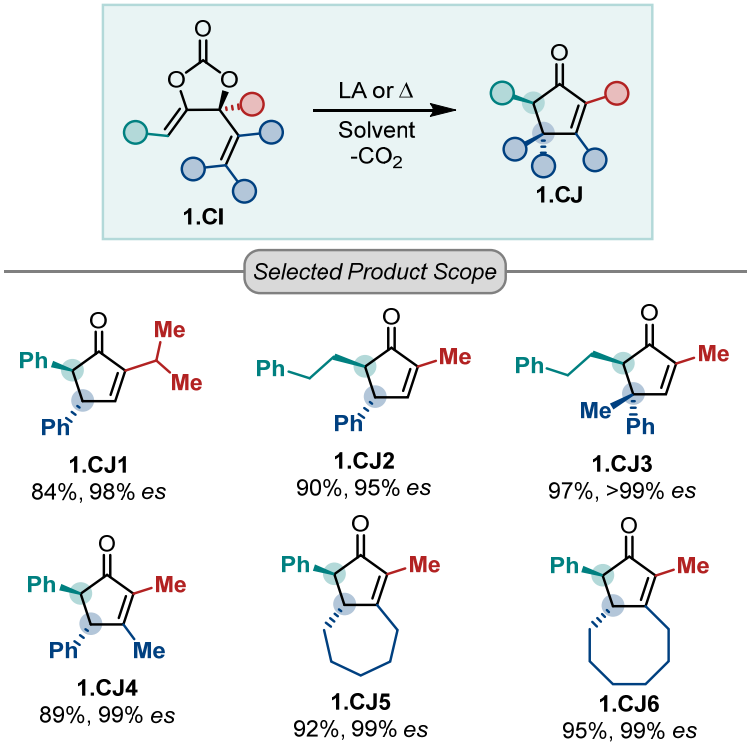

SCHEME 1.30. Stereospecific Nazarov cyclization from cyclic enol carbonates.

[75] a) Guo, W.; Kuniyil, R.; Gómez, J. E.; Maseras, F.; Kleij, A. W. *J. Am. Chem. Soc.* **2018**, *140*, 3981-3987. b) Wang, H.; Qiu, S.; Wang, S.; Zhai, H. *ACS Catal.* **2018**, *8*, 11960-11965. c) Yang, L.-C.; Tan, Z. Y.; Rong, Z.-Q.; Liu, R.; Wang, Y.-N.; Zhao, Y. *Angew. Chem. Int. Ed.* **2018**, *57*, 7860-7864. d) Xue, S.; Lücht, A.; Benet-Buchholz, J.; Kleij, A. W. *Chem. Eur. J.* **2021**, *27*, 10107-10114. e) Huang, Q.-W.; Qi, T.; Liu, Y.; Zhang, X.; Li, Q.-Z.; Gou, C.; Tao, Y.-M.; Leng, H.-J.; Li, J.-L. *ACS Catal.* **2021**, *11*, 10148-10158.

[76] a) Komatsuki, K.; Sadamitsu, Y.; Sekine, K.; Saito, K.; Yamada, T. *Angew. Chem. Int. Ed.* **2017**, *56*, 11594-11598. b) Komatsuki, K.; Kozuma, A.; Saito, K.; Yamada, T. *Org. Lett.* **2019**, *21*, 6628-6632. c) Kozuma, A.; Komatsuki, K.; Saito, K.; Yamada, T. *Chem. Lett.* **2020**, *49*, 60-63.

1.5 Thesis Aims

Given the importance of introducing functionalized allyl groups in the synthesis of complex molecular targets and advanced intermediates described throughout this chapter, the main goal of this thesis was to develop new stereoselective methods using vinyl cyclic carbonates as allylic surrogates, with a special focus on the construction of new C–C bonds.

Prior to the start date of these PhD studies (10/2017), our group introduced in 2016 novel methods using VCCs as electrophilic allyl sources, and their combination with nitrogen-,[50a,53c] oxygen-,[50c,53b] and sulfur-based[53d] pronucleophiles to give rise to various linear and branched allylic compounds. Additionally, the formal [3+2] cycloadditions reactions introduced by Zhang in 2014 involved primarily the formation of carbon-heteroatom bonds.[57-59a] Therefore, before starting the thesis work, general methods using VCCs as allylic surrogates aiming at making new C–C bonds were lacking.[77] Furthermore, applications of VCCs as reactive intermediates in the synthesis of natural products, rather than using them as temporary protecting groups, were also scarce.[48]

Taking the above limitations into account, the following objectives were formulated for this thesis, and these are delineated below per chapter:

- **Chapter 2:** Development of a broadly applicable and user-friendly method towards the allylation of nitroalkanes as carbon-based pronucleophiles, which relies on the selective formation of a palladacyclic intermediate to accomplish high (*Z*)-selectivity. Moreover, an initial exploration of modifications of the synthesized homoallylic nitroalkanes is targeted to reveal their potential as synthetic intermediates.
- **Chapter 3:** Application of the newly developed allylation of nitroalkanes (chapter 2) by using selected stereodefined building blocks towards the synthesis of biologically active indolizidine and quinolizidine alkaloids
- **Chapter 4:** Exploration and development of novel dual cobalt-photoredox catalytic processes to expand the scope of nucleophilic allyl species that can be generated from VCCs and focus specifically on the generation of quaternary carbon stereocenters.

[77] Before the start of this PhD thesis, examples merging carbon-based (pro)nucleophiles with VCCs were limited in the scope of VCCs and offered poor control over the stereoselectivity: See *refs.* 44, 47a, 49c, 53a, 67a-c, 68, 69a-d.

UNIVERSITAT ROVIRA I VIRGILI
STEREOSELECTIVE TRANSFORMATIONS OF VINYL CYCLIC CARBONATES AND APPLICATIONS IN NATURAL PRODUCT SYNTHESIS
Àlex Cristòfol Martínez

UNIVERSITAT ROVIRA I VIRGILI
STEREOSELECTIVE TRANSFORMATIONS OF VINYL CYCLIC CARBONATES AND APPLICATIONS IN NATURAL PRODUCT SYNTHESIS
Àlex Cristòfol Martínez

Good judgment comes from experience; experience comes from bad judgment.

— Dr Kerr L White

CHAPTER 2

PALLADIUM-CATALYZED (Z)-SELECTIVE ALLYLATION OF NITROALKANES: ACCESS TO HIGHLY FUNCTIONALIZED HOMOALLYLIC SCAFFOLDS

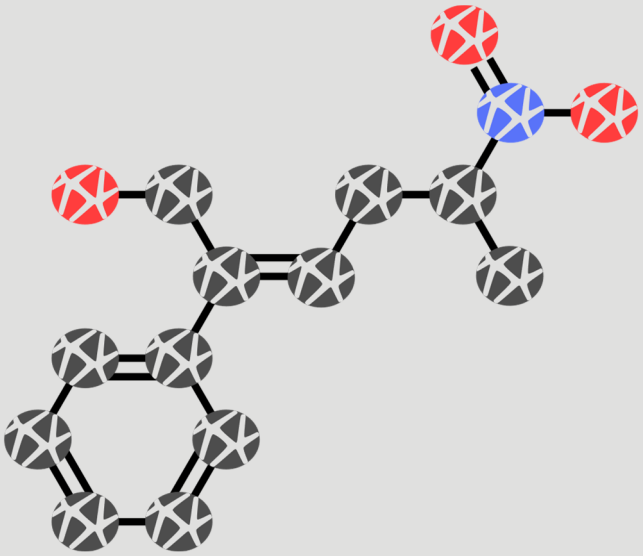

The results of this chapter have been published in:

Cristòfol, À.; Escudero-Adán, E. C.; Kleij, A. W. *J. Org. Chem.* **2018**, *83*, 9978–9990

2.1 Introduction

2.1.1 Nitroalkanes as Carbon Pronucleophiles in Organic Synthesis

The nitro group (NO_2) represents one of the most versatile functional groups that can be readily introduced into useful building blocks.[78] This is particularly true for aromatic nitro compounds, which are classically accessed through nitration of the corresponding arene precursor.[79] On the other hand, the utilization of aliphatic nitro compounds (also referred to as nitroalkanes) in organic synthesis has been less frequent, although they offer a feature that nitroaromatic compounds do not intrinsically possess: the acidic α-proton. Aliphatic nitro compounds (pK_a ~ 7-9)[80] are easily deprotonated by common bases, such as tertiary amines or inorganic carbonates, thus allowing practical and easy access to its nucleophilic nitronate species that serve as carbon nucleophiles. Despite the low pK_a value, the rate of deprotonation for nitroalkanes is not diffusion-controlled, as is the case for protons attached to heteroatoms, and therefore, the steric and electronic effects of the nitroalkane and the base, as well as the solvent play a major role in driving the deprotonation step forward.[81]

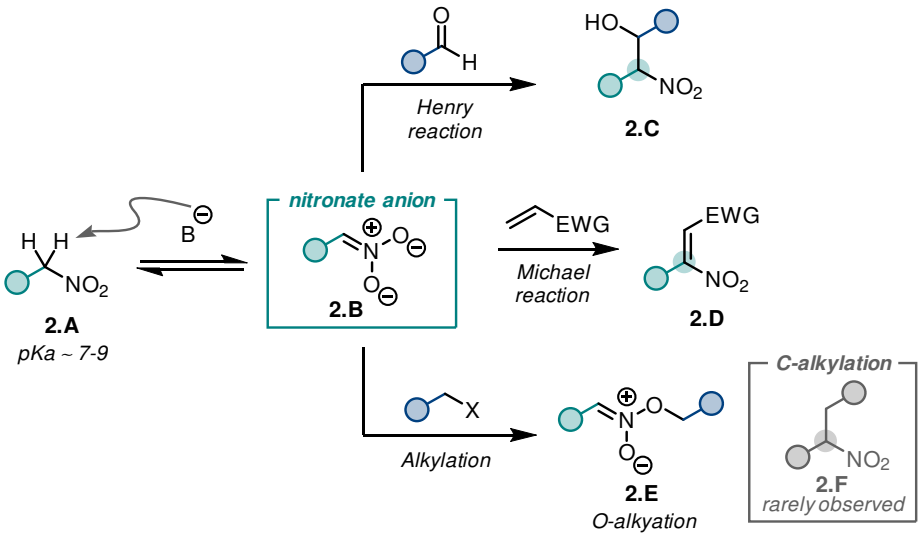

SCHEME 2.1. C–C bond-forming reactions using nitroalkanes as pronucleophiles.

[78] a) Ono, N., *The Nitro Group in Organic Synthesis*. John Wiley & Sons: New York, 2001. b) Ballini, R.; Petrini, M.; Rosini, G. *Molecules* **2008**, *13*, 319-330.

[79] For a review on metal-catalyzed denitrative cross-couplings, see: Muto, K.; Okita, T.; Yamaguchi, J. *ACS Catal.* **2020**, *10*, 9856-9871. For a nice example of a synthetically advantageous reductive coupling with alkyl halides, see: Cheung, C. W.; Hu, X. *Nat. Commun.* **2016**, *7*, 12494.

[80] For example, the reported pK_a in H_2O for nitroethane is 8.6 and for 2-nitropropane it is 7.74, see: Bell, R. P.; Higginson, W. C. E. *Pro. Royal Soc.* **1949**, *197*, 141-159.

[81] Bernasconi, C. F.; Pérez-Lorenzo, M.; Brown, S. D. *J. Org. Chem.* **2007**, *72*, 4416-4423.

Nonetheless, the generated nitronate species have been shown to react efficiently with some electrophiles, such as aldehydes (*cf.*, Henry reaction)[82] or α,β-unsaturated carbonyl compounds (*cf.*, Michael reaction)[83] and to a lesser extent, with halogenated electrophiles, such as alkyl bromides and iodides, as in this case the ambident nitronate anion prefers to react at the *O*-atom (**SCHEME 2.1**).[84]

2.1.2 Allylic Substitutions using Nitroalkanes as Pronucleophiles

A versatile and productive way to make a C–C bond is through a transition metal-catalyzed allylic substitution reaction. In this case, the nitronate anion prefers to react at the carbon atom (*i.e., C*-alkylation), instead of the oxygen atom (*O*-alkylation), thus providing an alternative method for the challenging *C*-alkylation of nitroalkanes.

While the introduction of a simple allyl group and disubstituted olefin units has been reported,[85] including enantioselective protocols,[86] the installation of more functional allyl groups featuring (*Z*)-configured tri- and tetrasubstituted olefins had not been reported (**SCHEME 2.2**) at the time of the execution of the envisioned project. Only one publication from Hesse *et. al.* in 1985 illustrated the allylation of 2-nitrocycloalkanones using substituted allylic carbonates or allylic epoxides leading to trisubstituted olefins as stereoisomeric mixtures or the expected (*E*)-stereoisomer.[87] Therefore, it would be highly desirable to address these shortcomings to expand on the variety of homoallylic scaffolds that cannot be easily accessed through other known methodologies.[88]

---

[82] a) Boruwa, J.; Gogoi, N.; Saikia, P. P.; Barua, N. C. *Tetrahedron: Asymmetry* **2006**, *17*, 3315-3326. b) Palomo, C.; Oiarbide, M.; Laso, A. *Eur. J. Org. Chem.* **2007**, 2561-2574.

[83] Ballini, R.; Bosica, G.; Fiorini, D.; Palmieri, A.; Petrini, M. *Chem. Rev.* **2005**, *105*, 933-972.

[84] The extent of *C*-alkylation can be improved by the addition of a suitable metal catalyst, as reported by Watson: a) Shimkin, K. W.; Gildner, P. G.; Watson, D. A. *Org. Lett.* **2016**, *18*, 988-991. b) Rezazadeh, S.; Devannah, V.; Watson, D. A. *J. Am. Chem. Soc.* **2017**, *139*, 8110-8113. c) Devannah, V.; Sharma, R.; Watson, D. A. *J. Am. Chem. Soc.* **2019**, *141*, 8436-8440.

[85] a) Aleksandrowicz, P.; Piotrowska, H.; Sas, W. *Tetrahedron* **1982**, *38*, 1321-1327. b) Genet, J. P.; Grisoni, S. *Tetrahedron Lett.* **1986**, *27*, 4165-4168. c) Maki, K.; Kanai, M.; Shibasaki, M. *Tetrahedron* **2007**, *63*, 4250-4257. d) Grenning, A. J.; Tunge, J. A. *Org. Lett.* **2010**, *12*, 740-742. e) Grenning, A. J.; Tunge, J. A. *Angew. Chem. Int. Ed.* **2011**, *50*, 1688-1691. f) Lang, S. B.; Locascio, T. M.; Tunge, J. A. *Org. Lett.* **2014**, *16*, 4308-4311. g) Chang, C. Y.; Wu, Y. K. *J. Org. Chem.* **2018**, *83*, 6217-6224.

[86] a) Rieck, H.; Helmchen, G. *Angew. Chem. Int. Ed. Engl.* **1996**, *34*, 2687-2689. b) Trost, B. M.; Surivet, J.-P. *J. Am. Chem. Soc.* **2000**, *122*, 6291-6292. c) Trost, B. M.; Jiang, C. *J. Am. Chem. Soc.* **2001**, *123*, 12907-12908. d) Uozumi, Y.; Suzuka, T. *J. Org. Chem.* **2006**, *71*, 8644-8646. e) Ohmatsu, K.; Ito, M.; Kunieda, T.; Ooi, T. *Nat. Chem.* **2012**, *4*, 473-477. f) Yang, X.-F.; Yu, W.-H.; Ding, C.-H.; Ding, Q.-P.; Wan, S.-L.; Hou, X.-L.; Dai, L.-X.; Wang, P.-J. *J. Org. Chem.* **2013**, *78*, 6503-6509. g) Jung, W.-O.; Mai, B. K.; Spinello, B. J.; Dubey, Z. J.; Kim, S. W.; Stivala, C. E.; Zbieg, J. R.; Liu, P.; Krische, M. J. *J. Am. Chem. Soc.* **2021**, *143*, 9343-9349.

[87] Ognyanov, V.; Hesse, M. *Synthesis* **1985**, 645-647.

[88] Chen, M. Z.; McLaughlin, M.; Takahashi, M.; Tarselli, M. A.; Yang, D.; Umemura, S.; Micalizio, G. C. *J. Org. Chem.* **2010**, *75*, 8048-8059.

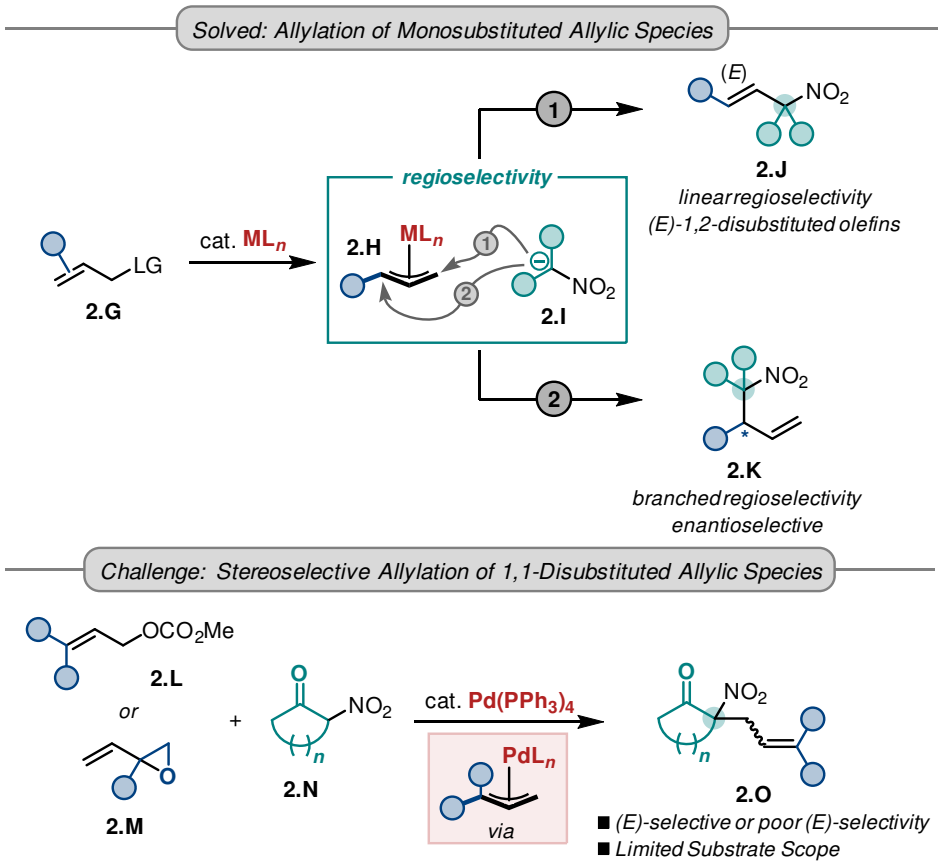

SCHEME 2.2. State-of-the-art in metal-catalyzed allylic substitution reactions using nitroalkanes.

2.1.3 Aims and Objectives

Given the lack of synthetic solutions for introducing functionalized allyl groups bearing (*Z*)-configured tri- and tetrasubstituted olefins through metal-catalyzed allylic substitution reactions, the main objective of the work presented in this chapter is to develop a general method that allows preparing (*Z*)-configured homoallylic nitroalkanes stereoselectively and in good yields (**SCHEME 2.3**). A new protocol would represent a significant synthetic advancement, as the current synthesis of tri- or tetrasubstituted olefins through robust and reliable olefination reactions (*e.g.*, Wittig or HWE reaction) usually yields a mixture of *Z* and *E* olefins, which are not easily separated.[89]

An additional focus of the present work is to explore streamlined transformations for the resulting (*Z*)-configured homoallylic nitroalkanes into more naturally occurring amines and ketones, thus positioning the

[89] Stereoselective synthesis of highly functionalized tri- and tetrasubstituted olefin scaffolds remains a highly challenging and attractive objective: a) Itami, K.; Yoshida, J. *Chem. Eur. J.* **2006**, *12*, 3966-3974. b) Flynn, A. B.; Ogilvie, W. W. *Chem. Rev.* **2007**, *107*, 4698-4745.

resulting methodology as an attractive tool for more elaborated synthesis providing scaffolds of value to natural product or pharmaceutical synthesis.

Based on previous research within the group,[90] we envisioned that the use of a suitable palladium precursor in conjunction with DPEPhos as ligand would represent an ideal starting point, as the high (*Z*)-selectivity may be guided by the formation of a (known) palladacyclic intermediate upon decarboxylation.

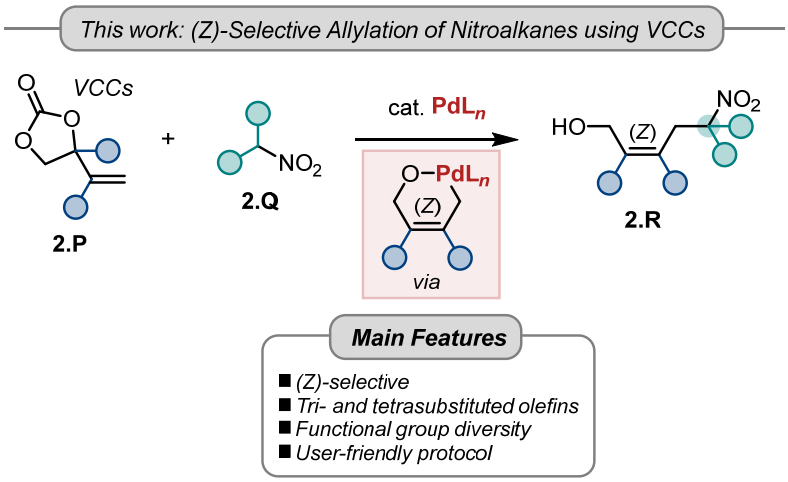

SCHEME 2.3. Schematic approach of the present work.

[90] See Kleij, A. W. *et al. Angew. Chem. Int. Ed.* **2016** (*ref.* 53b), Kleij, A. W. *et al. J. Am. Chem. Soc.* **2016** (*ref.* 53c), and Kleij, A. W. *et al. Org. Lett.* **2016** (*ref.* 53d) on page 30.

2.2 Results and Discussion

2.2.1 Optimization Studies

The reaction between vinyl cyclic carbonate **2.1a** and nitroethane **2.2a** was selected as a benchmark reaction. Inspired by previous research within the group, we initially run the reaction using $Pd_2(dba)_3{\cdot}CHCl_3$ and DPEPhos in THF. We were pleased to observe that the desired homoallylic nitroalkane **2.3a** was generated in 57% yield and 94:6 *Z*/*E* selectivity. As side products, we could also detect the formation of the bisallylated product **2.4a** and small amounts of aldehydes **2.5a**-**2.5b** (**SCHEME 2.4**).

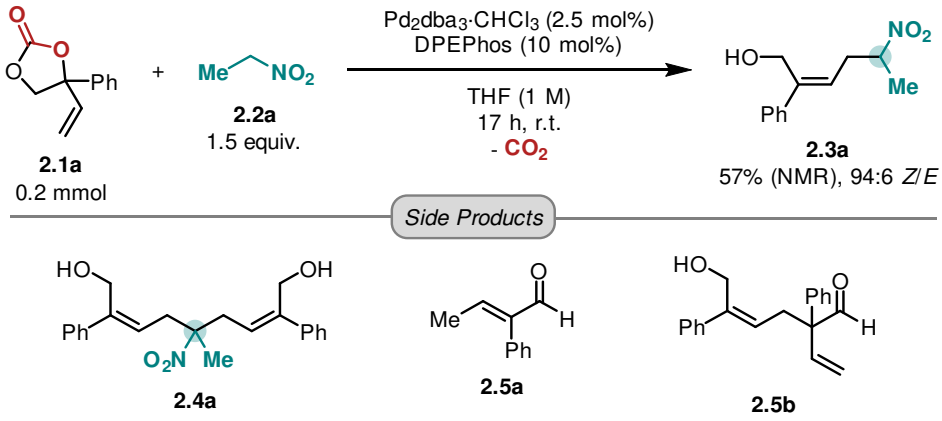

SCHEME 2.4. Initial discovery and side products investigation.

After this initial discovery, we set out to screen different reaction parameters, such as palladium precursor, solvent, ligand, nitroethane equivalents, and catalyst loading (**TABLE 2.1**). Replacing $Pd_2(dba)_3{\cdot}CHCl_3$ by $Pd(dba)_2$ afforded similar results (**TABLE 2.1**, entry 2), while the use of $Pd(PPh_3)_4$ negatively influenced the yield (**TABLE 2.1**, entry 3). Switching from zerovalent to Pd^{II} precursors was also detrimental to the yield of **2.3a** (**TABLE 2.1**, entries 4-6), so we decided to choose $Pd(dba)_2$ to continue with the screening of solvents. Non-polar to slightly polar solvents gave similar results compared to THF (**TABLE 2.1**, entries 7-9), while the reaction was more efficient when performed in polar solvents (**TABLE 2.1**, entries 10-12). In particular, running the reaction in MeCN boosted the yield and *Z*/*E* selectivity, affording 85% of **2.3a** in >99:1 *Z*/*E* selectivity, which was isolated after column chromatography in 50% yield when running the reaction at a 1.0 mmol scale (**TABLE 2.1**, entry 10). Replacing DPEPhos with other ligands resulted in a decrease in yield and *Z*/*E* ratio in most of the cases. A clear trend was observed when other diphosphine ligands with decreased bite angles were tested, resulting in a decrease in both, yield and *Z*/*E* selectivity (**TABLE 2.1**, entries 13-16). However, an increase in the bite angle of the ligand (*e.g.*, when using XantPhos) also negatively influenced the outcome of the reaction (**TABLE 2.1**, entries 17). This was also the case for other mono-

phosphine ligands (**TABLE 2.1**, entries 18-19) and structurally similar ligands to DPEPhos (**TABLE 2.1**, entries 20-21).

After finding the optimal conditions, we wanted to explore changes in the relative amount of nitroethane **2.2a** and catalyst loading. In an attempt to minimize the formation of the bisallylated product **2.4a**, we ran the reaction using 2.0 equivalents of nitroethane **2.2a**, but unfortunately, the yield of the desired monoallylated product **2.3a** did not increase (**TABLE 2.1**, entry 22). Lowering the amount of DPEPhos to 5 mol% was also disadvantageous, while decreasing the amount of $Pd(dba)_2$ and DPEPhos to 2 mol% and 4 mol%, respectively, was also less productive (**TABLE 2.1**, entries 23-24).

TABLE 2.1. Optimization of reaction conditions towards homoallylic nitroalkane **2.3a**

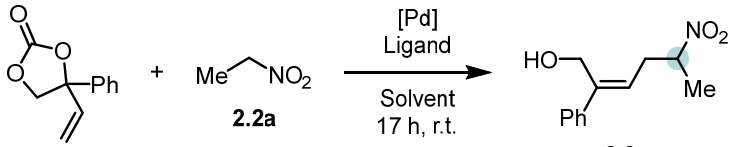

2.1a + **2.2a** → **2.3a**

Entry	[Pd]	Solvent	Ligand	Yield (%)[a]	Z/E[b]
1	$Pd_2(dba)_3{\cdot}CHCl_3$[c]	THF	DPEPhos	57	94:6
2	$Pd(dba)_2$	THF	DPEPhos	59	92:8
3	$Pd(PPh_3)_4$	THF	DPEPhos	41	93:7
4	$Pd(OAc)_2$	THF	DPEPhos	36	89:11
5	$Pd(acac)_2$	THF	DPEPhos	41	97:3
6	$[Pd(allyl)Cl]_2$[c]	THF	DPEPhos	53	93:7
7	$Pd(dba)_2$	PhMe	DPEPhos	59	93:7
8	$Pd(dba)_2$	CH_2Cl_2	DPEPhos	55	92:8
9	$Pd(dba)_2$	EtOAc	DPEPhos	60	97:3
10	$Pd(dba)_2$	MeCN	DPEPhos	85(50)[d]	>99:1
11	$Pd(dba)_2$	DMF	DPEPhos	76	98:2
12	$Pd(dba)_2$	DMSO	DPEPhos	73	97:3
13	$Pd(dba)_2$	MeCN	dppe	24	64:36
14	$Pd(dba)_2$	MeCN	dppp	56	89:11
15	$Pd(dba)_2$	MeCN	dppb	74	>99:1
16	$Pd(dba)_2$	MeCN	dppf	51	>99:1
17	$Pd(dba)_2$	MeCN	XantPhos	24	86:14
18	$Pd(dba)_2$	MeCN	PPh_3	26	72:28
19	$Pd(dba)_2$	MeCN	TFP	69	68:32

Continuation of **TABLE 2.1**

Entry	[Pd]	Solvent	Ligand	Yield (%)[a]	*Z*/*E*[b]
20	$Pd(dba)_2$	MeCN	**L1**	53	>99:1
21	$Pd(dba)_2$	MeCN	**L2**	56	87:13
22[e]	$Pd(dba)_2$	MeCN	DPEPhos	69	>99:1
23[f]	$Pd(dba)_2$	MeCN	DPEPhos	53	>99:1
24[g]	$Pd(dba)_2$	MeCN	DPEPhos	63	>99:1

Reaction conditions: **2.1a** (0.20 mmol), **2.2a** (1.5 equiv.), [Pd] (5 mol%), ligand (10 mol %), solvent (1 M), room temperature, open to air. Please refer to appendix A for the structure of each ligand. Full conversion of **2.1a** was noted in all instances; [a] NMR yield (%) using mesitylene as an internal standard; [b] Determined by ^{1}H NMR; [c] [Pd] (2.5 mol%); [d] Yield (%) of isolated product at 1.0 mmol scale; [e] **2.2a** (2.0 equiv.); [f] Ligand (5 mol%); [g] [Pd] (2 mol%), ligand (4 mol%).

2.2.2 Scope of Homoallylic Nitroalkanes

The effect of changing the nature and position of the substituents in both reactants was next examined by using structurally different vinyl cyclic carbonates **2.1a-2.1o** and nitroalkanes **2.2a-2.2q**. Most of the targeted products were isolated in moderate to high yields, and apart from the desired compound, typically bisallylated nitroalkanes (such as in **2.4a**) and minor amounts of aldehyde byproducts (such as in **2.5a-2.5b**) were noted. We first started varying the substitution on the nitroalkane reagent. The use of larger alkyl-substituted derivatives gave rise to consistently higher product yields, indicating a beneficial steric effect to diminish the rate of bisallylation (**SCHEME 2.5**, **2.3a-2.3c**). Nitroalkanes bearing an electron-withdrawing group at the α-carbon, such as Ph, SO_2Ph, or CO_2Et, are also effective reagents that provide access to their respective homoallylic nitroalkane products in good yields (**SCHEME 2.5**, **2.3d-2.3f**). Moreover, the introduction of additional functional groups within the nitroalkane backbone such as OH, Cl, and (thio)acetal were tolerated (**SCHEME 2.5**, **2.3g-2.3l**). In the case of compound **2.3g**, the stereoselectivity was, however, low (*Z*/*E* = 36:64), suggesting that the free alcohol group may have undesired interactions with the (allyl)Pd^{II} intermediate, possibly through hydrogen-bonding. Apart from that, the increased steric crowding imparted by the dimethyl acetal group could nearly suppress the undesired bisallylation, and thus excellent yields of **2.3j** were achieved (95%). Remarkably, the coexistence of a (nucleophilic) aniline group in **2.3l** did not influence the desired allylation of the nitroalkane. In addition, different heteroaryl groups in the nitroalkane reagent were found to be tolerated in this catalytic protocol (**SCHEME 2.5**, **2.3m-2.3o**), including a nucleophilic unprotected indole group in **2.3n** prone to potential side reactions. The assigned (*Z*)-configuration was unambiguously confirmed by X-ray diffraction of a single crystal of **2.3m** (see **TABLE 2.3** in subsection 2.4.6).

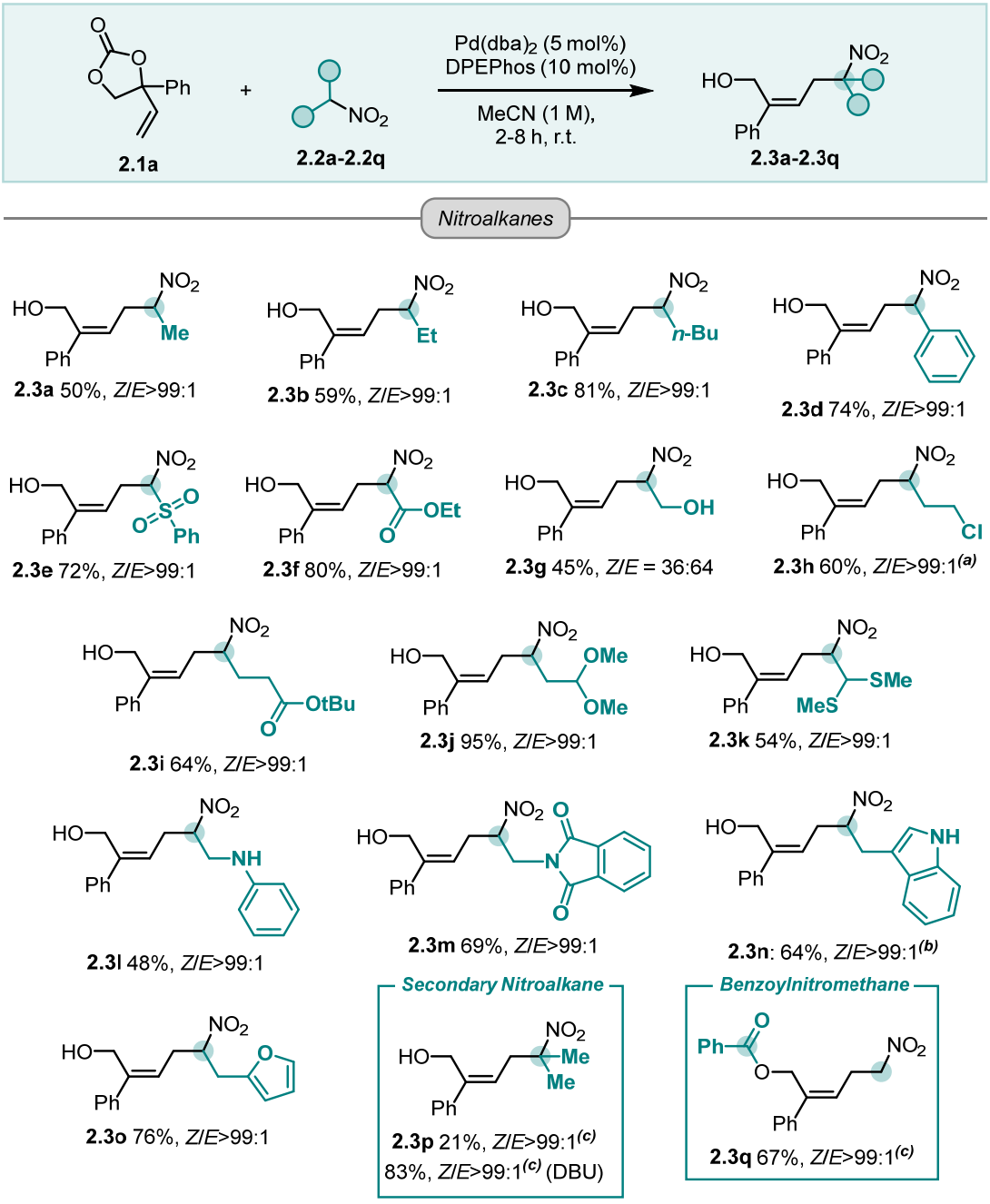

SCHEME 2.5. Variation of nitroalkane reagent to afford homoallylic compounds **2.3a-2.3q**. Reaction conditions: **2.1a** (1.0 mmol), nitroalkane **2.2a-2.2q** (1.5 equiv.), $Pd(dba)_2$ (5 mol%), DPEPhos (10 mol%), MeCN (1 M), room temperature, 2-8 h, open to air; [a] Reaction conducted at 0.23 mmol scale of **2.1a**; [b] Reaction conducted at 0.58 mmol scale of **2.1a**; [c] Reaction conducted at 0.20 mmol scale of **2.1a**.

When switching to a secondary nitroalkane (**SCHEME 2.5**, **2.3p**), the desired homoallylic nitroalkane was obtained in 21% yield, while noticing increased amounts of aldehyde byproducts **2.5a-2.5b**. We attribute this result to the diminished rate of deprotonation of the bulkier nitroalkane by the (allyl)Pd^{II} intermediate, which would favor parasitic β-*H*-elimination pathways in the (allyl)Pd^{II} intermediate leading to the aldehyde byproducts **2.5a-2.5b**. To circumvent this problem, we found that the addition of a catalytic amount of an exogenous base (DBU) greatly improved the yield of **2.3p** to 83%.[91]

While using benzoylnitromethane as pronucleophile, we observed that the benzoyl group was instead connected to the alcohol group in the final product **2.3q**, which is likely the result of an intramolecular acyl transfer (*i.e.,* through addition of the alcohol to the phenyl ketone and subsequent elimination of the nitronate as shown in **SCHEME 2.6**).

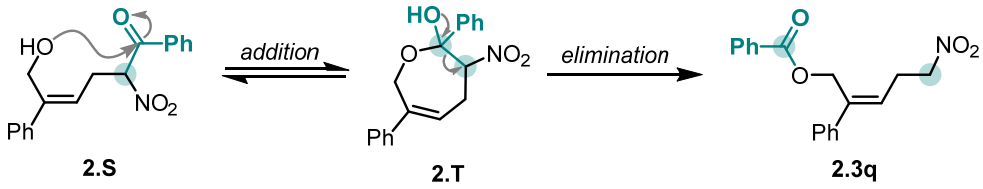

SCHEME 2.6. Postulated mechanism for the intramolecular acyl transfer to yield **2.3q**.

The scope of VCCs (**2.1b-2.1o**) was next examined. The presence of electron-withdrawing groups on the aromatic ring in the VCC decreased the yield of product (**SCHEME 2.7**, **2.3s-2.3t**), indicating that a more reactive (allyl)Pd^{II} intermediate could accelerate the competing bisallylation. In line with this hypothesis, electron-donating groups, such as in **2.3v**, improved the yield of the monoallylated product. The presence of other (hetero)aromatic substituents was tolerated (**SCHEME 2.7**, **2.3w-2.3y**), whereas the use of alkyl and *H*-substituted VCCs also gave access to the desired homoallylic nitroalkane products, though a loss of stereoselectivity was noted depending on the steric features of the substituent.[92] To our delight, (*Z*)-configured tetrasubstituted olefin products like **2.3ac** can also be achieved in the presence of a catalytic amount of DBU. Other *ortho*- and *meta*-substituted VCCs were tested in combination with other nitroalkane reagents (**SCHEME 2.7**, **2.3ad-2.3af**). While this increase in steric bulk did not prevent the oxidative addition step of

[91] Two other publications have also reported enhanced reactivity for secondary nitroalkane pronucleophiles when adding a catalytic amount of an exogenous base, namely DBU: See Shibasaki, M. *et al. Tetrahedron* **2007** (*ref.* 85c), and Wu, Y. K. *et al. J. Org. Chem.* **2018** (*ref.* 85g) on page 41.

[92] Presumably, the formation of the key palladacyclic intermediate is less favored with alkyl substituents, as delocalization of the electron density through hyperconjugation is less effective. Therefore, decarboxylation would likely lead to a mixture of zwitterionic *syn* and *anti* η^3-allylPd^{II} species governed mainly by steric effects (see subsection 2.2.5).

the VCC to the Pd(0) catalyst, a decrease in stereocontrol was noted in the conversion of *ortho*-substituted VCCs.[93]

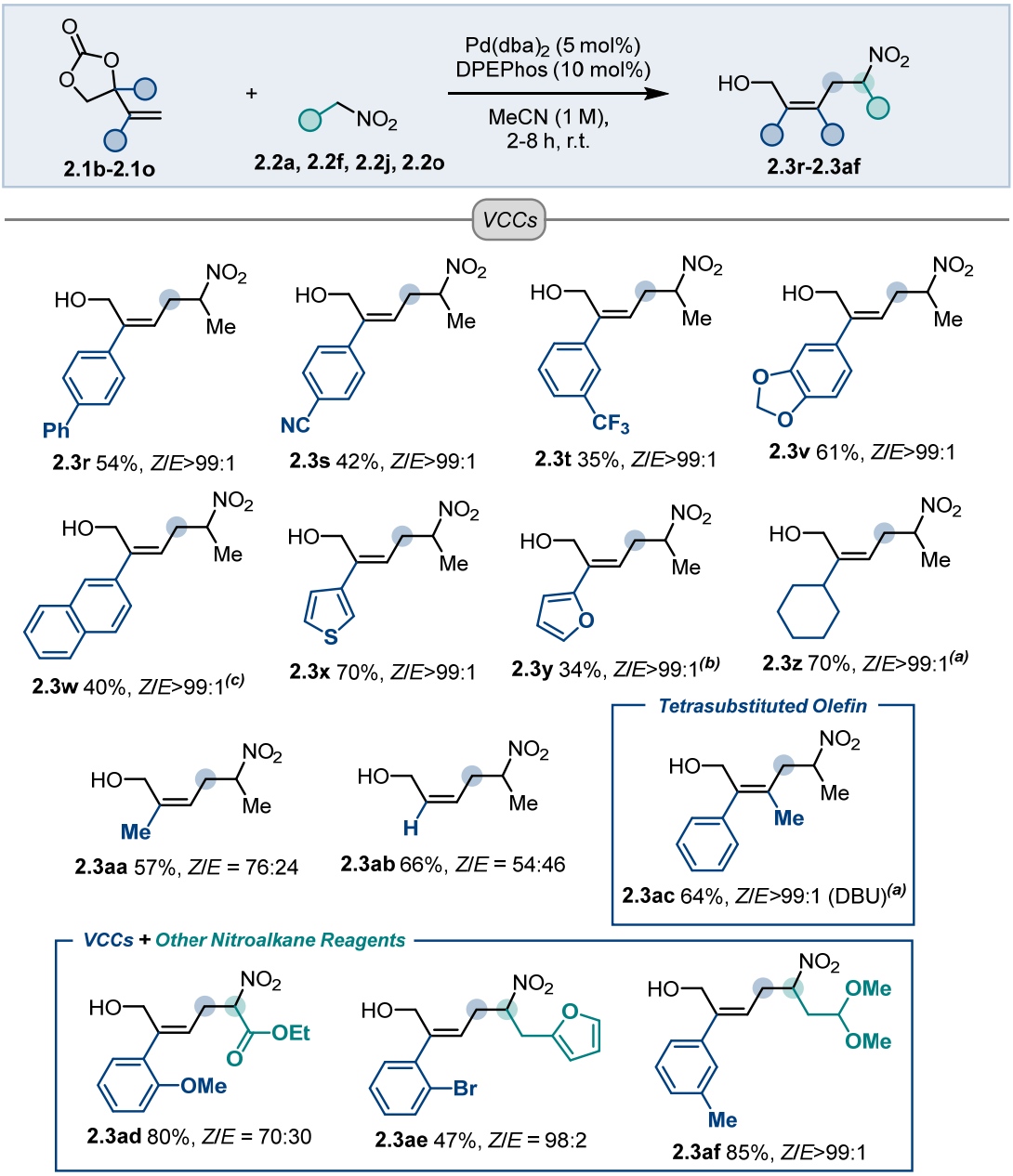

SCHEME 2.7. Variation of the VCC reactant to afford homoallylic compounds **2.3r-2.3af**. Reaction conditions: VCC **2.1b-2.1o** (1.0 mmol), nitroalkane **2.2a-2.2o** (1.5 equiv.), $Pd(dba)_2$ (5 mol%), DPEPhos (10 mol%), MeCN (1 M), room temperature, 2-8 h, open to air; [(a)] Reaction conducted at 0.20 mmol scale of VCC; [(b)] Reaction conducted at 0.46 mmol scale of VCC; [(c)] Reaction conducted at 0.22 mmol scale of VCC.

[93] The loss in stereoselectivity might likely be a result of a slower nucleophilic attack attributed to increased steric effects, which would allow for competitive *syn*/*anti* isomerization to occur (see subsection 2.2.5).

2.2.3 Synthesis of Multiallylated Nitroalkanes

Next, the introduction of multiple allyl groups using our VCCs within the nitroalkane scaffold was investigated. We were interested to see whether the stereoselectivity could be retained upon introduction of different allyl groups, while at the same time expanding our scope of allylated nitroalkanes.

To achieve this, we first focused on finding suitable reaction conditions for the monoallylation of nitromethane, as subsequent bis- and tris-allylations are more competitive compared with other primary nitroalkane reagents. We thought that using nitromethane also as solvent could greatly enhance the formation of the monoallylated product, and therefore we initially run the reaction using $Pd(dba)_2$ and DPEPhos in CH_3NO_2. We were pleased to observe the desired monoallylated homoallylic nitroalkane **2.4a** in 38% yield with >99:1 *Z*/*E* ratio (**TABLE 2.2**, entry 1), so we then decided to screen other palladium precursors, ligands, and different amounts of nitromethane. We found out that the best palladium precursor was $[Pd(allyl)Cl]_2$ (**TABLE 2.2**, entry 7), while the use of other ligands different from DPEPhos was detrimental in terms of product yield and substrate conversion (**TABLE 2.2**, entries 8-11). A further increase in the amount of CH_3NO_2 did unfortunately not lead to an increase in yield of **2.4a** (**TABLE 2.2**, entries 12-14), but by raising the catalyst loadings, the yield of monoallylated product could be raised to 57%, which was isolated after column chromatography in 53% when running the reaction at a 1.0 mmol scale (**TABLE 2.2**, entry 15).

TABLE 2.2. Optimization of the reaction conditions towards homoallylic nitroalkane **2.4a**

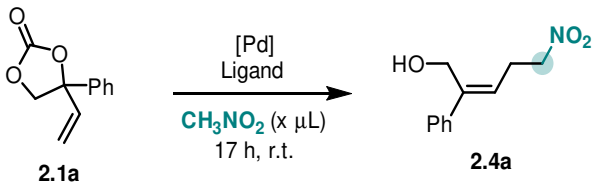

2.1a **2.4a**

Entry	[Pd]	Ligand	CH_3NO_2	Yield (%)[b]	*Z*/*E*[c]
1	$Pd(dba)_2$	DPEPhos	200 µL	38	>99:1
2	$Pd_2(dba)_3{\cdot}CHCl_3$[d]	DPEPhos	200 µL	28	95:5
3	$Pd(PPh_3)_4$	DPEPhos	200 µL	25	93:7
4	$Pd(OAc)_2$	DPEPhos	200 µL	28	>99:1
5	$Pd(acac)_2$	DPEPhos	200 µL	32	97:3
6	$PdCl_2(PPh_3)_2$	DPEPhos	200 µL	37	93:7
7	$[Pd(allyl)Cl]_2$[d]	DPEPhos	200 µL	49	>99:1
8	$[Pd(allyl)Cl]_2$[d]	dppe	200 µL	<1[e]	-
9	$[Pd(allyl)Cl]_2$[d]	dppp	200 µL	12[f]	-
10	$[Pd(allyl)Cl]_2$[d]	XantPhos	200 µL	37	>99:1
11	$[Pd(allyl)Cl]_2$[d]	TFP	200 µL	<1[g]	-

Continuation of **TABLE 2.2**

Entry	[Pd]	Ligand	CH_3NO_2	Yield (%)[b]	Z/E[c]
12	$[Pd(allyl)Cl]_2$[d]	DPEPhos	265 μL	47	>99:1
13	$[Pd(allyl)Cl]_2$[d]	DPEPhos	400 μL	42	>99:1
14	$[Pd(allyl)Cl]_2$[d]	DPEPhos	800 μL	39	>99:1
15[h]	$[Pd(allyl)Cl]_2$[d]	MeCN	200 μL	57(53)[i]	>99:1

[a] Reaction conditions: **2.1a** (0.20 mmol), [Pd] (2 mol%), ligand (5 mol %), CH_3NO_2, room temperature, open to air. Please refer to appendix A for the structure of each ligand. Full conversion of **2.1a** was noted in all instances, unless otherwise stated; [b] NMR yield (%) using mesitylene as an internal standard; [c] Determined by ^1H NMR; [d] [Pd] (1 mol%); [e] 27% conversion of **2.1a**; [f] 44% conversion of **2.1a**; [e] 42% conversion of **2.1a**; [h] [Pd] (2.5 mol%), ligand (10 mol%). [i] Yield (%) of isolated product at a 1.0 mmol scale.

After having found conditions to perform the monoallylation with nitromethane, we continued to explore the feasibility of introducing subsequent, different allyl groups to produce multiallylated nitroalkanes (**SCHEME 2.8**). Monoallylated nitroalkanes **2.4b** and **2.4c** were also successfully synthesized with a high degree of stereocontrol, although with a lower yield in the case of **2.4b**. Subsequent allylation with a different VCC (VCC_2) gave bisallylated nitroalkanes **2.5a-2.5c** with excellent stereocontrol (except for **2.5b**) and comparably good yields. After having prepared these nitroalkanes, we went on to attempt a further allylation with a different VCC (VCC_3), and we were pleased to find that hetero-trisallylated nitroalkanes **2.6a** and **2.6b** were prepared with excellent stereocontrol in the presence of a catalytic amount of DBU. Moreover, a related homo-trisallylation protocol was also developed (**2.6c**) combining 1 equivalent of nitromethane and 3.1 equivalents of VCC **2.1a**.

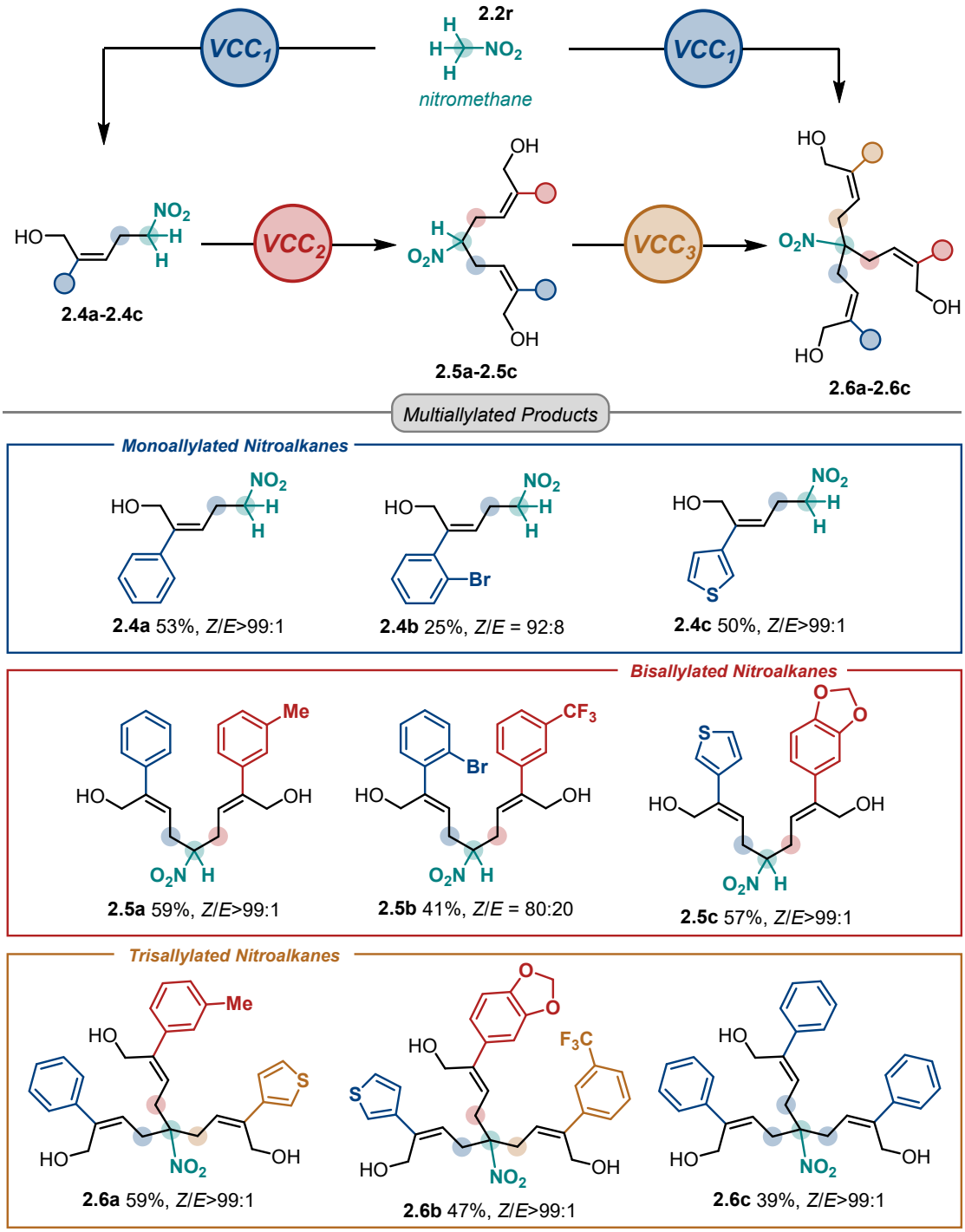

SCHEME 2.8. Stereoselective synthesis of mono-, bis- and trisallylated compounds. For the synthesis of monoallylated nitroalkanes **2.4a-2.4c**, please refer to entry 15 in **TABLE 2.2** for the reaction conditions. For the synthesis of bisallylated nitroalkanes **2.5a-2.5c**, please refer to entry 10 in **TABLE 2.1** for the reaction conditions. For the synthesis of unsymmetrical trisallylated nitroalkanes **2.6a-2.6b**, we added DBU (10 mol%) in addition to the conditions reported in entry 10 in **TABLE 2.1**. For the synthesis of symmetrical trisallylated nitroalkane **2.6c**, reaction conditions were as follows: VCC **2.1a** (3.1 equiv.), CH_3NO_2 (1.0 equiv.), $Pd(dba)_2$ (5.0 mol%), DPEPhos (10 mol%), DBU (10 mol%), MeCN (1 M), room temperature, open to air.

2.2.4 Scale-up and Synthetic Transformations

As previously discussed in subsection 2.1.1, the versatility of the NO_2 group is of great utility to synthetic chemists. As such, we explored the synthetic potential of our homoallylic nitroalkanes compounds, but first, we attempted to scale up our benchmark reaction between VCC **2.1a** and nitroethane **2.2a** to gram scale. As expected, the allylation process could be easily scaled up (using 1.14 g of VCC **2.1a**, 6 mmol) using the same experimental procedure, thus allowing to obtain larger amounts of homoallylic nitroalkane **2.3a** without affecting the efficiency of the process (62% yield, *Z*/*E* >99:1, **SCHEME 2.9**).

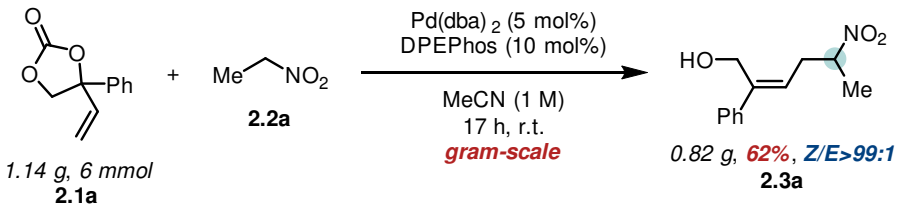

SCHEME 2.9. Scaled-up benchmark reaction between **2.1a** and **2.2a**.

After a successful scale-up, the reduction of homoallylic nitroalkanes **2.3a** and **2.3ac** to afford their homoallylic amines **2.7a** and **2.7b** using Zn under acidic conditions proved to be straightforward and these compounds were isolated in good yields (**SCHEME 2.10**). As far as we know, the synthesis of **2.7b** represents the first example of a (*Z*)-configured homoallylic amine incorporating a tetrasubstituted double bond. Further to this, a combined protection/Nef reaction sequence leading to ketone **2.9** illustrates that elusive β,γ-unsaturated (*Z*)-configured ketones can be easily accessed without any observed double bond isomerization.

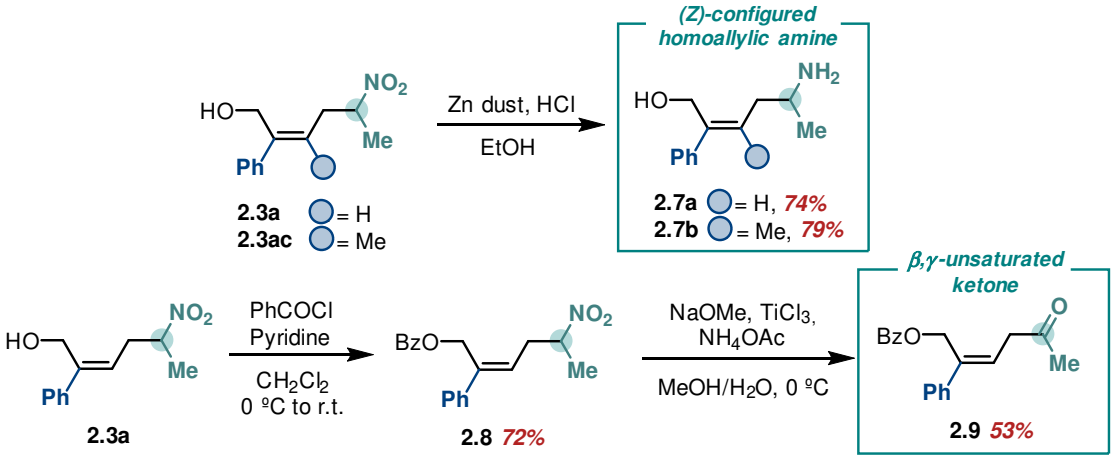

SCHEME 2.10. Synthetic modifications of homoallylic nitroalkanes **2.3a** and **2.3ac**.

2.2.5 Mechanistic Details

Based on previous mechanistic studies carried out in our group,[94] we envision that a similar mechanistic scenario might also be operative. The proposed catalytic cycle is depicted in **SCHEME 2.11**. The cycle starts with the formation of a Pd^0-DPEPhos coordination complex (**2.V**), which upon substrate coordination can undergo oxidative addition to furnish zwitterionic *syn* allyl-Pd^{II} (**2.W**) or *anti* allyl-Pd^{II} (**2.X**) complex. These two intermediates can rapidly interconvert to one another via a π–σ–π mechanism prior to decarboxylation, which is comparably a much slower process. Importantly to the high observed *Z*/*E* selectivity, the *syn* allyl-Pd^{II} (**2.W**) will undergo such decarboxylation process much faster than the *anti* allyl-Pd^{II} complex (**2.X**), with the primary reason being the direct formation of the palladacycle (**2.Y**) having the alkoxide directly coordinated to the Pd center, which is unfeasible to attain directly from the decarboxylation of the *anti* allyl-Pd^{II} complex (**2.X**). While palladacyclic intermediate **2.Y** is still able to undergo *syn*/*anti* isomerization via π–σ–π interconversion, the isomerization process is much slower than the subsequent step leading to the preferred (*Z*) product formation. However, in the absence of a suitable pronucleophile, this intermediate can decompose to aldehyde byproducts (**2.Z** and **2.AA**) via β-*H*-elimination.[95] In our case, this pathway is kinetically competitive when secondary nitroalkanes or 1,2-disubstituted VCCs are used, as the required deprotonation of the nitroalkane pronucleophile was kinetically slowed down. In those cases, the addition of DBU helped accelerate both the deprotonation of the nitroalkane and the subsequent protonation of the palladacylic intermediate (**2.Y**). The last step in the catalytic cycle is the final nucleophilic attack of the nitronate species (**2.AC**) onto the cationic allyl-Pd^{II} intermediate (**2.AB**), yielding the allylated nitroalkane product and regenerating the active Pd^0-DPEPhos species (**2.V**). Further allylation of the product can be explained by the direct deprotonation and subsequent nucleophilic attack onto the cationic allyl-Pd^{II} intermediate (**2.AB**). Analogous to the polyalkylation of amines with alkyl halides, the extent of further allylation is favored by electronic effects (*i.e.,* by electron donation through hyperconjugation of the additional allyl group to the nitronate anion), but is disfavored by steric effects. Therefore, sterically crowded primary nitroalkanes (*e.g.,* **2.2j**) gave the desired homoallylic nitroalkane products in better yields than less hindered derivatives (*e.g.*, nitroethane **2.2a**).

[94] See Kleij, A. W. *et al. Angew. Chem. Int. Ed.* **2016** (*ref.* 53b), and Kleij, A. W. *et al. J. Am. Chem. Soc.* **2016** (*ref.* 53c) on page 30.

[95] This process has been previously reported and studied by DFT calculations, see Kleij, A. W. *et al. J. Am. Chem. Soc.* **2018** (*ref.* 75a) on page 36.

Finally, is it worth noting that the nucleophilic attack happens exclusively at the terminal carbon of the allyl group (*i.e.,* the less hindered side). The observed regioselectivity is also in line with computational calculations on the (allyl)Pd^{II}-DPEPhos system using aryl amines as pronucleophiles, suggesting that an outer-sphere nucleophilic attack is favored at the terminal carbon.[96]

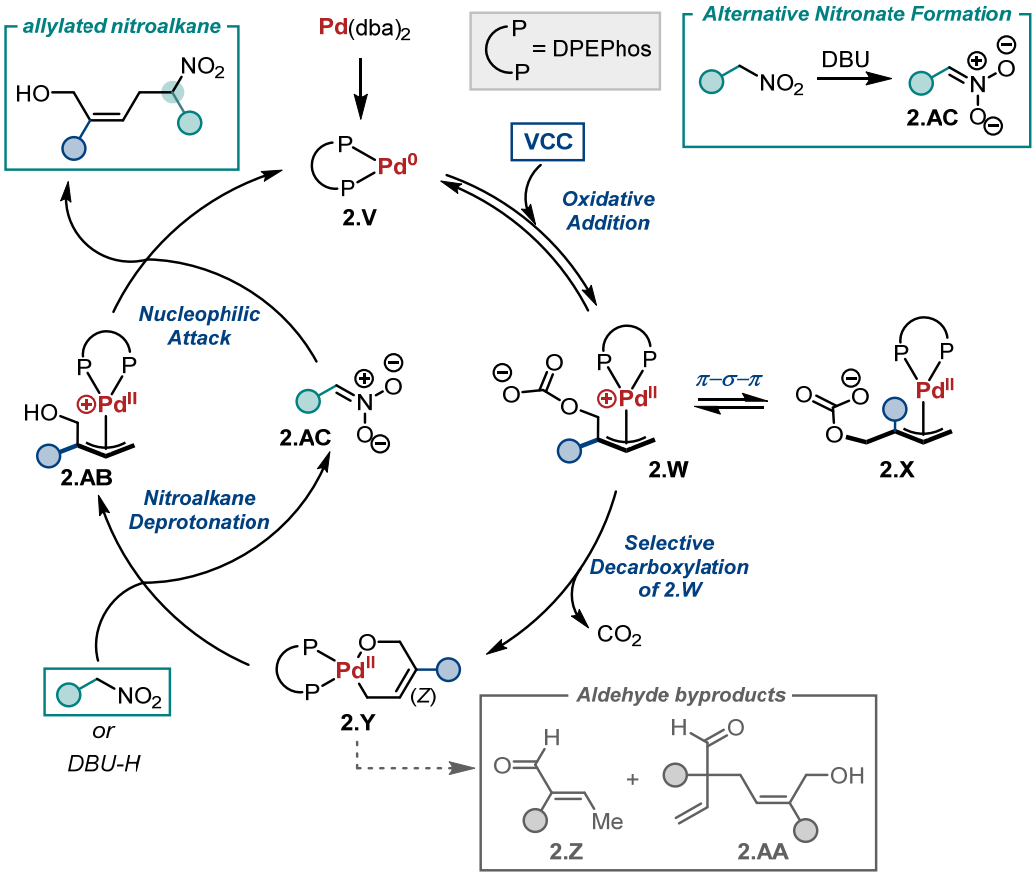

SCHEME 2.11. Mechanistic proposal for the (poly)allylation of nitroalkanes by VCCs.

[96] See Kleij, A. W. *et al. J. Am. Chem. Soc.* **2016** (*ref.* 50a) on page 29.

2.3 Conclusions

This chapter clearly demonstrates that the previously developed repertoire of (pro)nucleophiles (*N*-, *O*-, *S*- and *B*-based ones) used in allylic substitution reactions based on VCCs as reagents can be extended to carbon-based ones. A wide range of nitroalkanes can be effectively allylated with easily prepared and modular VCCs under effective Pd-catalysis. Moreover, the developed method features attractive functional group diversity and operational simplicity, and importantly, the produced homoallylic nitroalkane compounds are typically obtained in excellent (*Z*)-stereo- and linear regio-selectivity, thus allowing access to stereodefined tri- and tetrasubstituted olefins. Furthermore, our developed protocol allows for the introduction of multiple allyl groups within the nitroalkane scaffold using different VCCs, offering entries to bis- and trisallylated functional nitroalkanes while mostly preserving excellent stereoselectivity and good yields, even when starting from challenging nitromethane as pronucleophile. Lastly, these homoallylic nitroalkanes are easily transformed into useful (*Z*)-configured tri- and tetrasubstituted homoallylic amines or elusive (*Z*)-configured β,γ-unsaturated ketones, thus providing an entry for the synthesis of more elaborated compounds.

2.4 Experimental Section

2.4.1 General Information

Methods: Air and water-sensitive reactions were carried out in flame-dried glassware under an Ar atmosphere using standard Schlenk techniques. Reactions were monitored by TLC or ^{1}H NMR spectroscopy. TLC was carried out on 0.25 mm Merck aluminum-backed sheets coated with 60 F_{254} silica gel. Visualization of the silica plates was achieved using a UV lamp (λ = 254 nm) and/or by heating plates that were dipped into a $KMnO_4$ or a ceric ammonium molybdate stain. Flash chromatography was carried out on Sigma-Aldrich silica gel 60 (70-230 mesh) using the indicated eluent system. In the screening phase, the internal standard was added after the reaction. Hereafter, an aliquot of the resulting mixture was taken, and the yield was determined by means of ^{1}H NMR spectroscopy using $CDCl_3$ as the solvent.

Reagents and Solvents: Commercially available reagents and solvents were purchased from Sigma-Aldrich, TCI, Strem Chemicals, Abcr GmbH, Acros Organics, or Alfa Aesar, and were used without further purification. Zinc dust was activated using a previously reported procedure and was stored in a glovebox.[97] Solvents were dried using an Innovative Technology PURE SOLV solvent purification system.

Analytical Techniques: ^{1}H NMR, ^{13}C NMR, DEPT-90, DEPT-135, and related 2D NMR (gCOSY90, gHMQC, gHMBC, gNOESY) spectra were recorded at room temperature on a Bruker AV-300, AV-400, or AV-500 spectrometer and referenced to their residual deuterated solvent signals. ^{19}F NMR spectra were recorded on a Bruker AV-400. Coupling constants (J) are reported in Hertz with the following splitting abbreviations: s = singlet, d = doublet, t = triplet, q = quadruplet, quint = quintet, sextet = sext, br = broad and app = apparent. All reported NMR values are given in parts per million (ppm). FT-IR measurements were carried out on a Bruker Optics FTIR Alpha spectrometer. Mass spectrometric and X-ray analyses were performed by the Research Support Unit at ICIQ.

2.4.2 General Procedure for the Synthesis of Vinyl Cyclic Carbonates

Apart from 4-vinyl-1,3-dioxolan-2-one (**2.1k**), which was directly purchased from Sigma-Aldrich and used as received, vinyl cyclic carbonates **2.1a-2.1o** were prepared using a previously reported procedure from readily available aldehydes (**2.AD**) with minor modifications.[98] 4-Phenyl-4-vinyl-1,3-dioxolan-2-one (**2.1a**), 4-methyl-4-vinyl-1,3-dioxolan-2-one (**2.1j**), and 4-phenyl-4-(prop-1-en-2-yl)-1,3-dioxolan-2-one

[97] Yamamura, S.; Toda, M.; Hirata, Y. *Org. Synth.* **1973**, *53*, 86.
[98] See Kleij, A. W. *et al. Angew. Chem. Int. Ed.* **2016** (*ref.* 53b) on page 30.

(**2.1l**) were prepared directly from their commercially available hydroxymethyl ketones (**2.AF**). 4-Phenyl-4-(prop-1-en-2-yl)-1,3-dioxolan-2-one (**2.1l**) was prepared using isopropenylmagnesium bromide, instead of vinylmagnesium bromide. Organocatalyst **2.AE** was prepared according to a slightly modified literature procedure.[99]

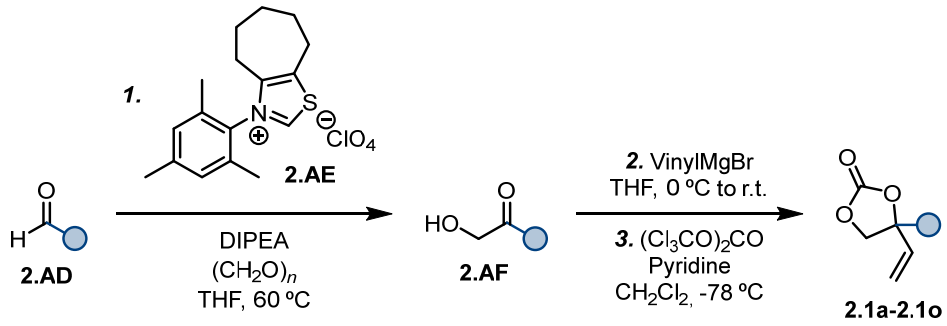

SCHEME 2.12. General synthesis of vinyl cyclic carbonates from readily available aldehydes.

Step 1: In a flame-dried round-bottomed flask, organocatalyst **2.AE** (10 mol%) and paraformaldehyde (3.0 equiv.) were suspended in dry THF (0.25 M) under N_2. Then, aldehyde **2.AD** (1.0 equiv.) and DIPEA (20 mol%) were added, respectively. The mixture was stirred at 60 °C (oil bath) for 24 h. Hereafter, the mixture was concentrated *in vacuo* and the residue was purified by flash chromatography on silica gel to afford the corresponding hydroxymethyl ketone **2.AF**.

Step 2: In a flame-dried Schlenk flask, the corresponding hydroxymethyl ketone **2.AF** (1.0 equiv.) was dissolved in dry THF (0.4 M) under N_2. The solution was cooled to 0 °C (ice-water bath) and vinylmagnesium bromide (2.5 equiv., 1 M in THF) was added dropwise over 20 min. After the addition, the mixture was allowed to warm to room temperature and was stirred for 2.5 h to 5 h. The reaction was quenched at 0 °C (ice-water bath) with aqueous saturated NH_4Cl and the phases were separated. The aqueous phase was extracted with EtOAc. The combined organic layers were washed with brine, dried over $MgSO_4$, filtered, and concentrated *in vacuo*. The crude product was used in the next step without further purification.

Step 3: In a flame-dried Schlenk flask, the crude 1,2-diol product was dissolved in dry CH_2Cl_2 (0.33 M) under N_2. Then, anhydrous pyridine (6.0 equiv.) was added, and the mixture was cooled to −78 °C (dry ice-acetone bath). Then, a solution of triphosgene (0.5 equiv.) in dry CH_2Cl_2 (0.5 M) was cannulated into the mixture dropwise over 15-30 min. Hereafter, the mixture was stirred for 30 min, and the reaction was monitored by TLC. In the case of incomplete conversion, the reaction mixture was allowed to warm to room temperature and was stirred for a further 0.5-2 h. The reaction was then quenched at 0 °C (ice-water bath)

[99] Piel, I.; Pawelczyk, M. D.; Hirano, K.; Fröhlich, R.; Glorius, F. *Eur. J. Org. Chem.* **2011**, 5475-5484.

with aqueous saturated NH_4Cl and the phases were separated. The aqueous phase was extracted with CH_2Cl_2 and the combined organic layers were washed with 1 M HCl and brine and were dried over Na_2SO_4, filtered, and concentrated *in vacuo*. The crude product was purified by flash chromatography on silica gel (CH_2Cl_2/hexanes) to afford the corresponding cyclic carbonates **2.1a-2.1o**. For all known VCC compounds that were synthesized in this chapter, spectroscopic data are in agreement with published data.[100]

Note: Yields of cyclic carbonates are always referred to as overall from steps 2 and 3.

4-Phenyl-4-vinyl-1,3-dioxolan-2-one (2.1a)

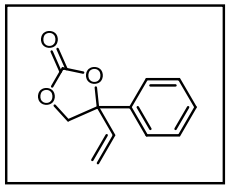

Yellowish oil (69 % yield); **^{1}H NMR** (400 MHz, $CDCl_3$) δ_H 7.46 - 7.34 (m, 5H), 6.16 (dd, J = 17.2, 10.7 Hz, 1H), 5.43 (d, J = 10.7 Hz, 1H), 5.42 (d, J = 17.2 Hz, 1H), 4.66 (d, J = 8.4 Hz, 1H), 4.58 (d, J = 8.4 Hz, 1H); **^{13}C NMR** (101 MHz, $CDCl_3$) δ_C 154.2, 138.5, 136.6, 129.1, 129.0, 125.0, 117.6, 85.6, 74.6.

4-([1,1'-Biphenyl]-4-yl)-4-vinyl-1,3-dioxolan-2-one (2.1b)

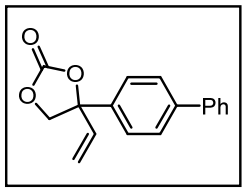

White solid (74% yield); **^{1}H NMR** (500 MHz, $CDCl_3$) δ_H 7.65 (d, J = 8.5 Hz, 2H), 7.60-7.54 (m, 2H), 7.49-7.35 (m, 5H), 6.20 (dd, J = 17.2; 10.7 Hz, 1H), 5.58-5.35 (m, 2H), 4.68 (d, J = 8.5 Hz, 1H), 4.62 (d, J = 8.5 Hz, 1H); **^{13}C NMR** (126 MHz, $CDCl_3$) δ_C 154.2, 142.1, 140.2, 137.4, 136.6, 130.5, 129.1, 128.0, 127.9, 127.3, 125.6, 117.9, 85.6, 74.7.

4-(2-Oxo-4-vinyl-1,3-dioxolan-4-yl)benzonitrile (2.1c)

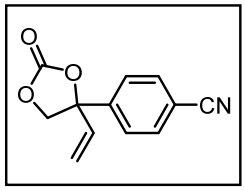

Light orange solid (277.9 mg, 24 % yield); **IR** (neat): ν = 3103, 3055, 2985, 2923, 2231, 1794, 1610, 1507, 1473, 1418, 1389, 1320, 1213, 1117, 1063, 985, 949, 841, 760, 740 cm^{-1}; **^{1}H NMR** (400 MHz, $CDCl_3$) δ_H 7.77–7.68 (m, 2H), 7.53–7.43 (m, 2H), 6.12 (dd, J = 17.2, 10.8 Hz, 1H), 5.46 (d, J = 10.8 Hz, 1H), 5.41 (d, J = 17.2 Hz, 1H), 4.70 (d, J = 8.7 Hz, 1H), 4.53 (d, J = 8.7 Hz, 1H); **^{13}C NMR** (101 MHz, $CDCl_3$) δ_C 153.4, 143.5, 135.6, 132.9, 125.8, 118.7, 118.0, 113.1, 84.9, 74.2; **HRMS** (ESI/TOF) m/z: $[M + Na]^+$ Calcd for $C_{12}H_9NO_3Na^+$ 238.0475; Found 238.0483.

Note: THF was used as solvent instead of CH_2Cl_2 in step 3 because of solubility issues.

[100] See Zhang, Y. J. *et al. Angew. Chem. Int. Ed.* **2014** (*ref.* 57) on page 31, Zhang, Y. J. *et al. Tetrahedron Lett.* **2016** (*ref.* 53a) on page 30, and Kleij, A. W. *et al. Angew. Chem. Int. Ed.* **2016** (*ref.* 53b) on page 30.

4-(3-(Trifluoromethyl)phenyl)-4-vinyl-1,3-dioxolan-2-one (2.1d)

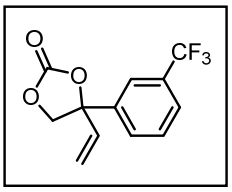

Light orange oil (1.28 g, 51 % yield); **IR** (neat): ν = 2924, 1801, 1481, 1446, 1414, 1378, 1332, 1251, 1167, 1122, 1055, 986, 940, 902, 805, 768, 701, 654 cm^{-1}; **^{1}H NMR** (400 MHz, $CDCl_3$) δ_H 7.70-7.64 (m, 1H), 7.63-7.60 (m, 1H), 7.60-7.55 (m, 2H), 6.16 (dd, J = 17.2, 10.8 Hz, 1H), 5.49 (d, J = 10.8 Hz, 1H), 5.44 (d, J = 17.2 Hz, 1H), 4.71 (d, J = 8.6 Hz, 1H), 4.56 (d, J = 8.6 Hz, 1H); **^{13}C NMR** (101 MHz, $CDCl_3$) δ_C 153.7, 139.8, 136.0, 131.7 (q, J = 32.7 Hz), 129.9, 128.4, 126.0 (q, J = 3.8 Hz), 122.0 (q, J = 3.8 Hz), 118.6, 85.1, 74.4; **^{19}F NMR** (376 MHz, $CDCl_3$) δ_F -62.9; **HRMS** (ESI/TOF) m/z: $[M + Na]^+$ Calcd for $C_{12}H_9F_3O_3Na^+$ 281.0396; Found 281.0400.

4-(Benzo[*d*][1,3]dioxol-5-yl)-4-vinyl-1,3-dioxolan-2-one (2.1e)

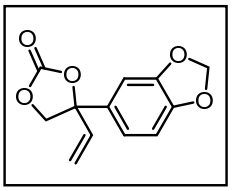

Yellowish oil (65% yield); **^{1}H NMR** (400 MHz, $CDCl_3$) δ_H 6.85– 6.82 (m, J = 3H), 6.11 (dd, J = 10.4,16.8 Hz, 1H), 6.00 (s, 2H), 5.44 (d, J = 3.2 Hz, 1H), 5.40 (d, J = 3.2 Hz, 1H), 4.60 (d, J = 8.4 Hz,1H), 4.54 (d, J = 8.4 Hz, 1H); **^{13}C NMR** (101 MHz, $CDCl_3$) δ_C 153.9, 148.3, 148.0, 136.4, 132.0, 118.6, 117.5, 108.4, 105.8, 101.5, 85.4, 74.4.

4-(Naphthalen-2-yl)-4-vinyl-1,3-dioxolan-2-one (2.1f)

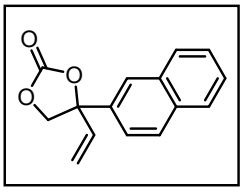

White solid (70% yield); **^{1}H NMR** (500 MHz, $CDCl_3$) δ_H 8.05-7.84 (m, 1H), 7.78 (dd, J = 7.4; 1.2 Hz, 1H), 7.56-7.40 (m, 2H), 6.40 (dd, J = 17.2; 10.7 Hz, 2H), 5.55-5.24 (m, 2H), 5.00 (d, J = 8.5 Hz, 1H), 4.79 (d, J = 8.5 Hz, 1H); **13C NMR** (126 MHz, $CDCl_3$) δ_C 153.8, 136.8, 134.5, 130.1, 129.7, 128.8, 126.7, 126.1, 125.4, 124.5, 123.4, 120.1, 86.1, 74.9.

4-(Thiophen-3-yl)-4-vinyl-1,3-dioxolan-2-one (2.1g)

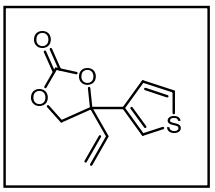

Yellowish oil (60% yield); **^{1}H NMR** (400 MHz, $CDCl_3$) δ_H 7.41-7.39 (m, 1H), 7.35-7.34 (m, 1H), 7.07-7.05 (m, 1H), 6.17 (dd, J = 10.4, 17.2, Hz, 1H), 5.43 (d, J = 17.2 Hz, 1H), 5.43 (d, J = 10.4 Hz, 1H), 4.59 (d, J = 8.4, Hz, 1H), 4.05 (d, J = 8.8, Hz, 1H); **^{13}C NMR** (101 MHz, $CDCl_3$) δ_C 153.9, 139.0, 135.6, 127.5, 124.9, 122.9, 117.6, 83.6, 74.2.

4-(Furan-2-yl)-4-vinyl-1,3-dioxolan-2-one (2.1h)

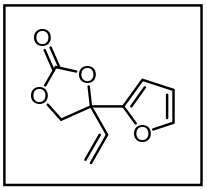

Yellowish oil (42% yield); **^{1}H NMR** (500 MHz, $CDCl_3$) δ_H 7.61-7.40 (m, 2H), 6.41 (dd, J = 1.7; 1.2 Hz, 1H), 6.13 (dd, J = 17.2; 10.7 Hz, 1H), 5.59-5.33 (m, 2H), 4.51 (d, J = 8.5 Hz, 1H), 4.48 (d, J = 8.5 Hz, 1H); **^{13}C NMR** (126 MHz, $CDCl_3$) δ_C 154.1, 144.8, 140.7, 135.2, 124.3, 118.5, 108.4, 81.7, 74.2.

4-Cyclohexyl-4-vinyl-1,3-dioxolan-2-one (2.1i)

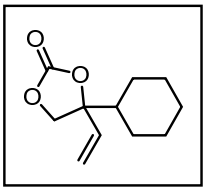

Yellowish oil (48% yield); **^{1}H NMR** (500 MHz, $CDCl_3$) δ_H 5.85 (dd, J = 17.2; 10.7 Hz, 1H), 5.61-5.27 (m, 2H), 4.32 (d, J = 8.4 Hz, 1H), 4.22 (d, J = 8.4 Hz, 1H), 1.91-1.61 (m, 7H), 1.40-0.93 (m, 4H); **^{13}C NMR** (126 MHz, $CDCl_3$) δ_C 154.7, 134.8, 116.9, 87.3, 72.2, 45.6, 26.7, 26.5, 26.2, 26.1, 25.8.

4-Methyl-4-vinyl-1,3-dioxolan-2-one (2.1j)

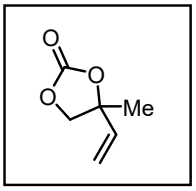

Yellowish oil (50% yield); **^{1}H NMR** (500 MHz, $CDCl_3$) δ_H 5.94 (dd, J = 17.2; 10.7 Hz, 1H), 5.44 (d, J = 17.2 Hz, 1H), 5.33 (d, J = 10.7 Hz, 1H), 4.27 (d, J = 8.3 Hz, 1H), 4.18 (d, J = 8.3 Hz, 1H), 1.60 (s, 3H); **^{13}C NMR** (126 MHz, $CDCl_3$) δ_C 154.5, 137.0, 116.7, 82.7, 74.5, 24.3.

4-Phenyl-4-(prop-1-en-2-yl)-1,3-dioxolan-2-one (2.1l)

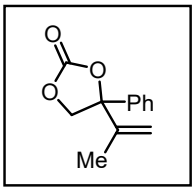

White solid (64% yield); **^{1}H NMR** (500 MHz, $CDCl_3$) δ_H 7.44–7.33 (m, 5H), 5.19 (s, 1H), 5.16 (s, 1H), 4.79 (d, J = 8.5 Hz, 1H), 4.63 (d, J = 8.5 Hz, 1H), 1.73 (s, 3H); **^{13}C NMR** (126 MHz, $CDCl_3$) δ_C 154.1, 143.0, 138.5, 129.0, 125.1, 114.1, 88.1, 73.2, 18.6.

4-(2-Methoxyphenyl)-4-vinyl-1,3-dioxolan-2-one (2.1m)

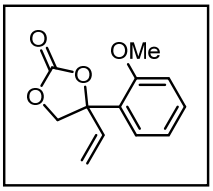

Yellowish oil (89% yield); **^{1}H NMR** (400 MHz, $CDCl_3$) δ_H 7.51 (dd, J = 7.6, 1.7 Hz, 1H), 7.35 (ddd, J = 8.2, 7.5, 1.7 Hz, 1H), 7.02 (td, J = 7.6, 1.1 Hz, 1H), 6.94 (dd, J = 8.2, 1.1 Hz, 1H), 6.23 (dd, J = 17.1, 10.7 Hz, 1H), 5.40 (d, J = 17.1 Hz, 1H), 5.25 (d, J =10.7 Hz, 1H), 4.74 (d, J = 8.8 Hz, 1H), 4.54 (d, J = 8.8 Hz, 1H), 3.85 (s, 3H); **^{13}C NMR** (101 MHz, $CDCl_3$) δ_C 154.9, 154.3, 136.4, 130.1, 127.6, 125.7, 121.4, 115.6, 111.2, 84.8, 75.2, 55.6.

4-(2-Bromophenyl)-4-vinyl-1,3-dioxolan-2-one (2.1n)

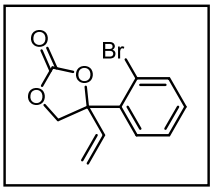

Yellowish oil (57% yield); **^{1}H NMR** (500 MHz, $CDCl_3$) δ_H 7.70 (dd, J = 7.8, 1.7 Hz, 1H), 7.62 (dd, J = 7.8, 1.2 Hz, 1H), 7.41 (td, J = 7.8, 1.2 Hz, 1H), 7.25 (td, J = 7.8, 1.9 Hz, 1H), 6.36 (dd, J = 17.0, 10.6 Hz, 1H), 5.40 (d, J = 10.6 Hz, 1H), 5.40 (d, J = 17.0 Hz, 1H), 4.97 (d, J = 9.0 Hz, 1H), 4.73 (d, J = 9.0 Hz, 1H); **^{13}C NMR** (126 MHz, $CDCl_3$) δ_C 153.5, 138.8, 135.1, 134.4, 130.5, 128.2, 127.5, 119.1, 118.6, 85.6, 74.6.

4-(*m*-Tolyl)-4-vinyl-1,3-dioxolan-2-one (2.1o)

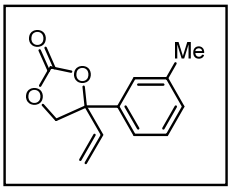

Yellowish oil (75% yield); **^{1}H NMR** (500 MHz, $CDCl_3$): δ_H 7.31-7.27 (m, 1H), 7.19-7.16 (m, 2H), 7.13-7.10 (m, 1H), 6.15 (dd, J = 17.2, 10.8 Hz, 1H), 5.42 (d, J = 17.2 Hz, 1H), 5.41 (d, J = 10.8 Hz, 1H), 4.64 (d, J = 8.4 Hz, 1H), 4.56 (d, J = 8.4 Hz, 1H), 2.38 (s, 3H); **^{13}C NMR** (126 MHz, $CDCl_3$) δ_C 154.2, 139.0, 138.5, 136.7, 129.7, 129.0, 125.5, 122.0, 117.5, 85.6, 74.7, 21.6.

2.4.3 Synthesis of Nitroalkanes Pronucleophiles

Nitroethane (**2.2a**), 1-nitropropane (**2.2b**), 1-nitropentane (**2.2c**), α-nitrotoluene (**2.2d**), nitromethyl phenyl sulfone (**2.2e**), ethyl nitroacetate (**2.2f**), 2-nitroethanol (**2.2g**), 2-nitropropane (**2.2p**), benzoylnitromethane (**2.2q**) and nitromethane (**2.2r**) were purchased from Sigma-Aldrich or TCI and were used without further purification.

1-Chloro-3-nitropropane (2.2h)

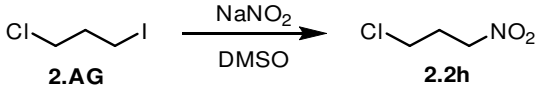

2.AG **2.2h**

According to a previously published procedure,[101] in a 100 mL round-bottomed flask, 1-chloro-3-iodopropane **2.AG** (2.09 g, 10.24 mmol) was dissolved in dry DMSO (20 mL) under Ar. The flask was then wrapped with aluminum foil and $NaNO_2$ (707 mg, 10.24 mmol) was added in small batches. The mixture was stirred at room temperature for 3 h. The reaction was quenched with H_2O and the product was extracted with Et_2O. The organic phase was washed three times with H_2O and once with brine. It was then dried over $MgSO_4$, filtered, and concentrated *in vacuo*. The crude product was purified by flash chromatography on silica gel using 10% EtOAc/cyclohexane to afford nitroalkane **2.2h** as a yellowish oil (43.4 mg, 3% yield).

[101] Kai, Y.; Knochel, P.; Kwiatkowski, S.; Dunitz, J. D.; Oth, J. F. M.; Seebach, D.; Kalinowski, H.-O. *Helv. Chim. Acta* **1982**, *65*, 137-161.

^{1}H NMR (500 MHz, $CDCl_3$) δ_H 4.58 (t, J = 6.6 Hz, 2H), 3.65 (t, J = 6.1 Hz, 2H), 2.45 (quint, J = 6.4 Hz, 2H); **^{13}C NMR** (126 MHz, $CDCl_3$) δ_C 72.2, 40.9, 29.8. Spectroscopic data are in agreement with published data.[102]

tert-Butyl 4-nitrobutanoate (2.2i)

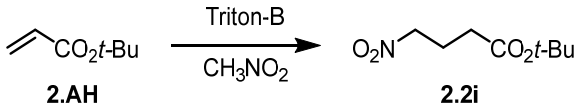

2.AH **2.2i**

According to a previously published procedure,[103] in a 100 mL round-bottomed flask, *tert*-butyl acrylate **2.AH** (1.5 mL, 10.0 mmol) was dissolved in CH_3NO_2 (27.5 mL). Then, Triton-B (90.0 μL, 0.20 mmol) was added in one portion and the mixture was stirred at room temperature for 16 h. After that, the mixture was concentrated in vacuo (approx. to 5 mL of CH_3NO_2). The residue was diluted with H_2O and extracted with Et_2O. The organic phase was washed with brine, dried over $MgSO_4$, filtered, and concentrated *in vacuo*. The product **2.2i** (1.06 g, 56% yield) was dried under high vacuum and was used without further purification. **^{1}H NMR** (500 MHz, $CDCl_3$) δ_H 4.46 (t, J = 6.7 Hz, 2H), 2.37 (t, J = 6.7 Hz, 2H), 2.27 (quint, J = 6.7 Hz, 2H), 1.45 (s, 9H); **^{13}C NMR** (126 MHz, $CDCl_3$) δ_C 171.3, 81.5, 74.6, 31.9, 28.4, 22.8. Spectroscopic data are in agreement with published data.[104]

1,1-Dimethoxy-3-nitropropane (2.2j)

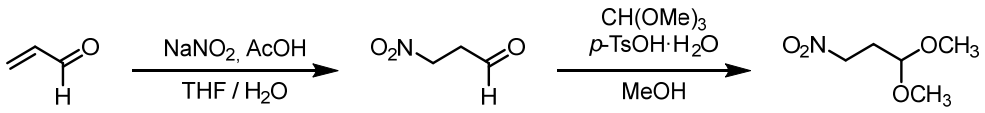

2.AI **2.AJ** **2.2j**

According to a previously published procedure,[105] in a 100 mL round-bottomed flask, $NaNO_2$ (1.74 g, 25.20 mmol) was dissolved in H_2O (5 mL) and THF (8 mL) under N_2. The mixture was cooled to 0 °C (ice-water bath) and acrolein **2.AI** (1.5 mL, 20.0 mmol) was added. The flask was wrapped with aluminum foil and AcOH (1.3 mL, 22.0 mmol) was added dropwise over 5 minutes. The mixture was stirred at 0 °C for 4 h. After that, the mixture was diluted with EtOAc (10 mL) and aqueous saturated $NaHCO_3$ (5 mL) was added. The organic phase was separated, and the aqueous phase was extracted with EtOAc twice. The combined organic layers were washed with brine, dried over Na_2SO_4, filtered, and concentrated *in vacuo*. The

[102] Zhao, M.; Lu, W. *Org. Lett.* **2017**, *19*, 4560-4563.
[103] Newkome, G. R.; Kim, H. J.; Moorefield, C. N.; Maddi, H.; Yoo, K.-S. *Macromolecules* **2003**, *36*, 4345-4354.
[104] See Watson, D. A. *et al. J. Am. Chem. Soc.* **2017** (*ref.* 84b) on page 41.
[105] Griesser, H.; Öhrlein, R.; Schwab, W.; Ehrler, R.; Jäger, V. *Org. Synth.* **2003**, *77*, 236-236.

yellowish oil was then azeotropically distilled with toluene once and was dried under high vacuum. Product **2.AJ** was used in the next step without further purification.

In a 25 mL round-bottomed flask, crude 3-nitropropanal **2.AJ** (1.43 g, 12.49 mmol) was dissolved in MeOH (5 mL) and $CH(OMe)_3$ (1.8 mL, 16.43 mmol) was added. The mixture was cooled to 0 ºC (ice-water bath) and *p*-TsOH H_2O (49.3 mg, 0.26 mmol) was added. The mixture was allowed to warm to room temperature and was stirred overnight. Hereafter, the reaction was quenched with aqueous saturated $NaHCO_3$ and was extracted with EtOAc three times. The combined organic layers were washed with brine, dried over Na_2SO_4, filtered, and concentrated *in vacuo*. The crude product was purified by flash chromatography on silica gel using 10-20% EtOAc/cyclohexane to afford nitroalkane **2.2j** as a yellowish oil (1.25 g, 67% yield). **^{1}H NMR** (500 MHz, $CDCl_3$) δ_H 4.47 (t, J = 5.6 Hz, 2H), 4.44 (t, J = 7.0 Hz, 1H), 3.36 (s, 6H), 2.30 (td, J = 6.9, 5.3 Hz, 2H); **^{13}C NMR** (126 MHz, $CDCl_3$) δ_C 102.0, 71.3, 54.2, 30.6. Spectroscopic data are in agreement with published data.[105]

(2-Nitroethane-1,1-diyl)bis(methylsulfane) (2.2k)

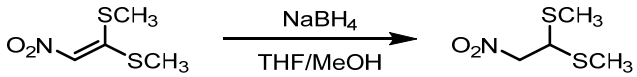

2.AK **2.2k**

The following protocol was adapted from a previously reported procedure.[106] In a flame-dried 100 mL round-bottomed flask, $NaBH_4$ (454 mg, 12.0 mmol) was dissolved in dry THF (11 mL) and dry MeOH (3.8 mL) under Ar. The solution was cooled to 0 °C (ice-water bath) and a solution of 1,1-bis(methylthio)-2-nitroethylene **2.AK** (1.65 g, 10.0 mmol) in dry THF (15 mL) was added. The mixture was warmed to room temperature and was stirred for 24 h. The reaction was quenched with aqueous saturated NH_4Cl, was diluted with H_2O, and was extracted with EtOAc. The organic phase was washed with H_2O and brine, dried over Na_2SO_4, filtered, and concentrated *in vacuo*. The crude product was purified by flash chromatography on silica gel using 3% EtOAc/cyclohexane to afford nitroalkane **2.2k** as a colorless oil (768.5 mg, 46% yield). **^{1}H NMR** (500 MHz, $CDCl_3$) δ_H 4.61 (d, J = 7.7 Hz, 2H), 4.36 (t, J = 7.7 Hz, 1H), 2.19 (s, 6H); **^{13}C NMR** (126 MHz, $CDCl_3$) δ_C 77.9, 50.2, 13.2. Spectroscopic data are in agreement with published data.[106]

[106] Hamberger, H.; Stütz, P.; Schulz, G. *Tetrahedron Lett.* **1977**, *18*, 3623-3624.

N-(2-Nitroethyl)aniline (2.2l)

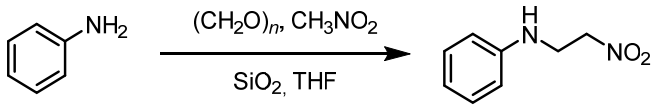

2.AL **2.2l**

According to a previously published procedure,[107] in a 100 mL round-bottomed flask, aniline **2.AL** (911 µL, 10.0 mmol) was suspended in THF (10 mL) and it was cooled to 0 °C (ice-water bath). Then, paraformaldehyde (316.1 mg, 10.0 mmol) was added, and the mixture was stirred for 1 h. After that, CH_3NO_2 (5.4 mL, 100 mmol) and silica gel (1 g) were added, and the resulting mixture was stirred at 70 °C (oil bath) for 72 h. The resulting yellow suspension was filtered, and the filtrate was concentrated *in vacuo*. The crude product was purified by flash chromatography on silica gel using 5-10% EtOAc/cyclohexane to afford nitroalkane **2.2l** as a yellowish oil (886.3 mg, 53% yield). **^{1}H NMR** (500 MHz, $CDCl_3$) δ_H 7.24-7.19 (m, 2H), 6.83-6.75 (m, 1H), 6.67-6.60 (m, 2H), 4.61-4.56 (m, 2H), 4.03 (br s, 1H), 3.85-3.79 (m, 2H); **^{13}C NMR** (126 MHz, $CDCl_3$) δ_C 146.3, 129.7, 118.9, 113.3, 74.4, 41.3. Spectroscopic data are in agreement with published data.[107]

N-(2-Nitroethyl)phthalimide (2.2m)

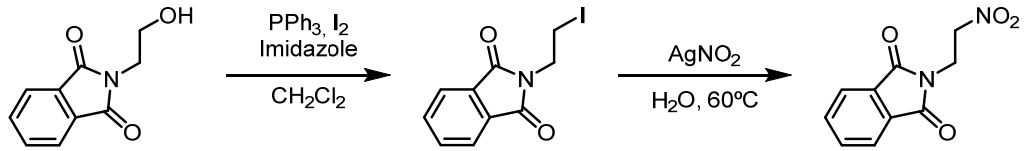

2.AM **2.AN** **2.2m**

The following protocol was adapted from a previously reported procedure.[108] In an oven-dried 100 mL round-bottomed flask, PPh_3 (4.72 g, 18.0 mmol) and imidazole (1.38 g, 19.5 mmol) were dissolved in dry CH_2Cl_2 under Ar. The mixture was cooled to 0 °C (ice-water bath), and I_2 (4.57 g, 18 mmol) was added. After stirring the mixture for 15 minutes, *N*-(2-hydroxyethyl)phthalimide **2.AM** (2.87 g, 15.0 mmol) was added. The mixture was stirred at 0 °C for 30 minutes and then at room temperature for 4 h. Hereafter, the reaction was diluted with H_2O and the layers were separated. The aqueous phase was extracted with CH_2Cl_2, and the combined organic layers were dried over Na_2SO_4, filtered, and concentrated *in vacuo*. The crude product was purified by flash chromatography on silica gel using 10% EtOAc/hexanes to afford *N*-(2-iodoethyl)phthalimide **2.AN** as a white solid (4.19 g, 93% yield).

[107] Manna, M. S.; Mukherjee, S. *J. Am. Chem. Soc.* **2015**, *137*, 130-133.
[108] See Watson, D. A. *et al. J. Am. Chem. Soc.* **2017** (*ref.* 84b) on page 41.

In a 100 mL round-bottomed flask, *N*-(2-iodoethyl)phthalimide **2.AN** (3.77 g, 12.5 mmol) was suspended in H_2O (25 mL) and then, $AgNO_2$ (7.70 g, 50.0 mmol) was added. The flask was wrapped with aluminum foil and the mixture was heated at 60 °C (oil-bath) for 6 h. Hereafter, the mixture was filtered through a pad of Celite, and the filtrate was extracted with EtOAc. The combined organic layers were washed with brine, dried over $MgSO_4$, filtered, and concentrated *in vacuo*. The crude product was purified by flash chromatography on silica gel using 20-30% EtOAc/cyclohexane to afford nitroalkane **2.2m** as a white solid (645 mg, 23% yield). **IR** (neat): ν = 3463, 3096, 3066, 3031, 3004, 2965, 2927, 1771, 1701, 1608, 1549, 1418, 1394, 1343, 1302, 1229, 1186, 1143, 1087, 1043, 1018, 961, 877, 806, 717 cm^{-1}; **^{1}H NMR** (500 MHz, $CDCl_3$) δ_H 7.91-7.84 (m, 2H), 7.79-7.72 (m, 2H), 4.72 (app t, J = 6.1 Hz, 2H), 4.32 (app t, J = 6.1 Hz, 2H); **^{13}C NMR** (126 MHz, $CDCl_3$) δ_C 167.6, 134.6, 131.8, 123.9, 72.3, 35.3; **HRMS** (ESI/TOF) *m/z*: $[M + Na]^+$ Calcd for $C_{10}H_8N_2O_4Na^+$ 243.0376; Found 243.0374.

3-(2-Nitroethyl)-1*H*-indole (2.2n)

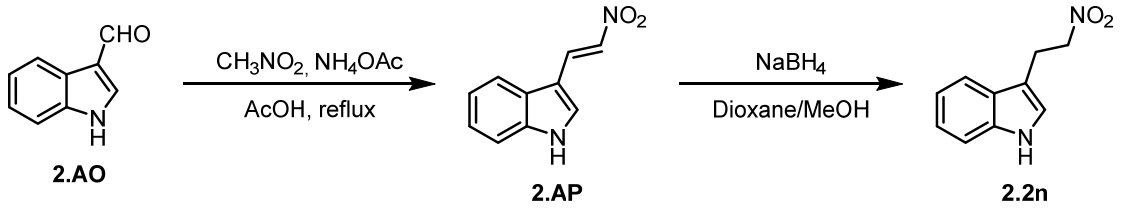

According to a previously published procedure,[109] in a 100 mL round-bottomed flask, indole 3-carboxaldehyde **2.AO** (1.45 g, 10.0 mmol) and NH_4OAc (1.93 g, 25.0 mmol) were dissolved in AcOH (20 mL). Then, CH_3NO_2 (1.7 mL, 31.0 mmol) was added dropwise, and the mixture was stirred overnight at reflux. Hereafter, the mixture was cooled to room temperature and poured into a beaker containing ice water. The resulting slurry was filtered under vacuum and the solid was washed with cold H_2O. The crude product was purified by flash chromatography on silica gel using 5-10% EtOAc/cyclohexane to afford (*E*)-3-(2-nitrovinyl)-1*H*-indole **2.AP** as a brownish solid (1.88 g, 43% yield).

In an oven-dried 100 mL round-bottomed flask, $NaBH_4$ (195.4 mg, 5.16 mmol) was dissolved in dry 1,4-dioxane (4.8 mL) and dry MeOH (1.6 mL) under Ar. The solution was cooled to 0 °C (ice-water bath) and a solution of (*E*)-3-(2-nitrovinyl)-1*H*-indole **2.AP** (810 mg, 4.30 mmol) in dry 1,4-dioxane (6.5 mL) was added dropwise over 20 minutes. Then, the mixture was allowed to warm to room temperature and was stirred overnight. The reaction was quenched with aqueous saturated NH_4Cl and was diluted with H_2O. The aqueous phase was extracted with CH_2Cl_2, and the organic phase was washed with brine, dried over Na_2SO_4, filtered, and concentrated *in vacuo*. The crude product was purified by flash chromatography on silica gel

[109] Cai, S.; Zhao, X.; Wang, X.; Liu, Q.; Li, Z.; Wang, D. Z. *Angew. Chem. Int. Ed.* **2012**, *51*, 8050-8053.

using 10% EtOAc/cyclohexane to afford nitroalkane **2.2n** as a white solid (186.7 mg, 23% yield). **^{1}H NMR** (400 MHz, $CDCl_3$) δ_H 8.08 (s, 1H), 7.62-7.55 (m, 1H), 7.42-7.35 (m, 1H), 7.28-7.19 (m, 1H), 7.22-7.12 (m, 1H), 7.10-7.04 (m, 1H), 4.67 (t, J = 7.3 Hz, 2H), 3.50 (t, J = 7.3 Hz, 2H); **^{13}C NMR** (101 MHz, $CDCl_3$) δ_C 136.4, 126.8, 122.7, 120.0, 118.3, 111.6, 110.2, 75.9, 23.8. Spectroscopic data are in agreement with published data.[109]

2-(2-Nitroethyl)furan (2.2n)

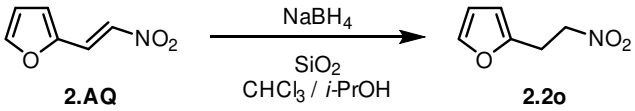

According to a previously published procedure,[107] in a 500 mL round-bottomed flask, 2-(2-nitrovinyl)furan **2.AQ** (1.39 g, 10.0 mmol) was dissolved in $CHCl_3$ (160 mL) and *i*-PrOH (30 mL). Then, silica gel (15 g) was added and the mixture was stirred vigorously. $NaBH_4$ (1.55 g, 41.0 mmol) was added in small batches over 15 minutes at room temperature. After the addition, the mixture was stirred for 2 h and then was quenched with 1 M HCl (40 mL). The resulting slurry was filtered, and the filtrate was concentrated *in vacuo*. The residue was dissolved in CH_2Cl_2 and was washed with 1 M HCl and brine. The resulting organic phase was dried over Na_2SO_4, filtered, and concentrated *in vacuo*. The crude product was purified by flash chromatography on silica gel using 5% EtOAc/cyclohexane to afford nitroalkane **2.2o** as a colorless oil (770 mg, 55% yield). **^{1}H NMR** (500 MHz, $CDCl_3$) δ_H 7.36-7.32 (m, 1H), 6.30 (dd, J = 3.2, 1.9 Hz, 1H), 6.16-6.12 (m, 1H), 4.64 (t, J = 7.1 Hz, 2H), 3.36 (t, J = 7.1 Hz, 2H); **^{13}C NMR** (126 MHz, $CDCl_3$) δ_C 149.5, 142.4, 110.6, 107.5, 73.5, 26.2. Spectroscopic data are in agreement with published data.[107]

2.4.4 General Procedure for the Synthesis of Homoallylic Nitroalkanes

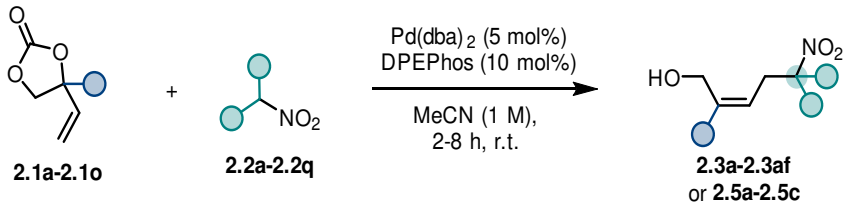

SCHEME 2.13. Standard procedure for the synthesis of homoallylic nitroalkanes.

General Procedure A: In a 5 mL vial, cyclic carbonate **2.1a-2.1o** (1.0 equiv.), $Pd(dba)_2$ (5 mol%), DPEPhos (10 mol%) and nitroalkane **2.2a-2.2q** (1.5 equiv.) were dissolved in MeCN (1.0 M). The vial was sealed with a septum and a needle was placed through the septum to release gaseous CO_2. The mixture was stirred open to air for 2-8 h at room temperature. Hereafter, the solvent was evaporated with a gentle stream

of N_2 and the residue was purified by flash chromatography on silica gel to afford the corresponding homoallylic nitroalkane **2.3a-2.3af** or bisallylated nitroalkane **2.5a-2.5c** (**SCHEME 2.13**).

(*Z*)-5-Nitro-2-phenylhex-2-en-1-ol (2.3a)

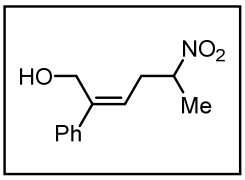

Yellowish oil (110.0 mg, 50% yield, *Z*/*E*>99:1); **IR** (neat): ν = 3573, 3387, 3058, 2938, 1543, 1493, 1446, 1388, 1359, 1312, 999, 767, 697 cm^{-1}. **^{1}H NMR** (400 MHz, $CDCl_3$) δ_H 7.42-7.26 (m, 5H), 5.74 (dd, *J* = 8.2, 7.2 Hz, 1H), 4.71 (dqd, *J* = 8.2, 6.7, 5.4 Hz, 1H), 4.61-4.50 (m, 2H), 3.02 (dt, *J* = 15.0, 8.2 Hz, 1H), 2.74 (ddd, *J* = 15.0, 7.2, 5.4 Hz, 1H), 1.62 (d, *J* = 6.7 Hz, 3H), 1.52-1.46 (m, 1H); **^{13}C NMR** (101 MHz, $CDCl_3$) δ_C 143.6, 140.3, 128.7, 128.0, 126.7, 124.3, 83.3, 59.9, 34.0, 19.1; **HRMS** (ESI/TOF) *m/z*: $[M + Na]^+$ Calcd for $C_{12}H_{15}NO_3Na^+$ 244.0950; Found 244.0944.

(*Z*)-5-Nitro-2-phenylhept-2-en-1-ol (2.3b)

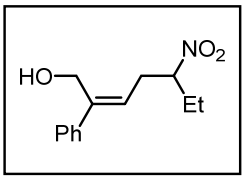

Yellowish oil (138.2 mg, 59% yield, *Z*/*E*>99:1); **IR** (neat): ν = 3574, 3403, 3057, 2973, 2937, 1543, 1493, 1460, 1443, 1373, 1326, 1011, 909, 766, 731, 697 cm^{-1}; **^{1}H NMR** (500 MHz, $CDCl_3$) δ_H 7.41-7.37 (m, 2H), 7.36-7.32 (m, 2H), 7.31-7.26 (m, 1H), 5.73 (dd, *J* = 8.8, 6.9 Hz, 1H), 4.59-4.49 (m, 3H), 3.01 (dt, *J* = 15.0, 8.8 Hz, 1H), 2.72 (ddd, *J* = 15.0, 6.9, 4.8 Hz, 1H), 2.07 (ddq, *J* = 14.6, 9.2, 7.4 Hz, 1H), 1.89 (dqd, *J* = 14.6, 7.4, 4.7 Hz, 1H), 1.52 (br t, *J* = 5.8 Hz, 1H), 1.01 (t, *J* = 7.4 Hz, 3H); **^{13}C NMR** (126 MHz, $CDCl_3$) δ_C 143.5, 140.4, 128.7, 127.9, 126.7, 124.5, 90.2, 59.9, 32.6, 27.1, 10.4; **HRMS** (ESI/TOF) *m/z*: $[M + Na]^+$ Calcd for $C_{13}H_{17}NO_3Na^+$ 258.1101; Found 258.1106.

(*Z*)-5-Nitro-2-phenylnon-2-en-1-ol (2.3c)

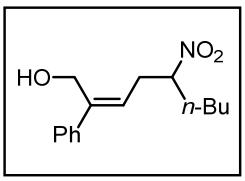

Dark red oil (212.2 mg, 81% yield, *Z*/*E*>99:1); **IR** (neat): ν = 3577, 3400, 3057, 2958, 2930, 2872, 1545, 1493, 1465, 1436, 1366, 1266, 1016, 764, 736, 697 cm^{-1}; **^{1}H NMR** (500 MHz, $CDCl_3$) δ_H 7.41-7.37 (m, 2H), 7.36-7.31 (m, 2H), 7.31-7.26 (m, 1H), 5.73 (dd, *J* = 8.5, 6.9 Hz, 1H), 4.64–4.49 (m, 3H), 3.01 (ddd, *J* = 15.0, 9.2, 8.5 Hz, 1H), 2.71 (ddd, *J* = 15.0, 6.9, 4.7 Hz, 1H), 2.11-2.01 (m, 1H), 1.85-1.77 (m, 1H), 1.49 (app dd, *J* = 6.5, 5.2 Hz, 1H), 1.41-1.30 (m, 4H), 0.95-0.89 (m, 3H); **^{13}C NMR** (126 MHz, $CDCl_3$) δ_C 143.5, 140.4, 128.7, 127.9, 126.7, 124.5, 88.8, 59.9, 33.5, 32.9, 28.0, 22.2, 13.9; **HRMS** (ESI/TOF) *m/z*: $[M + Na]^+$ Calcd for $C_{15}H_{21}NO_3Na^+$ 286.1414; Found 286.1416.

(*Z*)-5-Nitro-2,5-diphenylpent-2-en-1-ol (2.3d)

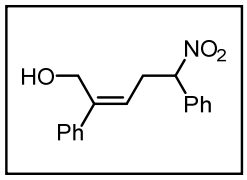

Yellowish oil (209.4 mg, 74% yield, *Z*/*E*>99:1); **IR** (neat): ν = 3574, 3402, 3061, 3032, 2899, 1546, 1494, 1455, 1364, 1010, 909, 765, 717, 694 cm^{-1}; **^{1}H NMR** (500 MHz, $CDCl_3$) δ_H 7.54-7.49 (m, 2H), 7.46-7.41 (m, 3H), 7.38-7.26 (m, 5H), 5.72 (dd, *J* = 8.2, 6.9 Hz, 1H), 5.60 (dd, *J* = 9.1, 6.0 Hz, 1H), 4.57 (d, *J* = 12.5 Hz, 1H), 4.53 (d, *J* = 12.5 Hz, 1H), 3.53 (ddd, *J* = 15.0, 9.1, 8.2 Hz, 1H), 3.03 (ddd, *J* = 15.0, 6.9, 6.0 Hz, 1H), 1.60 (br s, 1H); **^{13}C NMR** (126 MHz, $CDCl_3$) δ_C 143.6, 140.3, 134.1, 130.2, 129.3, 128.7, 127.9, 127.7, 126.6, 124.2, 91.1, 60.0, 33.3; **HRMS** (ESI/TOF) *m/z*: $[M + Na]^+$ Calcd for $C_{17}H_{17}NO_3Na^+$ 306.1101; Found 306.1110.

(*Z*)-5-Nitro-2-phenyl-5-(phenylsulfonyl)pent-2-en-1-ol (2.3e)

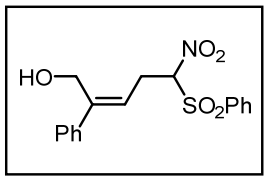

Yellowish oil (249.2 mg, 72% yield, *Z*/*E*>99:1); **IR** (neat): ν = 3563, 3064, 2963, 1558, 1493, 1448, 1334, 1221, 1154, 1082, 999, 908, 757, 724, 684, 600, 574, 530 cm^{-1}; **^{1}H NMR** (400 MHz, $CDCl_3$) δ_H 7.96-7.89 (m, 2H), 7.81-7.74 (m, 1H), 7.67-7.59 (m, 2H), 7.36-7.26 (m, 5H), 5.71 (dd, *J* = 9.2, 5.3 Hz, 1H), 5.65 (t, *J* = 7.7 Hz, 1H), 4.55 (d, *J* = 12.7 Hz, 1H), 4.51 (d, *J* = 12.7 Hz, 1H), 3.38-3.24 (m, 2H), 1.88 (br s, 1H); **^{13}C NMR** (101 MHz, $CDCl_3$) δ_C 145.6, 139.9, 135.8, 134.1, 130.0, 129.8, 128.7, 128.2, 126.6, 120.8, 101.6, 60.2, 27.3; **HRMS** (ESI/TOF) *m/z*: $[M + Na]^+$ Calcd for $C_{17}H_{17}NO_5SNa^+$ 370.0720; Found 370.0729.

(*Z*)-Ethyl-6-hydroxy-2-nitro-5-phenylhex-4-enoate (2.3f)

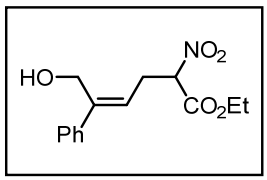

Yellowish oil (223.0 mg, 80% yield, *Z*/*E*>99:1); **IR** (neat): ν = 3576, 2984, 1745, 1557, 1493, 1445, 1371, 1260, 1209, 1013, 857, 766, 698 cm^{-1}; **^{1}H NMR** (400 MHz, $CDCl_3$) δ_H 7.43-7.27 (m, 5H), 5.73 (app t, *J* = 7.7 Hz, 1H), 5.26 (dd, *J* = 8.6, 6.0 Hz, 1H), 4.60 (d, *J* = 12.6 Hz, 1H), 4.56 (d, *J* = 12.6 Hz, 1H), 4.31 (qd, *J* = 7.2, 1.8 Hz, 2H), 3.29 (dt, *J* = 15.1, 8.3 Hz, 1H), 3.17 (ddd, *J* = 15.1, 7.4, 6.0 Hz, 1H), 1.81 (br s, 1H), 1.31 (t, *J* = 7.2 Hz, 3H); **^{13}C NMR** (101 MHz, $CDCl_3$) δ_C 164.2, 144.5, 140.2, 128.7, 128.1, 126.6, 122.7, 87.6, 63.5, 60.0, 29.7, 14.0; **HRMS** (ESI/TOF) *m/z*: $[M + Na]^+$ Calcd for $C_{14}H_{17}NO_5Na$ 302.0999; Found 302.0996.

5-Nitro-2-phenylhex-2-ene-1,6-diol (2.3g)

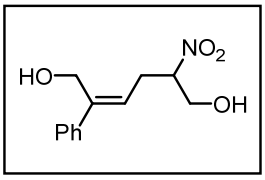

Yellowish oil (106.5 mg, 45% yield, *Z*/*E*=36:64); **IR** (neat): ν = 3338, 3082, 3056, 3027, 2928, 2893, 2477, 2071, 1542, 1493, 1445, 1362, 1012, 972, 853, 766, 697 cm^{-1}; **^{1}H NMR** (500 MHz, CD_3OD) δ_H 7.47-7.37 (m, 2H), 7.31 (ddt, *J* = 8.1, 6.3, 1.5 Hz, 2H), 7.27-7.21 (m, 1H), 5.76 (t, *J* = 7.7 Hz, 1H), 4.76 (tdd, *J* = 8.1, 5.9, 3.7 Hz, 1H), 4.49-4.42 (m, 2H), 4.00 (dd, *J* = 12.2, 7.8 Hz, 1H), 3.93 (dd, *J* = 12.2, 3.7 Hz, 1H), 2.94 (dt, *J* = 15.0, 8.1 Hz, 1H), 2.82 (ddd, *J* = 15.0, 7.6, 5.9 Hz, 1H); **^{13}C NMR** (126 MHz, CD_3OD) δ_C 144.5, 142.5, 129.3, 128.3, 127.5, 125.6, 95.8, 64.5, 59.8, 29.7; **HRMS** (ESI/TOF) *m/z*: $[M + Na]^+$ Calcd for $C_{12}H_{15}NO_4Na^+$ 260.0893; Found 260.0896.

Note: the reported NMR resonances here correspond only to the (*Z*) isomer.

(*Z*)-7-Chloro-5-nitro-2-phenylhept-2-en-1-ol (2.3h)

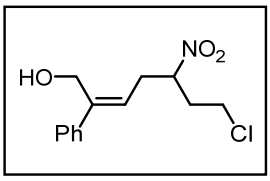

Yellowish oil (38.0 mg, 60% yield, *Z*/*E*>99:1); **IR** (neat): ν = 3575, 3383, 3082, 3057, 3028, 2924, 2853, 1545, 1493, 1445, 1375, 1331, 1293, 1010, 971, 910, 767, 735, 697 cm^{-1}; **^{1}H NMR** (400 MHz, $CDCl_3$) δ_H 7.42-7.27 (m, 5H), 5.73 (dd, *J* = 8.2, 7.1 Hz, 1H), 4.91 (tdd, *J* = 9.1, 5.2, 4.0 Hz, 1H), 4.55 (d, *J* = 12.7 Hz, 1H), 4.50 (d, *J* = 12.7 Hz, 1H), 3.65 (dt, *J* = 11.3, 5.5 Hz, 1H), 3.52 (ddd, *J* = 11.6, 9.1, 4.9 Hz, 1H), 3.02 (dt, *J* = 15.0, 8.4 Hz, 1H), 2.81 (ddd, *J* = 15.0, 7.1, 5.2 Hz, 1H), 2.58 (ddt, *J* = 14.8, 9.9, 5.1 Hz, 1H), 2.22 (dddd, *J* = 15.0, 9.4, 5.7, 4.0 Hz, 1H), 1.67 (br s, 1H); **^{13}C NMR** (101 MHz, $CDCl_3$) δ_C 144.0, 140.2, 128.7, 128.0, 126.6, 123.6, 85.2, 59.9, 40.4, 35.7, 32.6; **HRMS** (ESI/TOF) *m/z*: $[M + Na]^+$ Calcd for $C_{13}H_{16}ClNO_3Na^+$ 292.0711; Found 292.0713.

(*Z*)-*tert*-Butyl-8-hydroxy-4-nitro-7-phenyloct-6-enoate (2.3i)

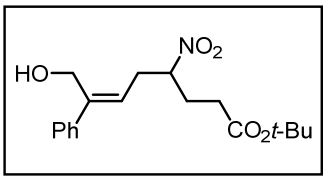

Yellowish oil (215.7 mg, 64% yield, *Z*/*E*>99:1); **IR** (neat): ν = 3566, 3434, 3083, 3059, 2979, 2933, 1724, 1547, 1493, 1445, 1367, 1320, 1251, 1150, 1009, 911, 844, 766, 732, 698 cm^{-1}; **^{1}H NMR** (400 MHz, $CDCl_3$) δ_H 7.41-7.25 (m, 5H), 5.72 (dd, *J* = 8.3, 7.1 Hz, 1H), 4.74-4.64 (m, 1H), 4.57-4.46 (m, 2H), 2.99 (dt, *J* =15.0, 8.6 Hz, 1H), 2.74 (ddd, *J* = 15.0, 7.1, 5.0 Hz, 1H), 2.40-2.08 (m, 4H), 1.88 (br t, *J* = 5.1 Hz, 1H), 1.45 (s, 9H); **^{13}C NMR** (101 MHz, $CDCl_3$) δ_C 171.3, 143.7, 140.4, 128.6, 127.8, 126.6, 124.0, 87.6, 81.4, 59.8, 32.8, 31.4, 28.6, 28.1; **HRMS** (ESI/TOF) *m/z*: $[M + Na]^+$ Calcd for $C_{18}H_{25}NO_5Na^+$ 358.1625; Found 358.1633.

(*Z*)-7,7-Dimethoxy-5-nitro-2-phenylhept-2-en-1-ol (2.3j)

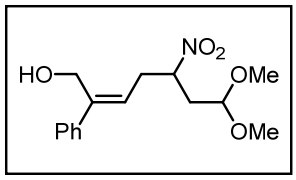

Yellowish oil (281.0 mg, 95% yield, *Z*/*E*>99:1); **IR** (neat): ν = 3568, 3422, 3081, 3058, 3029, 2992, 2937, 2911, 2836, 2251, 1548, 1493, 1445, 1370, 1325, 1267, 1194, 1127, 1065, 1023, 949, 909, 768, 730, 698 cm^{-1}; **^{1}H NMR** (500 MHz, $CDCl_3$) δ_H 7.42-7.37 (m, 2H), 7.37-7.32 (m, 2H), 7.31-7.27 (m, 1H), 5.73 (dd, *J* = 8.3, 7.1 Hz, 1H), 4.77 (tdd, *J* = 9.1, 5.1, 4.2 Hz, 1H), 4.58-4.47 (m, 2H), 4.41 (dd, *J* = 6.3, 4.5 Hz, 1H), 3.37 (s, 3H), 3.35 (s, 3H), 2.99 (dt, *J* = 14.9, 8.5 Hz, 1H), 2.79 (ddd, *J* = 15.0, 7.1, 5.1 Hz, 1H), 2.45 (ddd, *J* = 14.7, 9.2, 4.5 Hz, 1H), 2.05 (ddd, *J* = 14.7, 6.3, 4.2 Hz, 1H), 1.53 (br t, *J* = 4.7 Hz, 1H); **^{13}C NMR** (126 MHz, $CDCl_3$) δ_C 143.8, 140.3, 128.7, 128.0, 126.7, 124.0, 102.1, 84.5, 59.9, 54.5, 54.1, 36.4, 33.1; **HRMS** (ESI/TOF) *m/z*: $[M + Na]^+$ Calcd for $C_{15}H_{21}NO_5Na$ 318.1312; Found 318.1321.

(*Z*)-6,6-Bis(methylthio)-5-nitro-2-phenylhex-2-en-1-ol (2.3k)

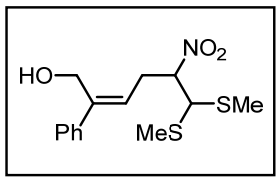

Yellowish oil (170.3 mg, 54% yield, *Z*/*E*>99:1); **IR** (neat): ν = 3565, 3396, 3081, 3055, 3026, 2919, 2854, 1550, 1493, 1423, 1365, 1308, 1011, 975, 957, 766, 698 cm^{-1}; **^{1}H NMR** (500 MHz, $CDCl_3$) δ_H 7.41-7.37 (m, 2H), 7.37-7.31 (m, 2H), 7.31-7.27 (m, 1H), 5.76 (dd, *J* = 8.7, 6.7 Hz, 1H), 4.70 (td, *J* = 9.7, 3.7 Hz, 1H), 4.57 (dd, *J* = 12.7, 3.4 Hz, 1H), 4.53 (dd, *J* = 12.7, 5.2 Hz, 1H), 4.13 (d, *J* = 9.6 Hz, 1H), 3.19 (ddd, *J* = 15.3, 6.7, 3.7 Hz, 1H), 3.09 (app dt, *J* = 15.3, 9.3 Hz, 1H), 2.21 (s, 3H), 2.19 (s, 3H), 1.57 (overlapped, 1H); **^{13}C NMR** (126 MHz, $CDCl_3$) δ_C 144.1, 140.3, 128.7, 128.0, 126.7, 123.8, 90.7, 60.0, 55.7, 31.5, 13.7, 13.5; **HRMS** (ESI/TOF) *m/z*: $[M + Na]^+$ Calcd for $C_{14}H_{19}NO_3S_2Na^+$ 336.0699; Found 336.0700.

(*Z*)-5-Nitro-2-phenyl-6-(phenylamino)hex-2-en-1-ol (2.3l)

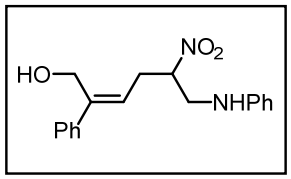

Yellowish oil (150.6 mg, 48% yield, *Z*/*E*>99:1); **IR** (neat): ν = 3567, 3408, 3055, 3026, 2922, 1602, 1544, 1497, 1444, 1381, 1355, 1314, 1256, 1182, 992, 908, 750, 692 cm^{-1}; **^{1}H NMR** (400 MHz, $CDCl_3$) δ_H 7.42-7.27 (m, 6H), 7.24-7.17 (m, 2H), 6.78 (tt, *J* = 7.4, 1.1 Hz, 1H), 6.66-6.59 (m, 2H), 5.77 (dd, *J* = 8.2, 7.4 Hz, 1H), 4.88 (tdd, *J* = 8.0, 5.6, 4.5 Hz, 1H), 4.56 (s, 2H), 4.13 (br s, 1H), 3.81 (dd, *J* = 14.7, 7.9 Hz, 1H), 3.65 (dd, *J* = 14.8, 4.5 Hz, 1H), 3.06 (dt, *J* = 15.0, 8.1 Hz, 1H), 2.90 (ddd, *J* = 15.0, 7.4, 5.6 Hz, 1H), 1.66 (br s, 1H); **^{13}C NMR** (101 MHz, $CDCl_3$) δ_C 146.4, 143.9, 140.3, 129.7, 128.8, 128.0, 126.6, 123.8, 118.9, 113.2, 86.5, 60.0, 46.4, 30.4; **HRMS** (ESI/TOF) *m/z*: $[M + H]^+$ Calcd for $C_{18}H_{21}N_2O_3$ 313.1547; Found 313.1545.

(*Z*)-2-(6-Hydroxy-2-nitro-5-phenylhex-4-en-1-yl)isoindoline-1,3-dione (2.3m)

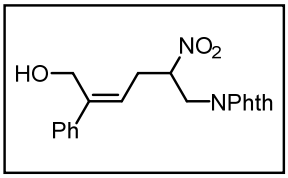

Pale yellow solid(251.1 mg, 69% yield, *Z*/*E*>99:1); **IR** (neat): ν = 3455, 3090, 3060, 3029, 2954, 2897, 1774, 1702, 1611, 1552, 1473, 1423, 1396, 1339, 1296, 1256, 1192, 1088, 1017, 992, 969, 931, 904, 881, 851, 771, 715, 690 cm^{-1}; **^{1}H NMR** (400 MHz, $CDCl_3$) δ_H 7.92-7.81 (m, 2H), 7.79-7.71 (m, 2H), 7.40-7.27 (m, 5H), 5.75 (t, *J* = 7.6 Hz, 1H), 5.06 (tt, *J* = 8.4, 5.1 Hz, 1H), 4.57 (d, *J* = 4.8 Hz, 2H), 4.42 (dd, *J* = 14.5, 8.3 Hz, 1H), 4.06 (dd, *J* = 14.5, 4.8 Hz, 1H), 3.11 (dt, *J* = 15.2, 8.3 Hz, 1H), 2.90 (ddd, *J* = 15.2, 7.2, 5.3 Hz, 1H), 1.66 (br t, *J* = 5.8 Hz, 1H); **^{13}C NMR** (101 MHz, $CDCl_3$) δ_C 167.7, 144.3, 140.1, 134.7, 131.7, 128.7, 128.0, 126.6, 123.9, 122.9, 84.9, 60.0, 40.0, 30.6; **HRMS** (ESI/TOF) *m/z*: $[M + Na]^+$ Calcd for $C_{20}H_{18}N_2O_5Na^+$ 389.1108; Found 389.1111.

(*Z*)-6-(1*H*-Indol-3-yl)-5-nitro-2-phenylhex-2-en-1-ol (2.3n)

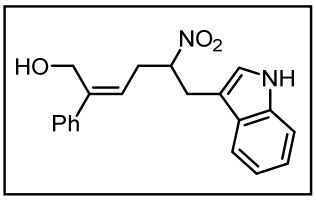

Yellowish oil (126.7 mg, 64% yield, *Z*/*E*>99:1); **IR** (neat): ν = 3556, 3415, 3056, 2924, 1747, 1543, 1492, 1457, 1370, 1339, 1279, 1230, 1097, 1010, 743, 697 cm^{-1}; **^{1}H NMR** (400 MHz, $CDCl_3$) δ_H 8.15 (br s, 1H), 7.59 (dt, *J* = 7.9, 1.0 Hz, 1H), 7.41-7.27 (m, 6H), 7.23 (ddd, *J* = 8.1, 7.0, 1.2 Hz, 1H), 7.17 (ddd, *J* = 8.0, 7.0, 1.1 Hz, 1H), 7.04 (d, *J* = 2.5 Hz, 1H), 5.75 (dd, *J* = 8.6, 6.7 Hz, 1H), 4.96 (dddd, *J* = 9.2, 7.7, 6.5, 4.5 Hz, 1H), 4.53 (d, *J* = 12.5 Hz, 1H), 4.48 (d, *J* = 12.5 Hz, 1H), 3.54 (ddd, *J* = 14.8, 7.7, 0.8 Hz, 1H), 3.32 (ddd, *J* = 14.8, 6.5, 0.7 Hz, 1H), 3.08 (dt, *J* = 15.2, 8.9 Hz, 1H), 2.80 (ddd, *J* = 15.2, 6.8, 4.5 Hz, 1H), 1.51 (br s, 1H); **^{13}C NMR** (101 MHz, $CDCl_3$) δ_C 143.5, 140.3, 136.3, 128.7, 127.9, 126.9, 126.6, 124.5, 123.2, 122.7, 120.1, 118.3, 111.6, 109.6, 88.8, 59.9, 32.5, 30.0; **HRMS** (ESI/TOF) *m/z*: $[M + Na]^+$ Calcd for $C_{20}H_{20}N_2O_3Na^+$ 359.1366; Found 359.1367.

(*Z*)-6-(Furan-2-yl)-5-nitro-2-phenylhex-2-en-1-ol (2.3o)

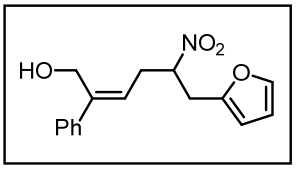

Yellowish oil (218.3 mg, 76% yield, *Z*/*E*>99:1); **IR** (neat): ν = 3574, 3398, 3027, 2920, 1599, 1547, 1506, 1493, 1429, 1371, 1325, 1208, 1145, 1077, 1010, 911, 732, 697 cm^{-1}; **^{1}H NMR** (400 MHz, $CDCl_3$) δ_H 7.42-7.26 (m, 6H), 6.31 (dd, *J* = 3.2, 1.9 Hz, 1H), 6.19-6.13 (m, 1H), 5.73 (dd, *J* = 8.4, 7.0 Hz, 1H), 4.91 (dddd, *J* = 8.8, 7.9, 6.0, 4.9 Hz, 1H), 4.54-4.45 (m, 2H), 3.40 (dd, *J* = 15.4, 7.9 Hz, 1H), 3.20 (dd, *J* = 15.4, 6.0 Hz, 1H), 3.01 (dt, *J* = 15.2, 8.6 Hz, 1H), 2.79 (ddd, *J* = 15.2, 7.1, 4.9 Hz, 1H), 1.80 (br s, 1H). **^{13}C NMR** (101 MHz, $CDCl_3$) δ_C 149.1, 143.7, 142.5, 140.3, 128.6, 127.9, 126.6, 123.8, 110.7, 108.3, 86.6, 59.7, 32.1, 31.9; **HRMS** (ESI/TOF) *m/z*: $[M + Na]^+$ Calcd for $C_{16}H_{17}NO_4Na^+$ 310.1050; Found 310.1046.

(*Z*)-5-Nitro-2-phenylpent-2-en-1-yl benzoate (2.3q)

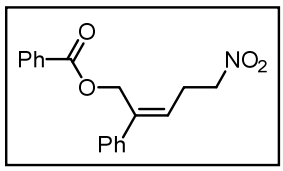

Brownish oil (41.9 mg, 67% yield, *Z*/*E*>99:1); **IR** (neat): ν = 3061, 3031, 2962, 2918, 1807, 1713, 1600, 1548, 1493, 1450, 1377, 1315, 1265, 1176, 1106, 1069, 1025, 954, 763, 710 cm^{-1}; **^{1}H NMR** (400 MHz, $CDCl_3$) δ_H 7.98-7.91 (m, 2H), 7.54 (app dt, *J* = 8.8, 1.4 Hz, 1H), 7.45-7.27 (m, 7H), 5.96 (t, *J* = 7.6 Hz, 1H), 5.28 (s, 2H), 4.55 (t, *J* = 6.8 Hz, 2H), 3.12 (q, *J* = 7.0 Hz, 2H); **^{13}C NMR** (101 MHz, $CDCl_3$) δ_C 166.5, 140.0, 138.9, 133.3, 130.0, 129.8, 128.7, 128.6, 128.0, 127.3, 126.5, 74.9, 61.6, 26.8; **HRMS** (ESI/TOF) *m/z*: $[M + Na]^+$ Calcd for $C_{18}H_{17}NO_4Na^+$ 334.1050; Found 334.1054.

(*Z*)-2-([1,1'-Biphenyl]-4-yl)-5-nitrohex-2-en-1-ol (2.3r)

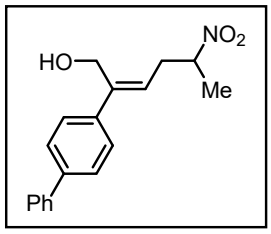

Yellowish oil (34.6 mg, 54% yield, *Z*/*E*>99:1); **IR** (neat): ν = 3428, 3029, 2924, 1538, 1486, 1448, 1388, 1357, 1000, 837, 763, 730, 692 cm^{-1}; **^{1}H NMR** (500 MHz, $CDCl_3$) δ_H 7.62-7.56 (m, 4H), 7.51-7.47 (m, 2H), 7.47-7.42 (m, 2H), 7.38-7.33 (m, 1H), 5.81 (dd, *J* = 8.3, 7.2 Hz, 1H), 4.73 (dqd, *J* = 8.1, 6.6, 5.3 Hz, 1H), 4.62 (d, *J* = 12.5 Hz, 1H), 4.58 (d, *J* = 12.5 Hz, 1H), 3.05 (dt, *J* = 14.9, 8.3 Hz, 1H), 2.77 (ddd, *J* = 14.9, 7.2, 5.4 Hz, 1H), 1.64 (d, *J* = 6.7 Hz, 3H), 1.56 (br s, 1H); **^{13}C NMR** (126 MHz, $CDCl_3$) δ_C 143.1, 140.8, 140.7, 139.2, 128.9, 127.5, 127.4, 127.1, 127.0, 124.3, 83.3, 59.8, 34.1, 19.1; **HRMS** (ESI/TOF) *m/z*: $[M + Na]^+$ Calcd for $C_{18}H_{19}NO_3Na^+$ 320.1257; Found 320.1271.

(*Z*)-4-(1-Hydroxy-5-nitrohex-2-en-2-yl)benzonitrile (2.3s)

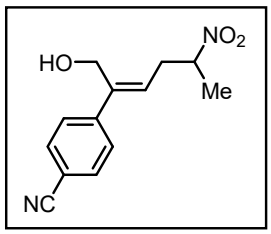

Yellowish oil (104.0 mg, 42% yield, *Z*/*E*>99:1); **IR** (neat): ν = 3494, 2989, 2939, 2898, 2227, 1605, 1544, 1504, 1449, 1389, 1360, 1312, 1008, 910, 830, 729 cm^{-1}; **^{1}H NMR** (400 MHz, $CDCl_3$) δ_H 7.63-7.58 (m, 2H), 7.54-7.48 (m, 2H), 5.85 (dd, *J* = 8.5, 7.0 Hz, 1H), 4.73 (dqd, *J* = 8.5, 6.7, 5.0 Hz, 1H), 4.56 (d, *J* = 12.6 Hz, 1H), 4.51 (d, *J* = 12.6 Hz, 1H), 3.04 (dt, *J* = 15.1, 8.5 Hz, 1H), 2.75 (ddd, *J* = 15.1, 7.0, 5.0 Hz, 1H), 1.73 (br s, 1H), 1.63 (d, *J* = 6.7 Hz, 3H); **^{13}C NMR** (101 MHz, $CDCl_3$) δ_C 145.2, 142.2, 132.4, 127.3, 127.2, 118.9, 111.3, 83.1, 59.4, 34.0, 19.2; **HRMS** (ESI/TOF) *m/z*: $[M + Na]^+$ Calcd for $C_{13}H_{14}N_2O_3Na^+$ 269.0897; Found 269.0907.

(*Z*)-5-Nitro-2-(3-(trifluoromethyl)phenyl)hex-2-en-1-ol (2.3t)

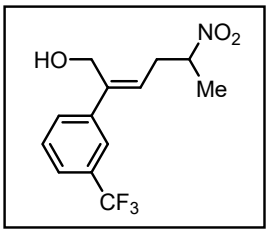

Yellowish oil (100.0 mg, 35% yield, *Z*/*E*>99:1); **IR** (neat): ν = 3578, 3371, 3077, 2992, 2924, 2899, 2854, 1806, 1547, 1489, 1436, 1390, 1331, 1262, 1164, 1118, 1075, 1066, 907, 800, 733, 701 cm^{-1}; **^{1}H NMR** (400 MHz, $CDCl_3$) δ_H 7.64 (d, *J* = 1.8 Hz, 1H), 7.62-7.52 (m, 2H), 7.45 (d, *J* = 7.7 Hz, 1H), 5.80 (dd, *J* = 8.4, 7.0 Hz, 1H), 4.73 (dqd, *J* = 8.5, 6.6, 5.1 Hz, 1H), 4.59 (dd, *J* = 12.6, 4.3 Hz, 1H), 4.53 (dd, *J* = 12.5, 5.5 Hz, 1H), 3.05 (dt, *J* = 15.0, 8.5 Hz, 1H), 2.75 (ddd, *J* = 15.0, 7.0, 5.2 Hz, 1H), 1.64 (d, *J* = 6.7 Hz, 3H), 1.56 (br t, *J* = 5.6 Hz, 1H); **^{13}C NMR** (101 MHz, $CDCl_3$) δ_C 142.5, 141.4, 131.0 (q, *J* = 32.4 Hz), 130.1, 129.1, 126.0, 125.5, 124.6 (q, *J* = 3.8 Hz), 123.4 (q, *J* = 4.0 Hz), 122.8, 83.2, 59.8, 34.0, 19.2; **^{19}F NMR** (376 MHz, $CDCl_3$) δ_F -62.7; **HRMS** (ESI/TOF) *m/z*: $[M + Na]^+$ Calcd for $C_{13}H_{14}F_3NO_3Na^+$ 312.0818; Found 312.0819.

(*Z*)-2-(Benzo[*d*][1,3]dioxol-5-yl)-5-nitrohex-2-en-1-ol (2.3v)

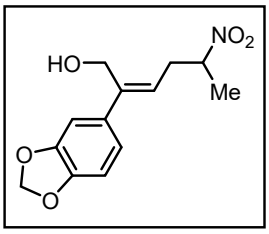

Yellowish oil (162.4 mg, 61% yield, *Z*/*E*>99:1); **IR** (neat): ν = 3567, 3401, 3068, 2989, 2897, 2779, 1720, 1606, 1545, 1503, 1486, 1436, 1388, 1360, 1326, 1232, 1110, 1036, 932, 891, 862, 808, 732 cm^{-1}; **^{1}H NMR** (400 MHz, $CDCl_3$) δ_H 6.91-6.84 (m, 2H), 6.77 (dd, *J* = 7.8, 0.6 Hz, 1H), 5.95 (s, 2H), 5.64 (dd, *J* = 8.3, 7.2 Hz, 1H), 4.68 (dqd, *J* = 8.3, 6.7, 5.4 Hz, 1H), 4.50 (d, *J* = 12.4 Hz, 1H), 4.46 (d, *J* = 12.4 Hz, 1H), 2.97 (dt, *J* = 15.0, 8.2 Hz, 1H), 2.70 (ddd, *J* = 15.0, 7.2, 5.4 Hz, 1H), 1.60 (d, *J* = 6.7 Hz, 3H), 1.58 (br s, 1H); **^{13}C NMR** (101 MHz, $CDCl_3$) δ_C 148.0, 147.4, 143.1, 134.5, 123.3, 120.2, 108.4, 107.2, 101.3, 83.3, 59.9, 34.0, 19.0; **HRMS** (ESI/TOF) *m/z*: $[M + Na]^+$ Calcd for $C_{13}H_{15}NO_5Na^+$ 288.0842; Found 288.0840.

(*Z*)-2-(Naphthalen-2-yl)-5-nitrohex-2-en-1-ol (2.3w)

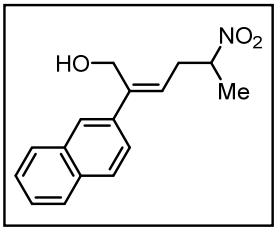

Yellowish oil (108.3 mg, 40% yield, *Z*/*E*>99:1); **IR** (neat): ν = 3574, 3390, 3057, 2939, 1543, 1448, 1388, 1360, 1013, 909, 802, 778, 730 cm^{-1}; **^{1}H NMR** (500 MHz, $CDCl_3$) δ_H 7.89-7.82 (m, 2H), 7.80 (app d, *J* = 8.3 Hz, 1H), 7.53-7.46 (m, 2H), 7.43 (dd, *J* = 8.3, 7.0 Hz, 1H), 7.28 (dd, *J* = 7.0, 1.2 Hz, 1H), 5.60 (dd, *J* = 8.3, 7.1 Hz, 1H), 4.79-4.69 (m, 1H), 4.58-4.48 (m, 2H), 3.12 (dt, *J* = 14.7, 8.3 Hz, 1H), 2.83 (ddd, *J* = 14.8, 7.0, 5.4 Hz, 1H), 1.66 (d, *J* = 6.7 Hz, 3H), 1.53 (br s, 1H); **^{13}C NMR** (126 MHz, $CDCl_3$) δ_C 143.6, 139.1, 133.8, 131.6, 128.5, 128.1, 126.7, 126.42, 126.40, 126.1, 125.43, 125.40, 83.3, 61.8, 33.9, 19.1; **HRMS** (ESI/TOF) *m/z*: $[M + Na]^+$ Calcd for $C_{16}H_{17}NO_3Na^+$ 294.1101. Found: 294.1101.

(*Z*)-5-Nitro-2-(thiophen-3-yl)hex-2-en-1-ol (2.3x)

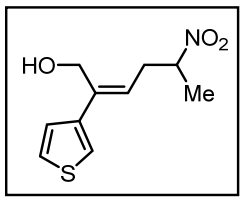

Yellowish oil (159.3 mg, 70% yield, *Z*/*E*>99:1); **IR** (neat): ν = 3567, 3381, 3108, 2988, 2938, 2897, 2248, 1678, 1544, 1449, 1388, 1360, 1312, 1004, 908, 861, 781, 728 cm^{-1}; **^{1}H NMR** (500 MHz, $CDCl_3$) δ_H 7.33 (dd, *J* = 3.0, 1.4 Hz, 1H), 7.28 (dd, *J* = 5.1, 2.9 Hz, 1H), 7.19 (dd, *J* = 5.1, 1.4 Hz, 1H), 5.85 (dd, *J* = 8.3, 7.3 Hz, 1H), 4.68 (dqd, *J* = 8.1, 6.7, 5.3 Hz, 1H), 4.51 (d, *J* = 12.2 Hz, 1H), 4.46 (d, *J* = 12.2 Hz, 1H), 2.99 (dt, *J* = 15.0, 8.3 Hz, 1H), 2.71 (ddd, *J* = 15.0, 7.2, 5.4 Hz, 1H), 1.73 (br s, 1H), 1.60 (d, *J* = 6.7 Hz, 3H); **^{13}C NMR** (126 MHz, $CDCl_3$) δ_C 141.2, 138.0, 126.1, 125.7, 122.8, 121.4, 83.3, 59.8, 33.7, 19.1; **HRMS** (ESI/TOF) *m/z*: $[M + Na]^+$ Calcd for $C_{10}H_{13}NO_3SNa^+$ 250.0508. Found: 250.0506.

(*E*)-2-(Furan-2-yl)-5-nitrohex-2-en-1-ol (2.3y)

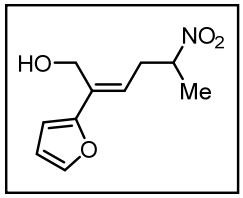

Yellowish oil (33.3 mg, 34% yield, *Z*/*E*>99:1); **IR** (neat): ν = 3577, 3390, 3152, 3138, 3119, 2987, 2938, 2900, 1544, 1459, 1388, 1360, 1313, 1320, 1159, 1013, 905, 884, 805, 731 cm^{-1}; **^{1}H NMR** (500 MHz, $CDCl_3$) δ_H 7.36 (d, *J* = 1.8 Hz, 1H), 6.42 (app d, *J* = 3.4 Hz, 1H), 6.40 (dd, *J* = 3.4, 1.8 Hz, 1H), 6.07 (t, *J* = 8.0 Hz, 1H), 4.69 (dqd, *J* = 8.0, 6.7, 5.5 Hz, 1H), 4.47 (d, *J* = 12.3 Hz, 1H), 4.42 (d, *J* = 12.3 Hz, 1H), 3.03 (dt, *J* = 15.0, 8.2 Hz, 1H), 2.74 (ddd, *J* = 15.0, 7.5, 5.6 Hz, 1H), 1.61 (overlapped, 1H), 1.61 (d, *J* = 6.7 Hz, 3H); **^{13}C NMR** (126 MHz, $CDCl_3$) δ_C 153.3, 142.4, 132.9, 120.9, 111.6, 106.9, 83.2, 58.2, 33.4, 19.1; **HRMS** (ESI/TOF) *m/z*: $[M + Na]^+$ Calcd for $C_{10}H_{13}NO_4Na^+$ 234.0737. Found: 234.0730.

Note: The obtained stereoconfiguration corresponds to the (*E*)-isomer, according to the Cahn-Ingold-Prelog priority rules, but is spatially oriented as in the other (*Z*)-isomers.

(*Z*)-2-Cyclohexyl-5-nitrohex-2-en-1-ol (2.3z)

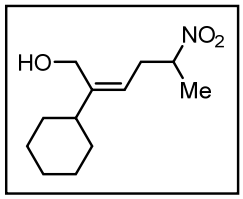

Brownish oil (32.0 mg, 70% yield, *Z*/*E*>99:1); **IR** (neat): ν = 3287, 3221, 2923, 2851, 1545, 1448, 1387, 1360, 998 cm^{-1}; **^{1}H NMR** (400 MHz, $CDCl_3$) δ_H 5.23 (ddd, *J* = 8.1, 6.9, 1.0 Hz, 1H), 4.60 (dqd, *J* = 8.3, 6.7, 5.4 Hz, 1H), 4.14 (dd, *J* = 11.9, 4.6 Hz, 1H), 4.09 (dd, *J* = 11.9, 5.7 Hz, 1H), 2.83 (dt, *J* = 14.7, 8.3 Hz, 1H), 2.55 (dt, *J* = 14.7, 6.7, 5.7 Hz, 1H), 2.09-1.98 (m, 1H), 1.83-1.63 (m, 6H), 1.55 (d, *J* = 6.7 Hz, 3H), 1.35-1.05 (m, 5H); **^{13}C NMR** (101 MHz, $CDCl_3$) δ_C 149.2, 119.8, 83.8, 59.7, 43.6, 33.5, 32.7, 32.6, 26.82, 26.79, 26.3, 19.0; **HRMS** (ESI/TOF) *m/z*: $[M + Na]^+$ Calcd for $C_{12}H_{21}NO_3Na^+$ 250.1414. Found: 250.1412.

2-Methyl-5-nitrohex-2-en-1-ol (2.3aa)

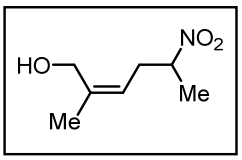

Yellowish oil (90.0 mg, 57% yield, *Z*/*E*=76:24); **IR** (neat): ν = 3377, 2976, 2941, 1542, 1451, 1388, 1361, 1008 cm^{-1}; **^{1}H NMR** (400 MHz, $CDCl_3$) δ_H 5.25-5.17 (m, 1H), 4.62-4.51 (m, 1H), 4.13 (app d, *J* = 12.3 Hz, 1H), 4.06 (dd, *J* = 12.6, 3.4 Hz, 1H), 2.85-2.70 (m, 1H), 2.55-2.42 (m, 1H), 1.80 (q, *J* = 1.2 Hz, 3H), 1.53 (d, *J* = 6.7 Hz, 3H), 1.51 (overlapped, 1H); **^{13}C NMR** (101 MHz, $CDCl_3$) δ_C 139.9, 120.6, 83.6, 61.4, 33.4, 21.6, 18.9; **HRMS** (ESI/TOF) *m/z*: $[M + Na]^+$ Calcd for $C_7H_{13}NO_3Na^+$ 182.0788. Found: 182.0787.

Note: the reported NMR resonances here correspond only to the (*Z*) isomer.

5-Nitrohex-2-en-1-ol (2.3ab)

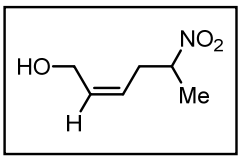

Yellowish oil (96.1 mg, 66% yield, *Z*/*E*=54:46); **IR** (neat): ν = 3570, 3353, 2940, 1543, 1451, 1389, 1361, 1314, 1004, 973, 857 cm^{-1}; **^{1}H NMR** (500 MHz, $CDCl_3$) δ_H 5.78 (overlapped, 1H), 5.46 (dddt, *J* = 11.1, 8.5, 7.2, 1.5 Hz, 1H), 4.63-4.55 (m, 1H), 4.25-4.14 (m, 2H), 2.86-2.77 (m, 1H), 2.52 (overlapped, 1H), 1.56 (dd, *J* = 12.1, 6.7 Hz, 3H), 1.45 (br s, 1H); **^{13}C NMR** (126 MHz, $CDCl_3$) δ_C 133.4, 125.1, 83.0, 58.4, 33.1, 18.9; **HRMS** (ESI/TOF) *m/z*: $[M + Na]^+$ Calcd for $C_6H_{11}NO_3Na^+$ 168.0631. Found: 168.0632.

Note: the reported NMR resonances here correspond only to the (*Z*) isomer.

Ethyl 6-hydroxy-5-(2-methoxyphenyl)-2-nitrohex-4-enoate (2.3ad)

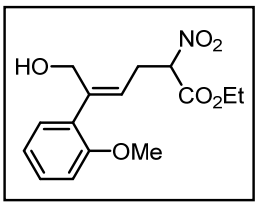

Yellowish oil (247.2 mg, 80% yield, *Z*/*E*=70:30); **IR** (neat): ν = 3570, 2982, 2963, 2940, 2838, 1747, 1598, 1558, 1489, 1464, 1435, 1373, 1240, 1119, 1050, 1021, 910, 858, 755, 730 cm^{-1}; **^{1}H NMR** (500 MHz, $CDCl_3$) δ_H 7.30-7.25 (m, 1H), 7.08 (dd, *J* = 7.5, 1.8 Hz, 1H), 6.96-6.91 (m, 1H), 6.89 (d, *J* = 8.2 Hz, 1H), 5.58 (t, *J* = 7.5 Hz, 1H), 5.32 (dd, *J* = 9.2, 5.7 Hz, 1H), 4.39 (dd, *J* = 12.5, 7.1 Hz, 1H), 4.33 (overlapped, 1H), 4.29 (qd, *J* = 7.2, 1.2 Hz, 2H), 3.85 (s, 3H), 3.28 (ddd, *J* = 15.1, 9.2, 7.8 Hz, 1H), 3.16 (ddd, *J* = 15.3, 7.4, 5.7 Hz, 1H), 2.47 (t, *J* = 6.5 Hz, 1H), 1.32 (t, *J* = 7.1 Hz, 3H); **^{13}C NMR** (126 MHz, $CDCl_3$) δ_C 164.2, 156.3, 144.7, 131.1, 130.3, 129.2, 125.4, 121.3, 110.7, 87.8, 63.2, 61.0, 55.7, 29.2, 14.0; **HRMS** (ESI/TOF) *m/z*: $[M + Na]^+$ Calcd for $C_{15}H_{19}NO_6Na^+$ 332.1105. Found: 332.1106.

Note: the reported NMR resonances here correspond only to the (*Z*) isomer.

2-(2-Bromophenyl)-6-(furan-2-yl)-5-nitrohex-2-en-1-ol (2.3ae)

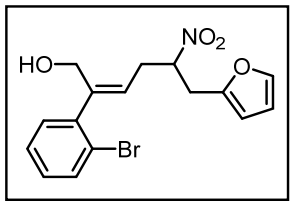

Yellowish oil (173.0 mg, 47% yield, *Z*/*E*=98:2); **IR** (neat): ν = 3581, 3407, 3119, 3055, 2919, 1548, 1506, 1468, 1431, 1370, 1145, 1010, 908, 728 cm^{-1}; **^{1}H NMR** (500 MHz, $CDCl_3$) δ_H 7.59-7.53 (m, 1H), 7.35 (d, *J* = 2.0 Hz, 1H), 7.31-7.24 (m, 1H), 7.18-7.13 (m, 2H), 6.31 (dd, *J* = 3.2, 2.0 Hz, 1H), 6.17 (d, *J* = 3.3 Hz, 1H), 5.49 (t, *J* = 7.7 Hz, 1H), 4.91 (tt, *J* = 8.2, 5.5 Hz, 1H), 4.42 (d, *J* = 6.1 Hz, 2H), 3.42 (dd, *J* = 15.4, 8.0 Hz, 1H), 3.24 (dd, *J* = 15.5, 6.0 Hz, 1H), 3.04 (dt, *J* = 15.1, 8.5 Hz, 1H), 2.82 (ddd, *J* = 15.1, 7.1, 5.0 Hz, 1H), 1.72 (t, *J* = 6.2 Hz, 1H); **^{13}C NMR** (126 MHz, $CDCl_3$) δ_C 149.1, 144.9, 142.5, 142.1, 132.7, 131.2, 129.2, 127.5, 126.7, 122.4, 110.7, 108.3, 86.4, 60.8, 31.9, 31.8; **HRMS** (ESI/TOF) *m/z*: $[M + Na]^+$ Calcd for $C_{16}H_{16}BrNO_4Na^+$ 388.0155. Found: 388.0149.

Note: the reported NMR resonances here correspond only to the (*Z*) isomer.

(*Z*)-7,7-Dimethoxy-5-nitro-2-(*m*-tolyl)hept-2-en-1-ol (2.3af)

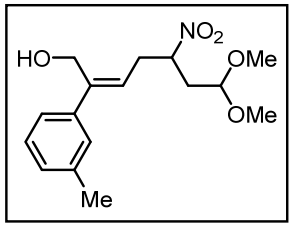

Yellowish oil (263.1 mg, 85% yield, *Z*/*E*>99:1); **IR** (neat): ν = 3576, 3441, 2937, 2835, 2250, 1603, 1548, 1446, 1370, 1192, 1127, 1066, 1010, 909, 786, 729, 702 cm^{-1}; **^{1}H NMR** (400 MHz, $CDCl_3$) δ_H 7.25-7.16 (m, 3H), 7.13-7.08 (m, 1H), 5.70 (dd, *J* = 8.3, 7.1 Hz, 1H), 4.76 (tdd, *J* = 9.1, 5.2, 4.1 Hz, 1H), 4.52 (dd, *J* = 14.5, 12.6 Hz, 1H), 4.48 (d, *J* = 12.6 Hz, 1H), 4.40 (dd, *J* = 6.3, 4.5 Hz, 1H), 3.36 (s, 3H), 3.34 (s, 3H), 2.97 (dt, *J* = 14.9, 8.4 Hz, 1H), 2.77 (ddd, *J* = 15.0, 7.1, 5.2 Hz, 1H), 2.44 (ddd, *J* = 14.7, 9.2, 4.5 Hz, 1H), 2.35 (s, 3H), 2.04 (ddd, *J* = 14.8, 6.3, 4.1 Hz, 1H), 1.72 (br s, 1H); **^{13}C NMR** (101 MHz, $CDCl_3$); δ_C 143.9, 140.3, 138.3, 128.6, 128.5, 127.4, 123.73, 123.71, 102.1, 84.5, 59.8, 54.4, 54.0, 36.3, 33.1, 21.6; **HRMS** (ESI/TOF) *m/z*: $[M + Na]^+$ Calcd for $C_{16}H_{23}NO_5Na^+$ 332.1468. Found: 332.1466.

(2*Z*,7*Z*)-5-Nitro-2-phenyl-8-(*m*-tolyl)nona-2,7-diene-1,9-diol (2.5a)

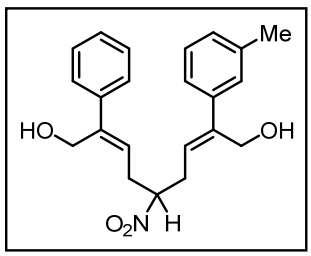

Yellowish foam (73.3 mg, 59% yield, *Z*/*E*>99:1); **IR** (neat): ν = 3575, 3376, 3080, 3056, 3028, 2920, 2249, 1602, 1546, 1491, 1436, 1371, 1323, 1220, 1008, 907, 786, 727, 697, 648 cm^{-1}; **^{1}H NMR** (500 MHz, $CDCl_3$) δ_H 7.42-7.37 (m, 2H), 7.36-7.31 (m, 2H), 7.31-7.27 (m, 1H), 7.23 (t, *J* = 7.5 Hz, 1H), 7.21-7.16 (m, 2H), 7.11 (d, *J* = 7.3 Hz, 1H), 5.75 (t, *J* = 7.9 Hz, 1H), 5.72 (t, *J* = 7.9 Hz, 1H), 4.75 (tt, *J* = 8.2, 5.4 Hz, 1H), 4.54 (s, 2H), 4.53 (s, 2H), 3.06 (dtd, *J* = 15.0, 8.1, 3.4 Hz, 2H), 2.87 (dddd, *J* = 15.1, 7.6, 5.4, 2.4 Hz, 2H), 2.35 (s, 3H), 1.84 (br s, 2H); **^{13}C NMR** (126 MHz, $CDCl_3$) δ_C 143.9, 143.8, 140.33, 140.27, 138.4, 128.8, 128.7, 128.6, 128.0, 127.4, 126.7, 124.0, 123.7, 87.9, 59.94, 59.91, 32.3, 21.6; **HRMS** (ESI/TOF) *m/z*: $[M + Na]^+$ Calcd for $C_{22}H_{25}NO_4Na^+$ 390.1676. Found: 390.1681.

(7*Z*)-2-(2-Bromophenyl)-5-nitro-8-(3-(trifluoromethyl)phenyl)nona-2,7-diene-1,9-diol (2.5b)

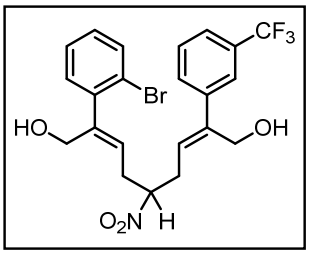

Yellowish foam (35.0 mg, 41% yield, *Z*/*E*=80:20); **IR** (neat): ν = 3574, 3364, 3056, 2924, 1546, 1468, 1433, 1372, 1332, 1265, 1164, 1119, 1074, 1021, 800, 754, 700, 657 cm^{-1}; **^{1}H NMR** (400 MHz, $CDCl_3$) δ_H 7.66 (app s, 1H), 7.63-7.50 (m, 3H), 7.46 (t, *J* = 7.6 Hz, 1H), 7.30-7.25 (m, 1H), 7.19-7.12 (m, 2H), 5.83 (dd, *J* = 8.4, 7.0 Hz, 1H), 5.51 (t, *J* = 7.7 Hz, 1H), 4.78 (tt, *J* = 8.3, 5.3 Hz, 1H), 4.60 (d, *J* = 12.5 Hz, 1H), 4.56 (d, *J* = 12.5 Hz, 1H), 4.48 (d, *J* = 13.3 Hz, 1H), 4.44 (d, *J* = 13.3 Hz, 1H), 3.19-3.04 (m, 2H), 2.97-2.86 (m, 2H), 1.75 (br s, 2H); **^{13}C NMR** (101 MHz, $CDCl_3$) δ_C 145.0, 142.8, 142.0, 141.4, 132.8, 131.2, 131.1 (q, *J* = 32.5 Hz), 130.1, 129.3, 129.2, 127.6, 126.9, 125.7, 124.6 (q, *J* = 3.9 Hz), 123.4 (q, *J* = 3.5 Hz), 122.5, 87.6, 61.0, 59.8, 32.3, 32.0; **^{19}F NMR** (376 MHz, $CDCl_3$) δ_F -62.7; **HRMS** (ESI/TOF) *m/z*: $[M + Na]^+$ Calcd for $C_{22}H_{21}BrF_3NO_4Na^+$ 522.0498. Found: 522.0521.

(2*Z*,7*Z*)-2-(Benzo[*d*][1,3]dioxol-5-yl)-5-nitro-8-(thiophen-3-yl)nona-2,7-diene-1,9-diol (2.5c)

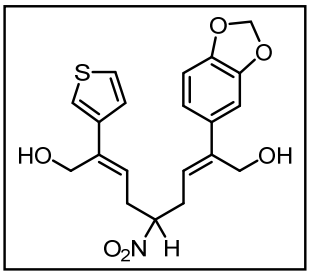

Yellowish foam (76.4 mg, 57% yield, *Z*/*E*>99:1); **IR** (neat): ν = 3561, 3353, 3107, 2894, 1606, 1544, 1502, 1486, 1434, 1370, 1325, 1233, 1102, 1035, 932, 892, 862, 810, 781, 729 cm^{-1}; **^{1}H NMR** (400 MHz, $CDCl_3$) δ_H 7.33 (dd, *J* = 2.9, 1.4 Hz, 1H), 7.29 (dd, *J* = 5.1, 3.0 Hz, 1H), 7.19 (dd, *J* = 5.0, 1.4 Hz, 1H), 6.88 (t, *J* = 1.7 Hz, 1H), 6.85 (overlapped, 1H), 6.77 (d, *J* = 7.9 Hz, 1H), 5.95 (s, 2H), 5.87 (t, *J* = 7.7 Hz, 1H), 5.65 (t, *J* = 7.7 Hz, 1H), 4.72 (tt, *J* = 8.2, 5.5 Hz, 1H), 4.50 (d, *J* = 12.4 Hz, 1H), 4.47 (d, *J* = 12.4 Hz, 1H), 4.46 (s, 2H), 3.10-2.95 (m, 2H), 2.89-2.76 (m, 2H), 1.88 (br s, 2H); **^{13}C NMR** (101 MHz, $CDCl_3$) δ_C 148.0, 147.5, 143.2, 141.2, 138.3, 134.5, 126.1, 125.7, 123.0, 122.4, 121.5, 120.2, 108.4, 107.2, 101.3, 87.9, 59.9, 59.8, 32.2, 32.0; **HRMS** (ESI/TOF) *m/z*: $[M + Na]^+$ Calcd for $C_{20}H_{21}NO_6SNa^+$ 426.0982. Found: 426.0982.

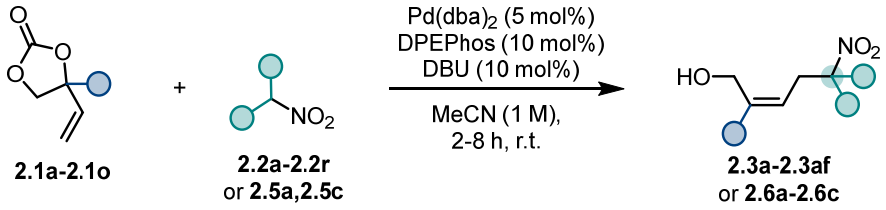

SCHEME 2.14. Synthesis of congested homoallylic nitroalkanes with co-catalytic DBU.

General Procedure B: In a 5 mL vial, cyclic carbonate **2.1a-2.1o** (1.0 equiv.), $Pd(dba)_2$ (5 mol%), DPEPhos (10 mol%) and nitroalkane **2.2a-2.2q** (1.5 equiv.) were dissolved in MeCN (1.0 M), and then, DBU (10 mol%) was added. The vial was sealed with a septum and a needle was placed through the septum to release gaseous CO_2. The mixture was stirred open to air for 2-8 h at room temperature. Hereafter, the solvent was evaporated with a gentle stream of N_2 and the residue was purified by flash chromatography on silica gel to afford the corresponding nitroalkane **2.3a-2.3af** or trisallylated nitroalkane **2.6a-2.6c** (**SCHEME 2.14**).

(*Z*)-5-Methyl-5-nitro-2-phenylhex-2-en-1-ol (2.3p)

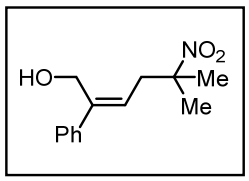

Yellowish oil (39.0 mg, 83% yield, *Z*/*E*>99:1); **IR** (neat): ν = 3575, 3405, 3057, 2987, 2930, 1533, 1493, 1468, 1445, 1396, 1372, 1347, 1261, 1137, 1019, 855, 766, 697 cm^{-1}; **^{1}H NMR** (400 MHz, $CDCl_3$) δ_H 7.43-7.27 (m, 5H), 5.72 (t, J = 7.9 Hz, 1H), 4.55 (s, 2H), 2.91 (d, J = 7.9 Hz, 2H), 1.67 (s, 6H), 1.49 (br s, 1H); **^{13}C NMR** (101 MHz, $CDCl_3$) δ_C 143.8, 140.5, 128.7, 127.9, 126.7, 123.9, 88.3, 59.9, 39.5, 26.0; **HRMS** (ESI/TOF) *m/z*: $[M + Na]^+$ Calcd for $C_{13}H_{17}NO_3Na^+$ 258.1101. Found: 258.1106.

(*Z*)-3-Methyl-5-nitro-2-phenylhex-2-en-1-ol (2.3ac)

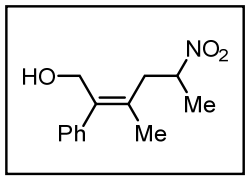

Yellowish oil (30.1 mg, 64% yield, *Z*/*E*>99:1); **IR** (neat): ν = 3568, 3396, 3080, 3057, 3021, 2989, 2937, 2921, 2861, 1599, 1546, 1492, 1442, 1388, 1361, 1314, 1218, 1118, 1051, 995, 910, 854, 768, 731, 701 cm^{-1}; **^{1}H NMR** (500 MHz, $CDCl_3$) δ_H 7.38-7.32 (m, 2H), 7.29-7.25 (m, 1H), 7.15-7.10 (m, 2H), 4.86 (dquint, J = 9.0, 6.5 Hz, 1H), 4.34 (d, J = 5.0 Hz, 2H), 3.13 (dd, J = 14.1, 9.0 Hz, 1H), 2.56 (dd, J = 14.1, 5.7 Hz, 1H), 1.64 (d, J = 6.6 Hz, 3H), 1.61 (s, 3H), 1.36 (br t, J = 6.2 Hz, 1H); **^{13}C NMR** (126 MHz, $CDCl_3$) δ_C 140.8, 140.3, 129.8, 128.9, 128.6, 127.2, 82.4, 62.9, 39.7, 20.2, 19.3; **HRMS** (ESI/TOF) *m/z*: $[M + Na]^+$ Calcd for $C_{13}H_{17}NO_3Na^+$ 258.1101. Found: 258.1108.

(2*Z*,7*Z*)-5-((*Z*)-4-Hydroxy-3-(*m*-tolyl)but-2-en-1-yl)-5-nitro-2-phenyl-8-(thiophen-3-yl)nona-2,7-diene-1,9-diol (2.6a)

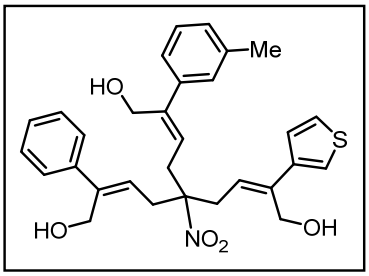

Yellowish foam (40.9 mg, 59% yield, *Z*/*E*>99:1); **IR** (neat): ν = 3559, 3336, 3106, 3028, 2921, 1719, 1601, 1535, 1486, 1433, 1357, 1286, 1230, 1122, 1076, 1010, 847, 780, 697 cm^{-1}; **^{1}H NMR** (500 MHz, $CDCl_3$) δ_H 7.40-7.24 (m, 7H), 7.24-7.14 (m, 4H), 7.10 (d, J = 7.4 Hz, 1H), 5.83 (t, J = 7.4 Hz, 1H), 5.72-5.64 (m, 2H), 4.48 (d, J = 3.3 Hz, 4H), 4.43 (s, 2H), 3.07 (d, J = 7.4 Hz, 6H), 2.47 (s, 3H), 2.43 (br s, 3H), 2.34 (s, 3H); **^{13}C NMR** (101 MHz, $CDCl_3$) δ_C 144.0, 141.3, 140.4, 140.3, 138.6, 138.5, 131.1, 129.0, 128.9, 128.8, 128.7, 128.0, 127.4, 126.7, 126.1, 125.8, 125.7, 123.8, 123.0, 122.7, 121.6, 121.4, 94.4, 59.93, 59.90, 59.85, 34.8, 34.6, 30.5, 21.7; **HRMS** (ESI/TOF) *m/z*: $[M + Na]^+$ Calcd for $C_{30}H_{33}NO_5SNa^+$ 542.1972. Found: 542.1982.

(2*Z*,7*Z*)-2-(Benzo[*d*][1,3]dioxol-5-yl)-5-((*Z*)-4-hydroxy-3-(3-(trifluoromethyl)phenyl)but-2-en-1-yl)-5-nitro-8-(thiophen-3-yl)nona-2,7-diene-1,9-diol (2.6b)

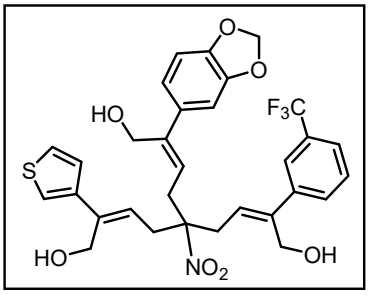

Yellowish foam (36.3 mg, 47% yield, *Z*/*E*>99:1); **IR** (neat): ν = 3642, 3559, 3350, 2954, 2922, 1722, 1607, 1536, 1503, 1487, 1433, 1334, 1233, 1163, 1119, 1075, 1036, 933, 893, 860, 780, 700 cm^{-1}; **^{1}H NMR** (500 MHz, $CDCl_3$) δ_H 7.63 (s, 1H), 7.54 (app t, J = 8.8 Hz, 2H), 7.42 (t, J = 7.8 Hz, 1H), 7.30 (dd, J = 2.9, 1.4 Hz, 1H), 7.28-7.24 (m, 1H), 7.18 (dd, J = 5.1, 1.4 Hz, 1H), 6.89-6.81 (m, 2H), 6.80-6.71 (m, 1H), 5.93 (s, 2H), 5.82 (t, J = 7.5 Hz, 1H), 5.75 (t, J = 7.3 Hz, 1H), 5.60 (t, J = 7.4 Hz, 1H), 4.48 (s, 2H), 4.45 (s, 2H), 4.43 (s, 2H), 3.12-3.01 (m, 6H), 2.55 (br s, 3H); **13C NMR** (126 MHz, $CDCl_3$) δ_C 148.0, 147.5, 143.3, 142.6, 141.5, 141.3, 138.3, 135.9, 134.6, 130.9 (q, J = 32.2 Hz), 130.1, 129.1, 126.1, 125.8, 125.6, 124.8, 124.5 (q, J = 3.7 Hz), 123.3 (q, J = 3.8 Hz), 122.1, 121.5, 120.2, 108.5, 107.2, 101.3, 94.2, 59.8, 59.7, 59.6, 34.9, 34.8, 34.4; **^{19}F NMR** (376 MHz, $CDCl_3$) δ_F -62.7; **HRMS** (ESI/TOF) *m/z*: $[M + Na]^+$ Calcd for $C_{31}H_{30}F_3NO_7SNa^+$ 640.1587. Found: 640.1582.

(2Z,7Z)-5-((Z)-4-Hydroxy-3-phenylbut-2-en-1-yl)-5-nitro-2,8-diphenylnona-2,7-diene-1,9-diol (2.6c)

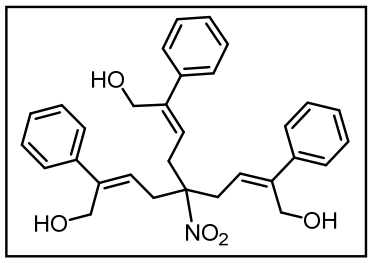

Yellowish foam (38.8 mg, 39% yield, *Z*/*E*>99:1); **IR** (neat): ν = 3568, 3326, 3055, 3024, 2953, 2922, 2851, 1598, 1534, 1492, 1443, 1353, 1013, 948, 847, 765, 695 cm^{-1}; **^{1}H NMR** (400 MHz, $CDCl_3$) δ_H 7.41-7.28 (m, 15H), 5.70 (t, J = 7.4 Hz, 3H), 4.54 (s, 6H), 3.12 (d, J = 7.4 Hz, 6H), 1.78 (br s, 3H); **^{13}C NMR** (101 MHz, $CDCl_3$) δ_C 144.1, 140.4, 128.8, 128.0, 126.7, 123.0, 94.4, 59.9, 34.8; **HRMS** (ESI/TOF) *m/z*: $[M + Na]^+$ Calcd for $C_{31}H_{33}NO_5Na^+$ 522.2251. Found: 522.2254.

Note: Nitromethane **2.2r** (10.8 μL, 0.20 mmol), 4-phenyl-4-vinyl-1,3-dioxolan-2-one **2.1a** (117.9 mg, 0.62 mmol) were used.

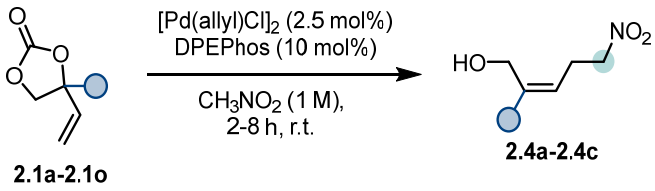

SCHEME 2.15. Synthesis of monoallylated nitroalkanes from nitromethane.

General Procedure C: In a 5 mL vial, cyclic carbonate **2.1a-2.1o** (1.0 equiv.), $[Pd(allyl)Cl]_2$ (2.5 mol%) and DPEPhos (10 mol%) were dissolved in CH_3NO_2 (1.0 M). The vial was sealed with a septum and a needle was placed through the septum to release gaseous CO_2. The mixture was stirred open to air for 2-8 h at room temperature. Hereafter, the solvent was evaporated with a gentle stream of N_2 and the residue was purified by flash chromatography on silica gel to afford the corresponding monoallylated nitroalkane **2.4a-2.4c** (**SCHEME 2.15**).

(Z)-5-Nitro-2-phenylpent-2-en-1-ol (2.4a)

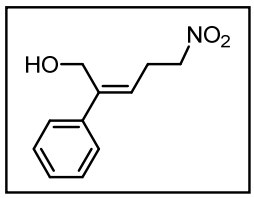

Yellowish oil (110.1 mg, 53% yield, *Z*/*E*>99:1); **IR** (neat): ν = 3563, 3376, 3082, 3056, 3028, 2924, 2852, 1545, 1492, 1430, 1376, 1190, 999, 955, 766, 697 cm^{-1}; **^{1}H NMR** (500 MHz, $CDCl_3$) δ_H 7.43-7.39 (m, 2H), 7.37-7.33 (m, 2H), 7.32-7.27 (m, 1H), 5.77 (t, J = 7.6 Hz, 1H), 4.59 (s, 2H), 4.53 (t, J = 6.9 Hz, 2H), 3.02 (q, J = 7.0 Hz, 2H), 1.54 (br s, 1H); **^{13}C NMR** (126 MHz, $CDCl_3$) δ_C 143.5, 140.3, 128.8, 128.0, 126.6, 124.6, 75.2, 60.1, 26.6; **HRMS** (ESI/TOF) *m/z*: $[M + Na]^+$ Calcd for $C_{11}H_{13}NO_3Na^+$ 230.0788. Found: 230.0790.

2-(2-Bromophenyl)-5-nitropent-2-en-1-ol (2.4b)

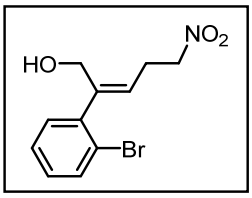

Orange oil (73.0 mg, 25% yield, *Z*/*E*=92:8); **IR** (neat): ν = 3570, 3384, 3055, 2919, 1546, 1467, 1428, 1376, 1264, 1192, 1118, 1023, 752 cm^{-1}; **^{1}H NMR** (400 MHz, $CDCl_3$) δ_H 7.60-7.54 (m, 1H), 7.31-7.26 (m, 1H), 7.20-7.13 (m, 2H), 5.52 (t, *J* = 7.6 Hz, 1H), 4.54 (t, *J* = 6.8 Hz, 2H), 4.49 (d, *J* = 6.3 Hz, 2H), 3.03 (q, *J* = 7.0 Hz, 2H), 1.65 (t, *J* = 6.3 Hz, 1H); **^{13}C NMR** (101 MHz, $CDCl_3$) δ_C 144.5, 142.1, 132.8, 131.2, 129.3, 127.7, 127.6, 122.5, 74.9, 61.0, 26.3; **HRMS** (ESI/TOF) *m/z*: $[M + Na]^+$ Calcd for $C_{11}H_{12}BrNO_3Na^+$ 307.9893. Found: 307.9891.

Note: the reported NMR resonances here correspond only to the (*Z*) isomer.

(*Z*)-5-Nitro-2-(thiophen-3-yl)pent-2-en-1-ol (2.4c)

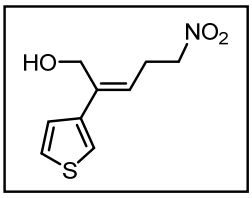

Yellowish oil (106.3 mg, 50% yield, *Z*/*E*>99:1); **IR** (neat): ν = 3565, 3376, 3106, 2916, 1544, 1428, 1376, 1336, 1267, 1178, 1001, 957, 861, 779, 734 cm^{-1}; **^{1}H NMR** (500 MHz, $CDCl_3$) δ_H 7.34 (dd, *J* = 3.0, 1.4 Hz, 1H), 7.30 (dd, *J* = 5.1, 2.9 Hz, 1H), 7.20 (dd, *J* = 5.2, 1.4 Hz, 1H), 5.89 (t, *J* = 7.7 Hz, 1H), 4.54 (s, 2H), 4.51 (t, *J* = 6.8 Hz, 2H), 2.99 (q, *J* = 7.0 Hz, 2H), 1.64 (br s, 1H); **^{13}C NMR** (126 MHz, $CDCl_3$) δ_C 141.2, 138.0, 126.2, 125.7, 123.1, 121.4, 75.1, 59.9, 26.3; **HRMS** (ESI/TOF) *m/z*: $[M + Na]^+$ Calcd for $C_9H_{11}NO_3SNa^+$ 236.0352. Found: 236.0356.

2.4.5 Synthetic Transformations of Homoallylic Nitroalkanes

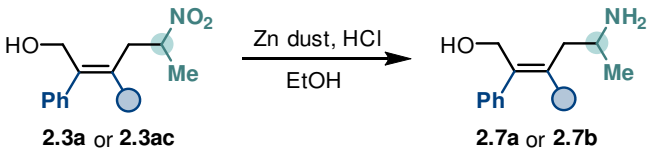

2.3a or **2.3ac** → **2.7a** or **2.7b**

SCHEME 2.16. Synthesis of homoallylic amines.

In a 25 mL round-bottomed flask, the homoallylic nitroalkane substrate **2.3a** or **2.3ac** (1.0 equiv.) was dissolved in EtOH (0.15 M) under Ar. Then, 1 M HCl (0.1 M) was added dropwise, followed by the addition of activated zinc dust (30 equiv.). The mixture was stirred at room temperature for 8 h. The mixture was basified with aqueous saturated $NaHCO_3$ and the solids were removed by filtration. The aqueous phase was extracted three times with EtOAc (20 mL). The combined organic layers were washed with brine, dried over Na_2SO_4, filtered, and concentrated *in vacuo*. The crude product was purified by flash chromatography on silica gel to afford the corresponding homoallylic amine **2.7a** or **2.7b**.

(*Z*)-5-amino-2-phenylhex-2-en-1-ol (2.7a)

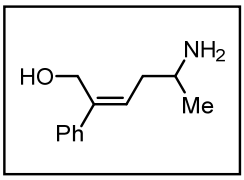

Yellowish oil (42.5 mg, 74% yield, *Z*/*E*>99:1); **IR** (neat): ν = 3344, 3283, 3080, 3055, 3025, 2959, 2925, 2871, 1727, 1597, 1493, 1445, 1374, 1343, 1009, 940, 765, 696 cm^{-1}; **^{1}H NMR** (500 MHz, CD_3OD) δ_H 7.50-7.43 (m, 2H), 7.34-7.27 (m, 2H), 7.26-7.19 (m, 1H), 5.90 (t, *J* = 7.7 Hz, 1H), 4.53 (d, *J* = 12.1 Hz, 1H), 4.50 (d, *J* = 12.1 Hz, 1H), 3.11 (sext, *J* = 6.5 Hz, 1H), 2.51-2.35 (m, 2H), 1.20 (d, *J* = 6.4 Hz, 3H); **^{13}C NMR** (126 MHz, CD_3OD) δ_C 143.0, 129.2, 129.1, 128.0, 127.5, 127.4, 59.7, 48.3, 38.2, 22.2; **HRMS** (ESI/TOF) *m/z*: $[M + H]^+$ Calcd for $C_{12}H_{18}NO^+$ 192.1383. Found: 192.1390.

(*Z*)-5-amino-3-methyl-2-phenylhex-2-en-1-ol (2.7b)

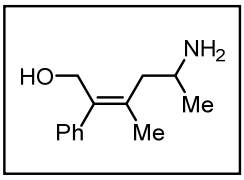

Yellowish oil (48.7 mg, 79% yield, *Z*/*E*>99:1); **IR** (neat): ν = 3375, 3051, 3019, 2974, 2931, 2506, 2188, 1600, 1492, 1441, 1386, 1202, 1156, 1109, 1058, 993, 768, 720, 701 cm^{-1}; **^{1}H NMR** (500 MHz, CD_3OD) δ_H 7.37-7.31 (m, 2H), 7.28-7.23 (m, 1H), 7.23-7.19 (m, 2H), 4.45 (d, *J* = 12.0 Hz, 1H), 4.25 (d, *J* = 12.0 Hz, 1H), 3.53 (sext, *J* = 6.9 Hz, 1H), 2.69 (dd, *J* = 13.6, 7.3 Hz, 1H), 2.54 (dd, *J* = 13.6, 7.4 Hz, 1H), 1.64 (s, 3H), 1.38 (d, *J* = 6.6 Hz, 3H); **^{13}C NMR** (126 MHz, CD_3OD) δ_C 143.3, 140.9, 132.3, 129.8, 129.2, 127.7, 63.2, 47.3, 40.3, 20.4, 19.3; **HRMS** (ESI/TOF) *m/z*: $[M + Na]^+$ Calcd for $C_{13}H_{19}NONa^+$ 228.1359. Found: 228.1364.

(*Z*)-5-oxo-2-phenylhex-2-en-1-yl benzoate (2.9)

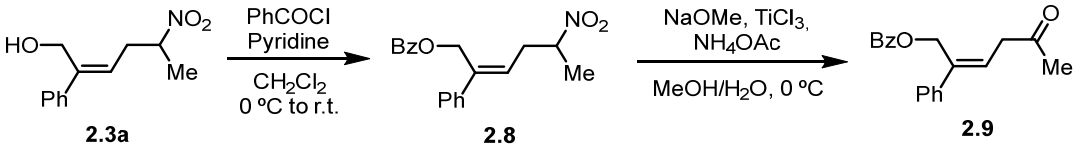

In a flame-dried 25 mL round-bottomed flask, compound **2.3a** (170.0 mg, 0.77 mmol) was dissolved in dry CH_2Cl_2 (2.3 mL) under Ar. Then, pyridine (249 µL, 3.07 mmol) was added dropwise and the mixture was cooled to 0 °C. Thereafter, benzoyl chloride (107 µL, 0.92 mmol) was added dropwise, and the mixture was allowed to warm to room temperature and was stirred for 14 h. The reaction was quenched with 1 M HCl and the phases were separated. The aqueous phase was extracted with CH_2Cl_2 (3 × 10 mL). The combined organic layers were washed with aqueous saturated $NaHCO_3$ and brine (1 × 15 mL), and were dried over Na_2SO_4, filtered, and concentrated *in vacuo*. The crude product was purified by flash chromatography on silica gel using 5% Et_2O/hexane to afford compound **2.8** (178.9 mg, 72% yield, *Z*/*E*>99:1) as a colorless oil; **IR** (neat): ν = 3061, 3032, 2990, 2938, 2899, 1714, 1601, 1546, 1492, 1449, 1389, 1359, 1313, 1264, 1214, 1176, 1107, 1098, 1070, 1024, 958, 762, 738, 710, 697 cm^{-1}; **^{1}H NMR** (500 MHz, $CDCl_3$) δ_H 7.97-

7.92 (m, 2H), 7.56-7.51 (m, 1H), 7.44-7.38 (m, 4H), 7.37-7.32 (m, 2H), 7.32-7.27 (m, 1H), 5.92 (t, J = 7.6 Hz, 1H), 5.30 (app d, J = 12.5 Hz, 1H), 5.19 (app d, J = 12.5 Hz, 1H), 4.71 (dqd, J = 8.1, 6.7, 5.5 Hz, 1H), 3.10 (dt, J = 15.2, 7.9 Hz, 1H), 2.88 (ddd, J = 15.2, 7.5, 5.5 Hz, 1H), 1.63 (d, J = 6.7 Hz, 3H); **^{13}C NMR** (126 MHz, $CDCl_3$) δ_C 166.5, 140.1, 139.0, 133.2, 130.0, 129.8, 128.6, 128.5, 128.0, 127.1, 126.5, 83.0, 61.5, 34.1, 19.1; **HRMS** (ESI/TOF) m/z: $[M + Na]^+$ Calcd for $C_{19}H_{19}NNaO_4$ 348.1206. Found: 348.1215.

In an argon-flushed 25 mL round-bottomed flask, compound **2.8** (65.1 mg, 0.20 mmol) was dissolved in MeOH (3.0 mL) under Ar. The solution was cooled to 0 °C and NaOMe (137 μL, 0.60 mmol, 25% in MeOH) was added. In a separate flask, NH_4OAc (531.9 mg, 6.90 mmol) was dissolved in H_2O (1.2 mL) and $TiCl_3$ (1.1 mL, 1.10 mmol, 12% in HCl) was added dropwise. Hereafter, the mixture of $TiCl_3$ was transferred with a cannula to the other reaction flask over 5 min. The resultant mixture was stirred at 0 °C for 3 h. Hereafter, the product was extracted with Et_2O (3 × 10 mL). The combined organic layers were washed with $NaHCO_3$ (2 × 10 mL) and brine (1 × 10 mL), dried over $MgSO_4$, filtered, and concentrated *in vacuo*. The crude product was purified by flash chromatography on silica gel using 5-15% EtOAc/hexanes to afford compound **2.9** (31.1 mg, 53% yield, Z/E>99:1) as a colorless oil; **IR** (neat): ν = 3060, 3032, 2960, 2924, 2854, 1713, 1601, 1493, 1451, 1356, 1315, 1264, 1175, 1159, 1107, 1098, 1070, 1024, 952, 759, 710, 697 cm^{-1}; **^{1}H NMR** (500 MHz, $CDCl_3$) δ_H 7.99-7.91 (m, 2H), 7.56-7.51 (m, 1H), 7.51-7.48 (m, 2H), 7.42-7.38 (m, 2H), 7.37-7.32 (m, 2H), 7.31-7.26 (m, 1H), 6.30 (t, J = 7.2 Hz, 1H), 5.24 (s, 2H), 3.59 (d, J = 7.2 Hz, 2H), 2.24 (s, 3H); **^{13}C NMR** (126 MHz, $CDCl_3$) δ_C 205.5, 166.6, 140.2, 137.4, 133.2, 130.1, 129.8, 128.6, 128.5, 127.8, 126.4, 125.9, 62.0, 43.3, 30.1; **HRMS** (ESI/TOF) m/z: $[M + Na]^+$ Calcd for $C_{19}H_{18}NaO_3$ 317.1148. Found: 317.1149.

2.4.6 Crystallographic Studies

Single crystals of compound **2.3m** suitable for X-ray diffraction were obtained by slow evaporation from an acetone solution. The measured crystal of **2.3m** was stable under atmospheric conditions; nevertheless, it was treated under inert conditions immersed in perfluoro-polyether as protecting oil for manipulation. Data Collection: measurements were made on a Bruker-Nonius diffractometer equipped with an APPEX II 4K CCD area detector, an FR591 rotating anode with MoKα radiation, Montel mirrors, and a Kryoflex low-temperature device (T = −173 °C). Full-sphere data collection was used with ω and ϕ scans. Programs used: Data collection Apex2 V2011.3 (Bruker-Nonius 2008), data reduction Saint+Version 7.60A (Bruker AXS 2008), and absorption correction SADABS V. 2008−1 (2008). Structure Solution: SHELXTL Version 6.10 (Shel-drick, 2000) was used.30 Structure Refinement: SHELXTL-97-UNIX VERSION.

TABLE 2.3. Crystal data and structure refinement for **2.3m** (CCDC-1837204).

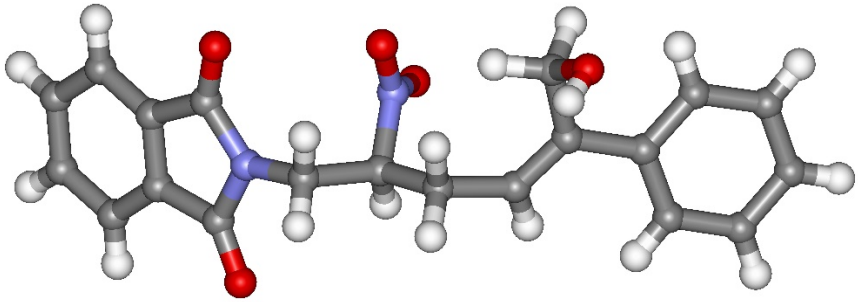

Empirical formula	$C_{21.5}H_{21}N_2O_{5.5}$	
Formula weight	395.40	
Temperature	100(2) K	
Wavelength	0.71073 Å	
Crystal system	monoclinic	
Space group	$P2_1/n$	
Unit cell dimensions	a = 13.6502(8) Å	α = 90°
	b = 5.5638(3) Å	β = 93.556(6)°
	c = 25.477(2) Å	γ = 90°
Volume	1931.2(2) Å^3	
Z	4	
Density (calculated)	1.360 mg·m^{-3}	
Absorption coefficient	0.099 mm^{-1}	
F(000)	832	
Crystal size	0.20 × 0.10 × 0.05 mm^3	
Theta range for data collection	1.74 to 27.80°.	
Index ranges	-4 <= h <= 8, -15 <= k <= 16, -19 <= l <= 18	
Reflections collected	5097	
Independent reflections	5097[R(int) = 0.0238]	
Completeness to theta =27.80°	88.6%	
Absorption correction	Multi-scan	
Max. and min. transmission	1.00 and 0.74	
Refinement method	Full-matrix least-squares on F^2	
Data / restraints / parameters	5097/ 0/ 256	
Goodness-of-fit on F^2	0.932	
Final R indices [I>2σ(I)]	R_1 = 0.0418, wR_2 = 0.0854	
R indices (all data)	R_1 = 0.0761, wR_2 = 0.0970	
Largest diff. peak and hole	0.245 and -0.202 e·Å^{-3}	

UNIVERSITAT ROVIRA I VIRGILI
STEREOSELECTIVE TRANSFORMATIONS OF VINYL CYCLIC CARBONATES AND APPLICATIONS IN NATURAL PRODUCT SYNTHESIS
Àlex Cristòfol Martínez

UNIVERSITAT ROVIRA I VIRGILI
STEREOSELECTIVE TRANSFORMATIONS OF VINYL CYCLIC CARBONATES AND APPLICATIONS IN NATURAL PRODUCT SYNTHESIS
Àlex Cristòfol Martínez

Each problem that I solved became a rule which served afterwards to solve other problems. — Rene Descartes

CHAPTER 3

FORMAL SYNTHESIS OF INDOLIZIDINE AND QUINOLIZIDINE ALKALOIDS FROM VINYL CYCLIC CARBONATES

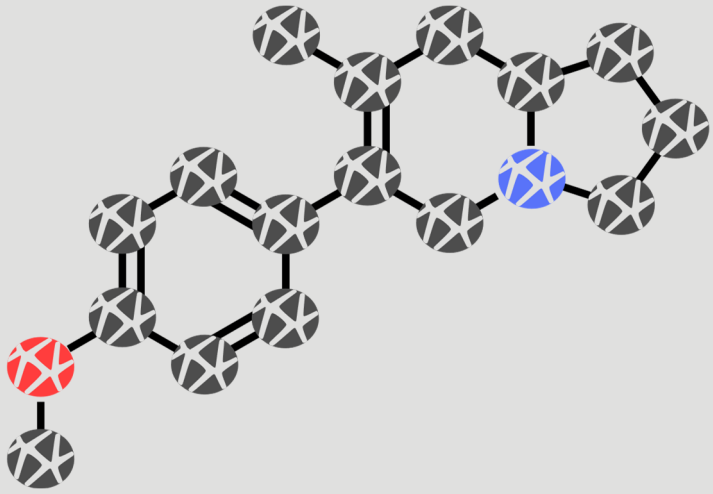

The results of this chapter have been published in:

Cristòfol, À.; Böhmer, C.; Kleij, A. W. *Chem. Eur. J.* **2019**, 25, 15055–15058

3.1 Introduction

3.1.1 Indolizidine and Quinolizidine Alkaloids

Members of the indolizidine and quinolizidine families of alkaloids possess a characteristic azabicyclic nucleus. The main difference is that the indolizidine bicycle is formed by a fused 6- and 5-membered ring, whereas the quinolizidine bicycle is formed by two fused 6-membered rings. These families comprise more than 740 compounds that have been identified and isolated, and are naturally present in many living organisms, such as in fungus, arthropods, plants, or marine sources (**FIGURE 3.1**).[110]

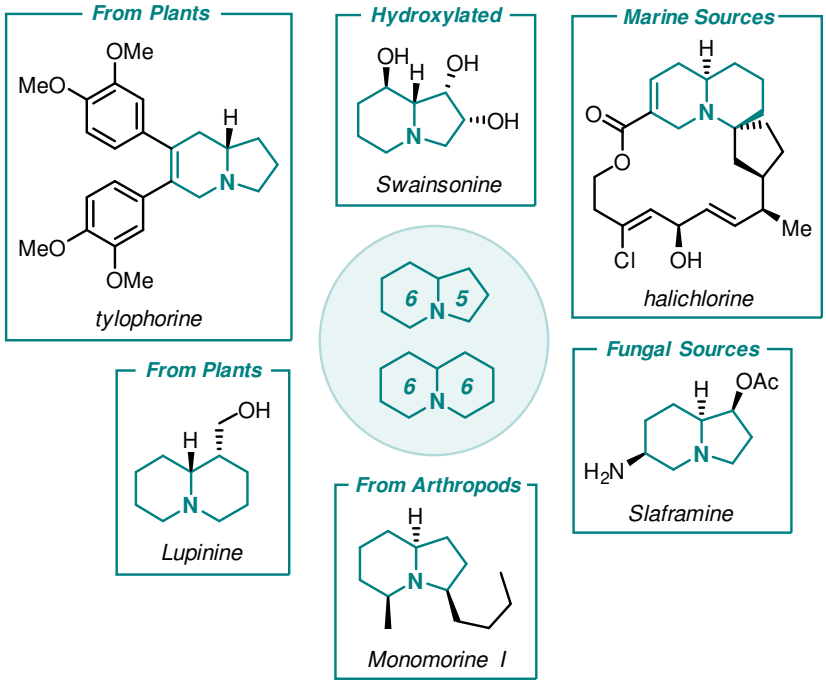

FIGURE 3.1. Representative examples of indolizidine and quinolizidine alkaloids.

Among these alkaloids, members containing an aryl-substituent, namely ipalbidine and the phenantroindolizidine and phenantroquinolizidine alkaloids (including their *seco*-analogs) have received widespread attention due to their extensive range of biological activities. Ipalbidine is a non-addictive analgesic, an oxygen-free radical scavenger, and has demonstrated inhibitory effects on the respiratory burst of leukocytes.[111] On the other hand, phenantroindolizidine and phenantroquinolizidine alkaloids have demonstrated

[110] a) Michael, J. P. *Nat. Prod. Rep.* **2008**, *25*, 139-165. b) Michael, J. P. The Alkaloids. In *Chemistry and Biology*, Vol. 75, 2016; pp 1-498.

[111] See references mentioned in Niphakis, M. J.; Georg, G. I. *J. Org. Chem.* **2010**, *75*, 6019-6022.

a broad range of biological activities ranging from anticancer and antiviral to anti-inflammatory activities.[112] These alkaloids are commonly isolated from plants from the genera of *Tylophora* (Asclepiadacea) and *Ficus* (Moraceae).

Several synthetic approaches towards these alkaloids have been previously reported. Most of these approaches rely on pericyclic reactions,[113] metal-catalyzed cyclizations,[114] radical cyclizations,[115] Pictet-Spengler reactions[116] or partial reductions of alkyl pyridinium salts[117] to build the key 1,2,3,6-tetrahydropyridine motif (**FIGURE 3.2**). However, a more unifying and flexible strategy would still be of general importance from a synthetic and medicinal chemistry point of view and could potentially allow for a more systematic exploration of SARs of a wider range of indolizidine and quinolizidine targets.

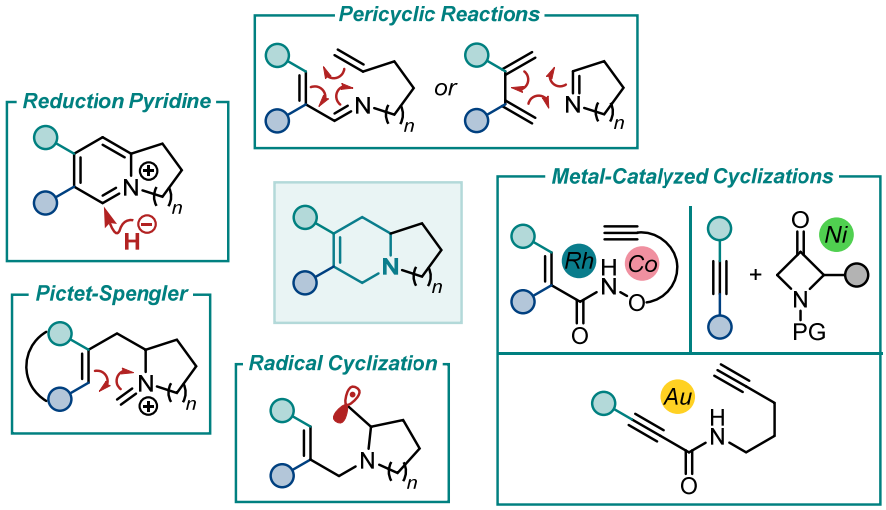

FIGURE 3.2. Illustrative synthetic approaches towards aryl-containing indolizidine and quinolizidine alkaloids.

[112] a) Huang, R.; Li, Z.; Jin, Z. *Synthesis* **2001**, 2365-2378. b) Lansky, E. P.; Paavilainen, H. M.; Pawlus, A. D.; Newman, R. A. *J. Ethnopharmacol.* **2008**, *119*, 195-213. c) Chemler, S. *Curr. Bioact. Compd.* **2009**, *5*, 2-19. d) Fatima Pereira, M.; Rochais, C.; Dallemagne, P. *Anti-Cancer Agents Med. Chem.* **2015**, *15*, 1080-1091. e) Su, B.; Cai, C.; Li, Y.; Wang, Q. *ACS Agric. Sci. Technol.* **2021**, *1*, 222-229.

[113] a) Danishefsky, S. J.; Vogel, C. *J. Org. Chem.* **1986**, *51*, 3915-3916. b) Lahm, G.; Stoye, A.; Opatz, T. *J. Org. Chem.* **2012**, *77*, 6620-6623. c) Chang, C.-F.; Li, C.-F.; Tsai, C.-C.; Chuang, T.-H. *Org. Lett.* **2016**, *18*, 638-641.

[114] a) McIver, A.; Young, D. D.; Deiters, A. *Chem. Commun.* **2008**, 4750-4752. b) Xu, X.; Liu, Y.; Park, C.-M. *Angew. Chem. Int. Ed.* **2012**, *51*, 9372-9376. c) Lerchen, A.; Knecht, T.; Koy, M.; Daniliuc, C. G.; Glorius, F. *Chem. Eur. J.* **2017**, *23*, 12149-12152. d) Renner, J.; Thakur, A.; Rutz, P. M.; Cowley, J. M.; Evangelista, J. L.; Kumar, P.; Prater, M. B.; Stolley, R. M.; Louie, J. *Org. Lett.* **2020**, *22*, 924-928. e) Tian, G.; Song, L.; Li, Z.; Robeyns, K.; Van Meervelt, L.; Van der Eycken, E. V. *Org. Lett.* **2020**, *22*, 8441-8445.

[115] a) Chea, J.; Clive, D. L. J. *J. Org. Chem.* **2015**, *80*, 10294-10298. b) Liu, G.-Q.; Reimann, M.; Opatz, T. *J. Org. Chem.* **2016**, *81*, 6142-6148.

[116] a) Fürstner, A.; Kennedy, J. W. J. *Chem. Eur. J.* **2006**, *12*, 7398-7410. b) Wang, Q. *et al. ACS Agric. Sci. Technol.* **2021**

[117] a) Ciufolini, M. A.; Roschangar, F. *J. Am. Chem. Soc.* **1996**, *118*, 12082-12089. b) Jo, Y.-I.; Burke, M. D.; Cheon, C.-H. *Org. Lett.* **2019**, *21*, 4201-4204.

3.1.2 Cyclic Carbonates in Natural Product Synthesis

Despite the vast interest in the synthesis of cyclic carbonates from carbon dioxide and epoxides,[118] their utilization in more complex multistep synthesis towards natural products and pharmaceuticals has been scarcely reported. Cyclic carbonates have so far been mostly used as protecting groups of 1,2-diols, especially in polyhydroxylated molecules (*e.g.*, carbohydrates or sphingolipids), thus playing a passive role in multistep synthetic sequences.[119] This intrinsic kinetic stability has likely hampered for a long time their use as reactive intermediates in synthetic campaigns towards more complex organic molecules.

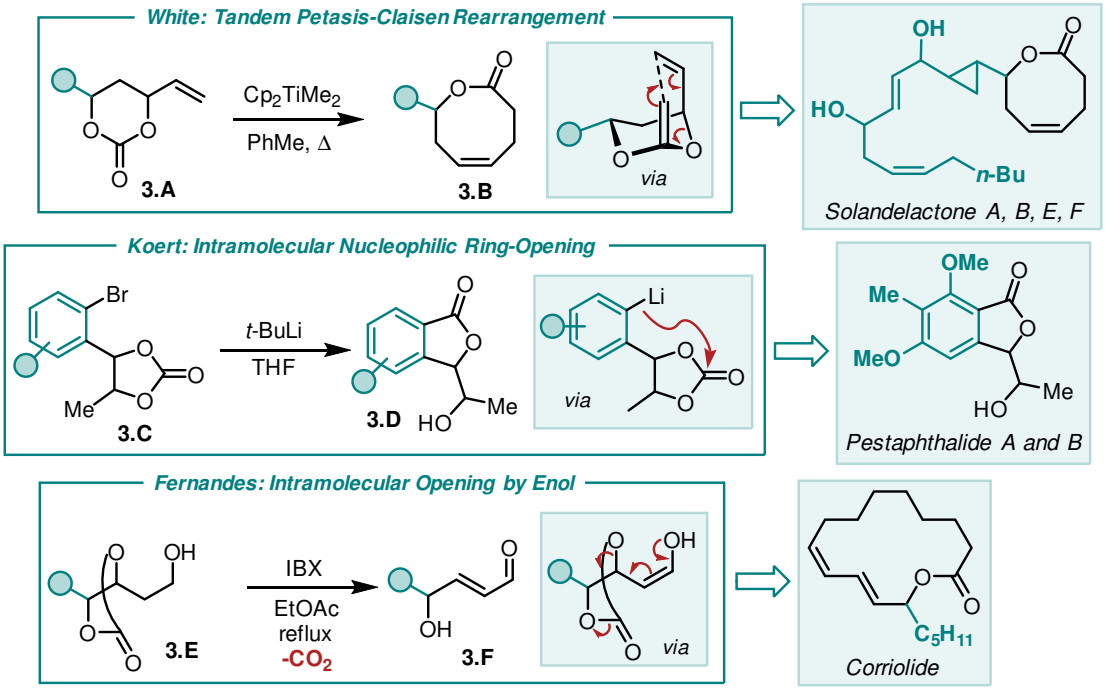

SCHEME 3.1. Synthesis of natural products using cyclic carbonates as reactive intermediates.

In this regard, only a few examples have been published where cyclic carbonates play an active role in accomplishing the synthesis of natural products (**SCHEME 3.1**). White and coworkers reported an elegant use of 6-membered cyclic carbonates (**3.A**) as precursors of cyclic ketene acetals, which is accomplished through a Petasis reaction with Cp_2TiMe_2. Upon heating, these intermediates undergo a stereospecific Claisen rearrangement to furnish the 8-membered lactones (**3.B**) present in Solandelactones A, B, E,

[118] a) Limburg, B.; Cristòfol, À.; Della Monica, F.; Kleij, A. W. *ChemSusChem* **2020**, *13*, 6056-6065. b) See Kleij, A. W. *et al. Green Chem.* **2021** (*ref.* 42c) on page 26.

[119] a) Pankau, W. M.; Kreiser, W. *Helv. Chim. Acta* **1998**, *81*, 1997-2004. b) Crich, D.; Vinod, A. U.; Picione, J. *J. Org. Chem.* **2003**, *68*, 8453-8458. c) Li, Z. *Carbohydr. Res.* **2010**, *345*, 1952-1957. d) Kancharla, P. K.; Navuluri, C.; Crich, D. *Angew. Chem. Int. Ed.* **2012**, *51*, 11105-11109. e) Wisse, P.; de Geus, M. A. R.; Cross, G.; van den Nieuwendijk, A. M. C. H.; van Rooden, E. J.; van den Berg, R. J. B. H. N.; Aerts, J. M. F. G.; van der Marel, G. A.; Codée, J. D. C.; Overkleeft, H. S. *J. Org. Chem.* **2015**, *80*, 7258-7265. f) Panza, L.; Compostella, F.; Imperio, D. *Carbohydr. Res.* **2019**, *472*, 50-57.

and F.[120] Koert and coworkers reported an intramolecular ring-opening of the cyclic carbonates (**3.C**) *en route* to Pestaphthalide A and B.[121] Lastly, Fernandes and coworkers took advantage of the more labile nature of the cyclic carbonate group to develop an intramolecular decarboxylative opening of cyclic carbonates intermediates (**3.E**) with *in situ* generated enol intermediates, affording the thermodynamically favored α,β-unsaturated enals (**3.F**).[122] These latter intermediates were used to accomplish the total synthesis of (*R*)- and (*S*)-Corriolide.

When considering vinyl cyclic carbonates (VCCs) as reactive intermediates for the synthesis of natural products, only two examples have been previously reported (**SCHEME 3.2**). The first example, communicated by Trost, describes a highly enantioselective allylic substitution of divinylethylene carbonate (**3.G**) with phenol nucleophiles. The protocol was applied to the total synthesis of macrolide *iso*-cladospolide B.[123] A second example reported by Fukuyama illustrates an intramolecular allylic alkylation that allows the consecutive construction of a fused 6- and 5-membered ring, which represents a key motif of the sesquiterpene Jiadifenin.[124]

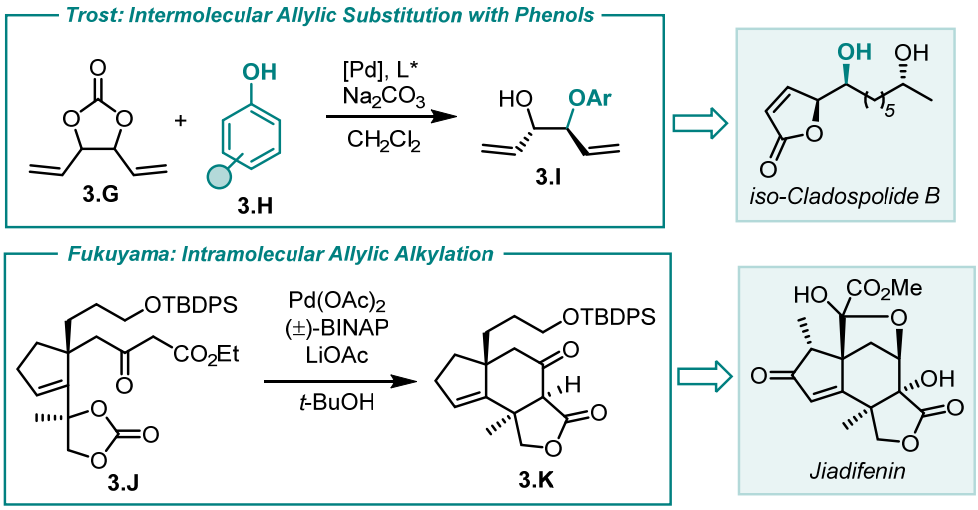

SCHEME 3.2. Synthesis of natural products using VCCs as reactive intermediates.

[120] White, J. D.; Lincoln, C. M.; Yang, J.; Martin, W. H. C.; Chan, D. B. *J. Org. Chem.* **2008**, *73*, 4139-4150. The model Claisen rearrangement was previously discovered by Holmes, refer to: O'Sullivan, P. T.; Buhr, W.; Fuhry, M. A. M.; Harrison, J. R.; Davies, J. E.; Feeder, N.; Marshall, D. R.; Burton, J. W.; Holmes, A. B. *J. Am. Chem. Soc.* **2004**, *126*, 2194-2207.

[121] Koert, U.; Schwaben, J.; Cordes, J.; Harms, K. *Synthesis* **2011**, 2929-2934.

[122] Kumari, A.; Gholap, S. P.; Fernandes, R. A. *Chem. Asian. J.* **2019**, *14*, 2278-2290.

[123] See Trost, B. M. *et al. J. Am. Chem. Soc.* **2006** (*ref.* 48) on page 28.

[124] a) Harada, K.; Imai, A.; Uto, K.; Carter, R. G.; Kubo, M.; Hioki, H.; Fukuyama, Y. *Org. Lett.* **2011**, *13*, 988-991. b) Harada, K.; Imai, A.; Uto, K.; Carter, R. G.; Kubo, M.; Hioki, H.; Fukuyama, Y. *Tetrahedron* **2015**, *71*, 2199-2209.

3.1.3 Aims and Objectives

In view of the potential of (functionalized) cyclic carbonates as synthetic intermediates and considering the value of developing a modular and efficient route to make biologically relevant indolizidine and quinolizidine alkaloids, the main objective of the work described in this chapter was to develop a flexible multistep synthetic route towards the synthesis of complex aryl-containing indolizidine and quinolizidine alkaloids using VCCs as key reactive intermediates. We envisaged that the previously described methodology in chapter 2 for the allylation of nitroalkanes with VCCs would provide suitable functionalized homoallylic nitroalkanes having an appropriate double bond configuration, which could be further elaborated towards biologically relevant aryl-containing indolizidine and quinolizidine alkaloids, and analogs thereof (**SCHEME 3.3**).

A second objective of the work presented in this chapter was to identify suitable conditions to generate the key fused azabicyclic structure typically present in the indolizidine and quinolizidine alkaloids using acyclic homoallylic nitroalkanes as starting point while applying a consecutive or sequential double cyclization strategy.

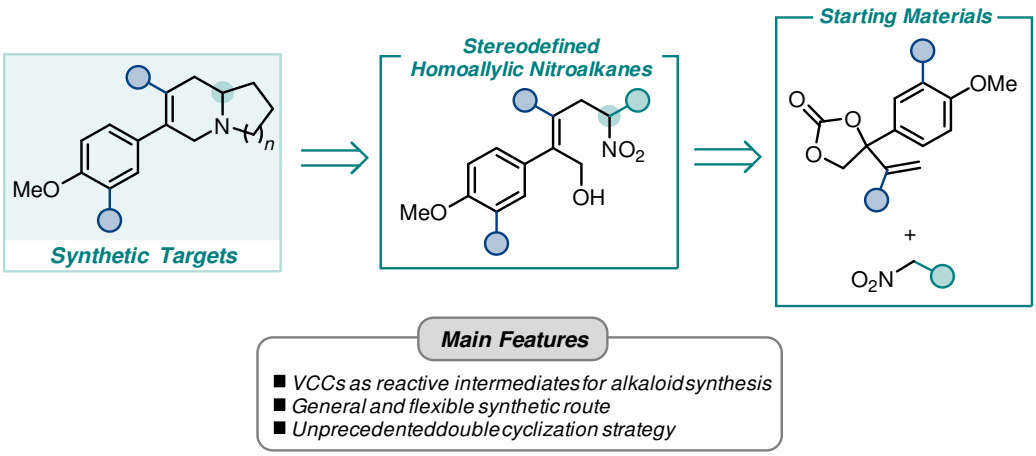

SCHEME 3.3. Schematic representation and objectives of the present work.

3.2 Results and Discussion

3.2.1 Preparation of Vinyl Cyclic Carbonates

TABLE 3.1. Synthesis of α-hydroxyketones **3.1a** and **3.1b** through reported methodologies.

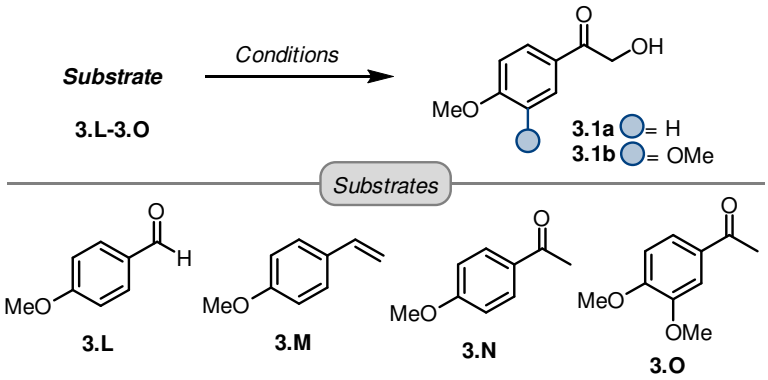

Entry	Substrate	Conditions	Scale (mmol) [a]	Yield (%) [b]
1	**3.L**	$(CH_2O)_n$, DIPEA, NHC precatalyst	10	5
2	**3.M**	$Pd(OAc)_2$, DAF, H_2O_2, TFA	12.5	21
3	**3.N**	***1.*** $PhI(OAc)_2$, KOH; ***2.*** *p*-TsOH·H_2O, H_2O	28.6	52
4	**3.O**	***1.*** $PhI(OAc)_2$, KOH; ***2.*** *p*-TsOH·H_2O, H_2O	30	10
5	**3.N**	***1.*** NBS, *p*-TsOH·H_2O; ***2.*** HCO_2Na, H_2O	33.9	73
6	**3.O**	***1.*** NBS, *p*-TsOH·H_2O; ***2.*** HCO_2Na, H_2O	13.9	75

Please refer to appendix A for the structure of the NHC precatalyst and DAF ligand; [a] mmol of substrate **3.L-3.O**; [b] Yield (%) of isolated product.

Initially, we attempted to synthesize suitable VCC starting materials from commercially available aldehydes through a hydroxymethylation reaction using formaldehyde, catalyzed by a thiazolium salt derived NHC, similarly as described for the VCCs in chapter 1. However, we found that the desired α-hydroxyketone (**3.1a**) was only produced in 5% yield at a 10 mmol scale reaction (**TABLE 3.1**, entry 1).[125] Therefore, we decided to screen other reported methodologies to make the desired α-hydroxyketone (**3.1a**). A palladium-catalyzed deoxygenation of styrene **3.M**, as reported by Jiang,[126] was attempted but unfortunately, the yield of product **3.1a** could not be reproduced in our hands when running the reaction using 12.5 mmol of **3.M**, and only 21% yield of product was obtained (**TABLE 3.1**, entry 2). We were pleased to obtain 52% yield of **3.1a** when applying a two-step protocol involving an initial α-acetoxylation of acetophenone **3.N** mediated by $PhI(OAc)_2$, followed by acid-catalyzed hydrolysis (**TABLE 3.1**, entry 3). However, a similar approach

[125] Presumably, the formation of the Breslow intermediate with less electrophilic aldehydes is more difficult and coupling of two formaldehyde molecules is competing: Kuhl, N.; Glorius, F. *Chem. Commun.* **2011**, *47*, 573-575.
[126] Huang, J.; Li, J.; Zheng, J.; Wu, W.; Hu, W.; Ouyang, L.; Jiang, H. *Org. Lett.* **2017**, *19*, 3354-3357.

only afforded 10% of **3.1b** when using aldehyde **3.O** (**TABLE 3.1**, entry 4).[127] Finally, a more conventional α-bromination/hydrolysis sequence afforded the desired α-hydroxyketone **3.1a** and **3.1b** in 73% and 75% yield, respectively, while also being highly reproducible (**TABLE 3.1**, entries 5-6).[128]

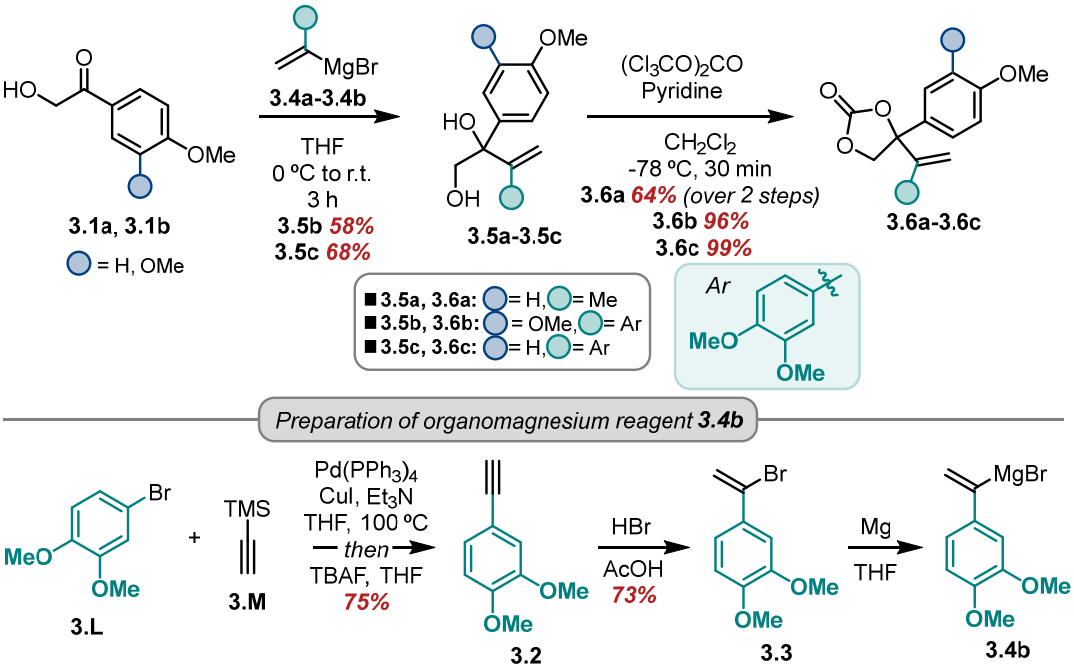

SCHEME 3.4. Synthetic route towards VCCs **3.6a-3.6c** from α-hydroxyketones **3.1a** and **3.1b**.

With α-hydroxyketones **3.1a** and **3.1b** in hand, a subsequent Grignard reaction to introduce the alkenyl group was straightforward and afforded 1,2-diols **3.5a-3.5c** in good yields (**SCHEME 3.4**). More than a two-fold excess of organomagnesium reagent **3.4a-3.4b** had to be employed due to deprotonation of the free alcohol group. While isopropenylmagnesium bromide (**3.4a**) can be directly purchased from commercial suppliers, aryl-substituted alkenyl organomagnesium reagent **3.4b** and its alkenyl bromide (**3.3**) had to be first prepared. This overall route to **3.4b** involved a Sonogashira coupling of 4-bromoveratrole (**3.L**) with trimethylsilylacetylene (**3.M**), fluoride-mediated deprotection of the TMS group, hydrobromination of the alkyne with HBr, and lastly, the synthesis of Grignard reagent **3.4b** with Mg turnings.[129] Chromatographic purification of 1,2-diol **3.5a** was not needed and the crude product was directly carried forward.[130] The

[127] Sahoo, S. C.; Nath, U.; Pan, S. C. *Eur. J. Org. Chem.* **2017**, 4434-4438.
[128] a) Tang, C.; Li, C.; Zhang, S.; Hu, Z.; Wu, J.; Dong, C.; Huang, J.; Zhou, H.-B. *J. Med. Chem.* **2015**, *58*, 4550-4572. b) Zhang, Y.; He, L.; Shi, L. *Adv. Synth. Catal.* **2018**, *360*, 1926-1931.
[129] a) Rosiak, A.; Frey, W.; Christoffers, J. *Eur. J. Org. Chem.* **2006**, 4044-4054. b) Roy, S.; Das, S. K.; Chattopadhyay, B. *Angew. Chem. Int. Ed.* **2018**, *57*, 2238-2243.
[130] While *in situ* generated propene is easily removed by venting the reaction, purification of **3.5b-3.5c** was needed to remove the non-volatile 3,4-dimethoxystyrene byproduct originated from alcohol deprotonation.

synthesis of VCCs **3.6a-3.6c** from 1,2-diols **3.5a-3.5c** was concluded by treatment of the latter with triphosgene in the presence of pyridine at -78 ºC.

3.2.2 Preparation of Stereodefined Homoallylic Nitroalkanes

After having completed the synthesis of the VCCs starting materials, we then focused on the preparation of the desired stereodefined homoallylic nitroalkanes. To this end, an appropriate nitroalkane partner needed to be selected that would allow for further elaboration towards the 5-or 6-membered ring of the indolizidine or quinolizidine core, while also being compatible with our developed palladium-catalyzed allylic substitution reaction (chapter 2). Taking these aspects into account, we thought that methyl 4-nitrobutyrate (**3.7a**) and methyl 5-nitropentanoate (**3.7b**) would represent excellent nitroalkane partners, as their ester functionalities can provide a versatile handle for finalizing the synthetic route through different pathways, while also being tolerated during the palladium-catalyzed allylic substitution reaction. Moreover, methyl 4-nitrobutyrate (**3.7a**) is commercially available, and methyl 5-nitropentanoate (**3.7b**) can be conveniently prepared in one step through a Victor-Mayer reaction.[131]

Based on our previously developed allylation methodology, we decided to perform the reaction in MeCN using $Pd_2(dba)_3{\cdot}CHCl_3$, DPEPhos, and DBU in catalytic amounts. We were pleased to obtain the desired compound **3.8a** in 64% yield and >99:1 *Z*/*E* selectivity (**TABLE 3.2**, entry 1). Hereafter, the synthesis of homoallylic nitroalkanes bearing two aryl groups was examined. Despite the increased steric crowding of having two aryl groups *cis* to each other, we were pleased to still be able to isolate these desired products with a tetrasubstituted double bond in 46% and 53% yield with >99:1 stereoselectivity (**TABLE 3.2**, entries 2-3). Furthermore, we could also obtain compound **3.8d** in 51% yield (**TABLE 3.2**, entry 4) when using methyl 5-nitropentanoate.

[131] Herr, J. R.; Jungheim, N. L.; McGill III, J. M.; Thrasher, K. J.; Valluri, M. Compounds, methods and formulations for the oral delivery of a glucagon-like peptide (GLP)-1 compound or a melanocortin-4 receptor (MC4) agonist peptide. US Patent WO2005019184A1, March 3, 2010.

TABLE 3.2. Stereoselective synthesis of homoallylic nitroalkanes **3.8a-3.8d**.

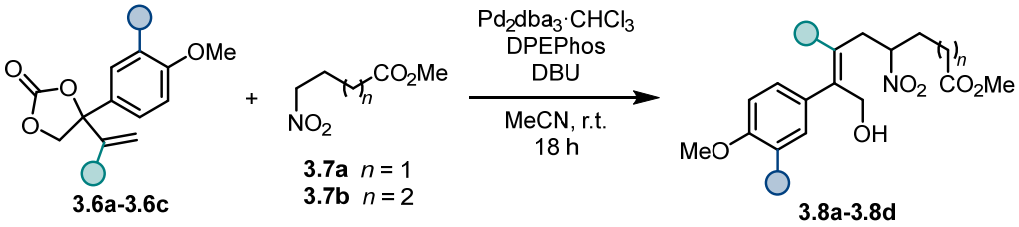

Entry	VCC	Nitroalkane	Product	Yield (%) [a]
1	**3.6a**	**3.7a**	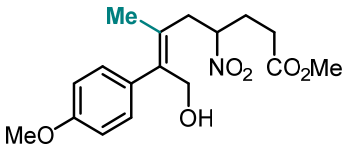 **3.8a**	64
2	**3.6b**	**3.7a**	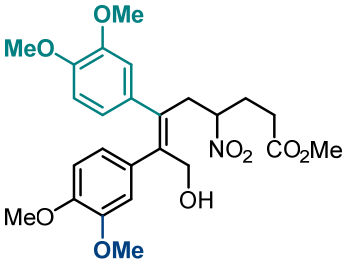 **3.8b**	46
3	**3.6c**	**3.7a**	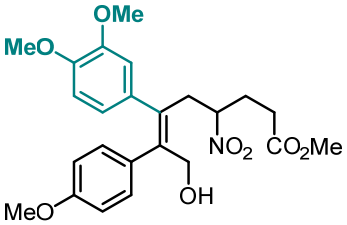 **3.8c**	53
4	**3.6c**	**3.7b**	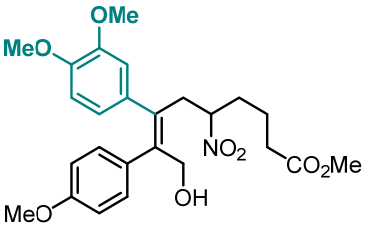 **3.8d**	51

Reaction conditions: VCC **3.6a-3.6c** (1 equiv.), nitroalkane **3.7a-3.7b** (1.5 equiv.), $Pd_2(dba)_3$·$CHCl_3$ (2.5 mol%), DPEPhos (10 mol%), DBU (10 mol%), MeCN (1 M), room temperature, 18 h, open to air. Full conversion of **3.6a-3.6c** and exclusive formation of one stereoisomer was noted in all instances;[a] Yield (%) of isolated product.

3.2.3 Consecutive Double Cyclization Strategy

After having successfully realized the preparation of stereodefined homoallylic nitroalkanes **3.8a-3.8d**, we explored the last sequence of steps leading to the final indolizidine and quinolizidine targets. We envisioned that the reduction of the NO_2 group to an amine, and the CO_2Me to an alcohol group should lead to a suitable amino-diol intermediate which could subsequently be used to explore a consecutive double cyclization approach. We directly attempted to reduce both functional groups (NO_2 and CO_2Me) in homoallylic nitroalkane **3.8a** simultaneously using $LiAlH_4$ in THF at room temperature, but unfortunately, these conditions did not produce any amino-diol product but led to a complex mixture. In addition, the combination of $NaBH_4$ and $ZrCl_4$ in THF at 40 ºC, which is known to reduce both functional groups,[132] did surprisingly showed no conversion.[133] Finally, we decided to perform the reduction of both groups in two steps. First, the reduction of the ester group was accomplished using DIBAL-H in THF, which cleanly produced nitro-diol intermediates **3.9a-3.9d** (**SCHEME 3.5**, step 1). Thereafter, reduction of the NO_2 group to the NH_2 group was easily accomplished using Zn dust under acidic conditions to cleanly produce amino-diol **3.10a-3.10d** without the need for any chromatographic purification (**SCHEME 3.5**, step 2). The polar nature of these compounds complicated the extraction with EtOAc from the aqueous phase, but the use of *n*-BuOH as extraction solvent, which is not miscible with water, could efficiently extract the amino-diol products from the aqueous phase.

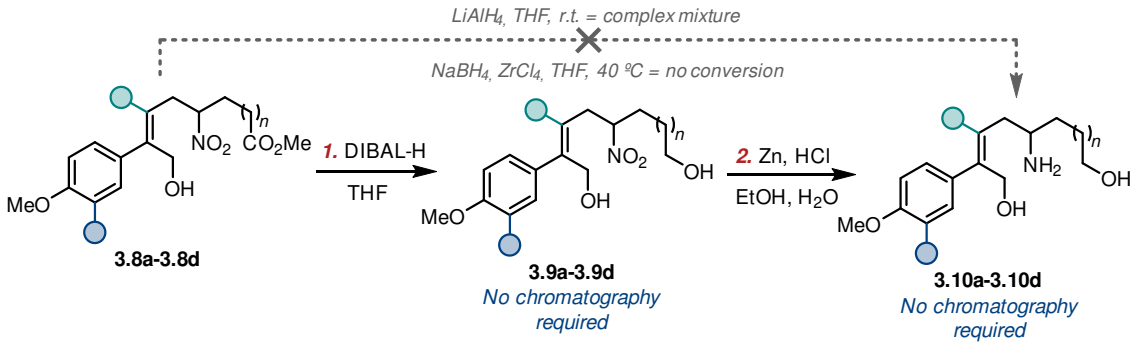

SCHEME 3.5. Reduction of homoallylic nitroalkanes **3.8a-3.8d** to give amino-diols **3.10a-3.10d**.

[132] a) Itsuno, S.; Sakurai, Y.; Ito, K. *Synthesis* **1988**, 995-996. b) Purushothama Chary, K.; Raja Ram, S.; Iyengar, D. S. *Synlett* **2000**, 683-685.

[133] The presence of the free alcohol group might have negatively interfered in this reaction.

We then explored a consecutive double cyclization reaction utilizing amino-diols **3.10a**-**3.10d** to afford the fused azabicyclic core of the targeted indolizidine and quinolizidine natural products. The success of this step heavily depends on the chemoselective activation of both OH groups (*i.e.,* transforming the OH group into a better leaving group) in the presence of the more nucleophilic NH_2 group. To address this (potential) chemoselectivity issue, different approaches were attempted exploiting the high affinity of specific reagents for oxygen. We initially selected the Appel reaction to transform the OH groups in **3.10a** to alkyl bromides,[134] but unfortunately, it did not produce the desired product and led to a complex mixture (**TABLE 3.3**, entry 1). Changing CBr_4 to I_2, or 1,2-diiodoethane and DMF,[135] was also not successful (**TABLE 3.3**, entries 2-3). Another strategy to make the alkyl iodides was attempted using NaI in combination with $CeCl_3{\cdot}7H_2O$[136] (this reagent has an oxyphilic character), but the reaction also failed to produce the cyclized product (**TABLE 3.3**, entry 4). In view of these problems, we decided to make the sulfonate using MsCl or TsCl, but again, the desired product was not produced (**TABLE 3.3**, entries 5-6). A different approach was then applied by means of a borrowing-hydrogen strategy using $[Ir(COD)Cl]_2$, dppf in refluxing PhMe (**TABLE 3.3**, entry 7).[137] As these conditions will likely favor a thermodynamic control, we hoped that the chemoselectivity issue could be avoided, as oxidation of both the amine and alcohol would be reversible, thereby favoring the formation of the thermodynamically most stable cyclized product. Despite this hypothesis, we were not able to observe any desired cyclized product. Returning to the original strategy aimed at finding a suitable reagent to chemoselectively activate the OH groups, we finally considered using *ex situ* generated SO_2F_2 gas, as recently communicated.[138] Using this described protocol, we were pleased to observe the formation of the indolizidine ring in only 1 h and we could isolate the desired MeO-Ipalbidine **3.11a** in 44% yield (**TABLE 3.3**, entry 8). The yield was slightly improved to 49% when running the reaction at room temperature (**TABLE 3.3**, entry 9), but was negatively influenced by the replacement of DMF for MeCN (**TABLE 3.3**, entry 10).

[134] Carroll, A. W.; Savaspun, K.; Willis, A. C.; Hoshino, M.; Kato, A.; Pyne, S. G. *J. Org. Chem.* **2018**, *83*, 5558-5576.
[135] Chen, J.; Lin, J.-H.; Xiao, J.-C. *Chem. Commun.* **2018**, *54*, 7034-7037.
[136] Di Deo, M.; Marcantoni, E.; Torregiani, E.; Bartoli, G.; Bellucci, M. C.; Bosco, M.; Sambri, L. *J. Org. Chem.* **2000**, *65*, 2830-2833.
[137] Cami-Kobeci, G.; Slatford, P. A.; Whittlesey, M. K.; Williams, J. M. J. *Bioorg. Med. Chem. Lett.* **2005**, *15*, 535-537.
[138] At the time, a shortly released contribution showed that SO_2F_2 can selectively activate fluorinated alcohols over primary and secondary amines, although a higher concentration of alcohol is required, see: Epifanov, M.; Foth, P. J.; Gu, F.; Barrillon, C.; Kanani, S. S.; Higman, C. S.; Hein, J. E.; Sammis, G. M. *J. Am. Chem. Soc.* **2018**, *140*, 16464-16468.

TABLE 3.3. Screening of conditions for the consecutive double cyclization of **3.10a**.

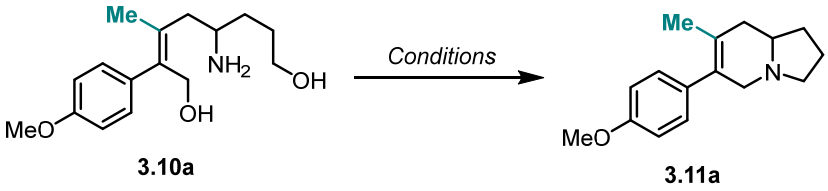

3.10a **3.11a**

Entry	Conditions	Yield (%) [(a)]
1	PPh_3, CBr_4, Et_3N, CH_2Cl_2, r.t. 16 h	-
2	PPh_3, I_2, Et_3N, CH_2Cl_2, r.t. 16 h	-
3	PPh_3, ICH_2CH_2I, Et_3N, DMF, r.t. 16 h	-
4	$CeCl_3{\cdot}7H_2O$, NaI, MeCN, reflux, 16 h	-
5	MsCl, Et_3N, CH_2Cl_2, 0 °C to r.t. 16 h	-
6	TsCl, Et_3N, CH_2Cl_2, 0 °C to r.t. 16 h	-
7	$[Ir(COD)Cl]_2$, dppf, PhMe, reflux, 16 h	-
8	SO_2F_2, DIPEA, DMF, 40 °C, 1 h	44
9	SO_2F_2, DIPEA, DMF, r.t. 1 h	49
10	SO_2F_2, DIPEA, MeCN, r.t. 1 h	16

Full conversion of **3.10a** was noted in all instances; [(a)] Yield (%) of isolated product over 3 steps.

These unique conditions proved to be more generally applicable and allowed to generate the other indolizidine alkaloids Septicine (**3.11b**) and *seco*-Antofine (**3.11c**) in 28% and 41% yield (3 steps overall yield, **SCHEME 3.6**). Remarkably, the targeted quinolizidine core of Julandine (**3.11d**) was also accomplished in 47% yield (3 steps overall yield) and its structure was unambiguously confirmed by X-ray analysis (see **TABLE 3.5** in subsection 3.4.8). Moreover, alkaloids **3.11a-3.11d** have been previously used to access Ipalbidine (**3.S**, by deprotection of the OMe group with BBr_3),[139] Tylophorine (**3.P**), Antofine (**3.Q**), and Cryptoleurine (**3.R**), through a dehydrogenative oxidative coupling mediated by VOF_3.[140]

[139] a) See Danishefsky, S. J. *et al. J. Org. Chem.* **1986** (*ref.* 113a), and Clive, D. L. J. *et al. J. Org. Chem.* **2015** (*ref.* 115a) on page 89.

[140] a) See Chuang, T.-H. *et al. Org. Lett.* **2016** (*ref.* 113c), and Glorius, F. *et al. Chem. Eur. J.* **2017** (*ref.* 114c) on page 89.

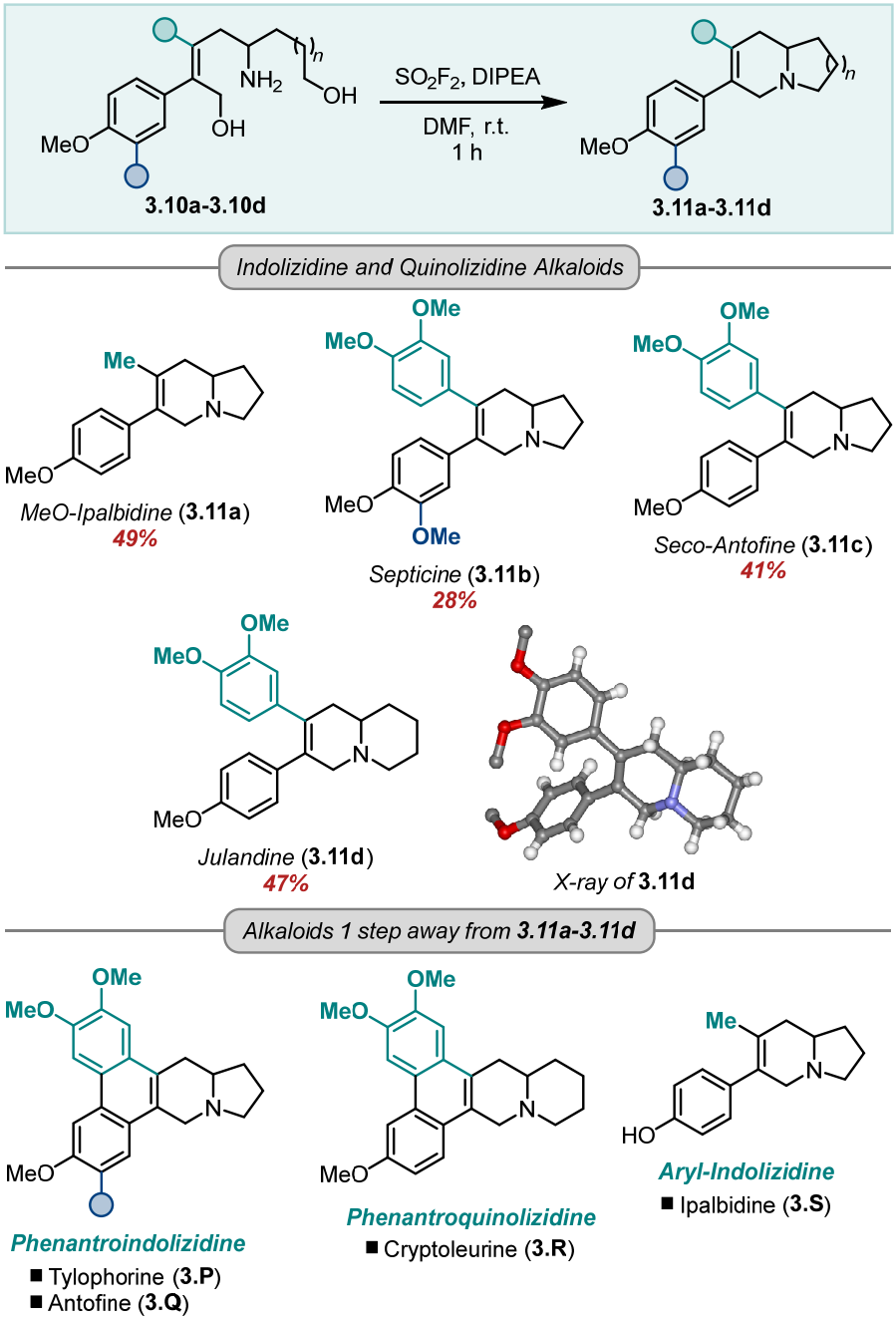

SCHEME 3.6. Synthesis of targeted indolizidine and quinolizidine alkaloids using SO_2F_2.

This unprecedented intramolecular double cyclization strategy represents a useful example of the utilization of SO_2F_2 to drive the overall chemoselectivity while allowing the efficient cyclization of an amino alcohol group. We assume that the hard electrophilicity of SO_2F_2 and/or hydrogen-bonding interactions between the oxygen atom of the OH group and the fluoride of SO_2F_2 might account for the observed chemoselectivity.

3.2.4 Sequential Double Cyclization Strategy

Whilst investigating the consecutive double cyclization reaction, we thought that a stepwise cyclization approach would also add flexibility and allow for the introduction of other groups to produce structural analogs of the natural products, thus further amplifying the synthetic potential towards medicinal chemistry programs. In this regard, we changed the reduction sequence by first reducing the NO_2 group to the NH_2 group with Zn in **3.8a** leading to intermediate **3.T**, of which we thought that it could spontaneously condense to form lactam **3.12**. To our surprise, the conversion was quite low after refluxing the reaction for 24 h in MeOH, so we repeated the reaction in MeCN at room temperature with the addition of a catalytic amount of TBD. Under these conditions, we were pleased to observe full conversion within 2 h and lactam **3.12** was isolated in 63% yield. The crude product after work-up was of sufficient quality to be carried forward to the next step without chromatographic purification.

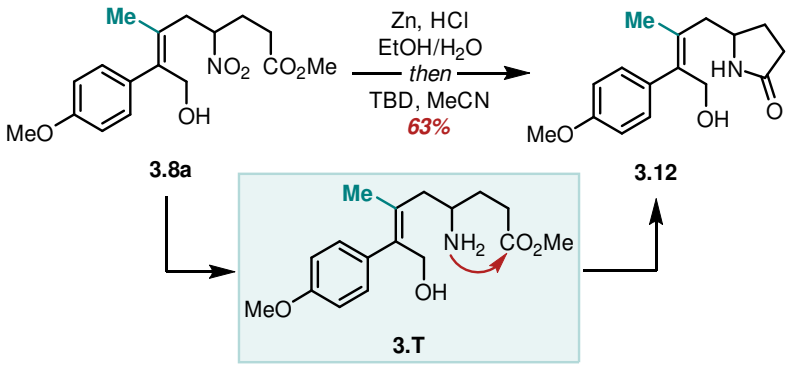

SCHEME 3.7. Synthesis of lactam **3.12**. through a reduction/condensation sequence.

After the formation of the first 5-membered ring, we continued the synthetic route by exploring an intramolecular Mitsunobu reaction leading prospectively to the formation of the second 6-membered ring. Unfortunately, using standard Mitsunobu reaction conditions did not induce the formation of the desired 1,2,3,6-tetrahydropyridine motif (**TABLE 3.4**, entry 1). This may be attributed to the lower basicity of the anion of the resulting hydrazine dicarboxylate intermediate to deprotonate the lactam NH proton, and therefore we decided to switch to TMAD as the diazo compound in combination with a more nucleophilic phosphine (**TABLE 3.4**, entry 2).[141] Under these conditions, the desired bicyclic lactam product **3.13** was produced in 73% yield. The structure was unambiguously confirmed by X-ray diffraction (see **TABLE 3.6** in subsection 3.4.8). Although we were pleased with this result, we decided to further optimize the reaction conditions. Switching to PhMe as solvent afforded similar results (**TABLE 3.4**, entry 3), but changing the

[141] A similar observation was previously made by Roush and coworkers when attempting an intramolecular Mitsunobu reaction of an amino-alcohol intermediate: Allais, C.; Roush, W. R. *Org. Lett.* **2017**, *19*, 2646-2649.

phosphine reagent to P(*n*-Bu)$_3$ increased the yield to 84% (**TABLE 3.4**, entry 4), while using the ubiquitous PPh_3 was detrimental for the overall reactivity (**TABLE 3.4**, entry 5). Further exploration of other diazo compounds combined with different phosphine reagents did not further improve the results (**TABLE 3.4**, entries 6-11).

TABLE 3.4. Optimization of the intramolecular Mitsunobu reaction.

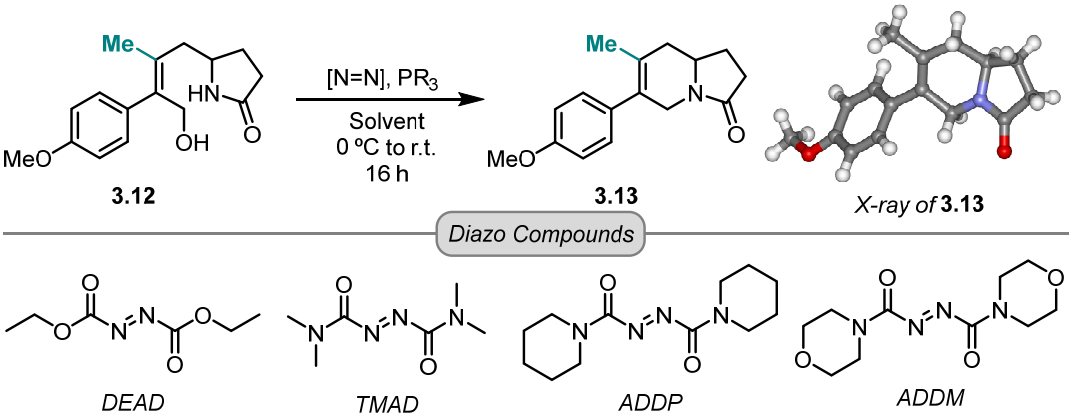

Entry	[N=N]	PR_3	Solvent	Yield (%) [a]
1	DEAD	PPh_3	CH_2Cl_2	-
2	TMAD	PMe_3	THF	73
3	TMAD	PMe_3	PhMe	71
4	TMAD	P(*n*-Bu)$_3$	THF	84
5	TMAD	PPh_3	THF	31
6	ADDP	PMe_3	THF	59
7	ADDP	P(*n*-Bu)$_3$	THF	62
8	ADDP	PPh_3	THF	30
9	ADDM	PMe_3	THF	21
10	ADDM	P(*n*-Bu)$_3$	THF	42
11	ADDM	PPh_3	THF	9

Reaction conditions: Lactam **3.12** (1 equiv.), [N=N] (1.5 equiv.), PR_3 (1.5 equiv.), solvent (0.1 M), 0 °C to room temperature, 16 h, under N_2. Full conversion of **3.12** was noted in all cases; [a] Yield (%) of isolated product.

Having already secured a shorter consecutive double cyclization strategy with SO_2F_2 for MeO-Ipalbidine **3.11a** (see subsection 3.2.4), we envisaged that this stepwise route might be more flexible and provide distinct indolizidine alkaloids analogs of interest for medicinal development programs, as the amide group in **3.13** can be conveniently transformed to accommodate alkyl groups at different positions.[142] In this respect, we first introduced a benzyl group at the 2-position through an α-alkylation of its lithium enolate, which proceeded in 51% yield and 8.5:1 *dr* (**SCHEME 3.8**). Subsequent reduction of **3.14** with $LiAlH_4$ afforded **3.15** in 77% yield. Finally, the introduction of two methyl groups at position 3 was accomplished through activation of amide **3.13** with Tf_2O in the presence of bulky 2,6-di-*tert*-butyl-4-methylpyridine (DTBMP). Subsequent addition of excess MeMgBr gave 3,3-dimethyl indolizidine **3.16** in 53% yield.

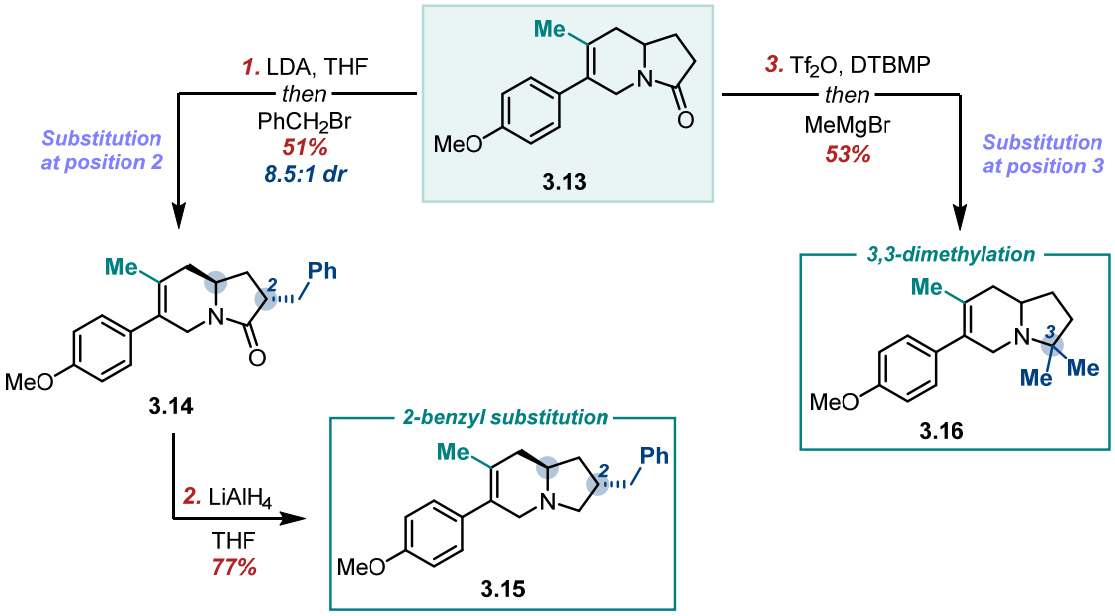

SCHEME 3.8. Synthesis of substituted indolizidine alkaloids analogs.

[142] Note that subsequent transformation of the amide group in **3.13** to the bridgehead tertiary amine, as in MeO-Ipalbidine **3.11a**, could be easily achieved by reduction with $LiAlH_4$, see: Pansare, S. V.; Lingampally, R.; Dyapa, R. *Eur. J. Org. Chem.* **2011**, 2235-2238.

3.3 Conclusions

This chapter demonstrates that cyclic carbonates, and VCCs in particular, can be effectively used as key reactive intermediates towards the formal synthesis of indolizidine and quinolizidine alkaloids. The nature of this work contrasts with the conventional use of cyclic carbonates as protecting groups in multistep synthetic campaigns.

The previously developed methodology for the palladium-catalyzed (*Z*)-selective allylation of nitroalkanes has been exploited here and extended to produce highly advanced homoallylic nitroalkanes intermediates with appropriate functionalities and configuration, which were rapidly converted into indolizidine and quinolizidine alkaloids in just three additional synthetic steps, including only a single chromatographic purification step. The synthesis of the final targets was successfully accomplished through an unprecedented consecutive double cyclization with *ex situ* generated SO_2F_2. Furthermore, the established multistep synthetic route can be easily adapted towards the introduction of alkyl groups at different positions of the 5-membered ring of the indolizidine motif through a common bicyclic lactam intermediate.

3.4 Experimental Section

3.4.1 General Information

Methods: Air and water-sensitive reactions were carried out in heat-gun-dried glassware under an Ar or N_2 atmosphere using standard Schlenk techniques. Reactions were monitored by TLC, ^{1}H NMR spectroscopy, FT-IR spectroscopy, or GC-FID chromatography. TLC was carried out on 0.25 mm Merck aluminum-backed sheets coated with 60 F_{254} silica gel. Visualization of the silica plates was achieved using a UV lamp (λ = 254 nm) and/or by heating plates that were dipped into a $KMnO_4$ or a ceric ammonium molybdate stain. Flash chromatography was carried out on Sigma-Aldrich silica gel 60 (70-230 mesh) using the indicated eluent system.

Reagents and Solvents: Commercially available reagents and solvents were purchased from Sigma-Aldrich, TCI, Fluorochem, Strem Chemicals, Abcr GmbH, Acros Organics, or Alfa Aesar, and were used without further purification. Zinc dust was activated using a previously reported procedure and was stored in a glovebox.[143] Solvents were dried using an Innovative Technology PURE SOLV solvent purification system.

Analytical Techniques: ^{1}H NMR, ^{13}C NMR, DEPT-90, DEPT-135, and related 2D NMR (gCOSY90, gHMQC, gHMBC, gNOESY) spectra were recorded at room temperature on a Bruker AV-300, AV-400, or AV-500 spectrometer and referenced to their residual deuterated solvent signals. Coupling constants (J) are reported in Hertz with the following splitting abbreviations: s = singlet, d = doublet, t = triplet, q = quadruplet, quint = quintet, sextet = sext, br = broad and app = apparent. All reported NMR values are given in parts per million (ppm). FT-IR measurements were carried out on a Bruker Optics FTIR Alpha spectrometer. Mass spectrometric and X-ray analyses were performed by the Research Support Area at ICIQ.

[143] See Hirata, Y. *et al. Org. Synth.* **1973** (*ref.* 97) on page 57.

3.4.2 General Procedure for the Synthesis of α-Hydroxyketones

α-Hydroxyketones (**3.1a-3.1b**, **SCHEME 3.9**) were prepared following previously reported literature procedures with minor modifications.[144]

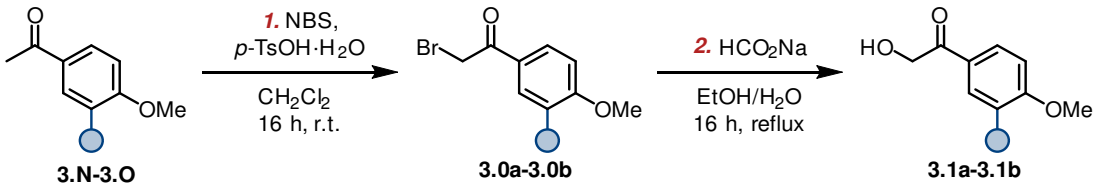

SCHEME 3.9. General synthesis of α-hydroxyketones from readily available acetophenone derivatives.

Step 1: In a round-bottomed flask, the corresponding acetophenone **3.N-3.O** (1 equiv. substrate) was dissolved in CH_2Cl_2 (1.20 mL/mmol substrate) open to air and cooled to 0 °C (ice-water bath). *p*-TsOH·H_2O (10 mol%) was added, and then NBS (1.1 equiv.) was added in small batches over 10 minutes. The reaction mixture was allowed to warm to room temperature and was stirred for 16 h. Hereafter, the reaction was quenched with aqueous saturated $Na_2S_2O_3$ and was diluted with aqueous saturated $NaHCO_3$ and water. The phases were separated, and the aqueous phase was extracted with CH_2Cl_2 twice. The combined organic layers were washed with $NaHCO_3$ twice and brine, dried over Na_2SO_4, filtered, and concentrated *in vacuo*. The crude product **3.0a-3.0b** was dried under high vacuum and used in the next step without further purification.

Note: The resulting α-bromoketones **3.0a-3.0b** were used as soon as possible in the next step because they decompose over time at room temperature.

Step 2: In a round-bottomed flask, the corresponding α-bromoketone **3.0a-3.0b** (1 equiv. substrate) was dissolved in EtOH (2.55 mL/mmol substrate) under N_2. A solution of HCO_2Na (6 equiv.) in H_2O (0.45 mL/mmol substrate) was added and the mixture was stirred at reflux for 16 h. The mixture was then concentrated *in vacuo*, diluted with H_2O, and extracted with EtOAc three times. The combined organic layers were washed with brine, dried over Na_2SO_4, filtered, and concentrated *in vacuo*. The crude product was purified by flash chromatography on silica gel to afford the corresponding α-hydroxyketones **3.1a-3.1b**

Note: Yields of α-hydroxyketones are always referred to as overall from steps 1 and 2.

[144] See Zhou, H.-B. *et al. J. Med. Chem.* **2015** (*ref.* 128a), and Shi, L. *et al. Adv. Synth. Catal.* **2018** (*ref.* 128b) on page 94.

2-Bromo-1-(4-methoxyphenyl)ethan-1-one (3.0a)

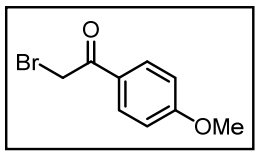

White solid; **^{1}H NMR** (500 MHz, $CDCl_3$) δ_H 7.97-7.86 (m, 2H), 6.97-6.86 (m, 2H), 4.37 (s, 2H), 3.84 (s, 3H). Spectroscopic data are in agreement with published data.[145]

2-Bromo-1-(3,4-dimethoxyphenyl)ethan-1-one (3.0b)

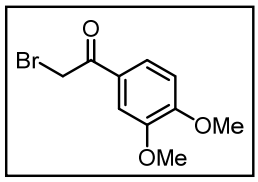

White solid; **^{1}H NMR** (400 MHz, $CDCl_3$) δ_H 7.62 (dd, J = 8.4, 2.1 Hz, 1H), 7.54 (d, J = 2.1 Hz, 1H), 6.91 (d, J = 8.4 Hz, 1H), 4.41 (s, 2H), 3.97 (s, 3H), 3.94 (s, 3H). Spectroscopic data are in agreement with published data.[146]

2-Hydroxy-1-(4-methoxyphenyl)ethan-1-one (3.1a)

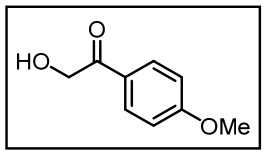

Yellowish solid (4.11 g, 73% yield); **^{1}H NMR** (500 MHz, $CDCl_3$) δ_H 7.93-7.87 (m, 2H), 7.00-6.94 (m, 2H), 4.82 (s, 2H), 3.88 (s, 3H); **^{13}C NMR** (75 MHz, $CDCl_3$) δ_C 196.9, 164.5, 130.2, 126.5, 114.3, 65.1, 55.7. Spectroscopic data are in agreement with published data.[147]

1-(3,4-Dimethoxyphenyl)-2-hydroxyethan-1-one (3.1b)

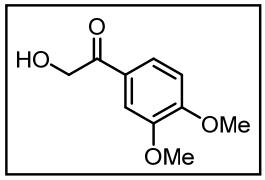

Yellowish solid (2.05 g, 75% yield); **^{1}H NMR** (500 MHz, $CDCl_3$) δ_H 7.52-7.47 (m, 2H), 6.90 (d, J = 8.2 Hz, 1H), 4.83 (s, 2H), 3.95 (s, 3H), 3.94 (s, 3H); **^{13}C NMR** (126 MHz, $CDCl_3$) δ_C 197.0, 154.4, 149.5, 126.6, 122.4, 110.5, 109.9, 65.1, 56.3, 56.2. Spectroscopic data are in agreement with published data.[148]

[145] Bestgen, B.; Kufareva, I.; Seetoh, W.; Abell, C.; Hartmann, R. W.; Abagyan, R.; Le Borgne, M.; Filhol, O.; Cochet, C.; Lomberget, T.; Engel, M. *J. Med. Chem.* **2019**, *62*, 1817-1836.

[146] Lancefield, C. S.; Teunissen, L. W.; Weckhuysen, B. M.; Bruijnincx, P. C. A. *Green Chem.* **2018**, *20*, 3214-3221.

[147] See Shi, L. *et al. Adv. Synth. Catal.* **2018** (*ref.* 128b) on page 94.

[148] Cho, D. W.; Parthasarathi, R.; Pimentel, A. S.; Maestas, G. D.; Park, H. J.; Yoon, U. C.; Dunaway-Mariano, D.; Gnanakaran, S.; Langan, P.; Mariano, P. S. *J. Org. Chem.* **2010**, *75*, 6549-6562.

3.4.3 Synthesis of Organomagnesium Reagents 3.4a-3.4b

Isopropenylmagnesium bromide (**3.4a**) was directly purchased from Sigma-Aldrich as a 0.5 M solution in THF and was used as received. (1-(3,4-Dimethoxyphenyl)vinyl)magnesium bromide (**3.4b**) was prepared as follows:

4-Ethynyl-1,2-dimethoxybenzene (3.2)

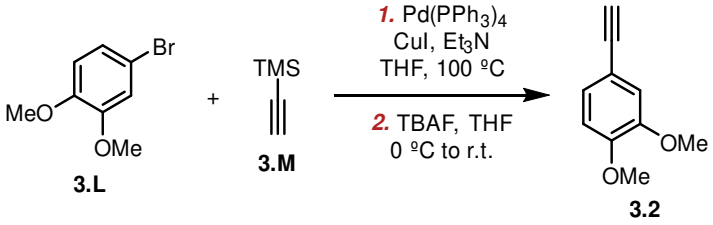

According to a previously reported procedure,[149] $Pd(PPh_3)_4$ (1.04 g, 5 mol%), CuI (343 mg, 10 mol%), 4-bromoveratrole **3.L** (3.91 g, 18 mmol), dry THF (9 mL), and Et_3N (7.2 mL) were charged into a pressure tube with a magnetic stirring bar inside a glovebox. Then, trimethylsilylacetylene **3.M** (3.0 mL, 1.2 equiv.) was added dropwise to the reaction mixture. The tube was sealed and stirred outside the glovebox at 100 ºC for 12 h. Hereafter, the reaction mixture was cooled to room temperature and was filtered through a short pad of Celite. The pad was rinsed with EtOAc and the solvent was evaporated *in vacuo*. The crude product was dissolved in dry THF (10 mL) under N_2 and the solution was cooled to 0 ºC (ice-water bath). TBAF (19.8 mL, 1 M in THF, 1.2 equiv.) was added dropwise and the solution was allowed to warm to room temperature and was stirred for 1 h. After completion, the reaction mixture was extracted with EtOAc three times. The combined organic layers were washed with water, brine, and were dried over Na_2SO_4, filtered, and concentrated *in vacuo*. The crude product was purified by flash chromatography on silica gel using hexane to afford alkyne **3.2** as a brown solid (2.20 g, 75% yield). **^{1}H NMR** (500 MHz, $CDCl_3$) δ_H 7.10 (dd, J = 8.3, 1.9 Hz, 1H), 6.99 (d, J = 1.9 Hz, 1H), 6.80 (d, J = 8.3 Hz, 1H), 3.89 (s, 3H), 3.88 (s, 3H), 3.00 (s, 1H); **^{13}C NMR** (126 MHz, $CDCl_3$) δ_C 150.0, 148.7, 125.6, 114.8, 114.3, 111.1, 83.9, 75.8, 56.01, 56.00. Spectroscopic data are in agreement with published data.[149]

[149] See Chattopadhyay, B. *et al. Angew. Chem. Int. Ed.* **2018** (*ref.* 129b) on page 94.

4-(1-Bromovinyl)-1,2-dimethoxybenzene (3.3)

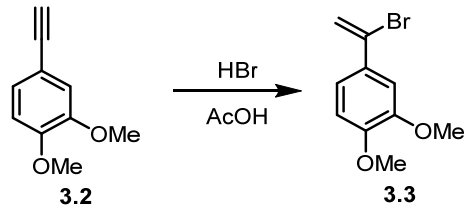

3.2 **3.3**

According to a previously reported procedure, alkyne **3.2** (1.19 g, 7.34 mmol) was carefully dried by lyophilization prior to use. Then, HBr (1.4 mL, 7.34 mmol, 33% in AcOH) was added dropwise at 0 °C (ice-water bath) and the mixture was allowed to warm to room temperature and was stirred for 25 minutes. Thereafter, water was added, and the mixture was extracted with CH_2Cl_2 three times. The combined organic layers were washed with aqueous saturated $NaHCO_3$, water, brine and were dried over $MgSO_4$, filtered, and concentrated *in vacuo*. The crude product was purified by flash chromatography on silica gel using 10-20% EtOAc/hexanes to afford alkenyl bromide **3.3** as a light brown oil (1.30 g, 73% yield). **^{1}H NMR** (500 MHz, $CDCl_3$) δ_H 7.14 (dd, J = 8.3 Hz, 2.0 Hz, 1H), 7.10 (d, J = 2.1 Hz, 1H), 6.81 (d, J = 8.4 Hz, 1H), 6.01 (d, J = 1.9 Hz, 1H), 5.68 (d, J = 1.9 Hz, 1H), 3.90 (s, 3H), 3.88 (s, 3H). **^{13}C NMR** (126 MHz, $CDCl_3$) δ_C 149.7, 148.3, 131.3, 130.7, 120.2, 116.1, 110.4, 110.4, 55.9, 55.8. Spectroscopic data are in agreement with published data.[150]

Note: Alkenyl bromide **3.3** was used as soon as possible in the next step because it decomposed over time at room temperature.

(1-(3,4-Dimethoxyphenyl)vinyl)magnesium bromide (3.4b)

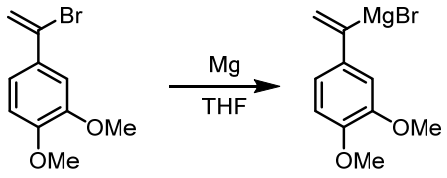

3.3 **3.4b**

In a heat-gun-dried two-necked round-bottomed flask, Mg turnings (124 mg, 1.0 equiv.) were suspended in dry THF (5 mL) under N_2. A solution of alkenyl bromide **3.3** (1.30 g, 1.0 equiv.) in dry THF (9 mL) was added dropwise over 5 minutes. After the addition, the mixture was heated at reflux for 1 h and then cooled to room temperature. The freshly prepared solution of **3.4b** was directly used in the next step as soon as possible.

[150] See Christoffers, J. *et al. Eur. J. Org. Chem.* **2006** (*ref.* 129a) on page 94.

3.4.4 General Procedure for the Synthesis of VCCs

Vinyl cyclic carbonates (**SCHEME 3.10**, **3.6a-3.6c**) were synthesized according to a previously reported procedure,[151] as also described in subsection 2.4.2 (**SCHEME 2.12**, steps 2-3). 1,2-Diol **3.5a** was carried forward to the next step without chromatographic purification, while 1,2-diols **3.5b-3.5c** were purified by flash chromatography over silica gel.

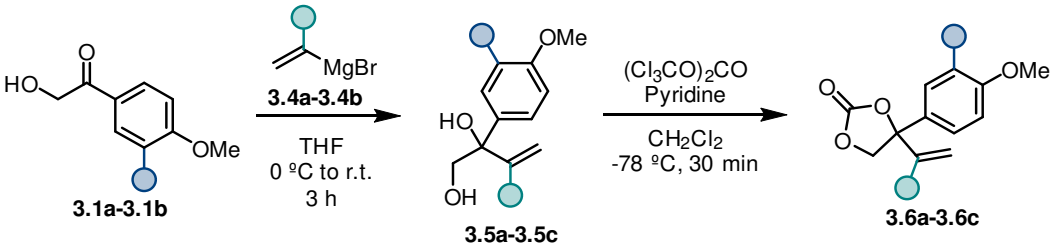

SCHEME 3.10. General synthesis of vinyl cyclic carbonates.

2-(4-Methoxyphenyl)-3-methylbut-3-ene-1,2-diol (3.5a)

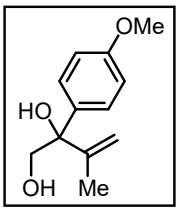

Yellowish oil; **IR** (neat): ν = 3542, 3283, 2955, 2840, 1673, 1646, 1605, 1582, 1510, 1452, 1309, 1253, 1182, 1168, 1087, 1033, 995, 899, 835, 820, 809, 584, 550 cm^{-1}; **^{1}H NMR** (300 MHz, $CDCl_3$) δ_H 7.41-7.32 (m, 2H), 6.95-6.82 (m, 2H), 5.15 (p, J = 1.0 Hz, 1H), 5.07 (p, J = 1.5 Hz, 1H), 4.02 (dd, J = 11.2, 5.0 Hz, 1H), 3.87 (dd, J = 11.3, 5.7 Hz, 1H), 3.80 (s, 3H), 2.78 (s, 1H), 1.76 (br t, J = 6.0 Hz, 1H), 1.65 (dd, J = 1.5, 1.0 Hz, 3H); **^{13}C NMR** (75 MHz, $CDCl_3$) δ_C 159.1, 147.2, 134.1, 127.2, 113.9, 111.9, 79.0, 68.1, 55.4, 19.4.; **HRMS** (ESI/TOF) m/z: $[M + Na]^+$ Calcd for $C_{12}H_{16}NaO_3$ 231.0992; Found 231.0985.

[151] See Kleij, A. W. *et al. J. Org. Chem.* **2018** (*ref.* 53e) on page 30.

2,3-Bis(3,4-dimethoxyphenyl)but-3-ene-1,2-diol (3.5b)

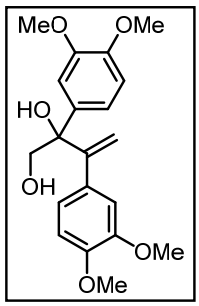

Yellowish foam (510 mg, 58% yield); **IR** (neat): ν = 3488, 2998, 2954, 2930, 2836, 1602, 1511, 1462, 1410, 1322, 1255, 1175, 1139, 1025, 913, 864, 812, 766, 735 cm^{-1}; **^{1}H NMR** (500 MHz, $CDCl_3$) δ_H 7.13 (d, J = 2.1 Hz, 1H), 7.03 (dd, J = 8.3, 2.1 Hz, 1H), 6.86 (d, J = 8.4 Hz, 1H), 6.70 (d, J = 8.3 Hz, 1H), 6.62 (dd, J = 8.3, 2.1 Hz, 1H), 6.54 (d, J = 2.1 Hz, 1H), 5.53 (d, J = 0.9 Hz, 1H), 5.44 (d, J = 0.9 Hz, 1H), 4.02 (dd, J = 11.2, 7.0 Hz, 1H), 3.89 (s, 3H), 3.87 (s, 3H), 3.84 (dd, J = 11.5, 5.8 Hz, 1H), 3.83 (s, 3H), 3.65 (s, 3H), 2.77 (s, 1H), 1.96 (t, J = 6.5 Hz, 1H); **^{13}C NMR** (126 MHz, $CDCl_3$) δ_C 150.6, 149.2, 148.8, 148.6, 148.3, 135.1, 132.4, 120.9, 118.6, 115.0, 111.9, 111.0, 110.8, 109.8, 79.2, 68.9, 56.1 (overlapping 2C), 56.0, 55.7; **HRMS** (ESI/TOF) m/z: $[M + Na]^+$ Calcd for $C_{20}H_{24}NaO_6$ 383.1465; Found 383.1466.

3-(3,4-Dimethoxyphenyl)-2-(4-methoxyphenyl)but-3-ene-1,2-diol (3.5c)

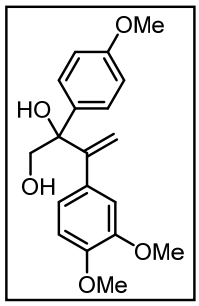

Yellowish foam (920 mg, 68% yield); **IR** (neat): ν = 3480, 3000, 2935, 2836, 1606, 1579, 1509, 1463, 1410, 1298, 1247, 1174, 1141, 1092, 1026, 916, 833, 767, 734 cm^{-1}; **^{1}H NMR** (500 MHz, $CDCl_3$) δ_H 7.48-7.41 (m, 2H), 6.94-6.88 (m, 2H), 6.70 (d, J = 8.3 Hz, 1H), 6.61 (dd, J = 8.3, 2.1 Hz, 1H), 6.49 (d, J = 2.1 Hz, 1H), 5.52 (d, J = 1.0 Hz, 1H), 5.41 (d, J = 1.0 Hz, 1H), 4.01 (dd, J = 11.3, 6.7 Hz, 1H), 3.82 (s, 3H), 3.81 (s, 3H), 3.79 (overlapped m, 1H), 3.64 (s, 3H), 2.75 (s, 1H), 2.01 (t, J = 6.5 Hz, 1H); **^{13}C NMR** (126 MHz, $CDCl_3$) δ_C 159.2, 150.7, 148.7, 148.3, 134.6, 132.5, 127.6, 120.9, 115.0, 113.9, 111.9, 110.8, 79.1, 68.8, 55.9, 55.7, 55.4; **HRMS** (ESI/TOF) m/z: $[M + Na]^+$ Calcd for $C_{19}H_{22}NaO_5$ 353.1359; Found 353.1343.

4-(4-Methoxyphenyl)-4-(prop-1-en-2-yl)-1,3-dioxolan-2-one (3.6a)

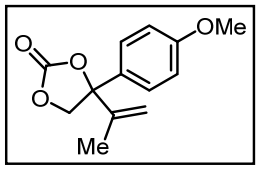

Yellowish solid (1.82 g, 64% yield over 2 steps); **IR** (neat): ν = 2956, 2935, 2911, 2837, 1787, 1652, 1611, 1582, 1510, 1484, 1456, 1374, 1299, 1255, 1223, 1212, 1178, 1123, 1105, 1042, 931, 916, 881, 828, 768, 736, 592, 552 cm^{-1}; **^{1}H NMR** (500 MHz, $CDCl_3$) δ_H 7.31-7.27 (m, 2H), 6.94-6.90 (m, 2H), 5.18 (br s, 1H), 5.15 (q, J = 1.5 Hz, 1H), 4.73 (d, J = 8.6 Hz, 1H), 4.62 (d, J = 8.6 Hz, 1H), 3.82 (s, 3H), 1.72 (dd, J = 1.5, 0.8 Hz, 3H); **^{13}C NMR** (75 MHz, $CDCl_3$) δ_C 160.0, 154.2, 143.0, 130.2, 126.7, 114.3, 113.8, 88.1, 73.1, 55.5, 18.6; **HRMS** (ESI/TOF) m/z: $[M + Na]^+$ Calcd for $C_{13}H_{14}NaO_4$ 257.0784; Found 257.0786.

4-(3,4-Dimethoxyphenyl)-4-(1-(3,4-dimethoxyphenyl)vinyl)-1,3-dioxolan-2-one (3.6b)

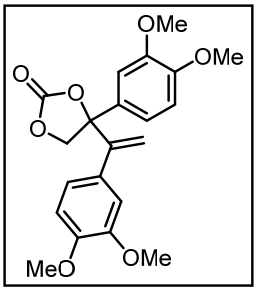

Yellowish foam (524 mg, 96% yield); **IR** (neat): ν = 3059, 3003, 2937, 2838, 1797, 1603, 1580, 1513, 1463, 1413, 1328, 1254, 1170, 1143, 1051, 1022, 916, 860, 812, 767, 731, 654 cm^{-1}; **^{1}H NMR** (500 MHz, $CDCl_3$) δ_H 6.97 (d, J = 2.2 Hz, 1H), 6.94 (dd, J = 8.3, 2.2 Hz, 1H), 6.87 (d, J = 8.4 Hz, 1H), 6.73 (d, J = 8.3 Hz, 1H), 6.60 (dd, J = 8.3, 2.1 Hz, 1H), 6.57 (d, J = 2.1 Hz, 1H), 5.58 (s, 1H), 5.53 (s, 1H), 4.72 (d, J = 8.8 Hz, 1H), 4.64 (d, J = 8.7 Hz, 1H), 3.90 (s, 3H), 3.86 (s, 3H), 3.84 (s, 3H), 3.72 (s, 3H); **^{13}C NMR** (126 MHz, $CDCl_3$) δ_C 154.0, 149.9, 149.5, 149.3, 148.7, 147.3, 130.7, 130.2, 121.0, 118.7, 116.8, 111.7, 111.04, 110.96, 109.6, 87.5, 73.3, 56.2, 56.1, 56.0, 55.9; **HRMS** (ESI/TOF) m/z: $[M + Na]^+$ Calcd for $C_{21}H_{22}NaO_7$ 409.1258; Found 409.1260.

4-(1-(3,4-Dimethoxyphenyl)vinyl)-4-(4-methoxyphenyl)-1,3-dioxolan-2-one (3.6c)

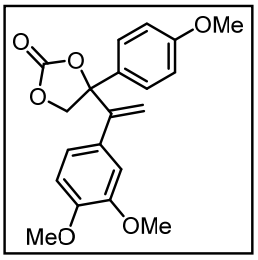

Yellowish foam (999 mg, 99% yield); **IR** (neat): ν = 3060, 3003, 2960, 2937, 2838, 1797, 1607, 1581, 1511, 1463, 1414, 1304, 1250, 1218, 1177, 1143, 1050, 1023, 920, 833, 812, 768, 732, 702 cm^{-1}; **^{1}H NMR** (400 MHz, $CDCl_3$) δ_H 7.41-7.34 (m, 2H), 6.97-6.91 (m, 2H), 6.73 (d, J = 8.3 Hz, 1H), 6.60 (ddd, J = 8.3, 2.1, 0.6 Hz, 1H), 6.56 (d, J = 2.1 Hz, 1H), 5.58 (s, 1H), 5.53 (s, 1H), 4.72 (d, J = 8.8 Hz, 1H), 4.63 (d, J = 8.8 Hz, 1H), 3.84 (s, 3H), 3.83 (s, 3H), 3.72 (s, 3H); **^{13}C NMR** (101 MHz, $CDCl_3$) δ_C 160.3, 154.0, 149.2, 148.7, 147.3, 130.4, 130.2, 127.7, 120.9, 116.7, 114.4, 111.6, 111.0, 87.4, 73.4, 56.0, 55.9, 55.5; **HRMS** (ESI/TOF) m/z: $[M + Na]^+$ Calcd for $C_{20}H_{20}NaO_6$ 379.1152; Found 379.1146.

3.4.5 General Procedure for the Synthesis of Homoallylic Nitroalkanes

Homoallylic nitroalkanes (**SCHEME 3.11**, **3.8a-3.8d**) were synthesized according to a previously reported procedure,[152] as described in subsection 2.4.4 (**SCHEME 2.14**). Methyl 4-nitrobutyrate (**3.7a**) was purchased from Sigma-Aldrich and used without further purification, while methyl 5-nitropentanoate (**3.7b**) was prepared in one step according to a previously reported procedure.[153]

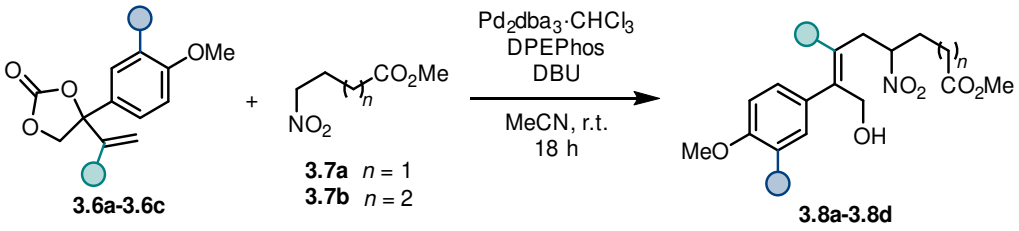

SCHEME 3.11. General synthesis of stereodefined homoallylic nitroalkanes.

Methyl 5-nitropentanoate (3.7b)

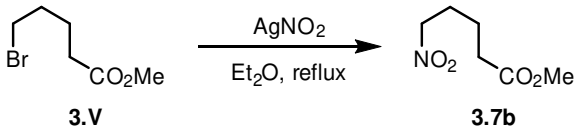

In a heat-gun dried 100 mL two-necked round-bottomed flask equipped with a condenser, methyl 5-bromopentanoate **3.V** (2.5 mL, 17.5 mmol) was dissolved in dry Et_2O (22 mL) under N_2. The flask was covered with aluminum foil, and $AgNO_2$ (4.03 g, 1.5 equiv.) was added in small batches. The mixture was stirred at reflux overnight and was thereafter cooled to room temperature. The mixture was then filtered through a small pad of Celite, and the filtrate was concentrated *in vacuo*. The crude product was purified by flash chromatography on silica gel using 0-20% EtOAc/hexanes to afford methyl 5-nitropentanoate **3.7b** (1.07 g, 38% yield) as a yellowish oil. **^{1}H NMR** (400 MHz, $CDCl_3$) δ_H 4.40 (t, J = 6.9 Hz, 2H), 3.68 (s, 3H), 2.39 (t, J = 7.2 Hz, 2H), 2.12-2.00 (m, 2H), 1.79-1.67 (m, 2H); **^{13}C NMR** (101 MHz, $CDCl_3$) δ_C 173.2, 75.3, 51.9, 33.1, 26.8, 21.7. Spectroscopic data are in agreement with published data.[153]

[152] See Kleij, A. W. *et al. J. Org. Chem.* **2018** (*ref.* 53e) on page 30.
[153] See Valluri, M. *et al.* US Patent WO2005019184A1, March 3, 2010. (*ref.* 131) on page 95.

Methyl (*Z*)-8-hydroxy-7-(4-methoxyphenyl)-6-methyl-4-nitrooct-6-enoate (3.8a)

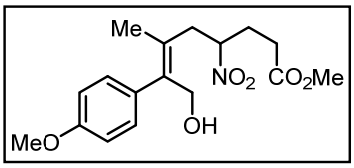

Yellowish solid (1.68 g, 64% yield, *Z*/*E*>99:1); **IR** (neat): ν = 3522, 2995, 2954, 2933, 2838, 1733, 1607, 1547, 1509, 1439, 1368, 1285, 1242, 1173, 1105, 1026, 834, 795 cm^{-1}; **^{1}H NMR** (400 MHz, $CDCl_3$) δ_H 7.08-7.01 (m, 2H), 6.92-6.85 (m, 2H), 4.86 (tdd, *J* = 9.3, 5.4, 3.6 Hz, 1H), 4.37-4.25 (m, 2H), 3.81 (s, 3H), 3.71 (s, 3H), 3.10 (dd, *J* = 14.1, 9.5 Hz, 1H), 2.59 (dd, *J* = 14.1, 5.4 Hz, 1H), 2.54-2.27 (m, 3H), 2.27-2.14 (m, 1H), 1.63 (s, 3H), 1.44 (br s, 1H); **^{13}C NMR** (126 MHz, $CDCl_3$) δ_C 172.5, 158.7, 139.9, 132.8, 130.1, 129.3, 114.0, 86.6, 62.9, 55.4, 52.1, 38.6, 30.0, 28.6, 20.2; **HRMS** (ESI/TOF) *m/z*: $[M + Na]^+$ Calcd for $C_{17}H_{23}NNaO_6$ 360.1418; Found 360.1425.

Methyl (*E*)-6,7-bis(3,4-dimethoxyphenyl)-8-hydroxy-4-nitrooct-6-enoate (3.8b)

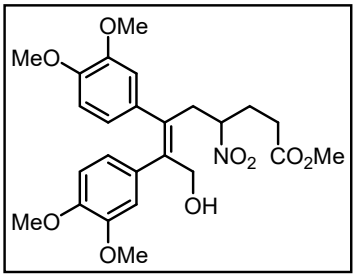

Yellowish foam (89.7 mg, 46% yield, *Z*/*E*>99:1); **IR** (neat): ν = 3518, 2999, 2954, 2934, 2837, 1736, 1602, 1581, 1548, 1513, 1464, 1441, 1410, 1321, 1251, 1167, 1141, 1025, 911, 859, 812, 765 cm^{-1}; **^{1}H NMR** (500 MHz, $CDCl_3$) δ_H 6.70-6.63 (m, 3H), 6.59 (dd, *J* = 8.2, 2.0 Hz, 1H), 6.49 (d, *J* = 1.7 Hz, 1H), 6.39 (d, *J* = 2.0 Hz, 1H), 4.59-4.49 (m, 2H), 4.49-4.41 (m, 1H), 3.81 (s, 3H), 3.79 (s, 3H), 3.63 (s, 3H), 3.60 (s, 3H), 3.60 (s, 3H), 3.50 (dd, *J* = 14.5, 9.8 Hz, 1H), 2.95 (dd, *J* = 14.6, 4.7 Hz, 1H), 2.40-2.23 (m, 3H), 2.17-2.07 (m, 1H), 1.62-1.54 (m, 1H); **^{13}C NMR** (126 MHz, $CDCl_3$) δ_C 172.2, 148.7, 148.5, 148.1, 147.9, 140.8, 134.6, 132.9, 132.7, 121.7, 121.2, 113.44, 113.40, 110.9, 110.8, 86.4, 63.1, 55.9 (overlapping 2C), 55.8, 52.0, 38.6, 30.2, 28.8; **HRMS** (ESI/TOF) *m/z*: $[M + Na]^+$ Calcd for $C_{25}H_{31}NNaO_9$ 512.1891; Found 512.1895.

Note: The stereoconfiguration corresponds to the (*E*)-isomer, according to the Cahn-Ingold-Prelog priority rules, but the spatial orientation of the olefinic substituents is similar to (Z)-**3.8a**. The same holds for the products described below.

Methyl (*E*)-6-(3,4-dimethoxyphenyl)-8-hydroxy-7-(4-methoxyphenyl)-4-nitrooct-6-enoate (3.8c)

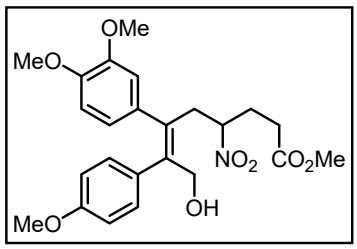

Yellowish oil (136.1 mg, 53% yield, *Z*/*E*>99:1); **IR** (neat): ν = 3515, 2998, 2954, 2837, 1736, 1606, 1549, 1510, 1464, 1441, 1245, 1174, 1026, 835 cm^{-1}; **^{1}H NMR** (400 MHz, $CDCl_3$) δ_H 6.97-6.90 (m, 2H), 6.71-6.63 (m, 3H), 6.60 (dd, *J* = 8.2, 2.0 Hz, 1H), 6.36 (d, *J* = 2.0 Hz, 1H), 4.58-4.49 (m, 2H), 4.45 (tt, *J* = 9.1, 4.0 Hz, 1H), 3.82 (s, 3H), 3.72 (s, 3H), 3.64 (s, 3H), 3.59 (s, 3H), 3.49 (dd, *J* = 14.6, 9.6 Hz, 1H), 2.95 (dd, *J* = 14.6, 4.7 Hz, 1H), 2.41-2.22 (m, 3H), 2.17-2.06 (m, 1H), 1.52 (dd, *J* = 7.0, 5.2 Hz, 1H); **^{13}C NMR** (101 MHz, $CDCl_3$) δ_C 172.2, 158.4, 148.5, 148.0, 140.8, 134.5, 132.8, 132.5, 130.7, 121.2, 113.67, 113.65, 110.8, 86.4, 63.2, 55.8 (overlapping 2C), 55.3, 52.0, 38.6, 30.2, 28.7; **HRMS** (ESI/TOF) *m/z*: $[M + Na]^+$ Calcd for $C_{24}H_{29}NNaO_8$ 482.1785; Found 482.1794.

Note: The obtained stereoconfiguration corresponds to the (*E*)-isomer, according to the Cahn-Ingold-Prelog priority rules, but is spatially oriented as in the other (*Z*)-isomers.

Methyl (*E*)-7-(3,4-dimethoxyphenyl)-9-hydroxy-8-(4-methoxyphenyl)-5-nitronon-7-enoate (5d)

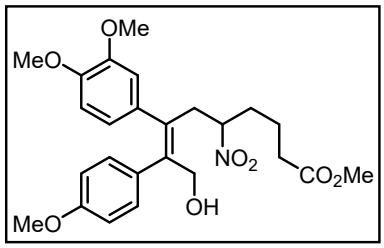

Yellowish oil (134.8 mg, 51% yield, *Z*/*E*>99:1); **IR** (neat): ν = 3515, 2953, 2838, 1734, 1606, 1548, 1511, 1463, 1440, 1245, 1173, 1026, 835 cm^{-1}; **^{1}H NMR** (400 MHz, $CDCl_3$) δ_H 6.96-6.90 (m, 2H), 6.72-6.63 (m, 3H), 6.59 (dd, *J* = 8.2, 2.0 Hz, 1H), 6.35 (d, *J* = 2.0 Hz, 1H), 4.58-4.45 (m, 2H), 4.38 (tt, *J* = 9.6, 4.5 Hz, 1H), 3.82 (s, 3H), 3.71 (s, 3H), 3.65 (s, 3H), 3.59 (s, 3H), 3.48 (dd, *J* = 14.6, 9.9 Hz, 1H), 2.89 (dd, *J* = 14.6, 4.4 Hz, 1H), 2.28 (t, *J* = 7.2 Hz, 2H), 2.11-1.98 (m, 1H), 1.85-1.73 (m, 1H), 1.73-1.64 (m, 1H), 1.64-1.56 (m, 2H); **^{13}C NMR** (101 MHz, $CDCl_3$) δ_C 173.2, 158.4, 148.5, 147.9, 140.7, 134.6, 132.9, 132.5, 130.7, 121.1, 113.6 (overlapping 2C), 110.8, 87.0, 63.2, 55.8 (overlapping 2C), 55.3, 51.8, 38.6, 33.1 (overlapping 2C), 21.2; **HRMS** (ESI/TOF) *m/z*: $[M + Na]^+$ Calcd for $C_{25}H_{31}NNaO_8$ 496.1942; Found 496.1929.

Note: The obtained stereoconfiguration corresponds to the (*E*)-isomer, according to the Cahn-Ingold-Prelog priority rules, but is spatially oriented as in the other (*Z*)-isomers.

3.4.6 General Procedure for the Consecutive Double Cyclization

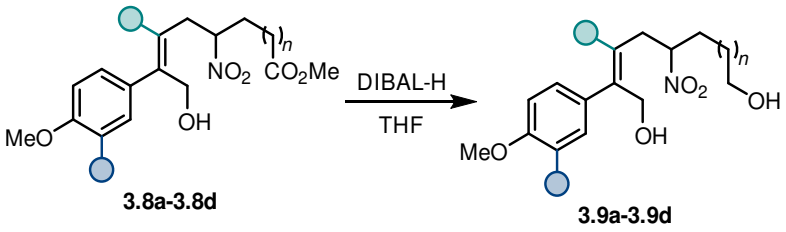

3.8a-3.8d 3.9a-3.9d

SCHEME 3.12. General synthesis of nitro-diols.

In a heat-gun-dried round-bottomed flask, the respective homoallylic nitroalkane **3.8a-3.8d** (1 equiv. substrate) was dissolved in dry THF (10 mL/mmol substrate) under N_2 and the solution was cooled to 0 °C (ice-water bath). DIBAL-H (3.45 equiv., 1 M in hexane) was added dropwise. Hereafter, the mixture was allowed to warm to room temperature and was stirred for 2 h. The mixture was then cooled to 0 °C (ice-water bath) and aqueous saturated Rochelle's salt was added dropwise. The mixture was diluted with Et_2O and was stirred for 30 min at room temperature. The phases were separated, and the aqueous phase was extracted with Et_2O three times. The combined organic layers were washed with brine, dried over $MgSO_4$, filtered, and concentrated *in vacuo*. The crude nitro-diol product **3.9a-3.9d** was dried under high vacuum and was used in the next step without further purification.

(*Z*)-2-(4-Methoxyphenyl)-3-methyl-5-nitrooct-2-ene-1,8-diol (3.9a)

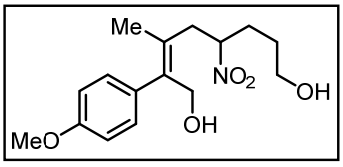

Yellowish oil; **IR** (neat): ν = 3265, 3002, 2951, 2930, 2878, 2844, 1608, 1556, 1539, 1509, 1442, 1377, 1333, 1283, 1243, 1177, 1109, 1055, 1010, 835, 795, 756, 741, 644, 612 cm^{-1}; **^{1}H NMR** (500 MHz, $CDCl_3$) δ_H 7.06-7.01 (m, 2H), 6.91-6.85 (m, 2H), 4.83 (tdd, *J* = 9.6, 5.3, 4.2 Hz, 1H), 4.34 (d, *J* = 12.3 Hz, 1H), 4.28 (d, *J* = 12.3 Hz, 1H), 3.81 (s, 3H), 3.75-3.66 (m, 2H), 3.08 (dd, *J* = 14.1, 9.5 Hz, 1H), 2.59 (dd, *J* = 14.2, 5.3 Hz, 1H), 2.17 (ddt, *J* = 14.6, 9.6, 7.2 Hz, 1H), 2.04-1.94 (m, 1H), 1.67-1.59 (m, 6H), 1.50 (br s, 1H); **^{13}C NMR** (126 MHz, $CDCl_3$) δ_C 158.7, 139.7, 132.9, 130.1, 129.6, 114.0, 87.5, 62.9, 61.7, 55.4, 38.5, 30.3, 28.7, 20.3; **HRMS** (ESI/TOF) *m/z*: $[M + Na]^+$ Calcd for $C_{16}H_{23}NNaO_5$ 332.1468; Found 332.1477.

(*E*)-2,3-Bis(3,4-dimethoxyphenyl)-5-nitrooct-2-ene-1,8-diol (3.9b)

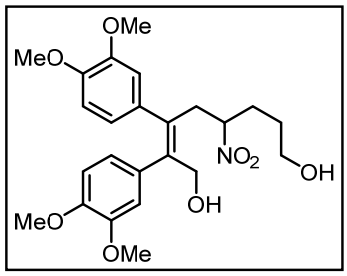

Brownish foam; **IR** (neat): ν = 3367, 3000, 2934, 2835, 1602, 1581, 1547, 1511, 1463, 1409, 1320, 1242, 1166, 1139, 1023, 912, 859, 810, 764, 728 cm^{-1}; **^{1}H NMR** (500 MHz, $CDCl_3$) δ_H 6.69 (d, J = 8.3 Hz, 1H), 6.65-6.63 (m, 2H), 6.59 (dd, J = 8.2, 2.0 Hz, 1H), 6.49 (d, J = 1.7 Hz, 1H), 6.40 (d, J = 2.0 Hz, 1H), 4.56 (d, J = 12.5 Hz, 1H), 4.52 (d, J = 12.5 Hz, 1H), 4.44 (tt, J = 9.2, 4.2 Hz, 1H), 3.82 (s, 4H), 3.79 (s, 3H), 3.62 (overlapped m, 2H), 3.60 (s, 6H), 3.50 (dd, J = 14.6, 10.0 Hz, 1H), 2.92 (dd, J = 14.7, 4.4 Hz, 1H), 2.17-2.07 (m, 1H), 1.95-1.86 (m, 1H), 1.56-1.49 (m, 2H), 1.52 (overlapped br s, 1H); **^{13}C NMR** (126 MHz, $CDCl_3$) δ_C 148.7, 148.5, 148.1, 147.9, 140.9, 134.9, 133.1, 132.8, 121.7, 121.2, 113.5, 113.4, 110.9, 110.8, 87.1, 63.0, 61.7, 55.92, 55.91, 55.90, 55.84, 38.7, 30.4, 28.7; **HRMS** (ESI/TOF) *m/z*: $[M + Na]^+$ Calcd for $C_{24}H_{31}NNaO_8$ 484.1942; Found 484.1950.

(*E*)-3-(3,4-Dimethoxyphenyl)-2-(4-methoxyphenyl)-5-nitrooct-2-ene-1,8-diol (3.9c)

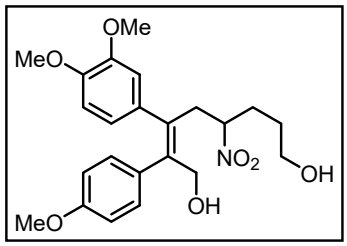

Brownish foam; **IR** (neat): ν = 3522, 2934, 2868, 2836, 1605, 1548, 1510, 1464, 1410, 1365, 1289, 1245, 1174, 1141, 1027, 834, 806, 765, 733 cm^{-1}; **^{1}H NMR** (400 MHz, $CDCl_3$) δ_H 6.97-6.91 (m, 2H), 6.72-6.62 (m, 3H), 6.59 (dd, J = 8.2, 2.0 Hz, 1H), 6.36 (d, J = 2.0 Hz, 1H), 4.55 (d, J = 12.5 Hz, 1H), 4.49 (d, J = 12.5 Hz, 1H), 4.43 (tt, J = 9.4, 4.4 Hz, 1H), 3.82 (s, 3H), 3.71 (s, 3H), 3.64-3.58 (m, 5H), 3.49 (dd, J = 14.6, 9.8 Hz, 1H), 2.93 (dd, J = 14.6, 4.5 Hz, 1H), 2.18-2.05 (m, 1H), 1.95-1.85 (m, 1H), 1.53 (d, J = 14.7 Hz, 1H), 1.57-1.48 (m, 2H), 1.25 (s, 1H); **^{13}C NMR** (101 MHz, $CDCl_3$) δ_C 158.4, 148.4, 147.9, 140.6, 134.8, 132.9, 132.6, 130.7, 121.2, 113.6 (overlapped 2C), 110.8, 87.1, 63.2, 61.7, 55.9, 55.8, 55.3, 38.6, 30.3, 28.7; **HRMS** (ESI/TOF) *m/z*: $[M + Na]^+$ Calcd for $C_{23}H_{29}NNaO_7$ 454.1836; Found 454.1835.

(*E*)-3-(3,4-dimethoxyphenyl)-2-(4-methoxyphenyl)-5-nitronon-2-ene-1,9-diol (3.9d)

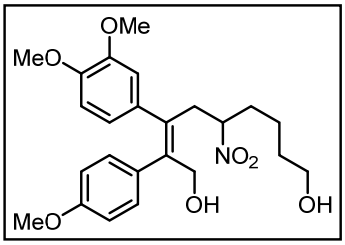

Brownish foam; **IR** (neat): ν = 3365, 2998, 2934, 2837, 1606, 1548, 1511, 1464, 1410, 1325, 1289, 1246, 1174, 1141, 1027, 835 cm^{-1}; **^{1}H NMR** (400 MHz, $CDCl_3$) δ_H 6.96-6.91 (m, 2H), 6.71-6.63 (m, 3H), 6.59 (dd, J = 8.2, 2.0 Hz, 1H), 6.35 (d, J = 2.0 Hz, 1H), 4.54 (d, J = 12.5 Hz, 1H), 4.49 (d, J = 12.5 Hz, 1H), 4.39 (tt, J = 9.4, 4.4 Hz, 1H), 3.82 (s, 3H), 3.71 (s, 3H), 3.61 (overlapped m, 2H), 3.59 (s, 3H), 3.49 (dd, J = 14.6, 10.0 Hz, 1H), 2.89 (dd, J = 14.6, 4.3 Hz, 1H), 2.12-2.00 (m, 1H), 1.81-1.70 (m, 1H), 1.66-1.44 (m, 3H), 1.41-1.30 (m, 2H), 1.25 (br s, 1H); **^{13}C NMR** (101 MHz, $CDCl_3$) δ_C 158.4, 148.4, 147.9, 140.5, 134.8, 132.9, 132.6, 130.7, 121.2, 113.6 (overlapped 2C), 110.8, 87.3, 63.2, 62.4, 55.9, 55.8, 55.3, 38.6, 33.7, 31.9, 22.3; **HRMS** (ESI/TOF) *m/z*: $[M + Na]^+$ Calcd for $C_{24}H_{31}NNaO_7$ 468.1993; Found 468.1991.

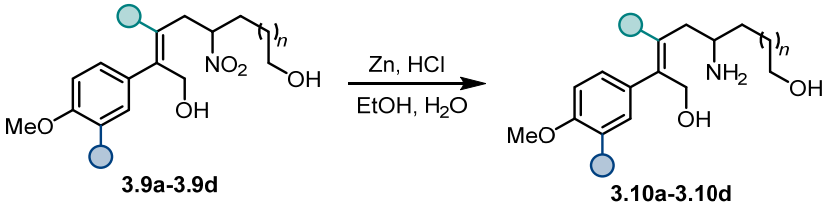

SCHEME 3.13. General synthesis of amino-diols.

In a round-bottomed flask, the respective crude nitro-diol compound **3.9a-3.9d** (1 equiv. substrate) was dissolved in EtOH (6.6 mL/mmol substrate) and HCl (10 mL/mmol substrate, 1 M in H_2O) was added dropwise. Then, activated zinc (30 equiv.) was added in small batches over 5 minutes. The resulting mixture was stirred for 1 h at room temperature. After that, the mixture was neutralized with aqueous saturated $NaHCO_3$. The mixture was then filtered, the solid was washed with EtOAc and the phases from the filtrate were separated. The aqueous phase was extracted with *n*-BuOH three times. The combined organic layers were concentrated *in vacuo*. The solid residue was suspended in CH_2Cl_2 and was filtered. The filtrate was then concentrated *in vacuo* and the respective crude amino-diol product **3.10a-3.10d** was dried under high vacuum and used in the next step without further purification.

(*Z*)-5-Amino-2-(4-methoxyphenyl)-3-methyloct-2-ene-1,8-diol (3.10a)

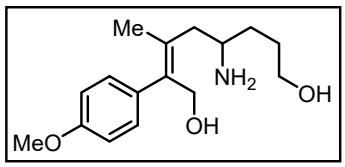

Yellowish oil; **IR** (neat): ν = 3350, 3289, 2931, 2854, 1646, 1606, 1508, 1443, 1377, 1284, 1241, 1176, 1105, 1053, 1026, 998, 832, 792 cm^{-1}; **^{1}H NMR** (400 MHz, CD_3OD) δ_H 7.17-7.10 (m, 2H), 6.93-6.86 (m, 2H), 4.44 (d, J = 11.8 Hz, 1H), 4.22 (d, J = 11.7 Hz, 1H), 3.79 (s, 3H), 3.64 (t, J = 6.9 Hz, 2H), 2.66 (dd, J = 13.8, 8.5 Hz, 1H), 2.49 (dd, J = 13.8, 5.8 Hz, 1H), 1.84-1.67 (m, 4H), 1.66 (s, 3H); **^{13}C NMR** (101 MHz, CD_3OD) δ_C 159.9, 140.1, 135.7, 132.9, 131.0, 114.5, 63.4, 62.5, 55.7, 50.9, 39.9, 32.4, 29.6, 20.4; **HRMS** (ESI/TOF) m/z: $[M + H]^+$ Calcd for $C_{16}H_{26}NO_3$ 280.1907; Found 280.1902.

(*E*)-5-Amino-2,3-bis(3,4-dimethoxyphenyl)oct-2-ene-1,8-diol (3.10b)

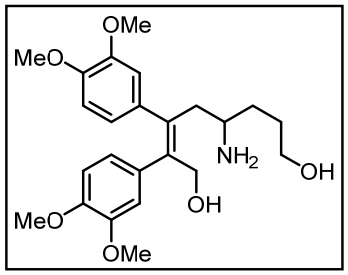

Yellowish foam; **IR** (neat): ν = 3349, 2935, 2836, 1602, 1580, 1512, 1464, 1409, 1320, 1250, 1166, 1140, 1025, 865, 811, 765 cm^{-1}; **^{1}H NMR** (500 MHz, CD_3OD) δ_H 6.80 (d, J = 8.3 Hz, 1H), 6.75-6.73 (m, 2H), 6.73-6.70 (m, 1H), 6.60 (dd, J = 10.9, 1.9 Hz, 2H), 4.63 (d, J = 12.0 Hz, 1H), 4.45 (d, J = 12.0 Hz, 1H), 3.76 (s, 3H), 3.75 (s, 3H), 3.55 (s, 3H), 3.55 (s, 3H), 3.50 (t, J = 5.9 Hz, 2H), 2.94-2.90 (m, 2H), 2.85-2.76 (m, 1H), 1.60-1.49 (m, 4H); .**^{13}C NMR** (126 MHz, CD_3OD) δ_C 150.0, 149.6, 149.4, 149.0, 140.9, 138.9, 136.5, 135.7, 123.1, 122.8, 115.51, 115.45, 112.6, 112.4, 63.8, 62.4, 56.41 (overlapping 2C), 56.39, 56.31, 50.8, 40.6, 32.9, 29.8; **HRMS** (ESI/TOF) m/z: $[M + H]^+$ Calcd for $C_{24}H_{34}NO_6$ 432.2381; Found 432.2397.

(*E*)-5-Amino-3-(3,4-dimethoxyphenyl)-2-(4-methoxyphenyl)oct-2-ene-1,8-diol (3.10c)

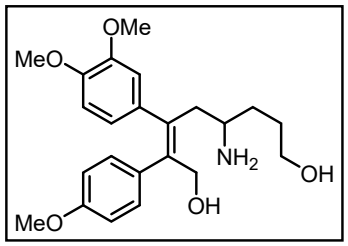

Yellowish foam; **IR** (neat): ν = 3354, 3002, 2934, 2837, 2252, 1605, 1580, 1509, 1464, 1441, 1410, 1321, 1288, 1242, 1174, 1140, 1026, 907, 833, 804, 725, 646 cm^{-1}; **^{1}H NMR** (500 MHz, CD_3OD) δ_H 7.01-6.99 (m, 2H), 6.75 (d, J = 8.3 Hz, 1H), 6.70-6.65 (m, 3H), 6.53 (d, J = 2.0 Hz, 1H), 4.60 (d, J = 11.9 Hz, 1H), 4.42 (d, J = 11.9 Hz, 1H), 3.75 (s, 3H), 3.70 (s, 3H), 3.53 (s, 3H), 3.49 (t, J = 5.9 Hz, 2H), 2.82-2.73 (m, 2H), 2.65-2.56 (m, 1H), 1.61-1.46 (m, 4H); **^{13}C NMR** (126 MHz, CD_3OD) δ_C 159.4, 149.7, 149.0, 140.2, 140.0, 136.3, 136.2, 131.8, 122.9, 115.5, 114.1, 112.4, 63.9, 62.8, 56.3 (overlapping 2C), 55.6, 50.2, 42.6, 34.6, 30.3; **HRMS** (ESI/TOF) m/z: $[M + H]^+$ Calcd for $C_{23}H_{32}NO_5$ 402.2275; Found 402.2268.

(*E*)-5-Amino-3-(3,4-dimethoxyphenyl)-2-(4-methoxyphenyl)non-2-ene-1,9-diol (3.10d)

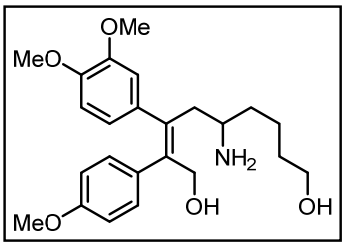

Yellowish foam; **IR** (neat): ν = 3363, 3002, 2934, 2860, 2837, 2252, 1605, 1580, 1509, 1463, 1441, 1410, 1321, 1288, 1242, 1173, 1140, 1026, 908, 833, 805, 765, 726, 646 cm^{-1}; **^{1}H NMR** (500 MHz, CD_3OD) δ_H 7.02-6.98 (m, 2H), 6.75 (d, J = 8.4 Hz, 1H), 6.70-6.65 (m, 3H), 6.53 (d, J = 2.0 Hz, 1H), 4.60 (d, J = 11.9 Hz, 1H), 4.41 (d, J = 11.9 Hz, 1H), 3.75 (s, 3H), 3.70 (s, 3H), 3.53 (s, 3H), 3.51 (t, J = 6.5 Hz, 2H), 2.83-2.72 (m, 2H), 2.61 (p, J = 6.0 Hz, 1H), 1.50-1.34 (m, 6H); **^{13}C NMR** (126 MHz, CD_3OD) δ_C 159.4, 149.7, 149.0, 140.2, 140.0, 136.3, 136.2, 131.8, 122.9, 115.5, 114.1, 112.4, 63.9, 62.9, 62.7, 56.3, 55.6, 50.2, 42.4, 37.8, 33.5, 23.4; **HRMS** (ESI/TOF) *m/z*: $[M + H]^+$ Calcd for $C_{24}H_{34}NO_5$ 416.2431; Found 416.2424.

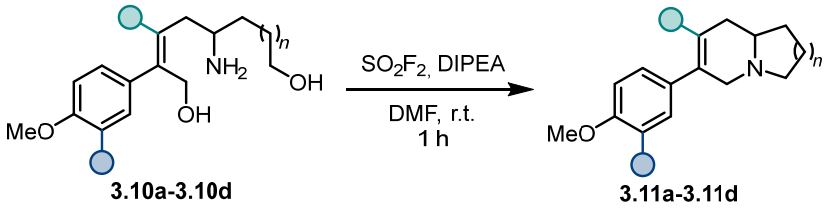

SCHEME 3.14. General synthesis of indolizidine and quinolizidine alkaloids.

Two screw-capped septum-protected vials, equipped with magnetic stir bars, were connected with a short PFA tube. Vial A was charged with 1,1'-sulfonyldiimidazole (SDI) (2.9 equiv.) and anhydrous CsF (7.8 equiv.). Vial B was charged with the respective crude amino-diol compound **3.10a-3.10d** (1 equiv. substrate). The two connected vials were purged with N_2 for 5 minutes. Anhydrous DMF (10 mL/mmol substrate) and DIPEA (11.5 equiv.) were added to vial B. Hereafter, trifluoroacetic acid (16.8 equiv.) was added in one portion into vial A. The mixture was stirred for 30 minutes at room temperature. Then, vial B was vented with a needle for 20 seconds, and the mixture was stirred for further 30 minutes. After that, vial B was diluted with H_2O and was extracted with EtOAc three times. The combined organic layers were washed with H_2O, brine, dried over Na_2SO_4, filtered, and concentrated *in vacuo*. The crude product was purified by flash chromatography on silica gel to afford the corresponding indolizidine or quinolizidine alkaloids **3.11a-3.11d**.

Note: Yields of indolizidine and quinolizidine alkaloids **3.11a-3.11d** are calculated over three steps.

6-(4-Methoxyphenyl)-7-methyl-1,2,3,5,8,8a-hexahydroindolizine (3.11a)

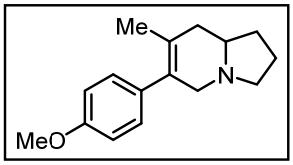

Yellowish oil (13.3 mg, 49% yield); **IR** (neat): ν = 3415, 2954, 2910, 2875, 2834, 2789, 2736, 2715, 1731, 1641, 1607, 1509, 1461, 1443, 1387, 1287, 1241, 1175, 1148, 1106, 1029, 996, 967, 832 cm^{-1}; **^{1}H NMR** (400 MHz, $CDCl_3$) δ_H 7.15-7.07 (m, 2H), 6.91-6.82 (m, 2H), 3.80 (s, 3H), 3.66 (br d, J = 15.5 Hz, 1H), 3.28 (td, J = 8.9, 1.7 Hz, 1H), 2.97 (br d, J = 15.6 Hz, 1H), 2.43-2.12 (m, 4H), 2.12-2.01 (m, 1H), 2.01-1.87 (m, 1H), 1.87-1.73 (m, 1H), 1.61 (s, 3H), 1.58-1.49 (m, 1H); **^{13}C NMR** (101 MHz, $CDCl_3$) δ_C 158.4, 133.5, 130.0, 129.9, 128.2, 113.7, 60.5, 57.6, 55.4, 54.2, 38.2, 30.8, 21.5, 20.2; **HRMS** (ESI/TOF) m/z: $[M + H]^+$ Calcd for $C_{16}H_{22}NO$ 244.1696; Found 244.1698. Spectroscopic data are in agreement with published data.[154]

6,7-Bis(3,4-dimethoxyphenyl)-1,2,3,5,8,8a-hexahydroindolizine (3.11b)

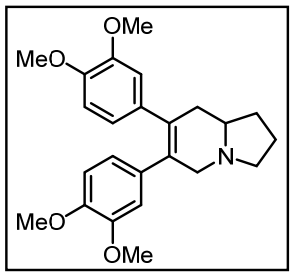

Yellowish oil (12.8 mg, 28% yield); **IR** (neat): ν = 3362, 2932, 2834, 1602, 1580, 1511, 1463, 1409, 1319, 1260, 1214, 1166, 1140, 1027, 860, 809, 764 cm^{-1}; **^{1}H NMR** (400 MHz, $CDCl_3$) δ_H 6.71-6.62 (m, 4H), 6.52 (dd, J = 10.1, 1.8 Hz, 2H), 3.91 (br d, J = 15.5 Hz, 1H), 3.80 (s, 3H), 3.80 (s, 3H), 3.60 (s, 3H), 3.57 (s, 3H), 3.43-3.26 (m, 1H), 3.24-3.00 (m, 1H), 2.75 (br d, J = 14.7 Hz, 1H), 2.58-2.39 (m, 2H), 2.39-2.21 (m, 1H), 2.21-2.05 (m, 1H), 2.05-1.92 (m, 1H), 1.92-1.76 (m, 1H), 1.71-1.52 (m, 1H); **^{13}C NMR** (101 MHz, $CDCl_3$) δ_C 148.4, 148.2, 147.7, 147.5, 135.1 (br s), 133.6 (br s), 133.1, 132.9, 121.2, 120.9, 113.1, 112.9, 110.8, 110.7, 60.6, 57.5 (br s), 57.5, 55.9, 55.8, 55.7, 54.3, 38.4 (br s), 30.8, 21.6; **HRMS** (ESI/TOF) m/z: $[M + H]^+$ Calcd for $C_{24}H_{30}NO_4$ 396.2169; Found 396.2150. Spectroscopic data are in agreement with published data.[155]

[154] See Clive, D. L. J. *et al. J. Org. Chem.* **2015** (*ref.* 115a) on page 89.
[155] See Glorius, F. *et al. Chem. Eur. J.* **2017** (*ref.* 114c) on page 89.

7-(3,4-Dimethoxyphenyl)-6-(4-methoxyphenyl)-1,2,3,5,8,8a-hexahydroindolizine (3.11c)

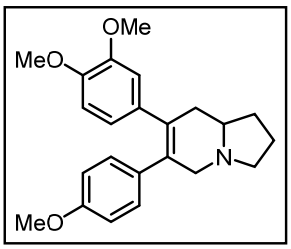

Yellowish oil (19.4 mg, 41% yield); **IR** (neat): ν = 2925, 2852, 2835, 1606, 1578, 1510, 1463, 1412, 1385, 1289, 1245, 1170, 1141, 1101, 1028, 832, 808 cm^{-1}; **^{1}H NMR** (400 MHz, $CDCl_3$) δ_H 7.00-6.93 (m, 2H), 6.73-6.63 (m, 4H), 6.46 (d, J = 1.6 Hz, 1H), 3.88 (br d, J = 15.9 Hz, 1H), 3.80 (s, 3H), 3.72 (s, 3H), 3.54 (s, 3H), 3.33 (br t, J = 8.0 Hz, 1H), 3.12 (br d, J = 16.1 Hz, 1H), 2.81-2.66 (m, 1H), 2.57-2.38 (m, 2H), 2.38-2.19 (m, 1H), 2.19-2.05 (m, 1H), 2.05-1.90 (m, 1H), 1.90-1.76 (m, 1H), 1.70-1.51 (m, 1H); **^{13}C NMR** (101 MHz, $CDCl_3$) δ_C 158.2, 148.0, 147.4, 135.0, 133.4, 132.8, 132.4 (br s), 130.3, 120.8, 113.5, 113.2, 110.6, 60.6, 57.7 (br s), 55.8, 55.6, 55.3, 54.3, 38.3 (br s), 30.8, 21.6; **HRMS** (ESI/TOF) m/z: $[M + H]^+$ Calcd for $C_{23}H_{28}NO_3$ 366.2064; Found 366.2067. Spectroscopic data are in agreement with published data.[155]

7-(3,4-Dimethoxyphenyl)-6-(4-methoxyphenyl)-1,2,3,5,8,8a-hexahydroindolizine (3.11d)

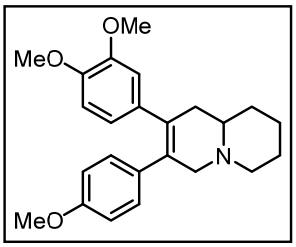

Yellowish solid (22.9 mg, 47% yield); **IR** (neat): ν = 2998, 2931, 2856, 2835, 2763, 1671, 1644, 1605, 1579, 1509, 1463, 1442, 1412, 1377, 1321, 1289, 1243, 1170, 1138, 1027, 910, 831, 807, 763, 727 cm^{-1}; **^{1}H NMR** (500 MHz, $CDCl_3$) δ_H 6.99-6.95 (m, 2H), 6.70-6.67 (m, 2H), 6.67-6.65 (m, 2H), 6.46 (d, J = 1.7 Hz, 1H), 3.80 (s, 3H), 3.72 (s, 3H), 3.62 (d, J = 15.3 Hz, 1H), 3.53 (s, 3H), 3.13-3.01 (m, 2H), 2.54 (dt, J = 17.1, 3.1 Hz, 1H), 2.46-2.24 (m, 2H), 2.16-2.06 (m, 1H), 1.89 -1.78 (m, 2H), 1.78-1.68 (m, 2H), 1.42-1.31 (m, 2H); **^{13}C NMR** (126 MHz, $CDCl_3$) δ_C 158.2, 148.0, 147.4, 134.6, 133.3, 131.4, 131.1, 130.3, 120.7, 113.6, 113.1, 110.6, 60.4, 58.1, 55.8, 55.7, 55.6, 55.3, 39.6, 33.4, 25.9, 24.4; **HRMS** (ESI/TOF) m/z: $[M + H]^+$ Calcd for $C_{24}H_{30}NO_3$ 380.2220; Found 380.2206. Spectroscopic data are in agreement with published data.[156]

[156] See Chuang, T.-H. *et al. Org. Lett.* **2016** (*ref.* 113c) on page 89.

3.4.7 Synthesis of Substituted Indolizidine Alkaloid Analogs

(Z)-5-(4-Hydroxy-3-(4-methoxyphenyl)-2-methylbut-2-en-1-yl)pyrrolidin-2-one (3.12)

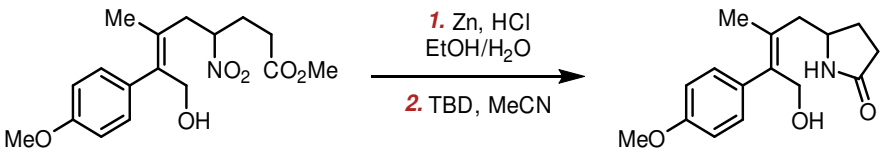

3.8a **3.12**

In a round-bottomed flask, compound **3.8a** (500 mg, 1.48 mmol) was dissolved in EtOH (10 mL) under N_2 and HCl (15 mL, 1 M in H_2O) was added dropwise. Then, activated zinc (2.91 g, 44.5 mmol) was added in small batches over 5 minutes. The resulting mixture was stirred for 1 h at room temperature. After that, the mixture was neutralized with aqueous saturated $NaHCO_3$. The mixture was then filtered, the solid was washed with EtOAc and the phases from the filtrate were separated. The aqueous phase was extracted with EtOAc three times. The combined organic layers were washed with brine, dried over Na_2SO_4, filtered, and concentrated in vacuo. The crude product was dried under high vacuum and used in the next step without further purification (note: the sample had partially condensed to product **3.12**).

In a round-bottomed flask, the crude compound from the previous step was dissolved in dry MeCN (4 mL) under N_2. 1,5,7-Triazabicyclo[4.4.0]dec-5-ene (TBD) (41.3 mg, 0.30 mmol) was added and the mixture was stirred at room temperature for 2 h. Hereafter, the mixture was concentrated *in vacuo* and was redissolved in CH_2Cl_2. Aqueous 1 M HCl was added dropwise, and the phases were separated. The aqueous phase was extracted with CH_2Cl_2 twice and the combined organic layers were washed with brine, dried over Na_2SO_4, filtered, and concentrated *in vacuo*. The resulting yellowish oil (**3.12**) was dried under high vacuum and used in the next step without further purification. **IR** (neat): ν = 3200, 2992, 2959, 2935, 2898, 2834, 2727, 1600, 1607, 1574, 1508, 1452, 1423, 1359, 1298, 1285, 1238, 1176, 1105, 1031, 997, 809, 791, 656 cm^{-1}; **^{1}H NMR** (500 MHz, $CDCl_3$) δ_H 7.13-7.08 (m, 2H), 6.92-6.87 (m, 2H), 6.89-6.80 (m, 1H), 4.45 (d, J = 11.5 Hz, 1H), 4.26 (d, J = 11.5 Hz, 1H), 3.89-3.82 (m, 1H), 3.81 (s, 3H), 2.65 (dd, J = 13.5, 9.5 Hz, 1H), 2.43-2.35 (m, 2H), 2.36-2.29 (m, 1H), 2.25 (dd, J = 13.5, 3.8 Hz, 1H), 2.20 (br s, 1H), 1.87-1.77 (m, 1H), 1.63 (s, 3H); **^{13}C NMR** (126 MHz, $CDCl_3$) δ_C 178.2, 158.6, 137.7, 133.6, 132.5, 130.1, 113.9, 62.9, 55.4, 53.2, 41.4, 30.8, 28.1, 20.8; **HRMS** (ESI/TOF) m/z: $[M - H]^-$ Calcd for $C_{16}H_{20}NO_3$ 274.1449; Found 274.1451.

6-(4-Methoxyphenyl)-7-methyl-1,5,8,8a-tetrahydroindolizin-3(2H)-one (3.13)

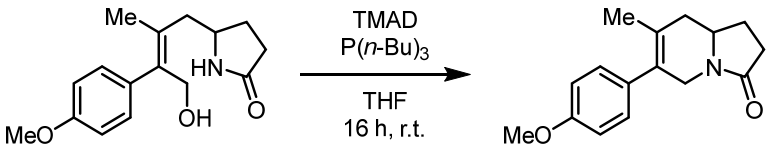

3.12 **3.13**

In a nitrogen-flushed 2 mL screw-capped septum vial, crude lactam **3.12** (19.3 mg, 0.07 mmol) was dissolved in dry THF (0.35 mL) under N_2. Tributylphosphine (21.2 mg, 0.11 mmol) was added and the mixture was cooled to 0 °C (ice-water bath). Then, a solution of 1,1'-azobis(*N*, *N*-dimethylformamide) (TMAD) (18.1 mg, 0.11 mmol) in dry THF (0.35 mL) was added dropwise. The mixture was allowed to warm to room temperature and was stirred for 16 h. Hereafter, the reaction mixture was concentrated with a gentle stream of N_2 and the residue was purified by flash chromatography on silica gel using 80-100% EtOAc/hexanes to afford bicyclic lactam **3.13** (15.2 mg, 53% yield) as a white solid. **IR** (neat): ν = 2908, 2832, 1665, 1605, 1508, 1445, 1421, 1281, 1239, 1174, 1035, 839, 794 cm^{-1}; **^{1}H NMR** (400 MHz, $CDCl_3$) δ_H 7.16-7.02 (m, 2H), 6.95-6.80 (m, 2H), 4.46 (d, *J* = 18.0 Hz, 1H), 3.81 (s, 3H), 3.74 (ddt, *J* = 9.9, 7.5, 4.9 Hz, 1H), 3.59 (d, *J* = 18.0 Hz, 1H), 2.51-2.41 (m, 2H), 2.41-2.23 (m, 2H), 2.19-2.06 (m, 1H), 1.80-1.67 (m, 1H), 1.62 (s, 3H); **^{13}C NMR** (101 MHz, $CDCl_3$) δ_C 173.9, 158.7, 132.0, 129.9, 128.6, 127.0, 113.8, 55.4, 53.2, 44.6, 38.5, 30.2, 25.2, 20.6; **HRMS** (ESI/TOF) *m/z*: $[M + H]^+$ Calcd for $C_{16}H_{20}NO_2$ 258.1489; Found 258.1488.

2-Benzyl-6-(4-methoxyphenyl)-7-methyl-1,5,8,8a-tetrahydroindolizin-3(2*H*)-one (3.14)

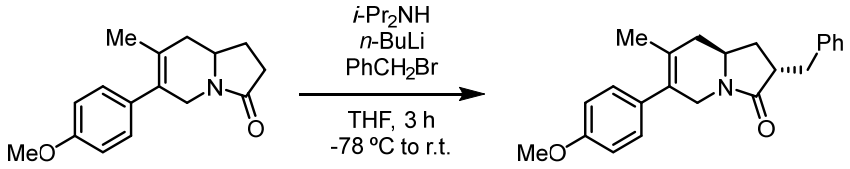

3.13 **3.14**

In an oven-dried 5 mL conical vial, *i*-Pr_2NH (16.3 µL, 0,12 mmol) was dissolved in dry THF (0.5 mL) under Ar. The solution was cooled to -78 °C (dry ice-acetone bath) and *n*-BuLi (42.6 µL, 0.11 mmol, 2.5 M in hexanes) was added dropwise. The mixture was stirred for 15 minutes and then a solution of compound **3.13** (24.9 mg, 0.10 mmol) in dry THF (0.5 mL) was added dropwise. After stirring the reaction mixture at -78 °C for 30 minutes, benzyl bromide (12.7 µL, 0.11 mmol) was added and the mixture was allowed to warm to room temperature. After 3 h, the reaction was quenched with aqueous saturated NH_4Cl and extracted with Et_2O three times. The combined organic layers were washed with brine, dried over $MgSO_4$, filtered, and concentrated *in vacuo*. The crude product was purified by flash chromatography on silica gel using 50-80% EtOAc/hexanes to afford product **3.14** (17.0 mg, 51% yield, 8.5:1 *dr*) as a yellowish oil. **IR** (neat): ν = 3028,

2915, 2835, 2241, 1681, 1607, 1510, 1440, 1242, 1175, 1033, 909, 831, 728, 700 cm^{-1}; **^{1}H NMR** (400 MHz, $CDCl_3$) δ_H 7.34-7.25 (m, 2H), 7.25-7.18 (m, 3H), 7.15-7.04 (m, 2H), 6.92-6.83 (m, 2H), 4.50 (br d, *J* = 17.9 Hz, 1H), 3.81 (s, 3H), 3.52 (br d, *J* = 18.0, 3.1 Hz, 1H), 3.48-3.38 (m, 1H), 3.21 (dd, *J* = 13.1, 3.6 Hz, 1H), 2.89-2.79 (m, 1H), 2.76 (dd, *J* = 13.2, 9.2 Hz, 1H), 2.18-1.99 (m, 3H), 1.81 (ddd, *J* = 13.1, 9.0, 3.9 Hz, 1H), 1.58 (s, 3H); **^{13}C NMR** (101 MHz, $CDCl_3$) δ_C 174.8, 158.7, 139.5, 132.0, 129.9, 129.3, 128.8, 128.6, 127.1, 126.5, 113.8, 55.4, 51.6, 44.6, 42.8, 37.8, 37.5, 30.6, 20.6; **HRMS** (ESI/TOF) *m/z*: $[M + H]^+$ Calcd for $C_{23}H_{26}NO_2$ 348.1958; Found 348.1974.

2-Benzyl-6-(4-methoxyphenyl)-7-methyl-1,2,3,5,8,8a-hexahydroindolizine (3.15)

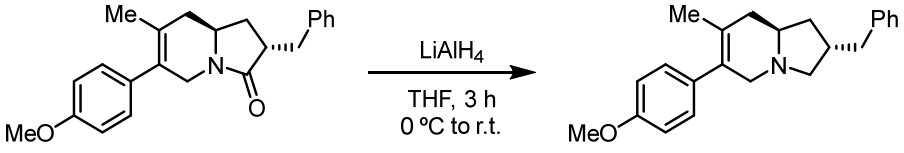

3.14 **3.15**

In a screw-capped septum-protected vial, a solution of compound **3.14** (23.0 mg, 0.07 mmol) in dry THF (0.2 mL) was added dropwise to $LiAlH_4$ (265 μL, 0.26 mmol, 1 M in THF) at 0 °C (ice-water bath) under N_2. The mixture was warmed to room temperature and was stirred for 3 h. The reaction was quenched at 0 °C (ice-water bath) with aqueous saturated Rochelle's salt and diluted with Et_2O. The mixture was allowed to warm to room temperature and was stirred for 30 minutes. The phases were separated, and the aqueous phase was extracted with Et_2O three times. The combined organic layers were washed with brine, dried over Na_2SO_4, filtered, and concentrated *in vacuo* to afford product **3.15** (17.0 mg, 77% yield) as a yellowish oil. **IR** (neat): *v* = 3027, 2928, 2833, 2785, 1607, 1509, 1453, 1288, 1242, 1175, 1031, 909, 831, 729, 609 cm^{-1}; **^{1}H NMR** (500 MHz, $CDCl_3$) δ_H 7.33-7.27 (m, 4H), 7.18-7.14 (m, 2H), 7.12-7.07 (m, 2H), 6.88-6.84 (m, 3H), 4.05 (d, *J* = 15.0 Hz, 1H), 3.91 (ddd, *J* = 10.9, 7.9, 4.7 Hz, 1H), 3.80 (s, 3H), 3.54-3.44 (m, 1H), 3.42-3.32 (m, 1H), 3.32-3.25 (m, 1H), 3.25-3.16 (m, 1H), 2.83 (dd, *J* = 14.0, 7.8 Hz, 1H), 2.76 (dd, *J* = 13.9, 7.9 Hz, 1H), 2.52-2.40 (m, 2H), 2.38-2.29 (m, 1H), 2.11-2.03 (m, 1H), 1.64 (s, 3H); **^{13}C NMR** (126 MHz, $CDCl_3$) δ_C 159.2, 138.3, 130.8, 130.7, 130.10, 130.05, 129.7, 129.6, 129.5, 129.4, 129.0, 128.9, 128.8, 128.3, 128.3, 127.0, 114.8, 114.1, 113.5, 58.6, 56.0, 55.4, 54.8, 40.8, 35.4, 34.2, 34.1, 20.2; **HRMS** (ESI/TOF) *m/z*: $[M + H]^+$ Calcd for $C_{23}H_{28}NO$ 334.2165; Found 334.2180.

Note: ^{1}H NMR and ^{13}C NMR of compound **3.15** were measured from its HCl salt.

6-(4-Methoxyphenyl)-3,3,7-trimethyl-1,2,3,5,8,8a-hexahydroindolizine (3.16)

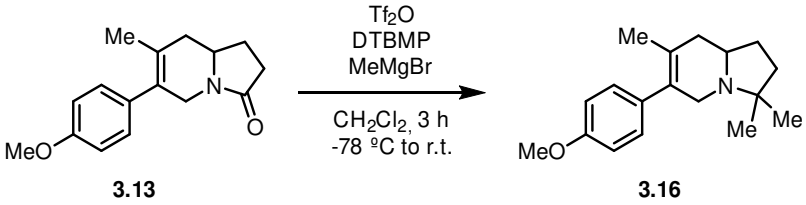

3.13 **3.16**

In an oven-dried 5 mL conical vial, compound **3.13** (14.0 mg, 0.05 mmol) and 2,6-di-*tert*-butyl-4-methylpyridine (DTBMP) (13.4 mg, 0.07 mmol) were dissolved in dry CH_2Cl_2 under N_2. The solution was cooled to -78 °C and triflic anhydride (11.0 µL, 0.07 mmol) was added dropwise. After 45 minutes, MeMgBr (163 µL, 0.16 mmol, 1 M in Bu_2O) was added dropwise. The mixture was allowed to warm to room temperature and was stirred for 3 h. The reaction was quenched with aqueous saturated NH_4Cl and was extracted with CH_2Cl_2 three times. The combined organic layers were washed with brine, dried over Na_2SO_4, filtered, and concentrated *in vacuo*. The crude product was purified by flash chromatography on silica gel using EtOAc/hexanes 80-100% to give compound **3.16** (7.8 mg, 53% yield) as a yellowish oil. **IR** (neat): ν = 2957, 2870, 2833, 1693, 1607, 1509, 1461, 1385, 1360, 1287, 1240, 1174, 1037, 830 cm^{-1}; **^{1}H NMR** (500 MHz, $CDCl_3$) δ_H 7.18-7.13 (m, 2H), 6.91-6.86 (m, 2H), 3.81 (s, 3H), 3.73 (br d, J = 13.8 Hz, 1H), 3.48-3.36 (m, 2H), 3.27-3.16 (m, 1H), 2.48-2.39 (m, 1H), 2.33-2.23 (m, 1H), 2.23-2.12 (m, 1H), 1.99-1.89 (m, 1H), 1.73 (s, 3H), 1.64 (s, 3H), 1.23 (s, 3H); **^{13}C NMR** (126 MHz, $CDCl_3$) δ_C 159.1, 131.1, 130.2, 130.0, 124.8, 114.1, 67.6, 58.9, 55.4, 47.2, 35.9, 35.0, 26.0, 23.5, 21.8, 20.1; **HRMS** (ESI/TOF) *m/z*: $[M + H]^+$ Calcd for $C_{18}H_{26}NO$ 272.2009; Found 272.2007.

Note: ^{1}H NMR and ^{13}C NMR of compound **3.16** were measured from its HCl salt.

3.4.8 Crystallographic Studies

The experimental procedure for measuring single crystals of compounds **3.11d** and **3.13** by X-ray diffraction has already been detailed in chapter 2. Single crystals of compound **3.11d** suitable for X-ray diffraction were obtained by slow evaporation from a CH_2Cl_2 solution, while single crystals of compound **3.13** were obtained by slow evaporation from an acetone solution.

TABLE 3.5. Crystal data and structure refinement for **3.11d** (CCDC-1951370).

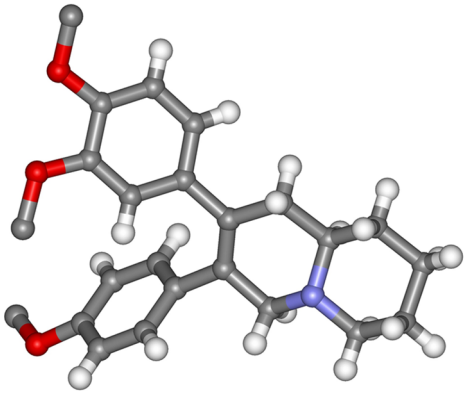

Empirical formula	$C_{24}H_{29}NO_3$	
Formula weight	379.48	
Temperature	100(2) K	
Wavelength	0.71073 Å	
Crystal system	triclinic	
Space group	*P*-1	
Unit cell dimensions	a = 5.9005(3) Å	α = 87.331(4)°
	b = 12.2469(6) Å	β = 80.374(4)°
	c = 14.0234(7) Å	γ = 81.982(4)°
Volume	989.06(9) Å^3	
Z	2	
Density (calculated)	1.274 mg·m^{-3}	
Absorption coefficient	0.083 mm^{-1}	
F(000)	408	
Crystal size	0.250 × 0.100 × 0.100 mm^3	
Theta range for data collection	2.947 to 29.614°.	
Index ranges	-4 <= h <= 8, -15 <= k <= 16, -19 <= l <= 18	
Reflections collected	10691	
Independent reflections	4814[R(int) = 0.0238]	
Completeness to theta =29.614°	86.4%	
Absorption correction	Multi-scan	
Max. and min. transmission	1.00 and 0.74	
Refinement method	Full-matrix least-squares on F^2	
Data / restraints / parameters	4814/ 0/ 256	
Goodness-of-fit on F^2	1.040	
Final R indices [I>2σ(I)]	R_1 = 0.0453, wR_2 = 0.1113	
R indices (all data)	R_1 = 0.0675, wR_2 = 0.1206	
Largest diff. peak and hole	0.414 and -0.260 e·Å^{-3}	

TABLE 3.6. Crystal data and structure refinement for **3.13**.[157]

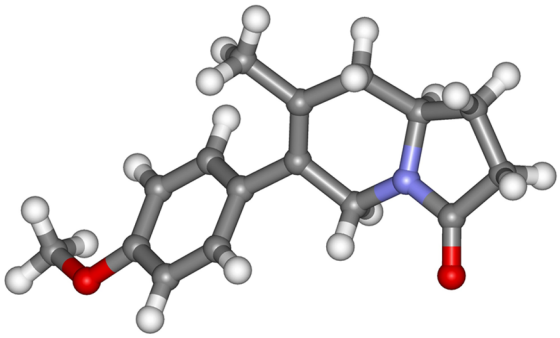

Empirical formula	$C_{16}H_{19}NO_2$	
Formula weight	257.32	
Temperature	100(2) K	
Wavelength	0.71073 Å	
Crystal system	monoclinic	
Space group	$P2_1/c$	
Unit cell dimensions	a = 14.3085(9) Å	α = 90°
	b = 7.9169(4) Å	β = 114.093(2)°
	c = 13.0833(8) Å	γ = 90°
Volume	1352.95(14) Å3	
Z	4	
Density (calculated)	1.263 mg·m^{-3}	
Absorption coefficient	0.083 mm^{-1}	
F(000)	552	
Crystal size	0.200 × 0.200 × 0.100 mm^3	
Theta range for data collection	3.009 to 30.535°.	
Index ranges	-20 <= h <= 19 , -11 <= k <= 10 , -11 <= l <= 18	
Reflections collected	14423	
Independent reflections	4102[R(int) = 0.0285]	
Completeness to theta =30.535°	98.9%	
Absorption correction	Multi-scan	
Max. and min. transmission	0.74 and 0.71	
Refinement method	Full-matrix least-squares on F^2	
Data / restraints / parameters	4102/ 0/ 174	
Goodness-of-fit on F^2	1.032	
Final R indices [I>2σ(I)]	R_1 = 0.0479, wR_2 = 0.1284	
R indices (all data)	R_1 = 0.0598, wR_2 = 0.1365	
Largest diff. peak and hole	0.645 and -0.361 e·Å^{-3}	

[157] This X-ray structure was not part of the original publication of this work but is added here for completion.

UNIVERSITAT ROVIRA I VIRGILI
STEREOSELECTIVE TRANSFORMATIONS OF VINYL CYCLIC CARBONATES AND APPLICATIONS IN NATURAL PRODUCT SYNTHESIS
Àlex Cristòfol Martínez

UNIVERSITAT ROVIRA I VIRGILI
STEREOSELECTIVE TRANSFORMATIONS OF VINYL CYCLIC CARBONATES AND APPLICATIONS IN NATURAL PRODUCT SYNTHESIS
Àlex Cristòfol Martínez

Important thing in science is not so much to obtain new facts as to discover new ways of thinking about them. — Sir William Bragg

CHAPTER 4

EXPEDIENT DUAL CO/ORGANOPHOTOREDOX CATALYZED STEREOSELECTIVE SYNTHESIS OF ALL-CARBON QUATERNARY CENTERS

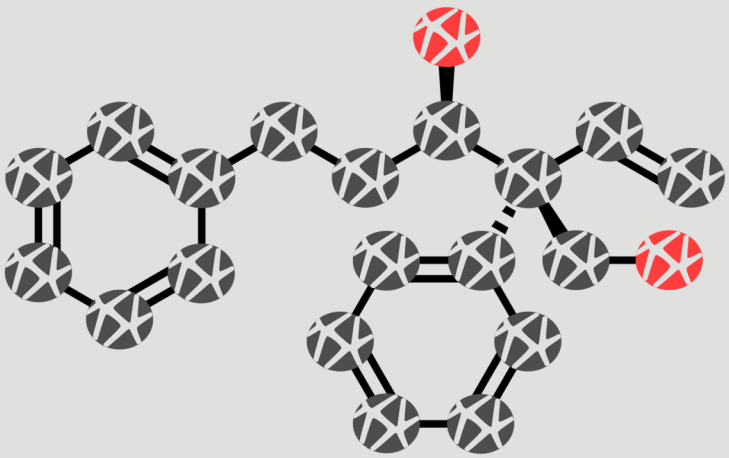

Most of the results of this chapter have been published in:

Cristòfol, À.; Limburg, B.; Kleij, A. W. *Angew. Chem. Int. Ed.* **2021**, *60*, 15266–15270

4.1 Introduction

4.1.1 Allylic Substitution: From Noble to 3d Transition Metals

The stereoselective introduction of allyl groups in organic molecules has been mainly dominated by the use of noble metals (*e.g.*, palladium, iridium, and rhodium).[158] Despite the success and efficiency of these TMs, a major drawback is represented by their high cost, which is mainly connected to their low natural abundance (**FIGURE 4.1**). Their (large) scale use is clearly frustrating sustainability due to limited availability and lack of renewability. To circumvent this problem, the use of more earth-abundant 3d transition metals has become a major topic of interest for the chemical community.

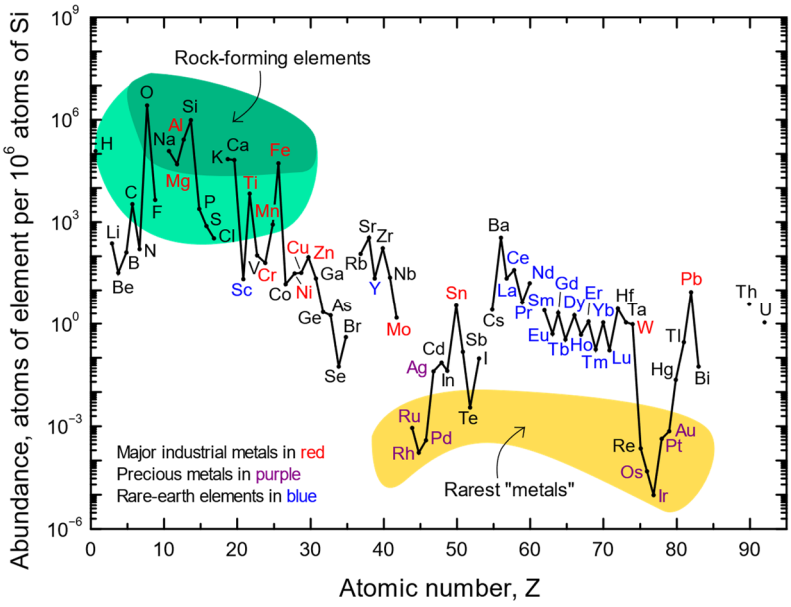

FIGURE 4.1. Abundance (atom fraction) of the chemical elements in Earth's upper continental crust as a function of atomic number.[159]

[158] a) Turnbull, B. W. H.; Evans, P. A. *J. Org. Chem.* **2018**, *83*, 11463-11479. b) Cheng, Q.; Tu, H.-F.; Zheng, C.; Qu, J.-P.; Helmchen, G.; You, S.-L. *Chem. Rev.* **2019**, *119*, 1855-1969. c) Pàmies, O.; Margalef, J.; Cañellas, S.; James, J.; Judge, E.; Guiry, P. J.; Moberg, C.; Bäckvall, J.-E.; Pfaltz, A.; Pericàs, M. A.; Diéguez, M. *Chem. Rev.* **2021**, *121*, 4373-4505.

[159] Haxel, G. B.; Boore, S.; Mayfield, S. Rare Earth Elements - Critical Resources for High Technology, 2002. U.S. Geological Survey. https://pubs.usgs.gov/fs/2002/fs087-02 (accessed Jul 05, 2021).

While attractive, the direct replacement of a noble metal by a more abundant 3d transition metal is not straightforward. In most cases, the reactivity of such 3d transition metal complexes is very distinct, as these complexes typically have different coordination geometries and/or operate through different redox states. A clear example is the cobalt-catalyzed allylic substitution of allyl electrophiles with organometallic or organic (pro)nucleophiles (**SCHEME 4.1**).[160] In contrast with well-known palladium- and iridium-catalyzed allylic substitution reactions, whose active Pd(0) and Ir(I) precursors are often bench-stable and/or commercially available, active Co(I) precursors are neither bench-stable nor commercially available, and must therefore be generated *in situ* by reduction of a Co(II) precursor with a suitable reductant. This can be accomplished using organometallic reagents, such as a Grignard or organozinc reagents, which also act as a nucleophile, as exemplified by Oshima and Knochel.[161] On the other hand, the reaction with more commonly used pronucleophiles requires the addition of a metal reductant, such as Zn, as demonstrated by Li and coworkers. [162]

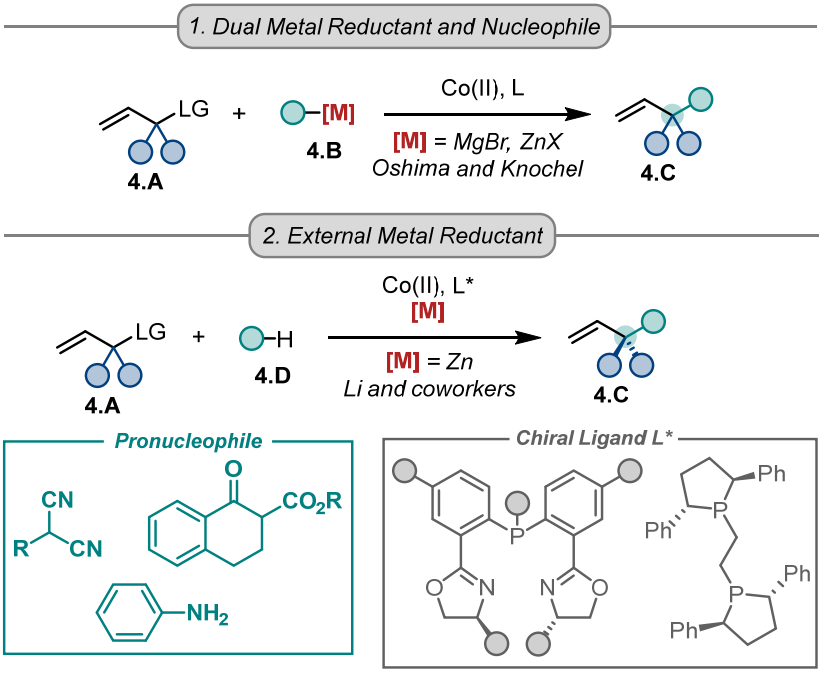

SCHEME 4.1. Cobalt-catalyzed allylic substitution reactions using (pro)nucleophiles.

[160] For a recent review on cobalt-catalyzed allylic functionalizations, see: Han, J.-F.; Guo, P.; Zhang, X.-G.; Liao, J.-B.; Ye, K.-Y. *Org. Biomol. Chem.* **2020**, *18*, 7740-7750.

[161] a) Reddy, C. K.; Knochel, P. *Angew. Chem. Int. Ed. Engl.* **1996**, *35*, 1700-1701. b) Mizutani, K.; Yorimitsu, H.; Oshima, K. *Chem. Lett.* **2004**, *33*, 832-833. c) Yasui, H.; Mizutani, K.; Yorimitsu, H.; Oshima, K. *Tetrahedron* **2006**, *62*, 1410-1415. d) Dunet, G.; Knochel, P. *Synlett* **2007**, 1383-1386.

[162] a) Ghorai, S.; Chirke, S. S.; Xu, W.-B.; Chen, J.-F.; Li, C. *J. Am. Chem. Soc.* **2019**, *141*, 11430-11434. b) Sun, M.; Chen, J.-F.; Chen, S.; Li, C. *Org. Lett.* **2019**, *21*, 1278-1282. c) Ghorai, S.; Ur Rehman, S.; Xu, W.-B.; Huang, W.-Y.; Li, C. *Org. Lett.* **2020**, *22*, 3519-3523.

A more elegant way to achieve the cobalt-catalyzed allylic substitution with malonates was reported by Kojima and Matsunaga,[163] who used a visible light source (namely a high-power blue LED) in conjunction with an exogenous organic photosensitizer (4CzIPN) and a sacrificial electron donor (DIPEA). Under these conditions, the reduction to the presumably active Co(I) species proceeded smoothly without the requirement of a metal reductant, thus allowing for a thermal Co(I)-Co(III) cycle to proceed via initial substrate coordination, oxidative addition, and nucleophilic attack (**SCHEME 4.2**).[164]

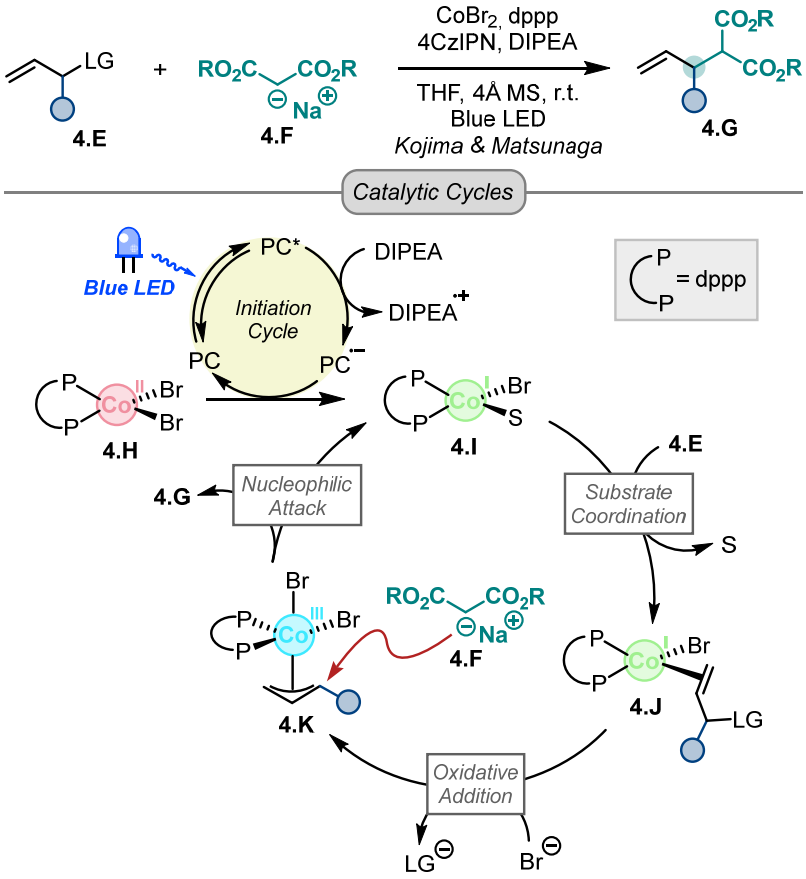

SCHEME 4.2. Photoinitiated cobalt-catalyzed allylic substitution.

[163] a) Takizawa, K.; Sekino, T.; Sato, S.; Yoshino, T.; Kojima, M.; Matsunaga, S. *Angew. Chem. Int. Ed.* **2019**, *58*, 9199-9203. b) Sekino, T.; Sato, S.; Kuwabara, K.; Takizawa, K.; Yoshino, T.; Kojima, M.; Matsunaga, S. *Synthesis* **2020**, *52*, 1934-1946.

[164] Light/dark experiments demonstrated that the thermal Co(I)-Co(III) cycle proceeds in the absence of light, although continuous light irradiation showed a marked beneficial effect.

4.1.2 Metallaphotoredox Catalysis for Carbonyl Allylations

Beyond the seminal work from Kojima and Matsunaga, a more profound application of metallaphotoredox catalysis in combination with allylic chemistry has been the formal *umpolung* of the allyl group (*i.e.,* from classically being electrophilic to becoming nucleophilic).[165] A seminal example of this concept is found in the stereoselective reductive allylation of carbonyl compounds (aldehydes and ketones), which has been commonly applied to the synthesis of complex natural products.[166] In contrast to the photoinitiated cycle, the photoreduction may as well be merged with the main catalytic cycle allowing to regenerate the active low-valent metal species to accommodate additional turnovers. Additionally, a second reduction of a high-valent to a lower valent allyl-metal species allows for the formal *umpolung* of the allyl group. This has only been realized on three occasions in the case of cobalt-catalyzed allylations, which require the additional reduction of a Co^{III}-allyl intermediate to the requisite nucleophilic Co^{II}-allyl species. The first report was published by Gosmini in 2003, where the allylation of aldehydes and ketones was effectively realized at room temperature through the combination of $CoBr_2$ with a two-fold excess of Zn dust in MeCN.[167] The reaction proceeded without the aid of an exogenous ligand and required a small amount of TFA for the activation of the Zn dust.

Despite this early report, it was not until 2021 that Gualandi, Marchini, and Cozzi published a photoredox version of the cobalt-catalyzed allylation of aldehydes using allylic acetates and a combination of $CoBr_2$, dtbbpy, $[Ir(dtbbpy)(ppy)_2]PF_6$, and DIPEA in DMF/H_2O using a blue LED bath as a light source (**SCHEME 4.3**).[168] A control reaction in the presence of TEMPO hardly had an effect on the product formation, indicating that a free radical pathway was not involved in the formation of the homoallylic alcohol product. Shortly hereafter, Shi and coworkers published an extension of Cozzi this work using minor modifications of Cozzi's reaction conditions, partially focusing on the formation of tertiary carbon stereocenters (**4.N5-4.N7**), albeit with poor diastereocontrol.[169] UV-Vis studies indicated that the reaction may proceed through a Co(II)-Co(I)-Co(III)-Co(II) cycle, as initially proposed by Gosmini.[167]

---

[165] a) Zanoni, G.; Pontiroli, A.; Marchetti, A.; Vidari, G. *Eur. J. Org. Chem.* **2007**, 3599-3611. b) Spielmann, K.; Niel, G.; de Figueiredo, R. M.; Campagne, J.-M. *Chem. Soc. Rev.* **2018**, *47*, 1159-1173. c) Huang, H.-M.; Bellotti, P.; Glorius, F. *Chem. Soc. Rev.* **2020**, *49*, 6186-6197.

[166] a) Yus, M.; González-Gómez, J. C.; Foubelo, F. *Chem. Rev.* **2013**, *113*, 5595-5698. b) Krische, M. J. *et al. Acc. Chem. Res.* **2017** c) Wang, P.-S.; Shen, M.-L.; Gong, L.-Z. *Synthesis* **2018**, *50*, 956-967. d) Doerksen, R. S.; Meyer, C. C.; Krische, M. J. *Angew. Chem. Int. Ed.* **2019**, *58*, 14055-14064.

[167] Gomes, P.; Gosmini, C.; Périchon, J. *Synthesis* **2003**, 1909-1915.

[168] Gualandi, A.; Rodeghiero, G.; Perciaccante, R.; Jansen, T. P.; Moreno-Cabrerizo, C.; Foucher, C.; Marchini, M.; Ceroni, P.; Cozzi, P. G. *Adv. Synth. Catal.* **2021**, *363*, 1105-1111.

[169] Shi, C.; Li, F.; Chen, Y.; Lin, S.; Hao, E.; Guo, Z.; Wosqa, U. T.; Zhang, D.; Shi, L. *ACS Catal.* **2021**, *11*, 2992-2998.

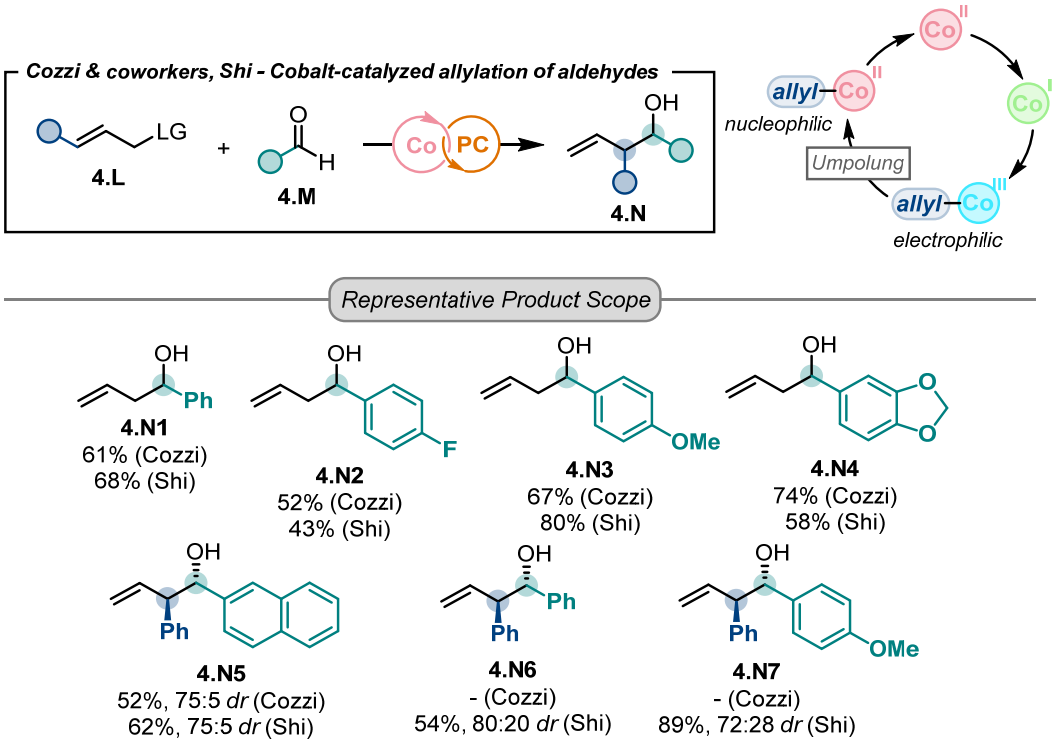

SCHEME 4.3. Allylation of aldehydes by dual photoredox and cobalt catalysis reported by Cozzi and Shi.

Before the introduction of dual cobalt/photoredox allylations, the group of Cozzi developed a method for the allylation of aldehydes using nickel as a base metal in combination with photoredox catalysis (**SCHEME 4.4**).[170] Mechanistic investigations suggested the involvement of a $[Ni^{I}(phen)_3]^{+}$ intermediate, which could react with allyl acetate (**4.O**) to generate the key allyl-Ni^{II} species responsible for nucleophilic addition onto the aldehyde. On the other hand, the group of Xia reported a methodology based on the intermediacy of a nickel hydride, which could react with 1,3-dienes substrates (**4.P**) to generate homoallylic alcohol products featuring tertiary carbon stereocenters in high yields, although with very poor diastereoselectivity (**4.N11**-**4.N13**).[171] Interestingly, the formation of the *syn*-diastereomer is slightly favored, which is opposite to what is usually found in other allylation protocols. It should be mentioned that the ligand backbone must play an important role in both of these discussed reactions to control multiple events, such as inducing a slight preference for the (*Z*)-σ-allyl-Ni^{II} over the (*E*)-σ-allyl-Ni^{II} species, or favoring a σ-allyl-Ni^{II} instead of a π-allyl-Ni^{II} coordination.

[170] Gualandi, A.; Rodeghiero, G.; Faraone, A.; Patuzzo, F.; Marchini, M.; Calogero, F.; Perciaccante, R.; Jansen, T. P.; Ceroni, P.; Cozzi, P. G. *Chem. Commun.* **2019**, *55*, 6838-6841. For a non-photoredox version, see: Suzuki, H.; Yamaguchi, E.; Itoh, A. *Synthesis* **2020**, *53*, 1489-1494.

[171] Li, Y.-L.; Li, W.-D.; Gu, Z.-Y.; Chen, J.; Xia, J.-B. *ACS Catal.* **2020**, *10*, 1528-1534.

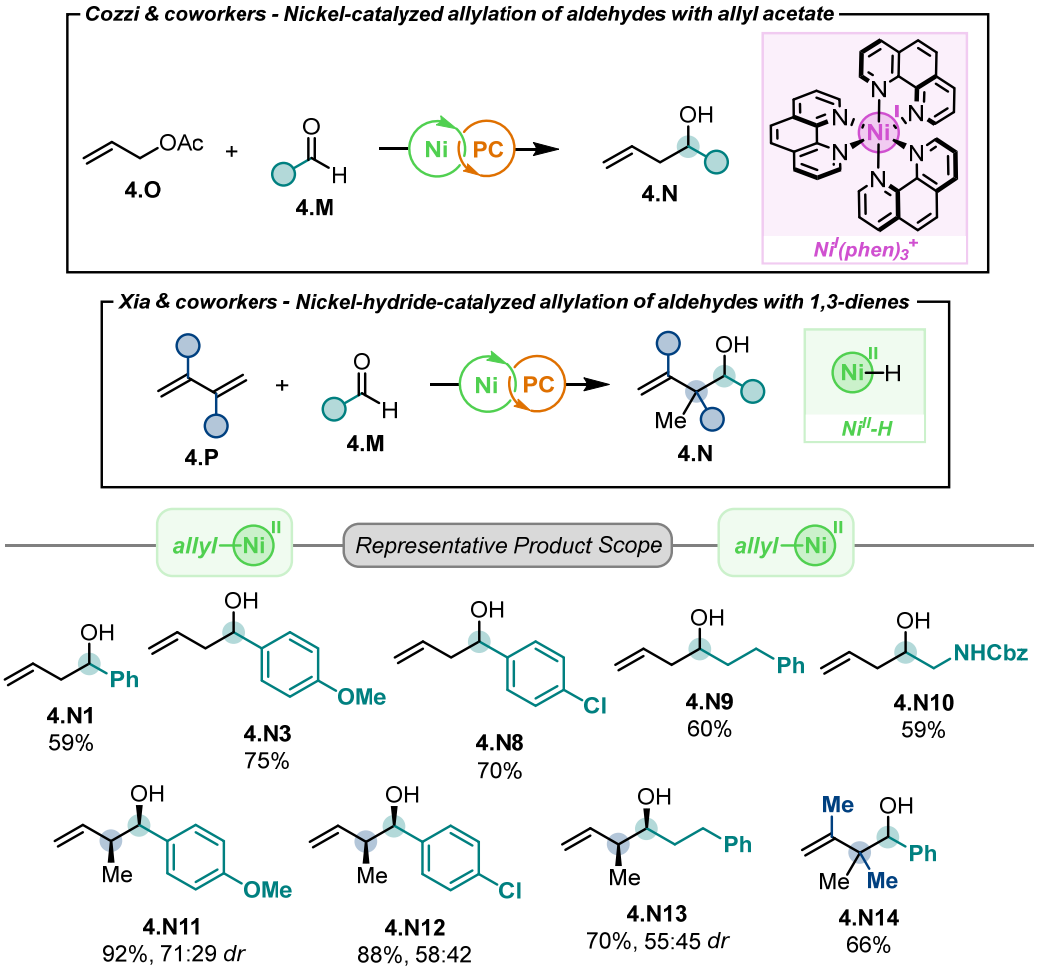

SCHEME 4.4. Allylation of aldehydes by dual photoredox and nickel catalysis reported by Cozzi, and Xia.

Apart from cobalt and nickel, the groups of Glorius and Kanai independently reported important breakthroughs in the area of carbonyl allylations by merging photoredox and chromium catalysis.[172] Similar to the well-known Nozaki-Hiyama-Kishi allylation, the reaction design relies on the catalytic generation of a nucleophilic allyl-Cr^{III} species. In contrast to cobalt-catalyzed allylations, in which a formal *umpolung* of the allyl group occurs via the reduction of a higher valent allyl-Co species, the generation of nucleophilic allyl-Cr^{III} species occurs through the interception of a free allyl radical by a Cr^{II} species (**SCHEME 4.5**). The generation of the free allyl radical has often been accomplished by photo-oxidation of electron-rich allylic substrates (**4.Q**) and subsequent deprotonation. In the case of electron-poor allylic substrates that cannot be directly photo-oxidized, the mediation of a suitable thiol-based HAT catalyst is required. The generation of the free allyl radical could in one case be accomplished through the radical addition of an alkyl radical (generated

[172] a) Schwarz, J. L.; Schäfers, F.; Tlahuext-Aca, A.; Lückemeier, L.; Glorius, F. *J. Am. Chem. Soc.* **2018**, *140*, 12705-12709. b) Mitsunuma, H.; Tanabe, S.; Fuse, H.; Ohkubo, K.; Kanai, M. *Chem. Sci.* **2019**, *10*, 3459-3465. c) Schäfers, F.; Quach, L.; Schwarz, J. L.; Saladrigas, M.; Daniliuc, C. G.; Glorius, F. *ACS Catal.* **2020**, *10*, 11841-11847. b) Schwarz, J. L.; Huang, H.-M.; Paulisch, T. O.; Glorius, F. *ACS Catal.* **2020**, *10*, 1621-1627. e) Tanabe, S.; Mitsunuma, H.; Kanai, M. *J. Am. Chem. Soc.* **2020**, *142*, 12374-12381.

from **4.R**) to a 1,3-diene (**4.P**). Overall, the product scope features high yields and high diastereoselectivity for the homoallylic alcohol products featuring tertiary carbon stereocenters (**4.N15**-**4.N22**), but these protocols do not allow to generate all-carbon quaternary stereocenters in high yield and diastereoselectivity (**4.N23**-**4.N24**).

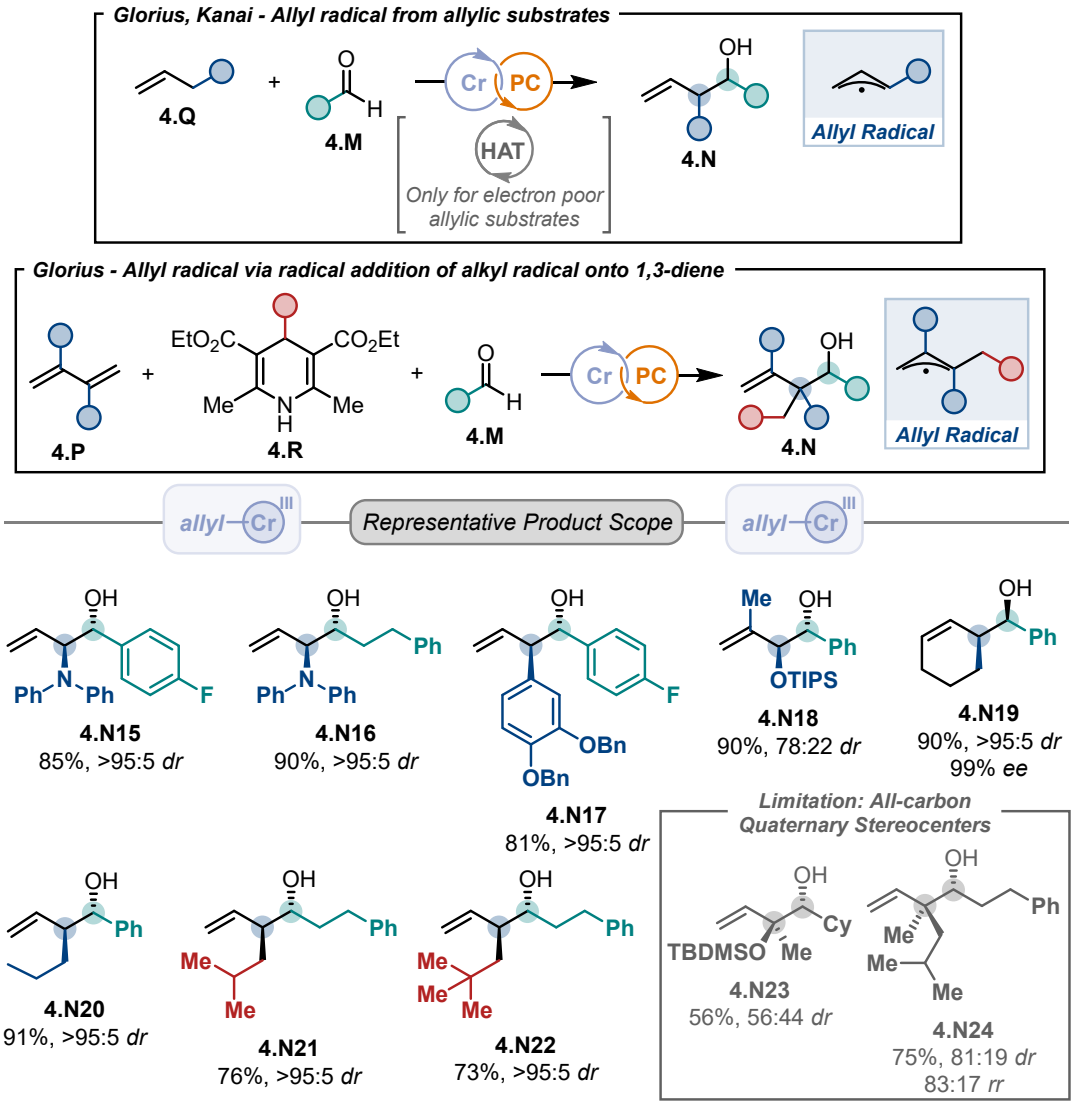

SCHEME 4.5. Aldehyde allylation by dual photoredox/chromium catalysis reported by Glorius, and Kanai.

In addition to the chromium-based allylations, the groups of Cozzi and Shi separately and successfully developed methodologies merging titanium and photoredox catalysis.[173] Analogous to the chromium-based allylations, the generation of a nucleophilic allyl-Ti^{IV} species proceeds through the interception of a free allyl radical with the Nugent-Rajanbabu reagent, $Cp_2Ti^{III}Cl$ (**SCHEME 4.6**). However, the generation of the free allyl radical takes place from an allyl halide substrate (**4.S**) or from the radical addition of an alkyl radical (generated from **4.V**) to 1,3-butadiene (**4.U**). Regarding the product scope, high yields are usually obtained for homoallylic alcohols featuring the most simple allyl group (**4.N1** and **4.N25-4.N26**), and high diastereoselectivities can be achieved for homoallylic alcohols featuring a tertiary carbon stereocenter (**4.N7**, **4.N13**, and **4.N27-4.N30**). Additionally, ketones were also shown to be suitable electrophiles in lieu of inherently more reactive aldehydes.

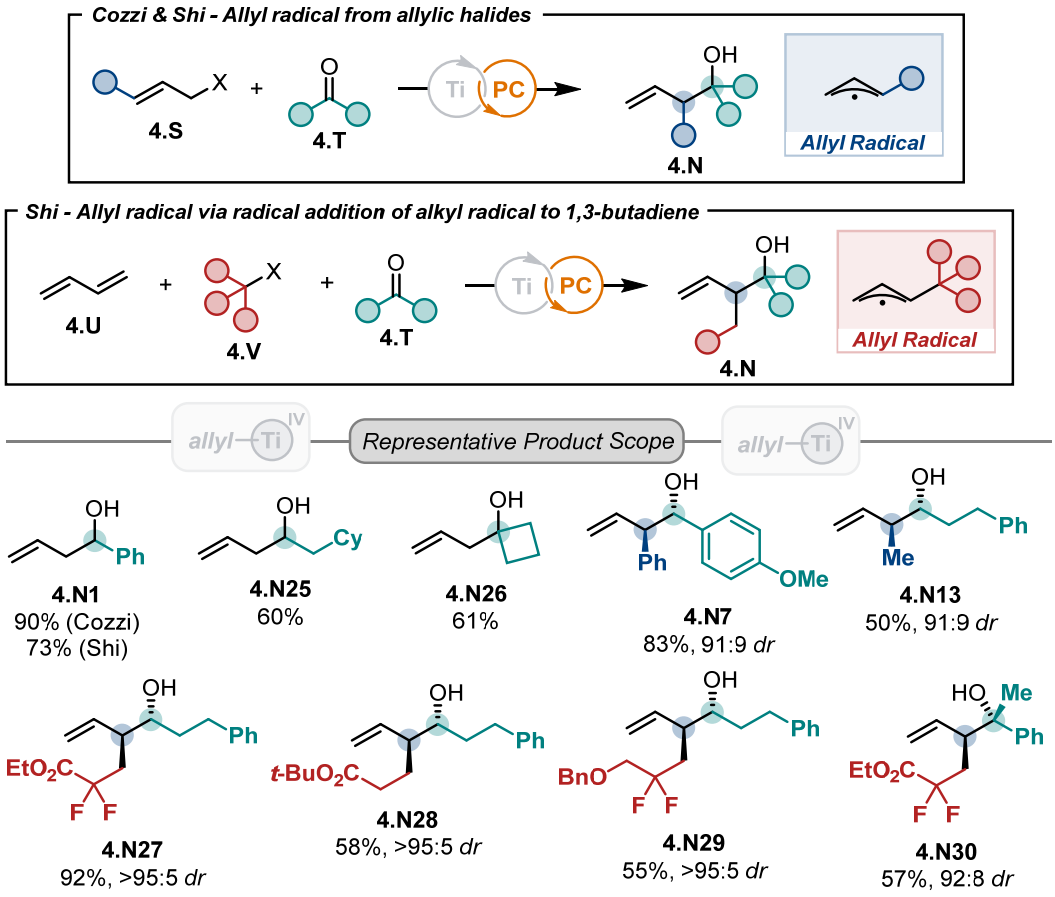

SCHEME 4.6. Carbonyl allylation by dual photoredox and titanium catalysis reported by Cozzi, and Shi.

[173] a) Gualandi, A.; Calogero, F.; Mazzarini, M.; Guazzi, S.; Fermi, A.; Bergamini, G.; Cozzi, P. G. *ACS Catal.* **2020**, *10*, 3857-3863. b) Li, F.; Chen, Y.; Lin, S.; Shi, C.; Li, X.; Sun, Y.; Guo, Z.; Shi, L. *Org. Chem. Front.* **2020**, *7*, 3434-3438. c) Li, F.; Lin, S.; Chen, Y.; Shi, C.; Yan, H.; Li, C.; Wu, C.; Lin, L.; Duan, C.; Shi, L. *Angew. Chem. Int. Ed.* **2021**, *60*, 1561-1566.

4.1.3 Stereoselective Formation of Quaternary Carbon Centers

Despite notable progress, carbonyl allylations using 3d transition metals have not successfully addressed the problem of generating homoallylic alcohol products featuring an all-carbon quaternary stereocenter with high levels of diastereocontrol. Moreover, the diastereocontrol when generating less congested tertiary carbon stereocenters with cobalt and nickel catalysts was shown to be problematic. In addition, the use of an iridium-based photocatalyst has been frequently necessary, which clearly compromises the overall sustainability of the process.

The challenging formation of such congested all-carbon quaternary centers in a stereoselective fashion has been primarily addressed by the use of noble metal catalysts or stoichiometric preformed allylmetal(oid) reagents, such as allylboron, allylsilane, or allylzinc reagents.[174] Several important breakthroughs in the allylation of carbonyl compounds have arisen from the utilization of chiral iridium catalysts developed by the group of Krische.[175] In particular, these chiral iridium catalysts were shown to produce homoallylic alcohol products featuring an all-carbon quaternary carbon stereocenter in high yields, high diastereoselectivity, and high enantioselectivity (**SCHEME 4.7**).[176] The reaction design relies on the catalytic generation of an allyl-Ir^{III} species[177] through oxidative addition of an allylic substrate to an Ir^{I} species, or alternatively, through migratory insertion of an Ir^{III}–H into 1,3-dienes or allenes. Related diastereoselective methodologies were also developed for ruthenium complexes, which also rely on the generation of a nucleophilic allyl-Ru^{II} species through migratory insertion of a Ru^{II}–H into 1,3-dienes or allenes. Importantly, these protocols work best when starting from the alcohol oxidation level, so these transformations are often regarded as redox-triggered carbonyl allylations via H_2 transfer. Moreover, the developed methods have found important applications in the total synthesis of complex natural products.[178]

---

[174] Marek, I.; Sklute, G. *Chem. Commun.* **2007**, 1683-1691.

[175] a) Santana, C. G.; Krische, M. J. *ACS Catal.* **2021**, *11*, 5572-5585. b) See Krische, M. J. *et al. Chem. Eur. J.* **2021** (*ref.* 41b) on page 24.

[176] a) Han, H.; Krische, M. J. *Org. Lett.* **2010**, *12*, 2844-2846. b) Feng, J.; Garza, V. J.; Krische, M. J. *J. Am. Chem. Soc.* **2014**, *136*, 8911-8914. c) Sam, B.; Luong, T.; Krische, M. J. *Angew. Chem. Int. Ed.* **2015**, *54*, 5465-5469. d) Nguyen, K. D.; Herkommer, D.; Krische, M. J. *J. Am. Chem. Soc.* **2016**, *138*, 14210-14213. e) Guo, Y.-A.; Lee, W.; Krische, M. J. *Chem. Eur. J.* **2017**, *23*, 2557-2559. f) Holmes, M.; Nguyen, K. D.; Schwartz, L. A.; Luong, T.; Krische, M. J. *J. Am. Chem. Soc.* **2017**, *139*, 8114-8117. g) Schwartz, L. A.; Holmes, M.; Brito, G. A.; Gonçalves, T. P.; Richardson, J.; Ruble, J. C.; Huang, K.-W.; Krische, M. J. *J. Am. Chem. Soc.* **2019**, *141*, 2087-2096.

[177] Note the amphiphilic character of these generated allyl-Ir^{III} species, which were also shown to react with nucleophiles, see: a) Meza, A. T.; Wurm, T.; Smith, L.; Kim, S. W.; Zbieg, J. R.; Stivala, C. E.; Krische, M. J. *J. Am. Chem. Soc.* **2018**, *140*, 1275-1279. b) Kim, S. W.; Schempp, T. T.; Zbieg, J. R.; Stivala, C. E.; Krische, M. J. *Angew. Chem. Int. Ed.* **2019**, *58*, 7762-7766. c) Kim, S. W.; Schwartz, L. A.; Zbieg, J. R.; Stivala, C. E.; Krische, M. J. *J. Am. Chem. Soc.* **2019**, *141*, 671-676.

[178] For selected examples, see: a) Gao, X.; Woo, S. K.; Krische, M. J. *J. Am. Chem. Soc.* **2013**, *135*, 4223-4226. b) Feng, J.; Noack, F.; Krische, M. J. *J. Am. Chem. Soc.* **2016**, *138*, 12364-12367. c) Shin, I.; Hong, S.; Krische, M. J. *J. Am.*

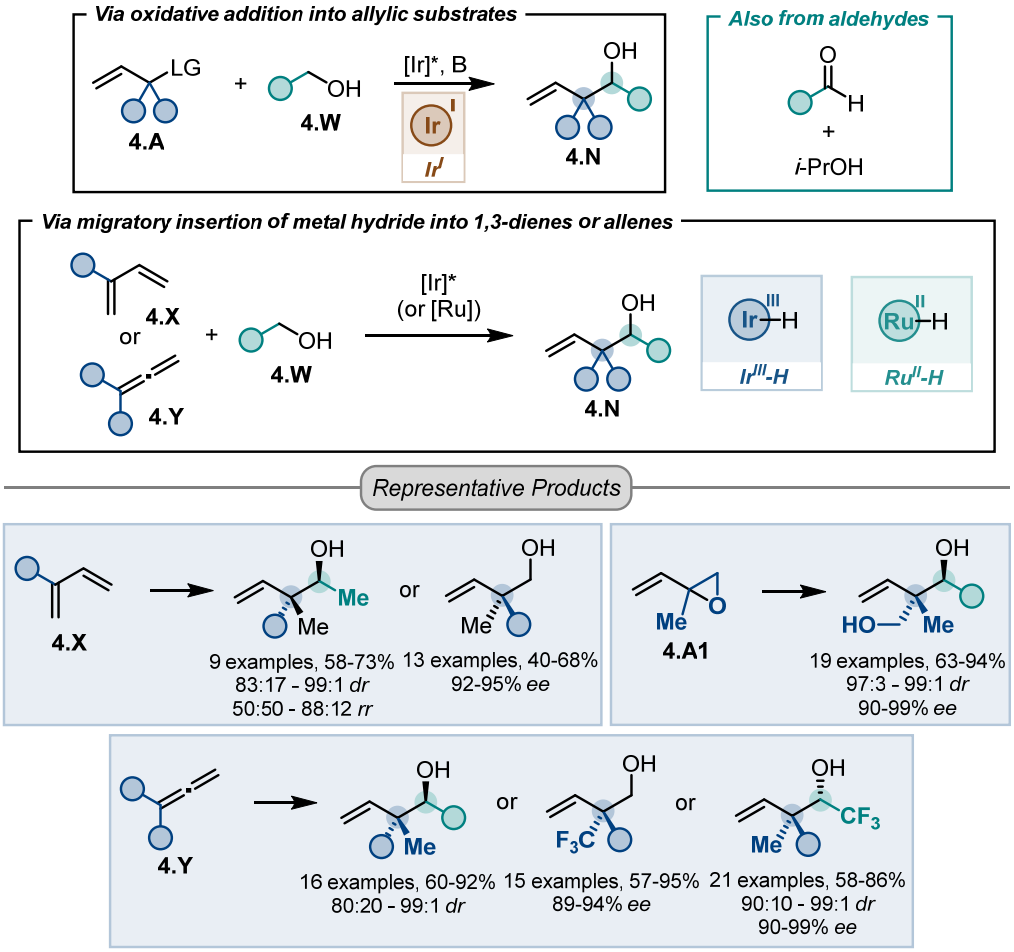

SCHEME 4.7. Redox-triggered carbonyl allylations via H_2 transfer for the formation of quaternary carbon stereocenters reported by Krische.

Among the various related allylation protocols, hydroxymethyl allylation[179] and *tert*-(hydroxyl)prenylation represent unique opportunities to increase the molecular functionality beyond a simple allyl group, giving rise to valuable and versatile 1,3-diols. Regarding *tert*-(hydroxyl)prenylation, which introduces a challenging quaternary carbon stereocenter, a catalytic approach towards these compounds was elegantly demonstrated by Krische, with the developed protocol featuring high yield and stereocontrol (**SCHEME 4.7**).[176b, 176e] While representing an important advancement, this transformation is limited to alkyl-vinyl-substituted epoxides, namely isoprene oxide (**4.A1**) and myrcene oxide, which are not easily diversified. Additionally, these reactions usually require a three-fold excess of the allylic precursor, prolonged reaction times under heating, and a significant loading (5 mol%) of an expensive iridium catalyst.

Chem. Soc. **2016**, *138*, 14246-14249. d) Zhou, J.; Gao, B.; Xu, Z.; Ye, T. *J. Am. Chem. Soc.* **2016**, *138*, 6948-6951. e) Manoni, F.; Rumo, C.; Li, L.; Harran, P. G. *J. Am. Chem. Soc.* **2018**, *140*, 1280-1284. f) Yang, L.; Wurm, T.; Sharma Poudel, B.; Krische, M. J. *Angew. Chem. Int. Ed.* **2020**, *59*, 23169-23173.

[179] See Krische, M. J. *et al. J. Am. Chem. Soc.* **2010** (*ref.* 56) on page 30.

4.1.4 Aims and Objectives

Given the lack of synthetic solutions for the stereoselective formation of quaternary carbon stereocenters using 3d transition metals and driven by our ongoing interest in the stereoselective synthesis of challenging tertiary and quaternary carbon centers, the main objective of the work presented in this chapter is to develop methods for the catalytic allylation of carbonyl compounds using highly modular and versatile VCCs as allylic surrogates (**SCHEME 4.8**). The merger of photoredox and cobalt catalysis would be a relevant starting point for several reasons:

- Cobalt is by far the most abundant element in group 9, compared to rhodium and iridium as its heavier congeners. (Relative concentration: Co / Rh / Ir = 10^4 / 5 / 1).[180]
- Cobalt-catalyzed carbonyl allylations are underdeveloped, compared to chromium, titanium, and nickel.[181]
- Cobalt/photoredox systems remain an unmatured area, compared to nickel/photoredox and copper/photoredox.[182]

However, several challenges will have to be addressed, such as the preference for 3,3-disubsituted allyl-Co species (leading to *branched* products) over 1,1-disubsituted allyl-Co species (leading to *linear* products). The control of the diastereoselectivity should be addressed from potential stabilizing and disruptive interactions in a Zimmermann-Traxler transition state, although a faster allyl isomerization rate compared to nucleophilic attack onto the aldehyde should be a prerequisite. In our case, we hoped to observe a faster rate for allyl isomerization due to the need for decarboxylation. Lastly, parasitic β-*H*-elimination, such as those observed for palladium in chapters 2 and 3, could also represent a potential issue and would generate undesired cobalt hydride species leading to other side-products.

[180] Hapke, M.; Hilt, G., *Cobalt Catalysis in Organic Synthesis: Methods and Reactions*. Wiley-VCH: 2020.
[181] Note that at the time we started the project, the only precedent of cobalt-catalyzed allylation was reported by Gosmini in 2003, see Gosmini, C. *et al. Synthesis* **2003** (*ref.* 167) on page 133.
[182] Kojima, M.; Matsunaga, S. *Trends Chem.* **2020**, *2*, 410-426.

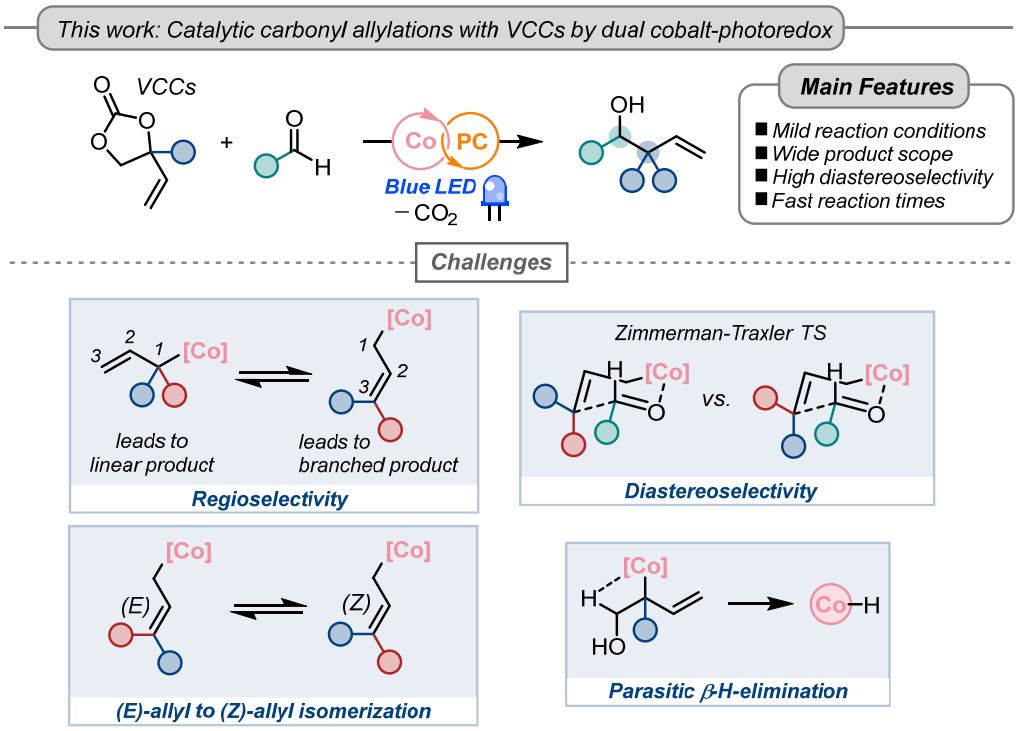

SCHEME 4.8. Schematic representation, challenges, and objectives of the work presented in this chapter.

4.2 Results and Discussion

4.2.1 Optimization Studies

The reaction between phenyl-substituted vinyl cyclic carbonate **4.1a** and benzaldehyde **4.2a** was selected as a model reaction to perform the screening and optimization studies (**SCHEME 4.9**). Initially, we chose to run the reaction under anaerobic conditions using $CoCl_2 \cdot 6H_2O$, DPEPhos as ligand, 4CzIPN as photocatalyst, DIPEA as sacrificial electron donor, and THF as solvent. To our delight, after irradiating the green mixture for 4 h at 20 ºC using a single high-power blue LED (λ_{em} = 445 nm, 700 mA, 1.2 μeinstein/s), we were pleased to identify and isolate the *syn*-1,3-diol **4.3a** in 56% yield and 91:9 *dr*.[183] In addition, hydrobenzoin **4.4** and homoallylic alcohol **4.5a** were noted as side-products in minor amounts (<10%). While the formation of hydrobenzoin **4.4** may be attributed to the dimerization of two ketyl radicals (pinacol coupling),[184] the formation of homoallylic alcohol **4.5a** should somehow arise from the coupling of one molecule of Ph-VCC **4.1a** and benzaldehyde **4.2a**, and thus constitutes a different type of allylated product.[185]

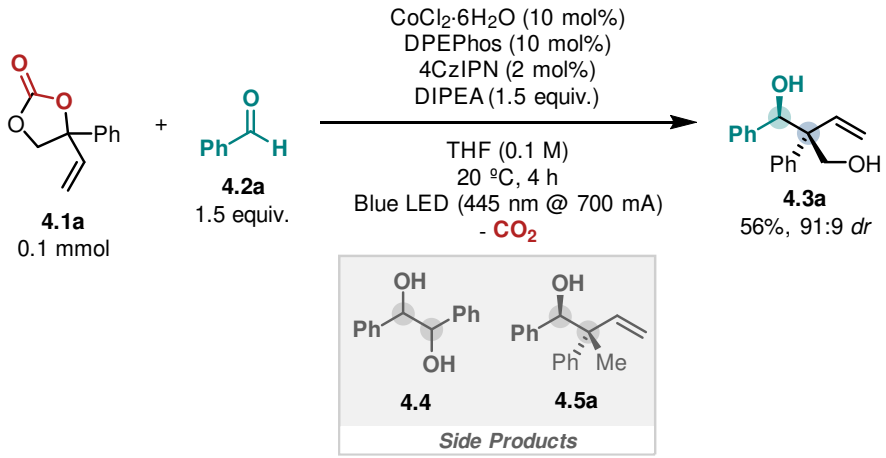

SCHEME 4.9. Initial results and product identification.

[183] It is worth noting that coupling on the less-hindered allylic carbon center to produce linear regioisomeric products was not observed, in contrast to earlier reports, see Cozzi, P. G. *et al. ACS Catal.* **2020** (*ref.* 173a) on page 137, and Cozzi, P. G. *et al. Adv. Synth. Catal.* **2021** (*ref.* 168) on page 133.

[184] Nakajima, M.; Fava, E.; Loescher, S.; Jiang, Z.; Rueping, M. *Angew. Chem. Int. Ed.* **2015**, *54*, 8828-8832.

[185] For the complete optimization of reaction conditions for homoallylic alcohol **4.5a**, and a preliminary scope of products, please refer to section 4.3.

After obtaining these initial results, we turned out attention to finding optimal reaction conditions for the synthesis of *syn*-1,3-diol **4.3a**. Surprisingly, replacing DIPEA for HE did not afford any desired *syn*-1,3-diol **4.3a** (**TABLE 4.1**, entry 1), but the combination of HE and DIPEA yielded 69% of 1,3-diol **4.3a** (**TABLE 4.1**, entry 2). Despite the apparent requirement of 2 protons for the formation of **4.3a**, we reasoned that DIPEA is, in fact, acting as a base, and HE is indeed the sacrificial electron donor, which in the absence of base would transiently lead to a highly acidic environment, thus potentially favoring the formation of undesired cobalt hydride species. Therefore, we decided to screen some bases while keeping HE as a sacrificial electron donor. To our delight, the use of other organic bases led to an increase in yield (**TABLE 4.1**, entries 3-5), especially when using 2,4,6-collidine (**TABLE 4.1**, entry 5). Switching to other inorganic bases was detrimental in terms of conversion and yield (**TABLE 4.1**, entries 6-8), probably due to the heterogeneous conditions. However, using more basic K_3PO_4 and LiOH gave quantitative yield of the desired product (**TABLE 4.1**, entries 9-10), while being able to obtain, in the case of the reaction with K_3PO_4, 93% of isolated *syn*-1,3-diol **4.3a** in 91:9 *dr*.[186] On the other hand, switching to KOH resulted in the hydrolysis of Ph-VCC **4.1a** (**TABLE 4.1**, entry 11). Lowering the amount of K_3PO_4 led to a decrease in conversion and yield (**TABLE 4.1**, entries 12-13). The reaction using LiOH was not highly reproducible due to the heterogeneous conditions and the very small amounts of LiOH required, so we decided to use K_3PO_4 to continue the optimization studies. The combination of K_3PO_4 and other electron donors had a negative influence on the conversion and yield (**TABLE 4.1**, entries 14-16).

[186] The chromatographic separation of HEPy (diethyl 2,6-dimethylpyridine-3,5-dicarboxylate) from 1,3-diol **4.3a** on a SiO_2 column was problematic, as they both exhibited similar R_f values in different eluents. Moreover, successive diluted HCl washes were not effective in removing HEPy from the organic phase. Gratifyingly, the separation was easily achieved through a small pad of basic Al_2O_3. This work-up method was effective for developing the entire product scope.

TABLE 4.1. Screening of bases for the allylation of benzaldehyde **4.2a** with VCC **4.1a**.

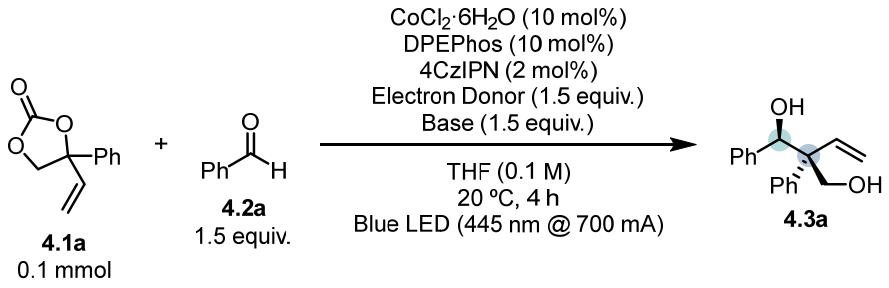

Entry	Base	Electron Donor	Conversion (%)[a]	Yield (%)[a]
1	-	HE	>99	-
2	DIPEA	HE	>99	69
3	Et_3N	HE	>99	74
4	2,6-lutidine	HE	>99	77
5	2,4,6-collidine	HE	>99	95
6	$KHCO_3$	HE	80	60
7	K_2CO_3	HE	75	35
8	$Na_2B_4O_7$	HE	84	17
9	K_3PO_4	HE	>99	>99(93)[b]
10	LiOH	HE	>99	>99
11	KOH	HE	>99	-[c]
12[d]	K_3PO_4	HE	78	66
13[e]	K_3PO_4	HE	50	22
14	K_3PO_4	BNAH	65	45
15	K_3PO_4	DIPEA	66	21
16	K_3PO_4	Et_3N	94	35

For the structures of 2,6-lutidine, 2,4,6-collidine and BNAH, please refer to Appendix A; [a] Reported conversions (%) and yields (%) of **4.3a** are based on ^{1}H NMR integration of the crude product using mesitylene as internal standard; [b] Yield (%) of isolated product, featuring 91:9 *dr*; [c] Hydrolysis of **4.1a** to 2-phenylbut-3-ene-1,2-diol was observed; [d] K_3PO_4 (1 equiv.) was used; [e] K_3PO_4 (0.5 equiv.) was used.

The screening of cobalt precursors and ligands was next examined. While $CoBr_2$ did not lower the yield substantially (**TABLE 4.2**, entry 1), switching to $Co(acac)_2$ and $Co(OAc)_2$ resulted in an important decrease of product yield (**TABLE 4.2**, entries 2-3). The choice of ligand was found to be a critical factor. Screening other commercially available phosphine ligands gave substantially lower yields (<30%) (**TABLE 4.2**, entries 4-7 and 9-13), except for XantPhos (**TABLE 4.2**, entry 8), which afforded 55% of **4.3a**, although with lower diastereoselectivity (80:20 *dr*). We, therefore, decided to keep DPEPhos to continue the optimization studies.

TABLE 4.2. Screening of cobalt precursors and ligands for the allylation of benzaldehyde **4.2a** with VCC **4.1a**.

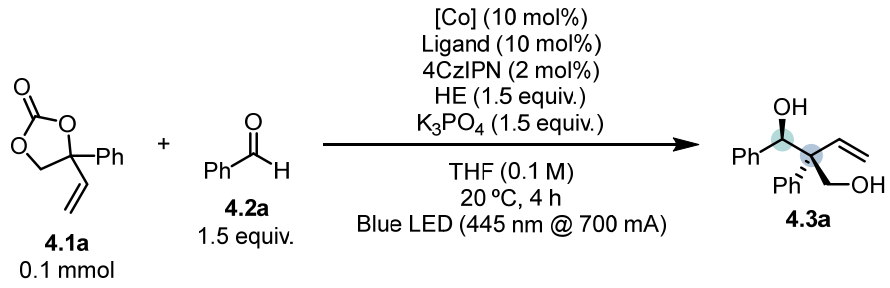

4.1a 0.1 mmol + **4.2a** 1.5 equiv. → **4.3a**

Entry	[Co]	Ligand	Conversion (%)[(a)]	Yield (%)[(a)]
1	$CoBr_2$	DPEPhos	>99	81
2	$Co(acac)_2$	DPEPhos	>99	50
3	$Co(OAc)_2$	DPEPhos	46	18
4	$CoCl_2{\cdot}6H_2O$	dppe	>99	24
5	$CoCl_2{\cdot}6H_2O$	dppp	>99	<5
6	$CoCl_2{\cdot}6H_2O$	dppb	84	8
7	$CoCl_2{\cdot}6H_2O$	dppf	>99	19
8	$CoCl_2{\cdot}6H_2O$	XantPhos	>99	55[(b)]
9	$CoCl_2{\cdot}6H_2O$	DBFPhos	>99	28
10	$CoCl_2{\cdot}6H_2O$	**L1**	86	30
11	$CoCl_2{\cdot}6H_2O$	**L3**	>99	8
12	$CoCl_2{\cdot}6H_2O$	**L4**	>99	15
13	$CoCl_2{\cdot}6H_2O$	PPh_3[(c)]	>99	23

For the structures of each ligand, please refer to Appendix A. [(a)] Reported conversions (%) and yields (%) of **4.3a** are based on ^{1}H NMR integration of the crude product using mesitylene as internal standard. [(b)] 80:20 *dr* was observed. [(c)] PPh_3 (20 mol%).

The screening of other photocatalysts (PCs) and solvents was next explored. The choice of Eosin B as an organic-based photosensitizer was not effective (**TABLE 4.3**, entry 1), while other iridium and ruthenium photocatalysts were not as effective as using 4CzIPN (**TABLE 4.3**, entries 2-5). The solvent was also found to be a critical factor. While 2-MeTHF gave a slightly lower yield (**TABLE 4.3**, entry 6), using other less polar solvents (**TABLE 4.3**, entries 7-9) or more polar aprotic solvents (**TABLE 4.3**, entries 10-11) gave very poor yields, so we decided to keep 4CzIPN as photocatalyst and THF as solvent.

TABLE 4.3. Screening of PCs and solvents for the allylation of benzaldehyde **4.2a** with VCC **4.1a**.

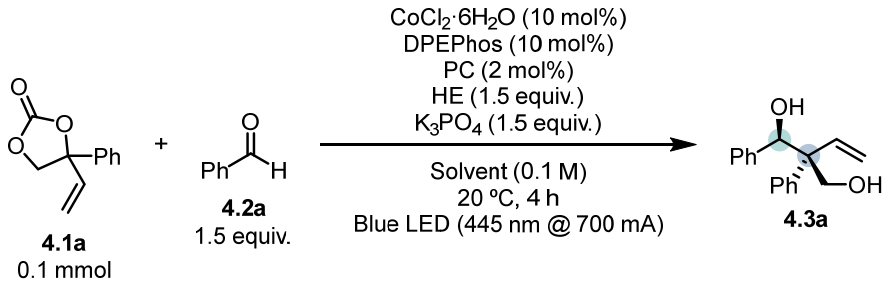

Entry	PC	Solvent	Conversion (%)[a]	Yield (%)[a]
1	Eosin B	THF	<5	-
2	$Ir(ppy)_3$	THF	69	39
3	$Ru(bpy)_3(PF_6)_2$	THF	36	16
4	$[Ir(dF,CF_3ppy)_2(dtbbpy)](PF_6)$	THF	96	77
5	$[Ir(dF,Meppy)_2(dtbbpy)](PF_6)$	THF	>99	82
6	4CzIPN	2-MeTHF	>99	86
7	4CzIPN	Et_2O	71	7
8	4CzIPN	PhMe	87	8
9	4CzIPN	CH_2Cl_2	<5	-
10	4CzIPN	MeCN	95	10[b]
11	4CzIPN	DMF	>99	21

For the structures of each photocatalyst, please refer to Appendix A; [a] Reported conversions (%) and yields (%) of **4.3a** are based on ^{1}H NMR integration of the crude product using mesitylene as internal standard; [b] 15% of homoallylic alcohol **4.5a** was observed.

Lastly, some control reactions were run to check the relevance of each factor. As expected, the reaction was unsuccessful when omitting either the $CoCl_2{\cdot}6H_2O$, HE, light, or DPEPhos (**TABLE 4.4**, entries 1-4). In the absence of 4CzIPN, the reaction showed a slight background reactivity (22% yield), which we ascribe to minimal light absorption and subsequent light-induced electron transfer by the HE (**TABLE 4.4**, entry 5). The reaction under anhydrous conditions afforded similar yields as the reaction under wet conditions (**TABLE 4.4**, entry 6). On the other hand, rigorous exclusion of dioxygen was required, not only to exclude quenching of the photoreactions or formation of reactive oxygen species, but also to avoid the reoxidation of air-sensitive Co(I) species (**TABLE 4.4**, entry 7).

TABLE 4.4. Control reactions for the allylation of benzaldehyde **4.2a** with VCC **4.1a**.

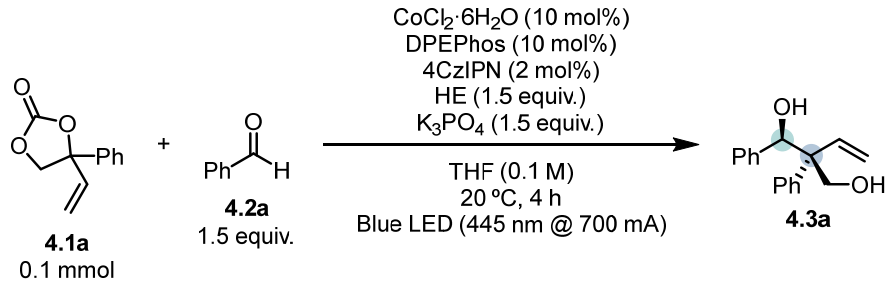

Entry	Change to Std. Cond.	Conversion (%)[(a)]	Yield (%)[(a)]
1	no $CoCl_2·6H_2O$	11	-
2	no HE	12	-
3	no light	7	-
4	no DPEPhos	>99	6
5	no 4CzIPN	22	22
6	anhydrous $CoCl_2$ and THF	>99	92
7	Air instead of N_2	<5	-

[(a)] Reported conversions (%) and yields (%) of **4.3a** are based on ^{1}H NMR integration of the crude product using mesitylene as internal standard.

4.2.2 Scope of 1,3-Diols

The optimized conditions were then applied to a larger set of structurally different vinyl cyclic carbonates **4.1a**-**4.1p** and aldehydes **4.2a**-**4.2x**. Generally, excellent yields and high diastereomeric ratios (*dr*) for most of the products were obtained, while noticing minor amounts of pinacol-type diol products (such as **4.4**). Aromatic aldehydes having electron-donating or electron-withdrawing groups (**SCHEME 4.10**, **4.3a**-**4.3j**) gave the desired products with minimal effect on the yield (except for **4.3i**), although showing a consistent reduction of diastereomeric ratio (*dr*) with substrates having more electron-withdrawing groups. Importantly, the photocatalytic reductive conditions allow for the presence of benzylic primary alcohols (**SCHEME 4.10**, **4.3g**) that were previously unattainable in the Krische allylation. *Meta* and *ortho* substituents in the aromatic ring of the aldehyde are well tolerated (**SCHEME 4.10**, **4.3k**-**4.3o**), as are disubstituted aldehydes (**SCHEME 4.10**, **4.3p**-**4.3r**). The absence of the initial green color was noted when using vanillin (**4.2s**) as aldehyde, indicating that deprotonation of the aromatic OH group was likely occurring, with the phenolate binding deactivating the cobalt catalyst. The latter was decisive to shut down the reaction, but fortunately, the desired product (**SCHEME 4.10**, **4.3s**) could be formed when switching to the less basic 2,4,6-collidine. The assigned *syn*-configuration was unambiguously confirmed by X-ray diffraction of a single crystal of **4.3s** (see **TABLE 4.12** in subsection 4.5.10). Other (hetero)aromatic aldehydes gave excellent results (**SCHEME 4.10**, **4.3t**-**4.3v**), while aliphatic aldehydes were less productive in terms of yield (likely due to steric crowding in the C–C bond formation step), but nonetheless, these reactions exhibited good diastereoselectivities (**SCHEME 4.10**, **4.3w**-**4.3x**).[187]

[187] Note that slightly modified reaction conditions were employed to produce **4.3y** in 45% yield (see caption in scheme 4.10), instead of an initial 24% yield. The modified reaction conditions had no beneficial effect when applied to the synthesis of **4.3w**.

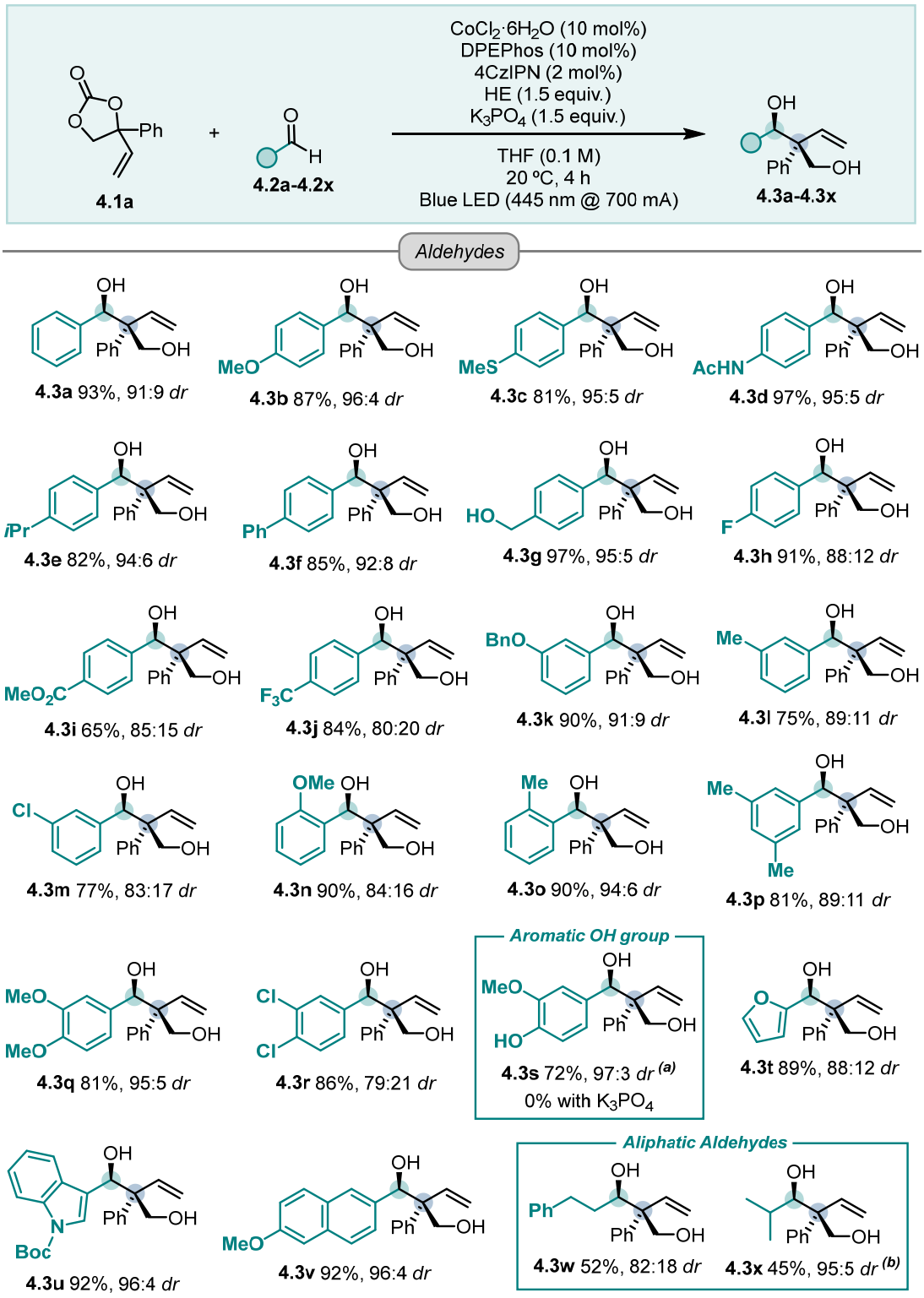

SCHEME 4.10. Variation of aldehyde reagent to afford *syn*-1,3-diols **4.3a-4.3x**. Reaction conditions: **4.1a** (0.1 mmol), aldehyde **4.2a-4.2x** (1.5 equiv.), $CoCl_2{\cdot}6H_2O$ (10 mol%), DPEPhos (10 mol%), 4CzIPN (2 mol%), HE (1.5 equiv.), K_3PO_4 (1.5 equiv.), THF (0.1 M), Blue LED (445 nm @ 700 mA, corresponding to 1.2 μeinstein/s), 20 °C, 4 h, under N_2; [a] 2,4,6-collidine (1.5 equiv.) was used instead of K_3PO_4; [b] 2,4,6-collidine (1.5 equiv.) instead of K_3PO_4, isobutyraldehyde **4.2x** (5 equiv.), 0 °C, 20 h, blue LED irradiation (λ_{em} = 445 nm @100 mA, corresponding to 0.2 μeinstein/s).

The scope of VCCs (**4.1b**-**4.1p**) was next examined. A usual limitation of catalytic allylation methods is the narrow scope for the allylic precursor. As VCCs can be easily prepared with a variety of substituents, we were able to synthesize 15 more product variations featuring aryl and heteroaryl groups in high yields and stereocontrol (**SCHEME 4.11**). VCCs having electron-donating groups and electron-withdrawing groups on the *para*- and *meta*-positions of the aryl-groups (**SCHEME 4.11**, **4.3x**-**4.3ah**) were tolerated and showed minimal impact on the yield and diastereoselectivity (except for a slight decrease in *dr* for **4.3ad**). As in the case of vanillin (**4.2s**), the presence of an aromatic OH group can be tolerated when using less basic 2,4,6-collidine as a base (**SCHEME 4.11**, **4.3ah**). More sterically crowded VCCs being substituted on the *ortho* position of the aryl group were more demanding substrates, requiring the presence of 2,4,6-collidine, as well as lower temperature and reduced light intensity (**SCHEME 4.11**, **4.3ai**). Nonetheless, the diastereoselectivity was positively influenced and product **4.3ai** was achieved with 98:2 *dr*. Disubstitution or the presence of other (hetero)aryl groups did not affect the catalytic protocol and produced the desired *syn*-1,3-diols in appreciable yield and stereocontrol (**SCHEME 4.11**, **4.3aj**-**4.3am**).

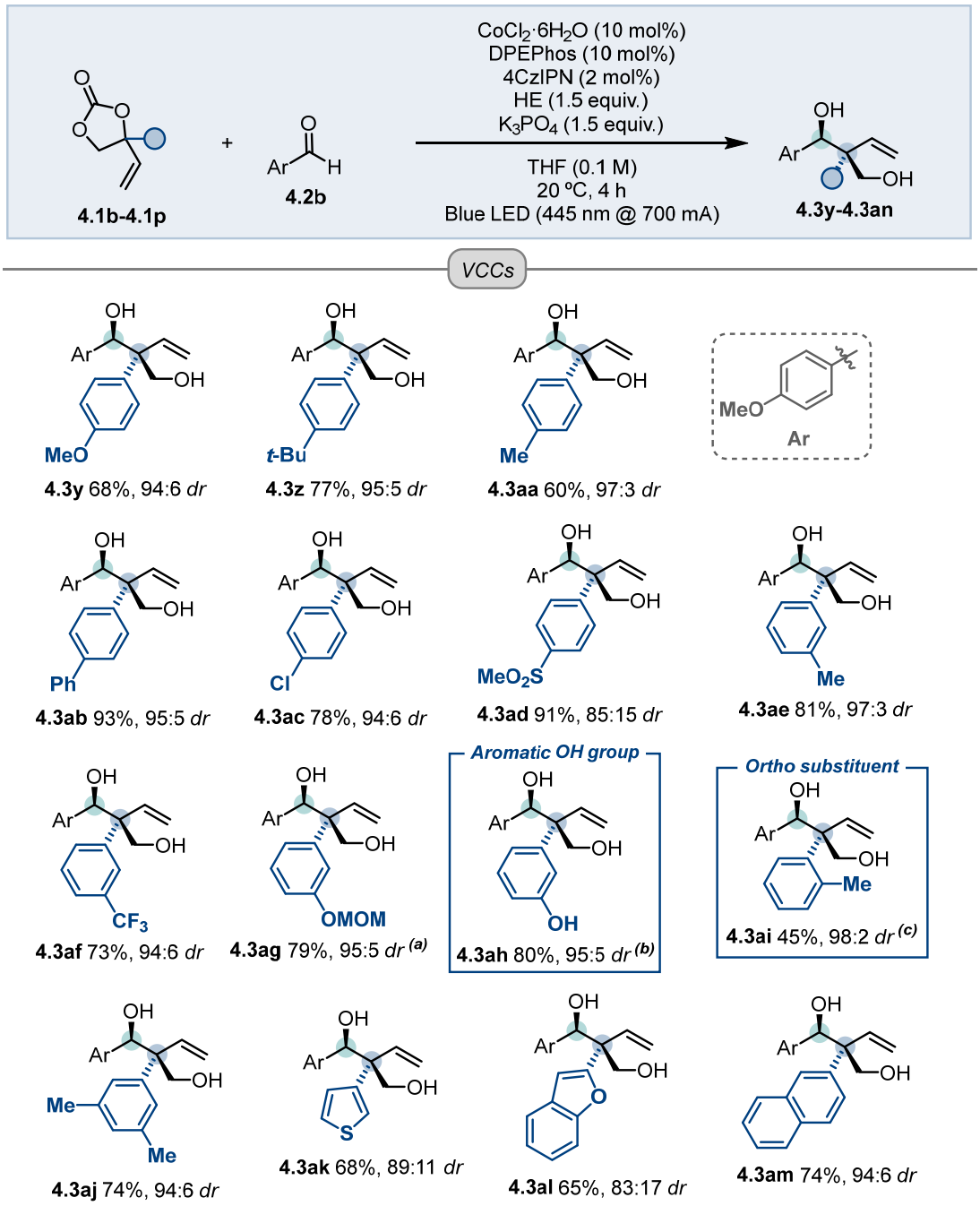

SCHEME 4.11. Variation of the VCC reagent to afford *syn*-1,3-diols **4.3y-4.3am**. Reaction conditions: **4.1b-4.1p** (0.1 mmol), *p*-anisaldehyde **4.2b** (1.5 equiv.), $CoCl_2·6H_2O$ (10 mol%), DPEPhos (10 mol%), 4CzIPN (2 mol%), HE (1.5 equiv.), K_3PO_4 (1.5 equiv.), THF (0.1 M), Blue LED (445 nm @ 700 mA, corresponding to 1.2 μeinstein/s), 20 °C, 4 h, under N_2; [a] Reaction time was 17 h; [b] 2,4,6-collidine (1.5 equiv.) was used instead of K_3PO_4; [c] 2,4,6-collidine (1.5 equiv.) instead of K_3PO_4, *p*-anisaldehyde **4.2b** (5 equiv.), 0 °C, 20 h, blue LED irradiation (λ_{em} = 445 nm @100 mA, corresponding to 0.2 μeinstein/s).

A few limitations of the current catalytic protocol were noted. Aromatic aldehydes having a *p*-NO_2, *p*-CN or *o*-F groups did not afford the desired 1,3-diol products (**SCHEME 4.12**, **4.3an-4.3an**). Instead, these aldehydes exhibited rapid reductive dimerization and produced pinacol diols **4.4**, as explained by facile ketyl radical formation. Competitive reductive dimerization was also observed for methylallylated 1,3-diol **4.3av**, which might be explained by the slower oxidative addition of the VCC substrate. The presence of a *p*-Br substituent was detrimental and probably interfered in the oxidative addition step (**SCHEME 4.12**, **4.3aq**). Moreover, the catalytic protocol was not tolerant towards the presence of unprotected indoles (**SCHEME 4.12**, **4.3ar**). On the other hand, sterically hindered tertiary aldehydes, such as pivalaldehyde, displayed poor reactivity, as in the case of an aromatic imine (**SCHEME 4.12**, **4.3as-4.3au**). Finally, alkyl-substituted VCCs showed poor selectivity towards the formation of the desired *syn*-1,3-diols (**SCHEME 4.12**, **4.3aw-4.3ax**), although the product having a -CH_2CH_2Ph substituent could be obtained in 28% and 83:17 *dr*, thus showing some potential to be further optimized.

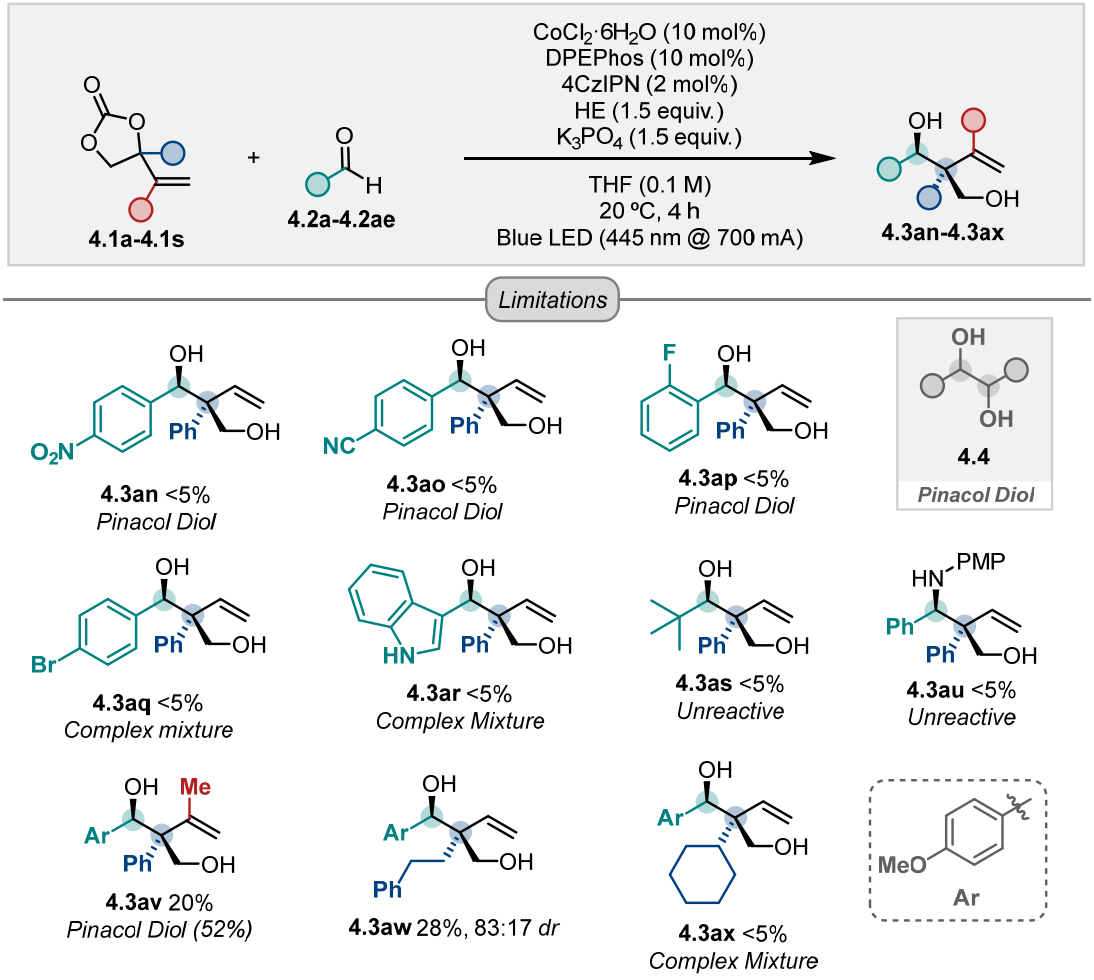

SCHEME 4.12. Limitations of the current catalytic protocol.

4.2.3 Scale-up Experiments

After having prepared a wide scope of products, we became interested in scaling up our benchmark reaction. A first attempt was conducted at 1 mmol scale of Ph-VCC **4.1a**, while keeping the same relative quantities of other reagents. However, for practical reasons, we reduced the relative amount of THF and decided to extend the reaction time to 17 h. Unfortunately, we noted no change of the initial green color and confirmed that no conversion of Ph-VCC **4.1a** had occurred (**TABLE 4.5**, entry 1). We thought that the high amount of deposited K_3PO_4 at the bottom of the flask was blocking the light, so we decided to make a second attempt using 2,4,6-collidine, which is a soluble base. We were pleased to observe full conversion of Ph-VCC **4.1a** and 99% yield of 1,3-diol **4.3a** (**TABLE 4.5**, entry 2). Moreover, we were able to obtain 91% of 1,3-diol **4.3a** (89:11 *dr*) using a catalytic amount (15 mol%) of K_3PO_4 and significantly reducing catalyst loadings (**TABLE 4.5**, entry 3). Lastly, another reaction was conducted at 5 mmol scale (≈1 g Ph-VCC **4.1a**) using 15 mol% of 2,4,6-collidine and reduced catalyst loadings, and we were pleased to obtain 93% yield of 1,3-diol **4.3a** (95:5 *dr*) while also keeping the amount of THF comparably low (**TABLE 4.5**, entry 4). In addition, the work-up procedure developed for obtaining pure 1,3-diols was also applicable for the reaction conducted at a larger scale.

TABLE 4.5. Scale-up studies of the benchmark reaction.

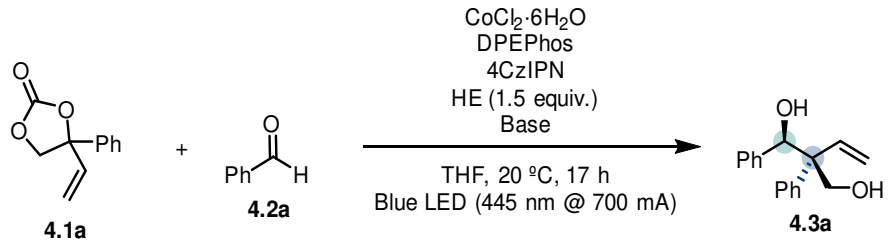

4.1a + **4.2a** → **4.3a**

Entry	Scale (mmol)	Base (mol%)	[Co] (mol%)	4CzIPN (mol%)	THF (M)	Yield (%)	*dr*
1	1	K_3PO_4 (150)	10	2	0.17	<5	-
2	1	2,4,6-collidine (150)	10	2	0.17	99	91:9
3	1	K_3PO_4 (15)	2	0.5	0.33	91	89:11
4[(a)]	5	2,4,6-collidine (15)	2	0.5	0.50	93	95:5

Full conversion of Ph-VCC **4.1a** was observed in all cases, except for entry 1 (<5% conversion). Reaction conditions: Ph-VCC **4.1a** (1 equiv.), benzaldehyde **4.2a** (1.5 equiv.), $CoCl_2·6H_2O$, DPEPhos, 4CzIPN, HE (1.5 equiv.), K_3PO_4 or 2,4,6-collidine, THF, Blue LED (445 nm @ 700 mA, corresponding to 1.2 μeinstein/s), 20 ºC, 17 h, under N_2. [Co] stands for $CoCl_2$-DPEPhos; [(a)] Reaction time was 20 h.

4.2.4 Mechanistic Details

Despite scarce mechanistic studies on cobalt-catalyzed allylations of carbonyl compounds, the catalytic cycle is believed to start with a single-electron transfer (SET) to the Co(II) precursor, that then provides a Co(III)-allyl species after an oxidative addition of the allylic surrogate to the *in situ* prepared Co(I) complex. A second SET gives rise to a nucleophilic Co(II)-allyl intermediate that reacts with the aldehyde reagent via a Zimmerman-Traxler TS. Finally, protodemetalation will release the product and regenerate the initial Co(II) complex.

Taking everything into account, we decided to conduct additional control experiments to give support to these findings. First, adding a radical scavenger (TEMPO or BHT) to the reaction mixture did not affect the reaction yield significantly (**SCHEME 4.13A**), thus corroborating that the formation of 1,3-diol **4.3a** does not involve a radical pathway (*e.g.*, via a free ketyl radical). Apart from that, the privileged nature of the vinyl cyclic carbonate in the protocol was demonstrated by using vinyl epoxide **4.6** as the allylic precursor, which only provided a low amount of **4.3a** (<10%, **SCHEME 4.13B**, part B) in the standard reaction.

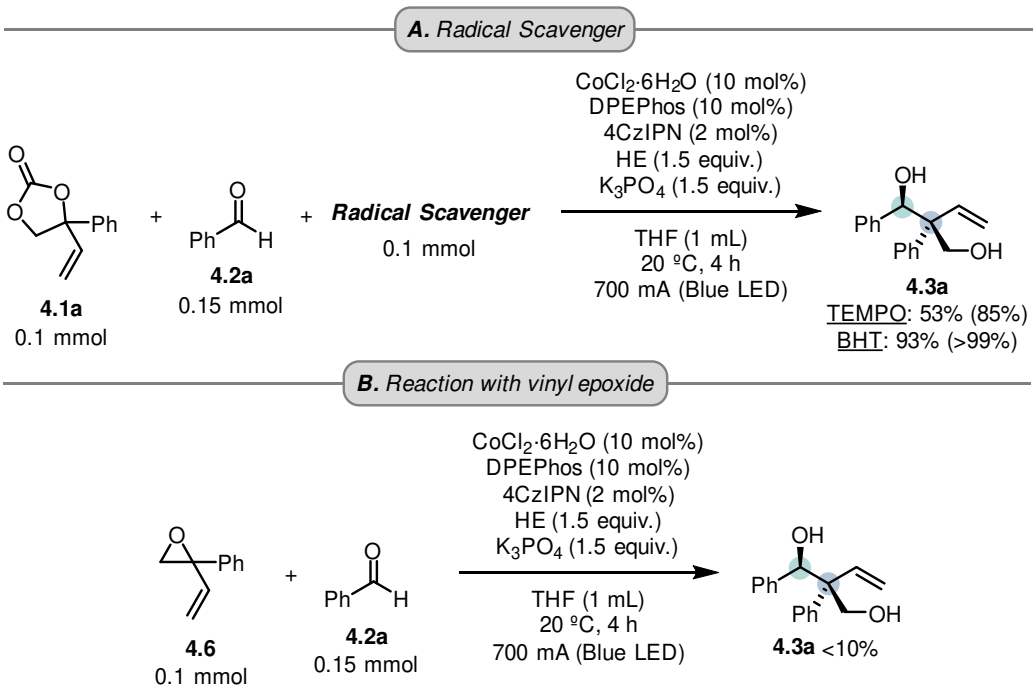

SCHEME 4.13. Reported conversions (%) in parenthesis and yields (%) of **4.3a** are based on ^{1}H NMR integration of the crude product using mesitylene as internal standard; **(A)** Radical scavenger experiments (yields are of the isolated product); **(B)** Reaction using vinyl epoxide **4.6** under standard conditions.

At this point, we wanted to get some insight into the observed high levels of diastereocontrol. The dependence upon the electronics of the aldehyde reagent was clearly seen as a critical factor, and therefore we decided to construct a Hammett plot of its *para*-substituent by plotting the logarithm of the *dr* as a function of the Hammett σ_{para} parameter (**SCHEME 4.14A**). A clear negative trend was observed (ρ = -1.8, R^2 = 0.94), indicating that electron-donating groups strongly favor the production of the *syn* isomer, whereas this effect is clearly diminished with electron-withdrawing groups. Interestingly, this trend is opposite to what was previously seen in a similar allylation reaction catalyzed by Cu.[188] Moreover, we did not observe a change in slope, suggesting that the diastereo-determining step is likely the same across the entire scope of aldehyde reagents that were used. On the basis of the Zimmerman-Traxler model (**SCHEME 4.14B**), we envisaged that the higher diastereocontrol in the presence of more electron-rich aldehyde substrates may be controlled by stronger intramolecular hydrogen-bonding between the pendent OH-group and the aldehyde thereby stabilizing the (*Z*)-allylic transition state. However, a control reaction using linear carbonate **4.7** (**SCHEME 4.14C**) leading to an intermediate devoid of such a potentially hydrogen-bonding motif even provided slightly increased diastereocontrol (*dr* = 96:4). To examine the rate of allyl isomerization, the use of (*E*) and (*Z*) *tert*-butyl 3-phenylbut-2-enyl carbonate was examined (**SCHEME 4.14D**). Despite the much slower nature of these conversions, both precursors convert preferentially to the same diastereomeric product, indicating a comparably fast allyl isomerization. When employing the methyl-substituted vinyl cyclic carbonate **4.1t** (**SCHEME 4.14E**), the corresponding *anti*-1,3-diol **3qb** was isolated in 76% yield and with a *dr* of 83:17 having opposite stereochemistry.[189] This result suggests a dominating steric effect in the Zimmermann-Traxler TS, as the methyl group is less sterically demanding than the hydroxymethyl group, therefore the latter is here preferentially placed *pseudo*-equatorial, thus reversing the diastereoselectivity.

[188] Wheatley, E.; Zanghi, J. M.; Meek, S. J. *Org. Lett.* **2020**, *22*, 9269-9275.
[189] For the determination of the relative configuration, please see subsection 4.5.8.

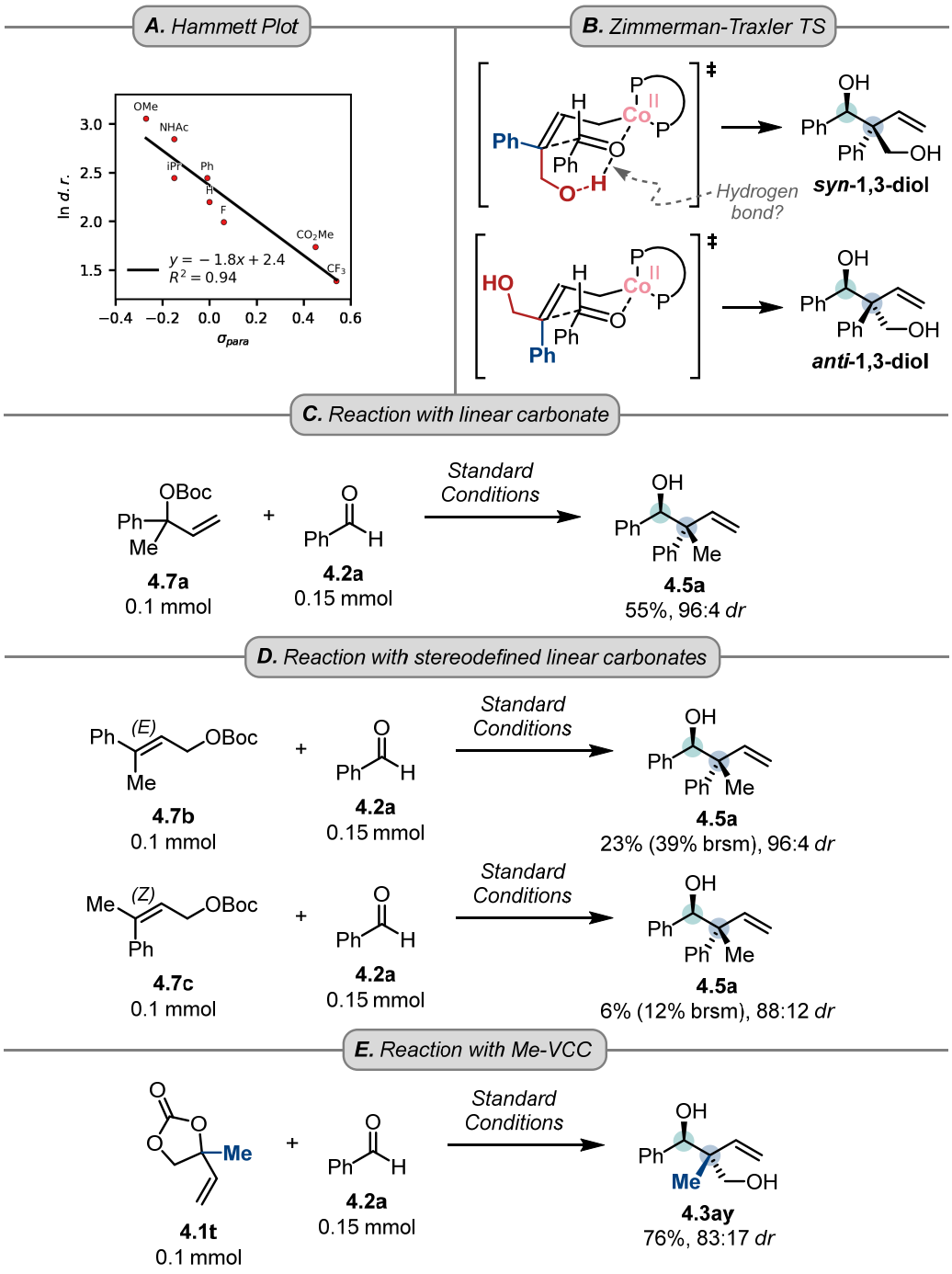

SCHEME 4.14. Reported yields (%) of **4.3a** are based on isolated material; **(A)** Hammett plot of the logarithm of the diastereomeric ratio as a function of σ_{para}; **(B)** Proposed Zimmerman-Traxler models; **(C)** Control reaction with linear carbonate **4.7a**; **(D)** Control reactions with perfectly defined linear carbonates **4.7b**-**4.7c**; **(E)** Control reaction with Me-VCC **4.1t**.

With this information in hand, we speculate that aldehyde coordination might influence the diastereo-determining step in the following way. Considering the Zimmerman-Traxler model, aldehyde pre-coordination is a prerequisite prior to the key C–C bond formation step. We presume that aldehyde coordination at the (*Z*)-allyl-Co^{II} intermediate **4.Z** might be higher in energy than for the (*E*)-allyl-Co^{II} intermediate **4.AA** because of a chelation effect (**SCHEME 4.15**). Considering that these two species are in equilibrium, the relative concentrations of these two species will be affected by the aldehyde C=O Lewis basicity, therefore a slightly higher concentration of species **4.AC** over **4.AB** will occur for electron-poor aldehydes.[190] Apart from that, the kinetic difference between k_{syn} and k_{anti} will primarily dictate the observed diastereoselectivity, with a major preference for the *syn*-1,3-diol.[191] This kinetic difference might arise, among other factors, from repulsive 1,2-gauche interactions between the substituents on the VCC and aldehyde reagents.

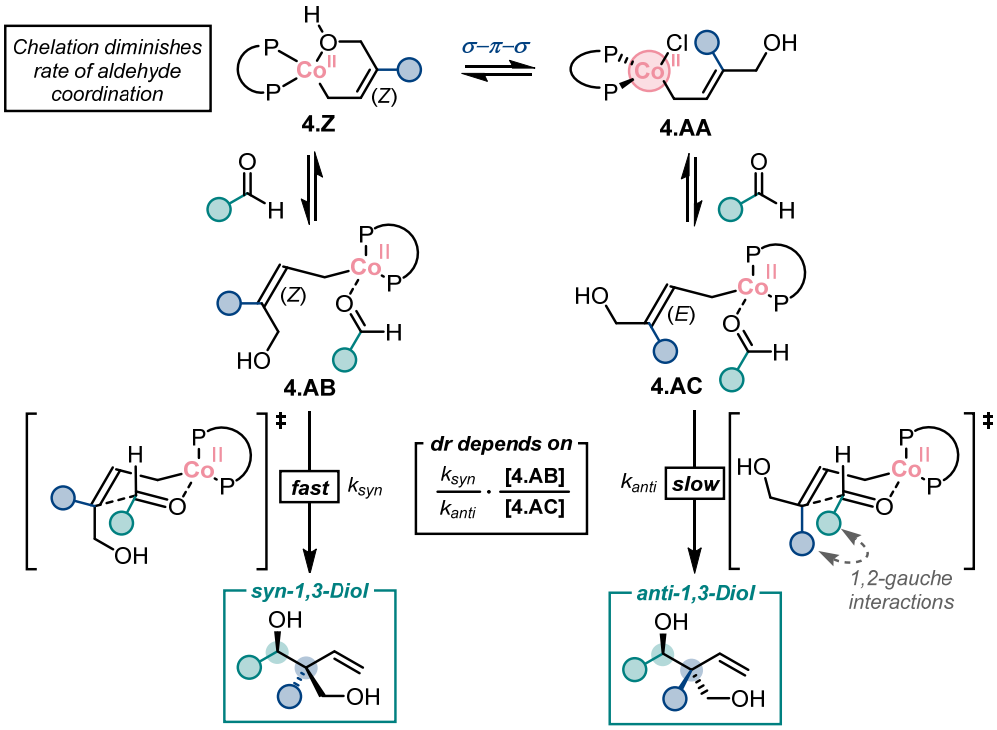

SCHEME 4.15. Possible explanation for the observed diastereoselectivity.

[190] Another mechanistic possibility is that allyl isomerization is slower than subsequent C–C bond formation, thereby affecting the relative concentrations of allyl-Co^{II} species over time, with this effect being more pronounced for more electrophilic aldehydes. Although this cannot be fully ruled out, control reactions with stereodefined linear carbonates **4.7b**-**4.7c** suggest otherwise.

[191] At this stage, we cannot fully rule out the possibility of the C–C bond formation step being reversible. Therefore, the diastereoselectivity difference could potentially arise from a kinetic difference in the irreversible protodemetalation step.

To gain insight into the photocatalytic cycle, we performed a Stern-Volmer analysis using both fluorimetry and time-correlated single-photon counting (TCSPC). We found efficient quenching with HE and [Co(DPEPhos)Cl$_2$], whereas no other components of the reaction quenched the fluorescence (**FIGURE 4.2A**). The deviation from linearity observed in the Stern-Volmer may be caused by complicated thermally activated delayed fluorescence (TADF) of 4CzIPN.[192] Since the dye fluoresces from both the initial singlet excited state (prompt fluorescence, PF), and through TADF, time-correlated single-photon counting was used to separate the two decay pathways in their individual rate constants (see subsection 4.5.6). By doing so, we identified efficient dynamic quenching of both PF and TADF by both HE and [Co(DPEPhos)Cl$_2$]. Under catalytic conditions, however, the concentration of HE is 15 times that of [Co(DPEPhos)Cl$_2$], so that it quenches 90% of the initial singlet excited state. We, therefore, propose that the reaction commences with a reductive quenching pathway from the initial singlet excited state. Although the quenching is efficient, the quantum yield of the reaction was measured to be 1.82%, indicating that much of the excitations are lost due to recombination processes (**FIGURE 4.2B**).

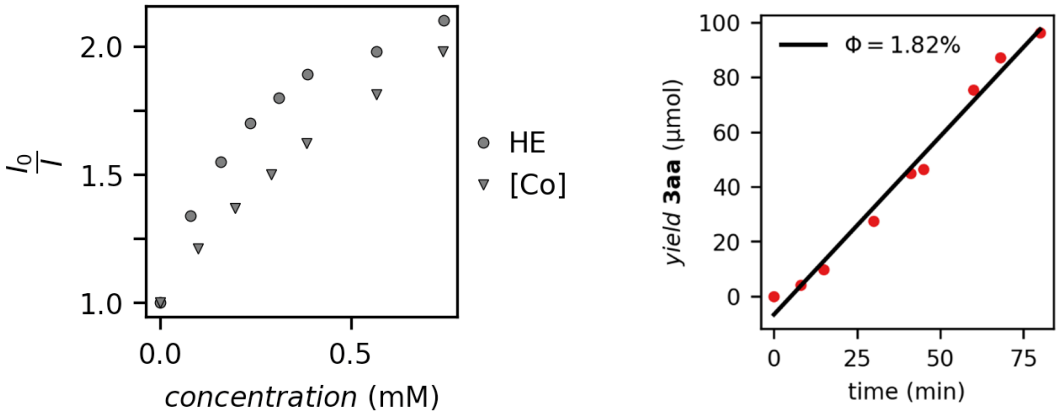

FIGURE 4.2. **(A)** Stern-Volmer plot of the TADF state using quenchers HE or [Co(DPEPhos)Cl$_2$]; **(B)** Overall quantum yield determination. Red dots indicate yield of **4.3a** from different reactions quenched at different times.

[192] a) Noda, H.; Chen, X.-K.; Nakanotani, H.; Hosokai, T.; Miyajima, M.; Notsuka, N.; Kashima, Y.; Brédas, J.-L.; Adachi, C. *Nat. Mater.* **2019**, *18*, 1084-1090. b) Kobayashi, T.; Kawate, D.; Niwa, A.; Nagase, T.; Goushi, K.; Adachi, C.; Naito, H. *Phys. Status Solidi A* **2020**, *217*, 1900616-1900621.

With all the information in hand, we propose the following catalytic cycle (**SCHEME 4.16**). The catalytic cycle starts from [Co^{II}(DPEPhos)Cl_2] complex **4.AD**, which is easily formed from $CoCl_2 \cdot 6H_2O$. Under light irradiation, [Co^{II}(DPEPhos)Cl_2] is reduced photocatalytically to [Co^{I}(DPEPhos)Cl] complex **4.AE**. Oxidative addition of the VCC substrate, followed by decarboxylation and protonation of the pendent alkoxide group will lead to allyl-Co^{III} **4.AF**, which undergoes a rapid reduction to allyl-Co^{II} intermediates **4.Z**-**4.AA**. It is worth mentioning that oxidative addition will likely require pre-coordination of the VCC substrate to the [Co^{I}(DPEPhos)Cl] **4.AE**, as hinted by the lower conversions observed for more sterically demanding substrates (as in **4.3av** and **4.7b**-**4.7c**).[193] In addition, allyl isomerization via σ-π-σ interconversion may well occur prior to decarboxylation and in the Co^{III} oxidation state. With the formation of key allyl-Co^{II} intermediates **4.AC**-**4.AD**, nucleophilic attack via a Zimmerman-Traxler TS must occur from these equilibrating allyl-Co^{II} intermediates independently, leading to a diastereomeric mixture of 1,3-diols after protodemetalation. As explained in **SCHEME 4.15**, the observed *dr* ratios will probably be a function of the relative concentrations of allyl-Co^{II} species, aldehyde C=O Lewis basicity, and steric effects between substituents in the VCC and aldehyde reagents in the Zimmerman-Traxler transition states. Apart from that, pinacol diol byproducts can be competitively formed via reductive dimerization of the aldehyde under photocatalytic conditions. Overall, the reaction requires two electrons and two protons, which will be produced in the photocatalytic cycle in the following manner. Blue light absorption by 4CzIPN leads to the excited PC*, which will be quenched by HE, thereby producing a PC radical anion and a HE radical cation **4.AH**. Despite charge recombination, accounting for the loss of quantum yield, productive single electron transfer (SET) from the PC radical anion will effectively reduce [Co^{II}(DPEPhos)Cl_2] **4.AD** (and possibly allyl-Co^{III} **4.AF**). Deprotonation of the HE radical cation **4.AH** will release one proton and produce a HE radical **4.AI**, which will also release one electron by SET to produce $HEPyH^+$ **4.AJ**. Subsequent deprotonation will release the second proton and produce the observed byproduct HEPy **4.AK**.

[193] Oxidative addition is likely the rate-determining step when using more substituted substrates, but this assumption cannot be extrapolated to the rest of the substrates.

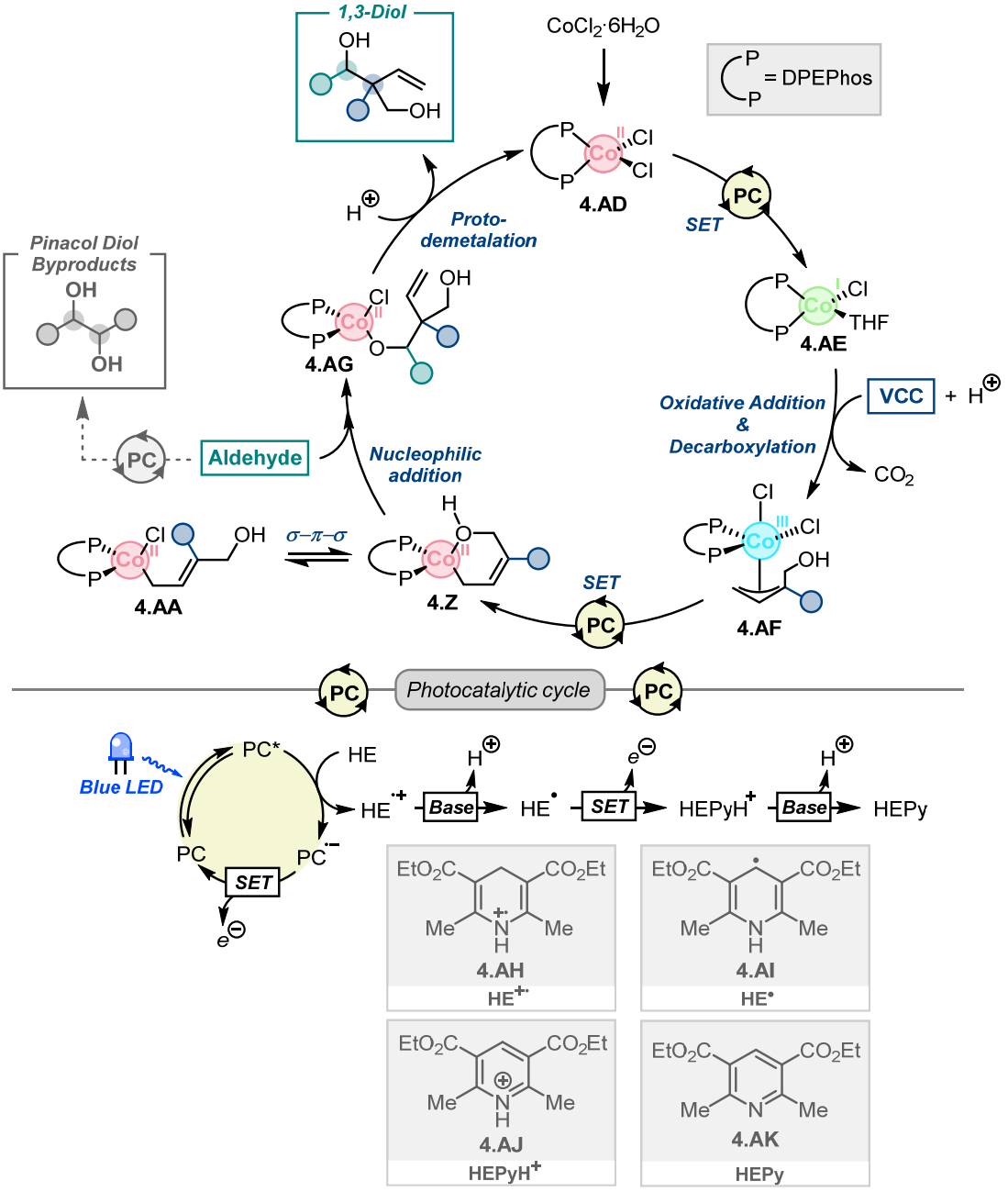

SCHEME 4.16. Proposed catalytic cycle for the generation of 1,3-diols by dual cobalt-photoredox catalysis.

4.3 Addendum: Synthesis of Homoallylic Alcohols

4.3.1 Optimization Studies

During the optimization of the synthesis of 1,3-diol **4.3a**, we noticed the unusual formation of homoallylic alcohol (**4.5a**) (**SCHEME 4.17**). Moreover, we noted that the formation of homoallylic alcohol **4.5a** was slightly favored in MeCN, with a 15% yield vs 10% yield of 1,3-diol **4.3a** (**TABLE 4.3**, entry 10). Furthermore, replacing HE for DIPEA resulted in 22% yield of **4.5a** (and 26% yield of **4.3a**), while the use of 10 mol% 2,2'-bipyridine as ligand, instead of DPEPhos, afforded 36% yield of **4.5a** with increased selectivity (17% yield of **4.3a**).

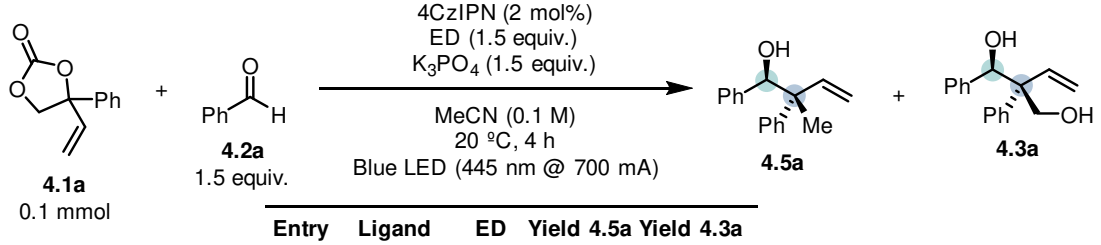

Entry	Ligand	ED	Yield 4.5a	Yield 4.3a
1	DPEPhos	HE	15%	10%
2	DPEPhos	DIPEA	22%	26%
3	bpy	DIPEA	36%	17%

SCHEME 4.17. Initial screening results for the synthesis of homoallylic alcohol **4.5a**.

With these results in hand, we decided to screen other reaction variables to optimize the yield of homoallylic alcohol **4.5a**. First, we evaluated the addition of different additives. Replacing K_3PO_4 for other less basic additives generally had a positive effect on the yield (**TABLE 4.6**, entries 1-4). To our surprise, acidic $B(OH)_3$ was tolerated, although it afforded a slightly lower yield of **4.5a** with respect to the utilization of other basic additives (**TABLE 4.6**, entry 5). The combination of HE and DIPEA gave slightly better results (52%, **TABLE 4.6**, entry 6), while the use of other tertiary amines as sacrificial electron donors produced inferior results (**TABLE 4.6**, entries 7-11). We decided to keep $NaHCO_3$ for further optimization, as the formation of the oxidized HE byproduct (HEPy) would cause separation problems during the chromatographic purification, while $NaHCO_3$ can be easily separated by filtration.

TABLE 4.6. Screening of various additives for the synthesis of homoallylic alcohol **4.5a**.

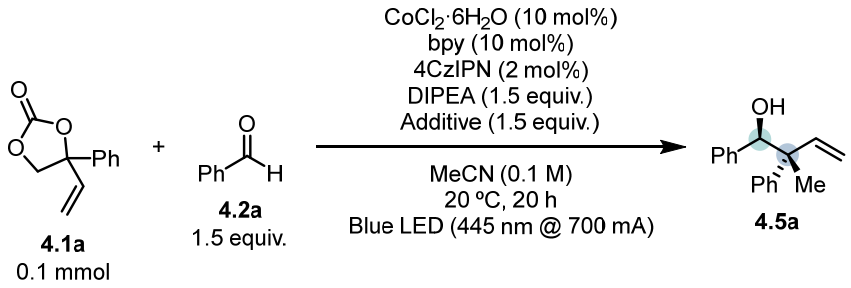

4.1a 0.1 mmol + **4.2a** 1.5 equiv. → **4.5a**

Entry	Additive	Electron Donor	Yield (%)[a]
1	2,4,6-collidine	DIPEA	42
2	Cs_2CO_3	DIPEA	20
3	$NaHCO_3$	DIPEA	50
4	Na_2HPO_4	DIPEA	50
5	$B(OH)_3$	DIPEA	42
6	HE	DIPEA	52
7	K_3PO_4	Et_3N	31
8	K_3PO_4	$(HOCH_2CH_2)_3N$	10
9	$NaHCO_3$	*i*-$PrMe_2N$	18
10	$NaHCO_3$	*n*-Bu_3N	42
11[b]	$NaHCO_3$	*N*-Me-TMP	11

Full conversion of **4.1a** was noted in all instances; [a] Reported yields (%) of **4.5a** are based on ^{1}H NMR integration of the crude product using mesitylene as internal standard; [b] bpy (20 mol %) was used.

We continued with the screening of different cobalt precursors. Using pre-synthesized cobalt-bipyridine complexes revealed that a ratio of 1:2 [Co]/bpy afforded better results (**TABLE 4.7**, entries 1-2), so we decided to increase the amount of 2,2'-bipyridine to 20 mol% for the rest of the optimization. The use of other cobalt halides displayed poor results (**TABLE 4.7**, entries 3-5), and switching to other inorganic cobalt salts did not improve the yield (**TABLE 4.7**, entries 6-7). To our delight, the presence of $Co(OAc)_2$ increased the yield of **4.5a** to 80%, showing a beneficial effect of having OAc in the reaction medium (**TABLE 4.7**, entry 9). Finally, cobalt precursors with relatively non-coordinating anions gave the best results obtained (**TABLE 4.7**, entries 10-11), providing 82% yield of **4.3a** in the case of $Co(ClO_4)_2{\cdot}6H_2O$.

TABLE 4.7. Screening of cobalt precursors for the synthesis of homoallylic alcohol **4.5a**.

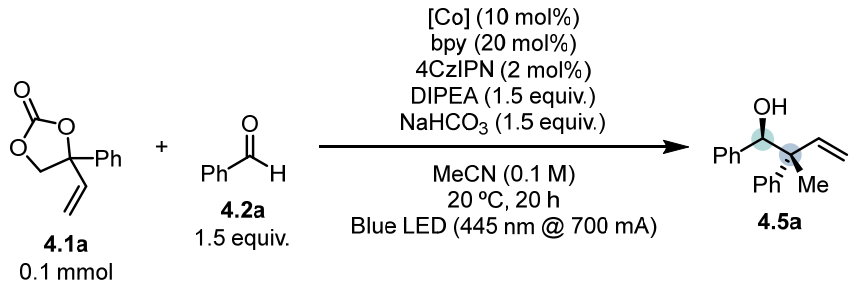

Entry	[Co]	Yield (%)[a]
1[b]	$CoCl_2(bpy)$	51
2[b]	$CoCl_2(bpy)_2{\cdot}3H_2O$	70
3	CoF_2	<5[c]
4	$CoBr_2$	29
5	CoI_2	30
6	$CoSO_4{\cdot}7H_2O$	11
7	$Co(NO_3)_2{\cdot}6H_2O$	55
8	$Co(acac)_2$	34
9	$Co(OAc)_2$	80
10	$Co(BF_4)_2{\cdot}6H_2O$	81
11	$Co(ClO_4)_2{\cdot}6H_2O$	82

Full conversion of **4.1a** was noted in all instances, unless otherwise stated; [a] Reported yields (%) of **4.5a** are based on ^{1}H NMR integration of the crude product using mesitylene as internal standard; [b] No exogenous 2,2'-bipyridine was added; [c] 75% substrate conversion.

However, a second run with freshly distilled benzaldehyde afforded 40% yield of **4.5a**. After some investigation, we found that the used benzaldehyde had minor $PhCO_2H$ impurities which positively impacted the yield. Indeed, a third run with freshly distilled benzaldehyde and adding 20 mol% of $PhCO_2H$ provided 84% yield of **4.3a** (**TABLE 4.8**, entry 1). This finding prompted us to screen other acid additives in combination with $Co(ClO_4)_2{\cdot}6H_2O$. The addition of acetic acid led to a slightly lower yield, while more acidic trifluoroacetic acid decreased the yield of **4.5a** (**TABLE 4.8**, entries 2-3). Adding more hindered carboxylic acids afforded slightly poorer product yields (**TABLE 4.8**, entries 4-6), while the presence of oxalic acid or *p*-$TsOH{\cdot}H_2O$ diminished the yield of **4.5a** substantially (**TABLE 4.8**, entries 7-8).

TABLE 4.8. Screening of various acids for the synthesis of homoallylic alcohol **4.5a**.

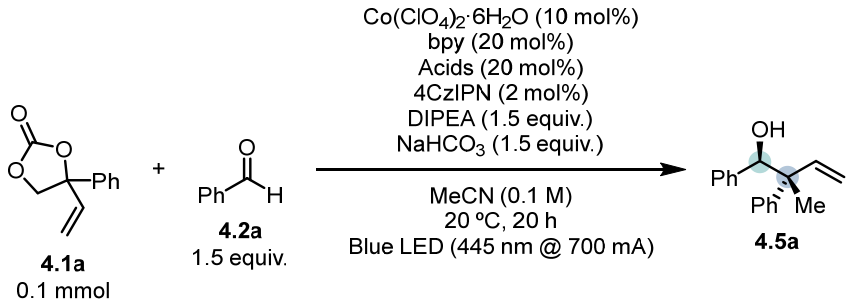

Entry	Acids	Yield (%)[(a)]
1	$PhCO_2H$	82
2	AcOH	79
3	TFA	60
4	PivOH	78
5	$MesCO_2H$	81
6	$1\text{-}AdCO_2H$	74
7	Oxalic Acid	45
8	*p*-TsOH·H_2O	<5

For the structure of the acids, please refer to Appendix A. Full conversion of **4.1a** was noted in all instances; [(a)] Reported yields (%) of **4.5a** are based on ^{1}H NMR integration of the crude product using mesitylene as internal standard.

Next, we decided to examine other dinitrogen ligands. To our surprise, despite being structurally similar to 2,2'-bipyridine, all the other ligands that we screened turned out to give significantly inferior results (**TABLE 4.9**, entries 1-13). These results suggest that the 2,2'-bipyridine ligand framework is rather privileged structure for this transformation.

TABLE 4.9. Screening of ligands for the synthesis of homoallylic alcohol **4.5a**.

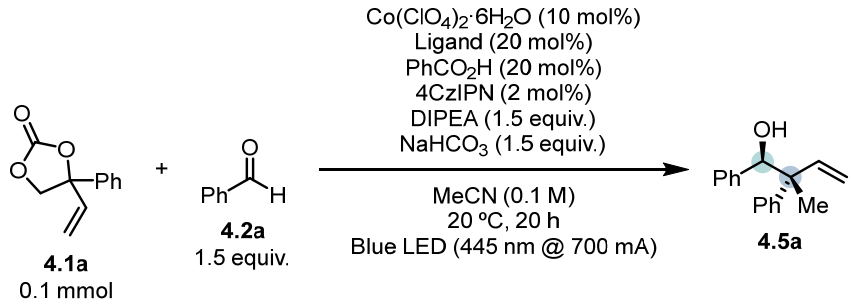

Entry	Ligand	Yield (%)[(a)]
1	dtbbpy	41
2	4,4'-OMe-bpy	35
3	4,4'-CF_3-bpy	8
4	5,5'-CF_3-bpy	34
5	6,6'-Me-bpy	31
6	phen	21
7	DAF	27
8	batho	22
9	**L1**	<5
10	**L2**	<5
11	**L3**	23
12	**L4**	<5[(b)]
13	**L5**	22

For the structure of the ligands, please refer to Appendix A. Full conversion of **4.1a** was noted in all instances, unless otherwise stated; [(a)] Reported yields (%) of **4.5a** are based on ^{1}H NMR integration of the crude product using mesitylene as internal standard; [(b)] 21% substrate conversion.

Hereafter, we moved on to investigate the influence of using different photocatalysts and solvents. Changing the structure of the organic photosensitizers afforded poor results (**TABLE 4.10**, entries 1-3). Switching to iridium-based photosensitizers also led to poor yields (**TABLE 4.10**, entries 4-5), or did not afford any homoallylic alcohol **4.5a** (**TABLE 4.10**, entries 6-7), while the presence of $Ru(bpy)_3(PF_6)_2$ only gave rise to 11% of **4.5a** (**TABLE 4.10**, entry 8). The reactions in DMF or NMP were sluggish (**TABLE 4.10**, entries 9-10), while the addition of H_2O to DMF afforded 41% yield (**TABLE 4.10**, entry 11). Finally, running the reaction in DCE or a micellar aqueous solution did not provide any desired homoallylic alcohol product **4.5a** (**TABLE 4.10**, entries 12-13).

TABLE 4.10. Screening of photocatalysts and solvents for the synthesis of homoallylic alcohol **4.5a**.

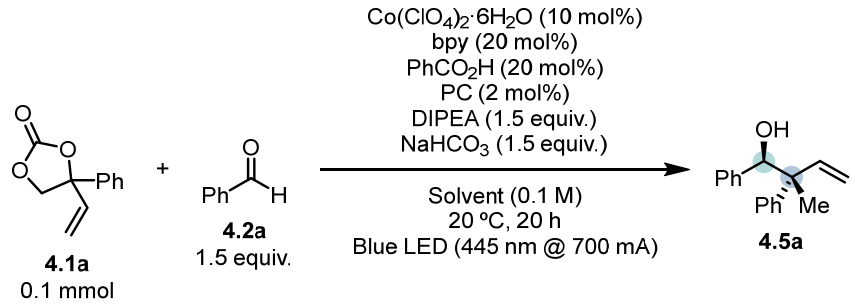

Entry	PC	Solvent	Yield (%)[a]
1	Eosin B[b]	MeCN	<5
2	4CzTPN	MeCN	5
3	3DPAFIPN	MeCN	<5
4	$[Ir(dF,CF_3ppy)_2(dtbbpy)](PF_6)$	MeCN	47
5	$[Ir(dF,Meppy)_2(dtbbpy)](PF_6)$	MeCN	41
6	$[Ir(dtbbpy)(ppy)_2](PF_6)$	MeCN	<5[b]
7	$Ir(ppy)_3$	MeCN	<5[b]
8	$Ru(bpy)_3(PF_6)_2$	MeCN	11
9	4CzIPN	DMF	<5[c]
10	4CzIPN	NMP	13
11	4CzIPN	DMF/H_2O (9:1)	41
12	4CzIPN	DCE	<5[d]
13	4CzIPN	TPGS-750-M	<5[e]

For the structure of the photocatalysts, please refer to Appendix A. Full conversion of **4.1a** was noted in all instances, unless otherwise stated; [a] Reported yields (%) of **4.5a** are based on ^1H NMR integration of the crude product using mesitylene as internal standard; [b] No conversion was observed; [c] 32% substrate conversion; [d] 66% substrate conversion; [e] 81% substrate conversion.

Before investigating the preliminary product scope, we conducted some control reactions. The reaction performed in the absence of $NaHCO_3$ surprisingly led to the same product yield (**TABLE 4.11**, entry 1), so apparently, $NaHCO_3$ does not play any significant role in this transformation. As expected, no reaction occurs in the absence of 4CzIPN or under air (**TABLE 4.11**, entries 2-3).

TABLE 4.11. Control reactions for the synthesis of homoallylic alcohol **4.5a**.

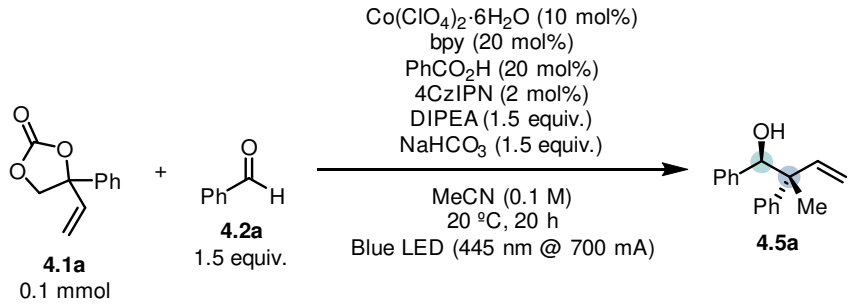

Entry	Change to std. condition	Yield (%)[a]
1	No $NaHCO_3$	82
2	No 4CzIPN	<5[b]
3	Under Air	<5[b]

Full conversion of **4.1a** was noted in all instances, unless otherwise stated; [a] Reported yields (%) of **4.5a** are based on ^{1}H NMR integration of the crude product using mesitylene as internal standard; [b] No conversion was observed.

4.3.2 Preliminary Scope of Products

To demonstrate that the reaction is applicable to a broader range of substrates, we prepared a preliminary scope of products (**SCHEME 4.18**, **4.5a**-**4.5g**). In this series of products, generally good yields and high diastereoselectivities were observed. Lower product yields were observed for strongly electron-donating or withdrawing groups on the aryl substituent in the VCC reagents (**SCHEME 4.18**, **4.5e**-**4.5f**). Apart from this, we generally detected small amounts (<20%) of 1,3-diol **4.3** as a byproduct in every reaction. Additionally, regioisomers **4.AO** are often formed in minor amounts, although a larger quantity was noted in the formation of product **4.5e**. Besides, competitive formation of olefins **4.AL**-**4.AN** in this reaction might account for the lower product yields. The assigned *anti*-configuration was unambiguously confirmed by X-ray diffraction of a single crystal of **4.5g** (see **TABLE 4.13** in subsection 4.5.10).

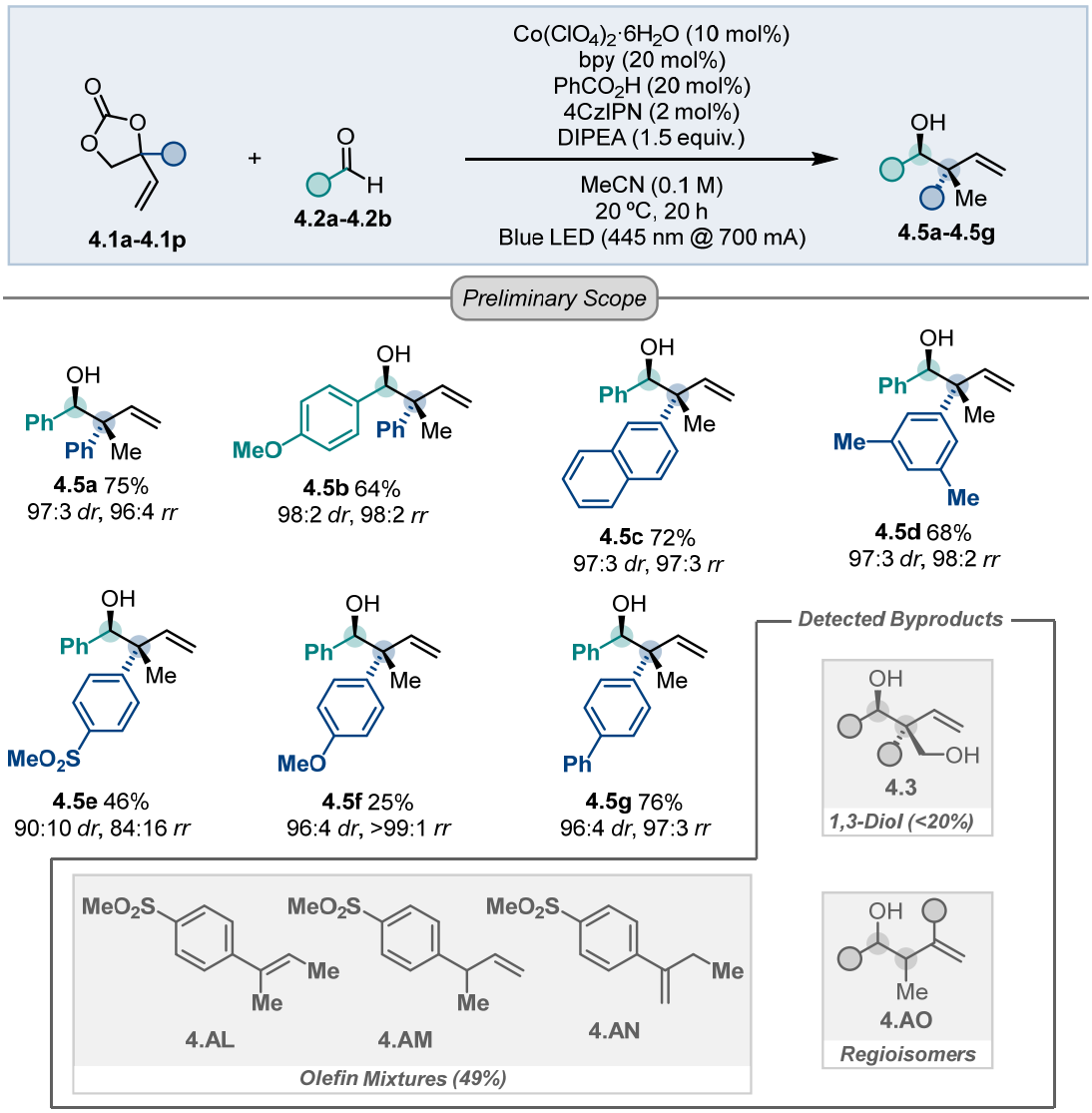

SCHEME 4.18. Preliminary variation of aldehyde and VCC reagents to afford *anti*-homoallylic alcohols **4.5a-4.5g**. The abbreviation *rr* refers to the regio-isomeric ratio between **4.5a-4.5g** and **4.AO**. Reaction conditions: VCC **4.1a-4.1p** (0.1 mmol), aldehyde **4.2a-4.2b** (1.5 equiv.), $Co(ClO_4)_2{\cdot}6H_2O$ (10 mol%), bpy (20 mol%), $PhCO_2H$ (20 mol%), 4CzIPN (2 mol%), DIPEA (1.5 equiv.), MeCN (0.1 M), Blue LED (445 nm @ 700 mA, corresponding to 1.2 μeinstein/s), 20 °C, 20 h, under N_2.

4.3.3 Mechanistic Details

In view of the detected byproducts, we hypothesized that the reaction might proceed through the intermediacy of a 1,3-diene generated from the VCC reagent. To support this hypothesis, we analyzed the reaction mixture by GC (**FIGURE 4.3**). To our delight, we could detect 1,3-diene **4.AP** after stirring the benchmark reaction mixture for 2 hours, while validating with an authentic sample of 1,3-diene (**FIGURE 4.3**, purple peak). Moreover, additional GC-MS analysis also corroborated the presence of 1,3-diene **4.AP** by comparison of their EI-MS spectra (see subsection 4.5.9).

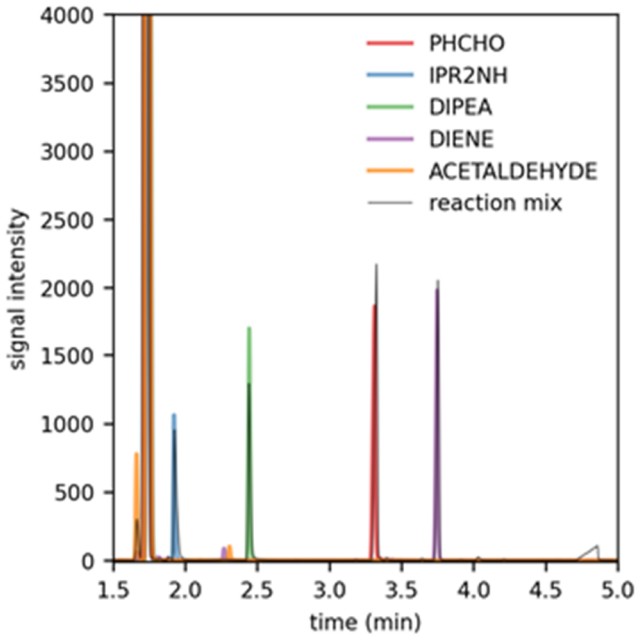

FIGURE 4.3. Superimposed GC chromatograms comparing the reaction mixture with authentic samples.

Additionally, we performed some control experiments to rule out other mechanistic scenarios. The reaction starting from 1,3-diol **4.3a** shows no conversion, indicating that 1,3-diol is only a byproduct and not a reaction intermediate towards **4.5a** (**SCHEME 4.19A**). Furthermore, the reaction starting from tertiary alcohol **4.AQ** also shows no conversion under a N_2 or a CO_2 atmosphere (**SCHEME 4.19B**). Beyond that, the reaction with isobutyraldehyde affords 17% of **4.5h**, while also producing 30% of **4.5i**, which is apparently the product arising from acetaldehyde (**SCHEME 4.19C**). The formation of acetaldehyde was confirmed in two ways. First, the reaction was run in the absence of benzaldehyde **4.2a**, producing homoallylic alcohol **4.5i** in 29% yield (**SCHEME 4.19D**), and secondly, comparing the retention times of the reaction mixture with authentic samples by GC-FID analysis confirmed the presence of acetaldehyde and diisopropylamine **4.AS** (**SCHEME 4.19E**), which is probably the result from the hydrolysis of iminium ion **4.AR** obtained after the oxidation of DIPEA.

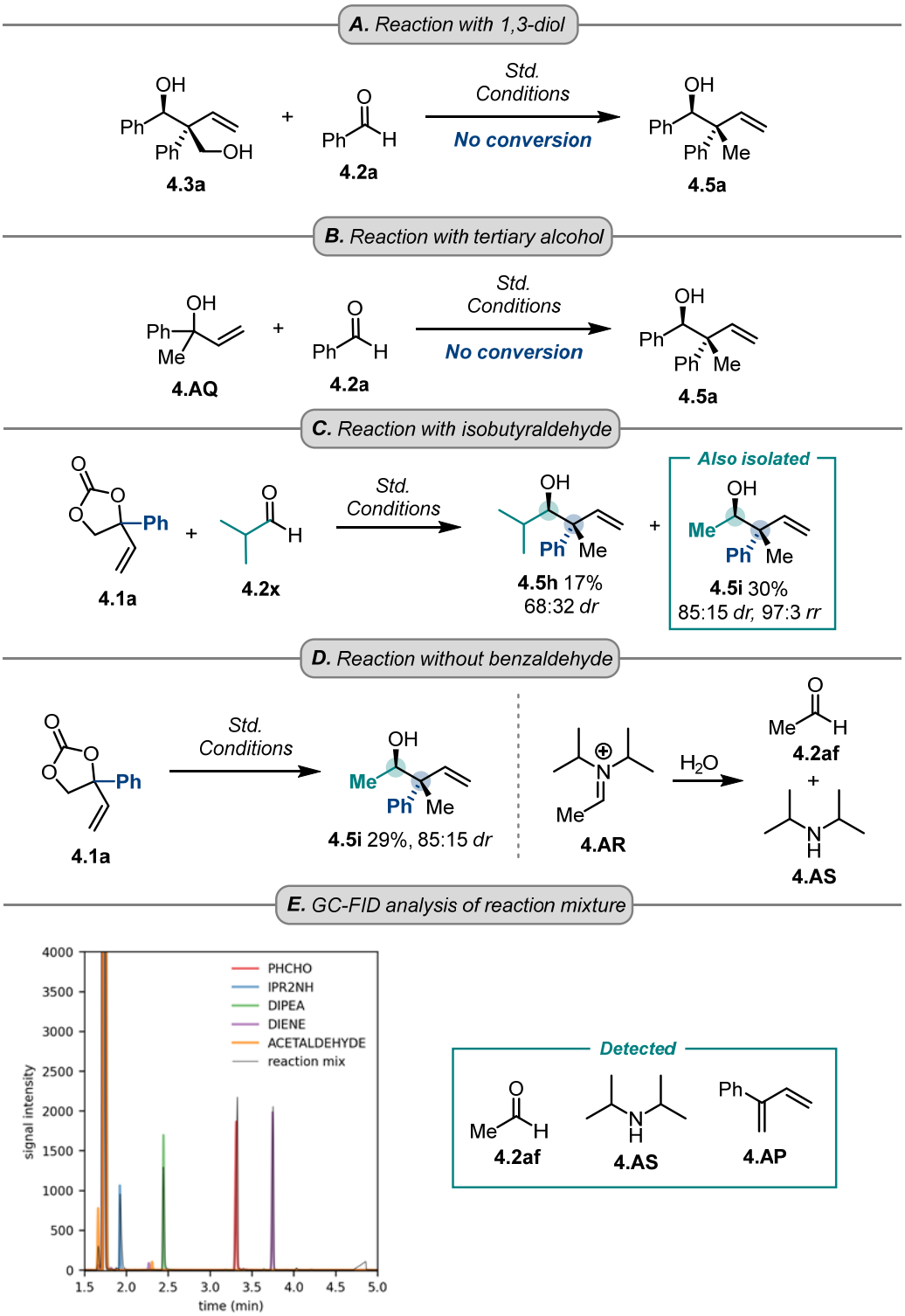

SCHEME 4.19. Reported conversions (%) are based on ^{1}H NMR integration of the crude product using mesitylene as internal standard, while reported yields are based on isolated product; **(A)** Control reaction with 1,3-diol **4.3a**; **(B)** Control reaction with tertiary alcohol **4.AQ**; **(C)** Reaction between Ph-VCC **4.1a** and isobutytaldehyde **4.2x** under standard conditions; **(D)** Reaction with Ph-VCC **4.1a** under standard conditions without the addition of benzaldehyde; **(E)** Comparison of GC-FID chromatograms between the reaction mixture and authentic samples.

Based on these control experiments/data, we tentatively propose the following mechanism. The overall mechanism consists of two cobalt catalytic cycles and the photoredox catalytic. The first cobalt cycle accounts for the formation of 1,3-diene intermediate (**SCHEME 4.20**, cobalt cycle A), while the second one explains the allylation of the aldehyde reagent (**SCHEME 4.20**, cobalt cycle B). The reaction is initiated by the photoreduction of the Co^{II} complex **4.AT** to the Co^{I} complex **4.AU**. Subsequent oxidative addition of the VCC reagent, decarboxylation, and protonation will generate an allyl-Co^{III} intermediate.[194] From here, the formation of the 1,3-diol byproduct follows the immediate SET reduction to a Co^{II}-allyl followed by nucleophilic attack onto the aldehyde. However, the major pathway that accounts for the formation of the observed 1,3-diene is presumably a β-*O*-elimination, thus leading to Co^{III}–OH complex **4.AW**.[195] The catalytic cycle is closed by the replacement of OH with BzOH and photoreduction to regenerate the starting Co^{II} complex **4.AT**. Moving to catalytic cycle B, we envision the formation of a Co^{III}–H complex **4.AX** from the initial Co^{II} complex 4**.AT** through either photoreduction followed by protonation, or hydrogen-atom transfer (HAT) with DIPEA radical cation. Hereafter, 1,3-diene insertion into the Co^{III}–H **4.AX** will produce Co^{III}-allyl **4.AY**. The observed regio-isomeric mixtures might well arise from the regioselective addition of a Co^{III}–H onto the 1,3-diene, which likely proceeds through a metal hydrogen-atom transfer (MHAT), thus favoring the addition product that generates the most stable radical. In addition, the observed olefin mixtures **4.AL**-**4.AN** should be formally the 1,2 and 1,4-addition products involving two Co–H species. From here, subsequent photoreduction to Co^{II}-allyl **4.AZ**, nucleophilic attack onto the aldehyde, and protodemetalation will eventually produce the observed homoallylic alcohol product. Regarding the photocatalytic cycle, blue light absorption by 4CzIPN leads transiently to the excited PC*, which will be reductively quenched by DIPEA. The release of one electron will then occur from the PC radical anion. The generation of an additional electron, and one proton should happen from deprotonation of DIPEA radical cation, followed by single electron transfer to yield iminium ion **4.AR**. Alternatively, hydrogen-atom transfer (HAT) would yield iminium ion **4.AR** directly. However, the overall cobalt catalytic cycles apparently require 4 electrons to produce the final homoallylic alcohol. We, therefore, postulate that the hydrolysis of iminium ion **4.AR**

[194] At this stage, we cannot rule out the possibility that the photoreduction reaches an initial Co^{0} intermediate upon which oxidative addition occurs. As 2,2'-bipyridine is a redox-active ligand, it might be easier to reach the Co(0) oxidation state than for the previously used $[Co^{II}(DPEPhos)Cl_2]$ complex in the preparation of *syn*-1,3-diols .

[195] Similar β–OH-eliminations from cobalt intermediates have been previously proposed, see: a) Suzuki, Y.; Sun, B.; Sakata, K.; Yoshino, T.; Matsunaga, S.; Kanai, M. *Angew. Chem. Int. Ed.* **2015**, *54*, 9944-9947. b) Bunno, Y.; Murakami, N.; Suzuki, Y.; Kanai, M.; Yoshino, T.; Matsunaga, S. *Org. Lett.* **2016**, *18*, 2216-2219. c) Kalsi, D.; Laskar, R. A.; Barsu, N.; Premkumar, J. R.; Sundararaju, B. *Org. Lett.* **2016**, *18*, 4198-4201.

into MeCHO **4.2af** and *i*Pr$_2$NH **4.AS**, which we could confirm by GC analysis, will eventually lead to the generation of an extra electron (and proton) from the oxidation of *i*Pr$_2$NH **4.AS** into imine **4.BA**.[196]

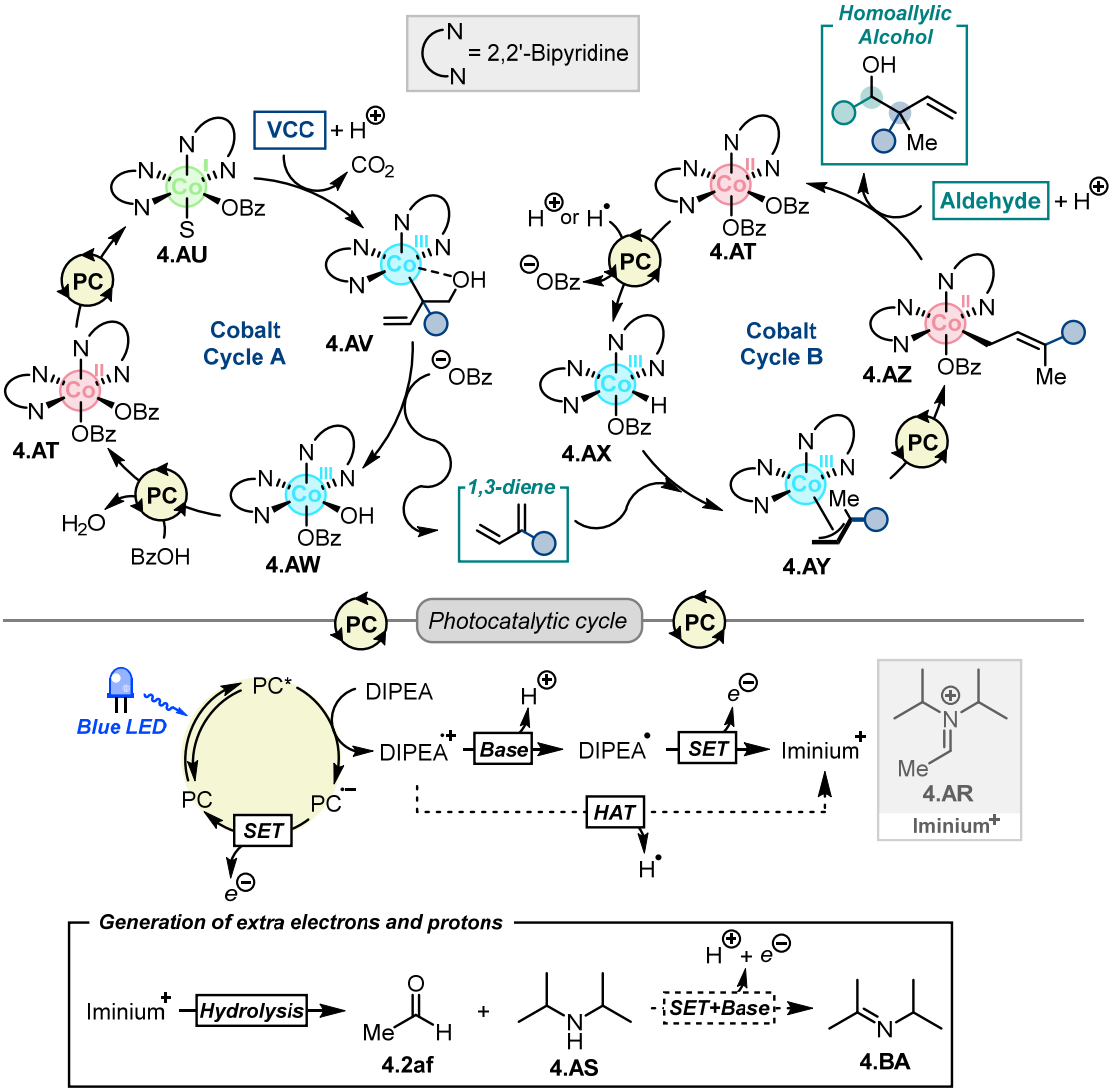

SCHEME 4.20. Proposed catalytic cycles for the transformation of VCCs into homoallylic alcohols by dual cobalt-photoredox catalysis.

[196] Evidence for this hypothesis could be gathered by running a control experiment between Ph-VCC **4.1a** and benzaldehyde **4.2a** using *i*Pr$_2$NH (2 equiv.) instead of DIPEA. Indeed, homoallylic alcohol **4.5a** was produced in 38% yield.

4.4 Conclusions

This chapter illustrates how two newly developed methods merging cobalt and organophotoredox catalysis can be effectively applied to generate acyclic quaternary carbon stereocenters in a stereoselective way. Compared to the previous palladium-catalyzed allylation of nitroalkanes developed in chapter 2, these protocols rely on the generation of nucleophilic allyl species from VCC reagents through an *umpolung* process, which can then be combined with electrophilic aldehydes. These methods feature mild reaction conditions that translate into a wide scope and attractive functional group tolerance. Relevant to the observed high diastereoselectivities are the presumably fast allyl isomerization rates imposed by the catalyst and the kinetic differentiation in the main C–C bond-forming step.

We believe that this work will provide a larger framework for the use of dual base metal/photocatalysis approaches in the creation of compounds with synthetically attractive quaternary carbon stereocenters, thus advancing the use of more sustainable processes that can obviate the utilization of scarce and expensive noble metals.

4.5 Experimental Section

4.5.1 General Information

Methods: Air and water-sensitive reactions were carried out in heat-gun-dried glassware under an Ar or N_2 atmosphere using standard Schlenk techniques. Reactions were monitored by TLC and/or ^{1}H NMR. TLC was carried out on 0.25 mm Merck aluminum-backed sheets coated with 60 F_{254} silica gel. Visualization of the silica plates was achieved using a UV lamp (λ = 254 nm) and/or by heating plates that were dipped in a $KMnO_4$ stain or a ceric ammonium molybdate stain. Flash chromatography was carried out on Sigma-Aldrich silica gel 60 (70-230 mesh) using the indicated eluent system. LED photo fluxes were determined by standard ferrioxalate actinometry.[197]

Reagents and Solvents: Commercially available reagents and solvents were purchased from Sigma-Aldrich, TCI, Fluorochem, Strem Chemicals, Abcr GmbH, Acros Organics, or Alfa Aesar, and were used without further purification. Benzaldehyde, *p*-anisaldehyde and, isobutyraldehyde were distilled under reduced pressure before use. 4CzIPN was synthesized according to a previously reported procedure.[198] Solvents were dried using an Innovative Technology PURE SOLV solvent purification system.

Analytical Techniques: ^{1}H NMR, ^{13}C NMR, DEPT-90, DEPT-135, and related 2D NMR (gCOSY90, gHMQC, gHMBC, gNOESY) spectra were recorded at room temperature on a Bruker AV-300, AV-400, or AV-500 spectrometer and referenced to their residual deuterated solvent signals. Coupling constants (J) are reported in hertz with the following splitting abbreviations: s = singlet, d = doublet, t = triplet, q = quadruplet, quint = quintet, sextet = sext, heptet = hept, br = broad and app = apparent. All reported NMR values are given in parts per million (ppm). FT-IR measurements were carried out on a Bruker Optics FTIR Alpha spectrometer. Mass spectrometric and X-ray analyses were performed by the Research Support Unit at ICIQ. UV-Vis measurements were carried out on a Shimadzu UV1700PC spectrophotometer equipped with a photomultiplier detector, double beam optics, and D2 and W light sources. Fluorescence measurements were carried out on a Fluorolog Horiba Jobin Yvon spectrofluorimeter equipped with a photomultiplier detector, double monochromator, and Xenon light source. Lifetime measurements were carried out on an Edinburgh Instruments LifeSpec-II based on the time-correlated single-photon counting (TCSPC) technique, equipped with a PMT detector, double subtractive monochromator, and a picosecond pulsed diode laser source with a wavelength of 405 nm.

[197] Hatchard, C. G.; Parker, C. A. *Proc. R. Soc. London. Ser. A. Math. Phys. Sci.* **1956**, *235*, 518-536.
[198] Luo, J.; Zhang, J. *ACS Catal.* **2016**, *6*, 873-877.

Photocatalysis Set-up: Photoreactions were performed in a parallel photoreactor with 8 spots using flat-bottom J-young Schlenk flasks (**FIGURE 4.4**). The reactions were thermostated using a Heidolph rota-cool and stirred using 3x7 mm stirring bars. OSRAM Oslon SSL 80 royal-blue LEDs mounting on a star PCB were used and cooled passively by a common heatsink. The LEDs were powered in series using a current limited power supply (RS Pro RS-3005D).

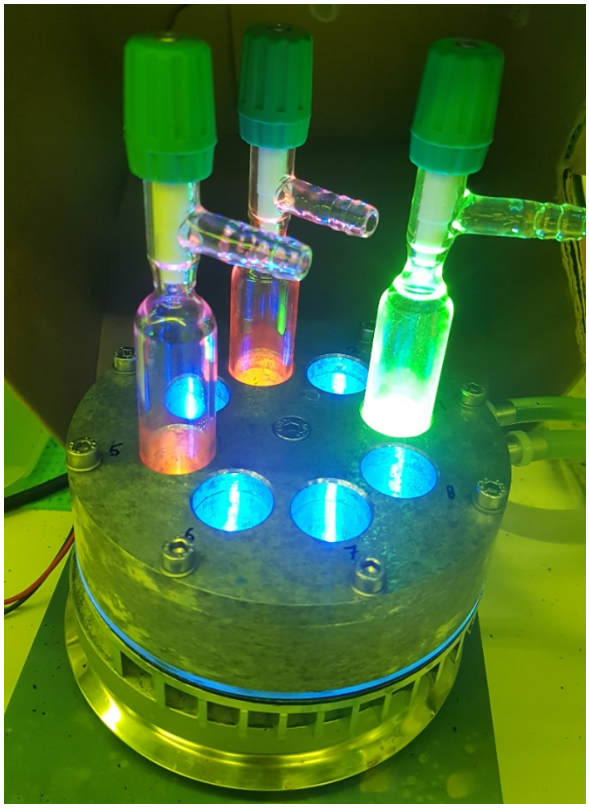

FIGURE 4.4. Photoreactor setup with 8 parallel reactors photographed through a 450 nm notch filter.

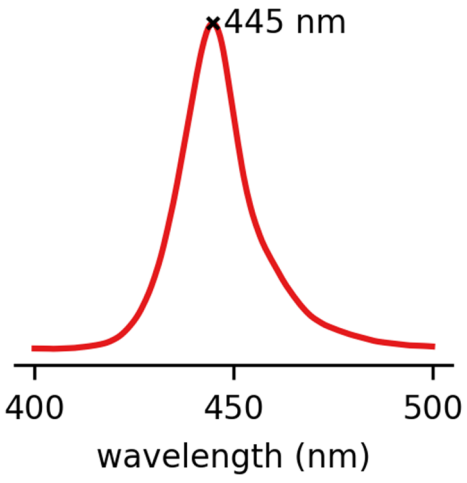

FIGURE 4.5. Emission spectrum of the blue LED.

4.5.2 General Procedure for the Synthesis of Vinyl Cyclic Carbonates

Vinyl cyclic carbonates **4.1a-4.1p** were synthesized according to a previously reported procedure,[199] as previously described in subsection 2.4.2 (**SCHEME 2.12**). 4-(3-Hydroxyphenyl)-4-vinyl-1,3-dioxolan-2-one (**4.1k**) was prepared by deprotection of the MOM group in 4-(3-(methoxymethoxy)phenyl)-4-vinyl-1,3-dioxolan-2-one (**4.1j**) using trifluoroacetic acid in dichloromethane following a standard procedure.[200] Characterization data for newly prepared VCC compounds are provided below:

4-(4-(Methylsulfonyl)phenyl)-4-vinyl-1,3-dioxolan-2-one (4.1g)

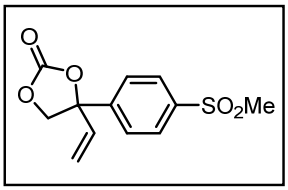

White solid (820 mg, 66% yield); **IR** (neat): ν = 2929, 1798, 1304, 1148, 1052, 954, 766 cm^{-1}; **^{1}H NMR** (400 MHz, $CDCl_3$) δ_H 8.06-7.98 (m, 2H), 7.63-7.55 (m, 2H), 6.15 (dd, J = 17.2, 10.8 Hz, 1H), 5.49 (d, J = 10.7 Hz, 1H), 5.45 (d, J = 17.1 Hz, 1H), 4.72 (d, J = 8.6 Hz, 1H), 4.56 (d, J = 8.6 Hz, 1H), 3.07 (s, 3H); **^{13}C NMR** (101 MHz, $CDCl_3$) δ_C 153.5, 144.6, 141.4, 135.7, 128.4, 126.1, 118.9, 85.0, 74.3, 44.6; **HRMS** (ESI/TOF) m/z: $[M + Na]^+$ Calcd for $C_{12}H_{12}NaO_5S$ 291.0298; Found 291.0292.

4-(3-(Methoxymethoxy)phenyl)-4-vinyl-1,3-dioxolan-2-one (4.1j)

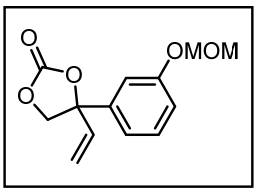

Colorless oil (1.37 g, 59% yield); **IR** (neat): ν = 2909, 2828, 1798, 1585, 1150, 1052, 982, 768, 699 cm^{-1}; **^{1}H NMR** (400 MHz, $CDCl_3$) δ_H 7.34 (t, J = 8.0 Hz, 1H), 7.06 (ddd, J = 8.2, 2.5, 0.9 Hz, 1H), 7.02 (t, J = 2.1 Hz, 1H), 6.97 (ddd, J = 7.7, 1.8, 0.9 Hz, 1H), 6.14 (dd, J = 17.2, 10.7 Hz, 1H), 5.45 (d, J = 11.2 Hz, 1H), 5.41 (d, J = 4.8 Hz, 1H), 5.18 (s, 2H), 4.63 (d, J = 8.4 Hz, 1H), 4.55 (d, J = 8.4 Hz, 1H), 3.48 (s, 3H); **^{13}C NMR** (101 MHz, $CDCl_3$) δ_C 157.9, 154.1, 140.2, 136.5, 130.3, 118.3, 117.7, 116.5, 113.3, 94.6, 85.4, 74.6, 56.3; **HRMS** (ESI/TOF) m/z: $[M + Na]^+$ Calcd for $C_{13}H_{14}NaO_5$ 273.0733; Found 273.0733.

4-(3-Hydroxyphenyl)-4-vinyl-1,3-dioxolan-2-one (4.1k)

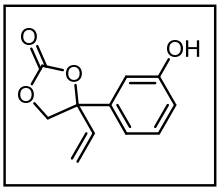

Colorless oil (408 mg, 99% yield); **IR** (neat): ν = 3387, 1767, 1590, 1450, 1191, 1052, 940, 770, 698 cm^{-1}; **^{1}H NMR** (400 MHz, $CDCl_3$) δ_H 7.31-7.22 (m, 1H), 6.92-6.80 (m, 3H), 6.12 (dd, J = 17.2, 10.7 Hz, 1H), 6.08 (br s, 1H), 5.41 (dd, J = 13.9, 3.2 Hz, 2H), 4.64 (d, J = 8.5 Hz, 1H), 4.57 (d, J = 8.5 Hz, 1H); **^{13}C NMR** (101 MHz, $CDCl_3$) δ_C 156.6, 154.7, 140.1, 136.3, 130.5, 117.9, 116.9, 116.2, 112.1, 85.8, 74.8; **HRMS** (ESI/TOF) m/z: $[M + Na]^+$ Calcd for $C_{11}H_{10}NaO_4$ 229.0471; Found 229.0465.

[199] See Kleij, A. W. *et al. J. Org. Chem.* **2018** (*ref.* 53e) on page 30.
[200] Banerjee, U.; DeBerardinis, A. M.; Hadden, M. K. *Bioorganic Med. Chem.* **2015**, *23*, 548-555.

4.5.3 Synthesis of Other Starting Materials

***tert*-Butyl 3-formyl-1*H*-indole-1-carboxylate (4.2u)**

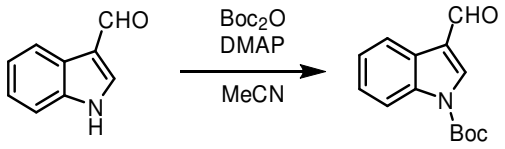

4.2ac **4.2u**

According to a previously published procedure,[201] in a heat-gun-dried 50 mL round-bottomed flask, indole **4.2ac** (1.45 g, 10 mmol) was dissolved in dry MeCN (15 mL) under N_2. Hereafter, DMAP (122.2 mg, 1 mmol) was added to the reaction mixture, and then Boc_2O (2.5 mL, 11 mmol) was added dropwise. The mixture was stirred at room temperature overnight. The solvent was evaporated, and the resulting solid was dissolved in CH_2Cl_2, followed by one washing with $NaHCO_3$ and water. The organic phase was dried over Na_2SO_4, filtered, and concentrated *in vacuo*. The resulting solid was purified by flash chromatography on silica gel using 10% EtOAc/hexanes to afford indole **4.2u** as a white solid (2.43 g, 99% yield). **^{1}H NMR** (300 MHz, $CDCl_3$) δ_H 10.10 (s, 1H), 8.36-8.26 (m, 1H), 8.23 (s, 1H), 8.19-8.08 (m, 1H), 7.40 (pd, J = 7.3, 1.5 Hz, 2H), 1.71 (s, 9H); **^{13}C NMR** (75 MHz, $CDCl_3$) δ_C 186.0, 148.9, 136.7, 136.1, 126.2, 124.7, 124.4, 122.2, 121.7, 115.3, 85.8, 28.2; Spectroscopic data are in agreement with published data.[201]

2-Phenyl-2-vinyloxirane (4.6)

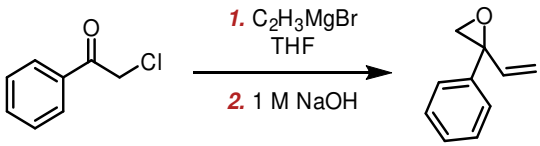

4.BB **4.6**

According to a previously published procedure,[202] in a heat-gun-dried 250mL round-bottomed flask, 2-chloroacetophenone **4.BB** (3.86 g, 25 mmol) was dissolved in dry THF under N_2. The reaction mixture was cooled to 0 °C (ice-water bath) and vinylmagnesium bromide (30 mL, 30 mmol, 1 M in THF) was added dropwise over 30 min. The mixture was stirred at 0 °C for 15 min and then warmed to room temperature over 30 min. The reaction was quenched with aqueous saturated NH_4Cl and was extracted with Et_2O twice. The combined organic layers were washed with brine, dried over $MgSO_4$, filtered, and was concentrated *in vacuo*. The crude product was purified by flash chromatography on silica gel using 10% EtOAc/hexanes to give the title compound (1.85 g) as a yellow oil.

---

[201] Fredrich, S.; Bonasera, A.; Valderrey, V.; Hecht, S. *J. Am. Chem. Soc.* **2018**, *140*, 6432-6440.
[202] Trost, B. M.; Brown, B. S.; McEachern, E. J.; Kuhn, O. *Chem. Eur. J.* **2003**, *9*, 4442-4451.

The product from the last step was redissolved in Et_2O (50 mL) and was stirred over 1 M NaOH for 2 h, and then the phases were separated. The aqueous layer was extracted with Et_2O, and the combined organic layers were dried over Na_2SO_4, filtered, and concentrated *in vacuo*. The crude product was used without further purification (1.50 g, 41% yield). **^{1}H NMR** (300 MHz, $CDCl_3$) δ_H 7.30-7.42 (m, 5H), 6.05 (dd, J = 17.2, 10.6 Hz, 1H), 5.33 (dd, J = 10.6, 1.2, Hz, 1H), 5.25 (dd, J = 17.2, 1.2 Hz, 1H), 3.10 (d, J = 5.7 Hz, 1H), 3.03 (d, J = 5.7 Hz, 1H); **^{13}C NMR** (75 MHz, $CDCl_3$) δ_C 137.3, 128.2, 127.8, 127.0, 119.0, 56.7; Spectroscopic data are in agreement with published data.[202]

***tert*-Butyl (2-phenylbut-3-en-2-yl) carbonate (4.7a)**

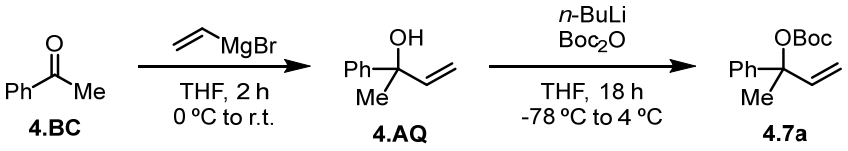

According to a previously published procedure,[203] in a 100 mL round-bottomed flask, acetophenone **4.BC** (1.20 g, 10 mmol) was dissolved in dry THF (10 mL) under N_2. The solution was cooled to 0 °C (ice-water bath) and vinylmagnesium bromide (15 mL, 15 mmol, 1 M in THF) was added dropwise over 10 minutes. The reaction mixture was allowed to warm to room temperature and was stirred for further 2 h. The reaction was quenched with aqueous saturated NH_4Cl and was extracted with Et_2O three times. The combined organic layers were washed with brine, dried over $MgSO_4$, filtered, and concentrated *in vacuo*. The crude product was purified by flash chromatography over silica gel using 10% EtOAc/hexanes to afford tertiary alcohol **4.AQ** as a yellowish oil (1.20 g, 81% yield).

In a heat-gun-dried 100 mL round-bottomed flask, tertiary alcohol **4.AQ** (1.20 g, 8.1 mmol) was dissolved in dry THF (16 mL) under N_2. The solution was cooled to -78 °C (dry ice-acetone bath), and *n*-BuLi (3.55 mL, 8.5 mmol, 2.5 M in hexane) was added dropwise over 5 minutes. After stirring the reaction mixture for 30 minutes, a solution of Boc_2O (2.29 g, 10.5 mmol) in dry THF (5 mL) was added dropwise over 5 minutes. The reaction mixture was then allowed to warm to 4 °C (cryocooler) and was stirred for further 18 h. Hereafter, the reaction was diluted with Et_2O and water, and the phases were separated. The aqueous layer was extracted with Et_2O three times. The combined organic layers were washed with brine, dried over $MgSO_4$, filtered, and concentrated *in vacuo*. The crude product was purified by flash chromatography on silica gel using EtOAc/hexanes/Et_3N (1:98:1) to afford carbonate **4.7a** as a yellowish oil (1.65 g, 82% yield). **^{1}H NMR** (500 MHz, $CDCl_3$) δ_H 7.40-7.37 (m, 2H), 7.36-7.32(m, 2H), 7.27-7.24 (m, 1H), 6.34 (dd, J =

[203] Zhang, P.; Le, H.; Kyne, R. E.; Morken, J. P. *J. Am. Chem. Soc.* **2011**, *133*, 9716-9719.

17.4, 10.8 Hz, 1H), 5.30-5.26 (m, 2H), 1.87 (s, 3H), 1.41 (s, 9H); Spectroscopic data are in agreement with published data.[204]

(*E*)-*tert*-Butyl (3-phenylbut-2-en-1-yl) carbonate (4.7b) and (*Z*)-*tert*-butyl (3-phenylbut-2-en-1-yl) carbonate (4.7c)

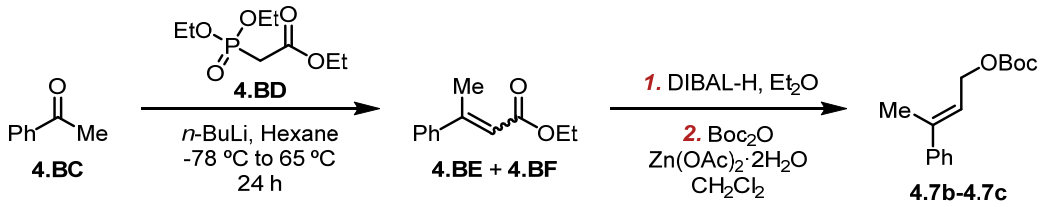

According to a previously published procedure,[205] in a heat-gun-dried Schlenk tube, triethyl phosphonoacetate **4.BD** (4.0 mL, 20 mmol) was suspended in dry hexane (20 mL) under N_2. The suspension was cooled to -78 ºC (dry ice-acetone bath), and *n*-BuLi (8 mL, 20 mmol, 2.5 M in hexane) was added dropwise over 10 minutes. The mixture was stirred at -78 ºC for 30 minutes, and then at 0 ºC (ice-water bath) for further 30 minutes. Hereafter, acetophenone **4.BC** (2.3 mL, 20 mmol) was added dropwise and the reaction mixture was stirred at 65 ºC (oil bath) for 24 h. After cooling the mixture to room temperature, the reaction was quenched with aqueous saturated Na_2CO_3 and extracted with Et_2O twice. The combined organic phases were washed with water and brine, dried over Na_2SO_4, filtered, and concentrated *in vacuo*. The crude product (mixture of **4.BE**-**4.BF**) was purified by flash chromatography over silica gel using EtOAc/hexanes (20:1) to afford separated α,β-unsaturated esters **4.BE** and **4.BF** as yellowish oils

Ethyl (*E*)-3-phenylbut-2-enoate (**4.BE**): Obtained 1.51 g, 40% yield; **^{1}H NMR** (300 MHz, $CDCl_3$) δ_H 7.53-7.43 (m, 2H), 7.43-7.30 (m, 3H), 6.13 (q, *J* = 1.3 Hz, 1H), 4.22 (q, *J* = 7.1 Hz, 2H), 2.58 (d, *J* = 1.3 Hz, 3H), 1.32 (t, *J* = 7.1 Hz, 3H).

Ethyl (*Z*)-3-phenylbut-2-enoate (**4.BF**): Obtained 400 mg, 11% yield; **^{1}H NMR** (400 MHz, $CDCl_3$) δ_H 7.39-7.27 (m, 3H), 7.24-7.16 (m, 2H), 5.91 (q, *J* = 1.5 Hz, 1H), 4.00 (q, *J* = 7.1 Hz, 2H), 2.18 (d, *J* = 1.5 Hz, 3H), 1.08 (t, *J* = 7.1 Hz, 3H).

[204] Tom, M.-J.; Evans, P. A. *J. Am. Chem. Soc.* **2020**, *142*, 11957-11961.
[205] Cabré, A.; Garçon, M.; Gallen, A.; Grisoni, L.; Grabulosa, A.; Verdaguer, X.; Riera, A. *ChemCatChem* **2020**, *12*, 4112-4120.

Following a previously published procedure,[205] the respective α,β-unsaturated ester (1 equiv.) was dissolved in dry Et_2O (0.5 M) under N_2. The solution was cooled to -78 ºC (dry ice-acetone bath) and DIBAL-H (2.2 equiv., 1 M in hexane) was added dropwise. The mixture was stirred at -78 ºC for 3 h, and was then quenched at 0 ºC (ice-water bath) with aqueous saturated NH_4Cl. The mixture was stirred at room temperature for 1 h, producing a white precipitate. The mixture was filtered through a pad of Celite and washed with Et_2O. The resulting solution was washed with brine, dried over $MgSO_4$, filtered, and concentrated *in vacuo*. The resulting crude allylic alcohols were used in the next step without further purification.

According to a previously published procedure,[206] the respective crude allylic alcohol product from the previous step was dissolved in CH_2Cl_2 (1 M) under N_2. Hereafter, $Zn(OAc)_2{\cdot}2H_2O$ (10 mol%) and Boc_2O (1 equiv.) were successively added, and the mixture was stirred at reflux for 6 h. The reaction was then diluted with H_2O and was extracted twice with CH_2Cl_2. The combined organic layers were dried over Na_2SO_4, filtered, and concentrated *in vacuo*. The crude product was purified by flash chromatography on silica gel using 20% EtOAc/hexanes to give pure carbonates **4.7b**-**4.7c** as yellowish oils. Spectroscopic data are in agreement with published data. [203]

(*E*)-*tert*-Butyl (3-phenylbut-2-en-1-yl) carbonate (**4.7b**): Obtained 1.74 g, 88% yield; **^{1}H NMR** (400 MHz, $CDCl_3$) δ_H 7.44-7.37 (m, 2H), 7.37-7.28 (m, 2H), 7.32-7.22 (m, 1H), 5.92 (tq, *J* = 7.0, 1.4 Hz, 1H), 4.79 (dq, *J* = 7.0, 0.8 Hz, 2H), 2.12 (dt, *J* = 1.5, 0.8 Hz, 3H), 1.50 (s, 9H).

(*Z*)-*tert*-Butyl (3-phenylbut-2-en-1-yl) carbonate (**4.7c**): Obtained 471.9 mg, 90% yield; **^{1}H NMR** (400 MHz, $CDCl_3$) δ_H 7.39-7.27 (m, 2H), 7.32-7.23 (m, 1H), 7.21-7.14 (m, 2H), 5.68 (tt, *J* = 7.2, 1.5 Hz, 1H), 4.50 (dq, *J* = 7.2, 1.1 Hz, 2H), 2.10 (q, *J* = 1.2 Hz, 3H), 1.47 (s, 9H).

[206] Bartoli, G.; Bosco, M.; Carlone, A.; Dalpozzo, R.; Locatelli, M.; Melchiorre, P.; Palazzi, P.; Sambri, L. *Synlett* **2006**, 2104-2108.

4.5.4 General Procedure for the Synthesis of 1,3-diols

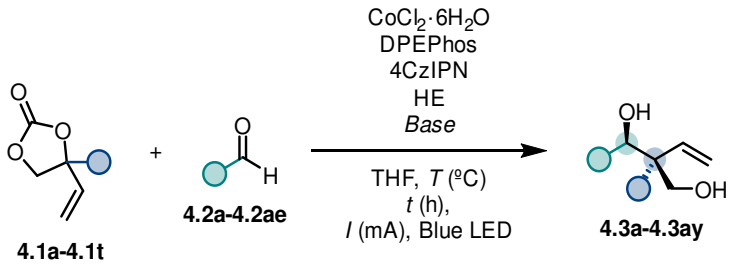

SCHEME 4.21. General synthesis of 1,3-diols.

Method A: 4CzIPN (2 μmol, 1.6 mg), $CoCl_2 \cdot 6H_2O$ (10 μmol, 2.4 mg), DPEPhos (10 μmol, 5.4 mg), K_3PO_4 (0.15 mmol, 31.8 mg) and Hantzsch ester (0.15 mmol, 38.0 mg) were weighed in a flat-bottom Schlenk flask. The solids were dissolved in THF (1 mL), and VCC **4.1a-4.1t** (0.1 mmol) and aldehyde **4.2a-4.2ae** (0.15 mmol) were added, affording a green suspension. The flask was sealed with a Teflon cap and the mixture was freeze-pump-thawed 3 times and stirred under N_2 at room temperature for 5–20 minutes after which it was irradiated for 4 hours at 20 °C using a single high-power blue LED (λ_{em} = 445 nm, 700 mA, 1.2 μeinstein s^{-1}) from the bottom. After the reaction, the mixture was aerated and evaporated to dryness. The residue was dissolved in CH_2Cl_2 and passed through basic Al_2O_3 (3 cm, Ø = 0.5 cm) eluting with CH_2Cl_2 (10 mL), and subsequently CH_2Cl_2/MeOH (9:1, 5 mL). The second fraction was evaporated to dryness and purified by column chromatography (SiO_2, EtOAc/cyclohexane or EtOAc/CH_2Cl_2) to afford 1,3-diol product **4.3a-4.3ay**.

Method B: 4CzIPN (2 μmol, 1.6 mg), $CoCl_2 \cdot 6H_2O$ (10 μmol, 2.4 mg), DPEPhos (10 μmol, 5.4 mg) and Hantzsch ester (0.15 mmol, 38.0 mg) were weighed in a flat-bottom Schlenk flask. The solids were dissolved in THF (1 mL) and 2,4,6-collidine (0.15 mmol, 19.8 μL), VCC **4.1a-4.1t** (0.1 mmol) and aldehyde **4.2a-4.2ae** (0.15 mmol or 0.5 mmol) were added, affording a green solution. The flask was sealed with a Teflon cap and the mixture was freeze-pump-thawed 3 times and stirred under N_2 at room temperature for 5–20 minutes after which it was irradiated for 4 hours at 20 °C using a single high-power blue LED (λ_{em} = 445 nm, 700 mA, 1.2 μeinstein s^{-1}) from the bottom. After the reaction, the mixture was aerated and evaporated to dryness. The residue was dissolved in CH_2Cl_2 and passed through basic Al_2O_3 (3 cm, Ø = 0.5 cm) eluting with CH_2Cl_2 (10 mL), and subsequently CH_2Cl_2/MeOH (9:1, 5 mL). The second fraction was evaporated to dryness and purified by column chromatography (SiO_2, EtOAc/cyclohexane or EtOAc/CH_2Cl_2) to afford product **4.3a-4.3ay**.

Method C: 4CzIPN (2 μmol, 1.6 mg), $CoCl_2 \cdot 6H_2O$ (10 μmol, 2.4 mg), DPEPhos (10 μmol, 5.4 mg) and Hantzsch ester (0.15 mmol, 38.0 mg) were weighed in a flat-bottom Schlenk flask. The solids were

dissolved in THF (1 mL) and 2,4,6-collidine (0.15 mmol, 19.8 μL), VCC **4.1a-4.1t** (0.1 mmol) and aldehyde **4.2a-4.2ae** (0.15 mmol or 0.5 mmol) were added, affording a green solution. The flask was sealed with a Teflon cap and the mixture was freeze-pump-thawed 3 times and stirred under N_2 at room temperature for 5–20 minutes after which it was irradiated for 20 hours at 0 °C using a single high-power blue LED (λ_{em} = 445 nm, 100 mA, 0.2 μeinstein s^{-1}) from the bottom. After the reaction, the mixture was aerated and evaporated to dryness. The residue was dissolved in CH_2Cl_2 and passed through basic Al_2O_3 (3 cm, Ø = 0.5 cm) eluting with CH_2Cl_2 (10 mL), and subsequently CH_2Cl_2/MeOH (9:1, 5 mL). The second fraction was evaporated to dryness and purified by column chromatography (SiO_2, EtOAc/cyclohexane or EtOAc/CH_2Cl_2) to afford product **4.3a-4.3ay**.

1,2-Diphenyl-2-vinylpropane-1,3-diol (4.3a)

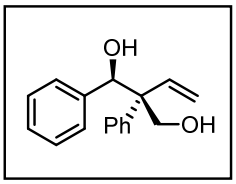

Yellowish oil (Method A, 23.6 mg, 93% yield, 90:10 *dr*); **IR** (neat): ν = 3361, 3060, 3030, 2890, 1636, 1600, 1494, 1446, 1049, 910, 728, 697 cm^{-1}; **^{1}H NMR** (500 MHz, $CDCl_3$) (major) δ_H 7.30-7.21 (m, 5H), 7.21-7.14 (m, 3H), 7.08-7.03 (m, 2H), 6.25 (dd, *J* = 18.0, 11.3 Hz, 1H), 5.44 (dd, *J* = 11.3, 1.1 Hz, 1H), 5.30 (s, 1H), 5.18 (dd, *J* = 18.0, 1.1 Hz, 1H), 4.00 (d, *J* = 11.2 Hz, 1H), 3.80 (d, *J* = 11.2 Hz, 1H), 2.62 (br s, 1H), 1.93 (br s, 1H); **^{1}H NMR** (500 MHz, $CDCl_3$) (minor, diagnostic peaks) δ_H 5.92 (dd, *J* = 17.8, 11.1 Hz, 1H), 5.36 (dd, *J* = 11.1, 1.1 Hz, 1H), 5.26 (s, 1H), 5.07 (dd, *J* = 17.8, 1.1 Hz, 1H); **^{13}C NMR** (126 MHz, $CDCl_3$) (major) δ_C 140.8, 140.3, 139.3, 128.6, 128.4, 128.0, 127.7, 127.6, 127.2, 117.8, 78.1, 66.0, 55.16; **^{13}C NMR** (126 MHz, $CDCl_3$) (minor, diagnostic peaks) δ_C 139.6, 118.4, 79.0, 65.8, 55.23; **HRMS** (ESI/TOF) *m/z*: $[M + Na]^+$ Calcd for $C_{17}H_{18}NaO_2$ 277.1199; Found 277.1200.

1-(4-Methoxyphenyl)-2-phenyl-2-vinylpropane-1,3-diol (4.3b)

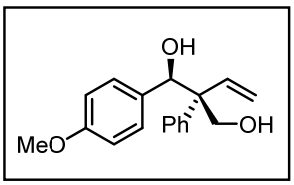

Yellowish oil (Method A, 24.8 mg, 87% yield, 96:4 *dr*); **IR** (neat): ν = 3403, 2935, 2904, 2836, 1724, 1610, 1511, 1243, 1175, 1031, 834, 699 cm^{-1}; **^{1}H NMR** (400 MHz, $CDCl_3$) (major) δ_H 7.32-7.22 (m, 5H), 7.04-6.96 (m, 2H), 6.78-6.71 (m, 2H), 6.27 (dd, *J* = 18.0, 11.3 Hz, 1H), 5.47 (dd, *J* = 11.3, 1.1 Hz, 1H), 5.29 (s, 1H), 5.21 (dd, *J* = 18.0, 1.1 Hz, 1H), 4.02 (d, *J* = 11.1 Hz, 1H), 3.82 (d, *J* = 10.5 Hz, 1H), 3.77 (s, 3H), 2.65 (br s, 1H), 1.95 (br s, 1H); **^{1}H NMR** (400 MHz, $CDCl_3$) (minor, diagnostic peaks) δ_H 5.96 (dd, *J* = 17.8, 11.1 Hz, 1H), 5.39 (dd, *J* = 11.1, 1.1 Hz, 1H), 5.25 (s, 1H), 5.11 (dd, *J* = 17.8, 1.2 Hz, 1H); **^{13}C NMR** (101 MHz, $CDCl_3$) (major) δ_C 159.1, 140.9, 139.4, 132.4, 129.1, 128.6, 128.4, 127.1, 117.7, 113.0, 77.7, 66.1, 55.3, 55.2; **^{13}C NMR** (101 MHz, $CDCl_3$) (minor, diagnostic peaks) δ_C 118.3, 65.2, 55.4; **HRMS** (ESI/TOF) *m/z*: $[M + Na]^+$ Calcd for $C_{18}H_{20}NaO_3$ 307.1305; Found 307.1308.

1-(4-(Methylthio)phenyl)-2-phenyl-2-vinylpropane-1,3-diol (4.3c)

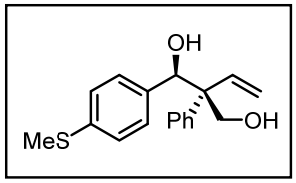

Yellowish oil (Method A, 24.2 mg, 81% yield, 95:5 *dr*); **IR** (neat): ν = 3366, 2921, 1598, 1493, 1050, 1013, 728, 699 cm^{-1}; **^{1}H NMR** (500 MHz, $CDCl_3$) (major) δ_H 7.30-7.20 (m, 5H), 7.08-7.03 (m, 2H), 7.00-6.94 (m, 2H), 6.22 (dd, J = 18.1, 11.3 Hz, 1H), 5.43 (dd, J = 11.3, 1.1 Hz, 1H), 5.26 (s, 1H), 5.17 (dd, J = 18.0, 1.1 Hz, 1H), 3.98 (d, J = 11.1 Hz, 1H), 3.78 (d, J = 11.1 Hz, 1H), 2.77 (br s, 1H), 2.42 (s, 3H), 1.95 (br s, 1H); **^{1}H NMR** (500 MHz, $CDCl_3$) (minor, diagnostic peaks) δ_H 5.91 (dd, J = 17.9, 11.1 Hz, 1H), 5.37 (dd, J = 11.1, 1.1 Hz, 1H), 5.22 (s, 1H), 5.09 (dd, J = 17.9, 1.1 Hz, 1H), 4.01 (d, J = 11.5 Hz, 1H), 3.96 (d, J = 11.5 Hz, 1H, partially overlaps); **^{13}C NMR** (126 MHz, $CDCl_3$) (major) δ_C 140.7, 139.3, 137.8, 137.2, 128.6, 128.5, 128.5, 127.2, 125.7, 117.8, 77.7, 66.1, 55.15, 15.9; **^{13}C NMR** (126 MHz, $CDCl_3$) (minor, diagnostic peaks) δ_C 139.5, 118.4, 78.6, 66.0, 55.23, 16.1; **HRMS** (ESI/TOF) *m/z*: $[M + Na]^+$ Calcd for $C_{18}H_{20}NaO_2S$ 323.1076; Found 323.1078.

***N*-(4-(1-Hydroxy-2-(hydroxymethyl)-2-phenylbut-3-en-1-yl)phenyl)acetamide (4.3d)**

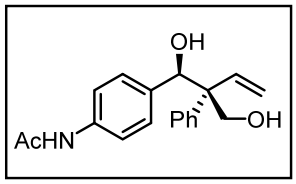

Yellowish oil (Method A, 30.3 mg, 97% yield, 95:5 *dr*); **IR** (neat): ν = 3307, 3061, 1666, 1601, 1536, 1515, 1411, 1371, 1317, 1052, 1017, 906, 726, 700 cm^{-1}; **^{1}H NMR** (400 MHz, $CDCl_3$) (major) δ_H 7.60-7.43 (m, 1H), 7.37-7.18 (m, 6H), 7.02-6.95 (m, 2H), 6.26 (dd, J = 18.0, 11.2 Hz, 1H), 5.46 (dd, J = 11.2, 1.1 Hz, 1H), 5.29 (s, 1H), 5.21 (dd, J = 18.0, 1.1 Hz, 1H), 4.02 (d, J = 11.1 Hz, 1H), 3.81 (d, J = 11.0 Hz, 1H), 2.35 (br s, 2H, partially overlaps), 2.12 (s, 3H); **^{1}H NMR** (400 MHz, $CDCl_3$) (minor, diagnostic peaks) δ_H 5.91 (dd, J = 17.8, 11.1 Hz, 1H), 5.36 (d, J = 11.3 Hz, 1H), 5.26 (s, 1H), 5.10 (d, J = 11.0 Hz, 1H), 2.17 (s, 3H); **^{13}C NMR** (101 MHz, $CDCl_3$) (major) δ_C 168.7, 140.7, 139.4, 137.3, 136.4, 128.6, 128.5, 128.4, 127.2, 119.0, 117.7, 77.8, 66.0, 54.9, 24.6; **^{13}C NMR** (101 MHz, $CDCl_3$) (minor, diagnostic peaks) δ_C 78.8; **HRMS** (ESI/TOF) *m/z*: $[M + Na]^+$ Calcd for $C_{19}H_{21}NNaO_3$ 334.1414; Found 334.1413.

1-(4-Isopropylphenyl)-2-phenyl-2-vinylpropane-1,3-diol (4.3e)

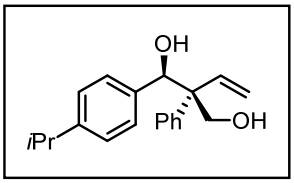

Yellowish oil (Method A, 24.2 mg, 82% yield, 94:6 *dr*); **IR** (neat): ν = 3370, 2960, 2872, 1446, 1051, 1016, 909, 730, 698 cm^{-1}; **^{1}H NMR** (500 MHz, $CDCl_3$) (major) δ_H 7.29-7.25 (m, 4H), 7.24-7.18 (m, 1H), 7.05-7.01 (m, 2H), 7.01-6.95 (m, 2H), 6.24 (dd, *J* = 18.0, 11.2 Hz, 1H), 5.43 (dd, *J* = 11.2, 1.1 Hz, 1H), 5.26 (s, 1H), 5.16 (dd, *J* = 18.1, 1.1 Hz, 1H), 3.97 (d, *J* = 11.2 Hz, 1H), 3.79 (d, *J* = 11.1 Hz, 1H), 2.83 (hept, *J* = 6.9 Hz, 1H), 2.44 (br s, 1H), 1.91 (br s, 1H), 1.18 (dd, *J* = 7.0, 1.0 Hz, 6H); **^{1}H NMR** (500 MHz, $CDCl_3$) (minor, diagnostic peaks) δ_H 5.89 (dd, *J* = 17.8, 11.1 Hz, 1H), 5.33 (dd, *J* = 11.1, 1.2 Hz, 1H), 5.23 (s, 1H), 5.03 (dd, *J* = 17.8, 1.2 Hz, 1H); **^{13}C NMR** (126 MHz, $CDCl_3$) (major) δ_C 148.4, 140.9, 139.3, 137.7, 128.7, 128.4, 127.9, 127.1, 125.7, 117.7, 77.9, 66.2, 55.3, 33.9, 24.10, 24.05; **^{13}C NMR** (126 MHz, $CDCl_3$) (minor, diagnostic peaks) δ_C 139.8, 118.3, 79.1, 65.7; **HRMS** (ESI/TOF) *m/z*: $[M + Na]^+$ Calcd for $C_{20}H_{24}NaO_2$ 319.1669; Found 319.1668.

1-([1,1'-Biphenyl]-4-yl)-2-phenyl-2-vinylpropane-1,3-diol (4.3f)

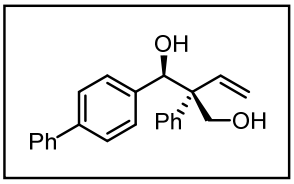

Yellowish solid (Method A, 28.1 mg, 85% yield, 92:8 *dr*); **IR** (neat): ν = 3301, 3031, 2934, 2896, 1635, 1600, 1486, 1052, 914, 695 cm^{-1}; **^{1}H NMR** (400 MHz, $CDCl_3$) (major) δ_H 7.62-7.54 (m, 2H), 7.49-7.40 (m, 4H), 7.38-7.24 (m, 6H), 7.19-7.12 (m, 2H), 6.32 (dd, *J* = 18.0, 11.3 Hz, 1H), 5.50 (dd, *J* = 11.3, 1.1 Hz, 1H), 5.38 (s, 1H), 5.24 (dd, *J* = 18.0, 1.1 Hz, 1H), 4.07 (d, *J* = 11.2 Hz, 1H), 3.88 (d, *J* = 11.2 Hz, 1H), 2.72 (br s, 1H), 2.19 (br s, 1H); **^{1}H NMR** (400 MHz, $CDCl_3$) (minor, diagnostic peaks) δ_H 6.00 (dd, *J* = 17.8, 11.1 Hz, 1H), 5.43 (dd, *J* = 11.1, 1.1 Hz, 1H), 5.35 (s, 1H), 5.15 (dd, *J* = 17.8, 1.1 Hz, 1H); **^{13}C NMR** (101 MHz, $CDCl_3$) (major) δ_C 140.8, 140.7, 140.4, 139.4, 139.3, 128.9, 128.6, 128.5, 128.4, 127.4, 127.2, 127.1, 126.2, 117.9, 77.8, 66.1, 55.2; **^{13}C NMR** (101 MHz, $CDCl_3$) (minor, diagnostic peaks) δ_C 139.5, 118.5, 78.8, 65.9, 55.3; **HRMS** (ESI/TOF) *m/z*: $[M + Na]^+$ Calcd for $C_{23}H_{22}NaO_2$ 353.1512; Found 353.1511.

1-(4-(Hydroxymethyl)phenyl)-2-phenyl-2-vinylpropane-1,3-diol (4.3g)

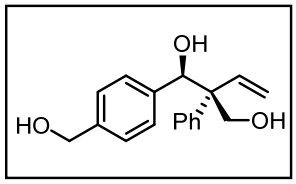

Yellowish oil (Method A, 27.7 mg, 97% yield, 95:5 *dr*); **IR** (neat): ν = 3346, 3089, 3058, 3025, 2881, 1420, 1042, 1013, 909, 728, 699 cm^{-1}; **^{1}H NMR** (400 MHz, $CDCl_3$) (major) δ_H 7.34-7.22 (m, 5H), 7.20-7.14 (m, 2H), 7.09-7.03 (m, 2H), 6.27 (dd, *J* = 18.0, 11.2 Hz, 1H), 5.46 (dd, *J* = 11.2, 1.1 Hz, 1H), 5.32 (s, 1H), 5.19 (dd, *J* = 18.0, 1.1 Hz, 1H), 4.61 (s, 2H), 4.00 (d, *J* = 11.1 Hz, 1H), 3.80 (d, *J* = 11.1 Hz, 1H), 2.25 (br s, 3H); **^{1}H NMR** (400 MHz, $CDCl_3$) (minor, diagnostic peaks) δ_H 5.92 (dd, *J* = 17.8, 11.1 Hz, 1H), 5.38 (dd, *J* = 11.1, 1.1 Hz, 1H), 5.28 (s, 1H), 5.08 (dd, *J* = 17.8, 1.1 Hz, 1H); **^{13}C NMR** (101 MHz, $CDCl_3$) (major) δ_C 140.7, 140.2, 139.7, 139.3, 128.6, 128.4, 128.2, 127.2, 126.2, 117.8, 77.8, 66.0, 65.1, 55.0; **^{13}C NMR** (101 MHz, $CDCl_3$) (minor, diagnostic peaks) δ_C 78.8, 65.9; **HRMS** (ESI/TOF) *m/z*: $[M + Na]^+$ Calcd for $C_{18}H_{20}NaO_3$ 307.1305; Found 307.1311.

1-(4-Fluorophenyl)-2-phenyl-2-vinylpropane-1,3-diol (4.3h)

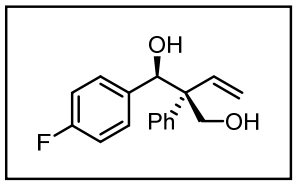

Yellowish oil (Method A, 24.8 mg, 91% yield, 88:12 *dr*); **IR** (neat): ν = 3358, 3059, 2894, 1603, 1509, 1222, 1158, 1051, 909, 838, 731, 699 cm^{-1}; **^{1}H NMR** (500 MHz, $CDCl_3$) (major) δ_H 7.30-7.25 (m, 2H), 7.24-7.20 (m, 3H), 7.04-6.98 (m, 2H), 6.89-6.81 (m, 2H), 6.21 (dd, *J* = 18.0, 11.3 Hz, 1H), 5.43 (dd, *J* = 11.3, 1.0 Hz, 1H), 5.29 (s, 1H), 5.16 (dd, *J* = 18.0, 1.0 Hz, 1H), 3.96 (d, *J* = 11.2 Hz, 1H), 3.76 (d, *J* = 11.2 Hz, 1H), 2.74 (br s, 1H), 1.84 (br s, 1H); **^{1}H NMR** (500 MHz, $CDCl_3$) (minor, diagnostic peaks) δ_H 5.92 (dd, *J* = 17.9, 11.1 Hz, 1H), 5.39 (dd, *J* = 11.1, 1.0 Hz, 1H), 5.23 (s, 1H), 5.11 (dd, *J* = 17.8, 1.0 Hz, 1H), 4.02 (d, *J* = 11.5 Hz, 1H), 3.94 (d, *J* = 11.5 Hz, 1H, partially overlaps); **^{13}C NMR** (126 MHz, $CDCl_3$) (major) δ_C 162.3 (d, *J* = 245.8 Hz), 140.6, 139.1, 136.02 (d, *J* = 3.2 Hz), 129.6 (d, *J* = 8.0 Hz), 128.52, 128.51, 127.3, 117.9, 114.4 (d, *J* = 21.3 Hz), 77.4, 65.97, 55.1; **^{13}C NMR** (126 MHz, $CDCl_3$) (minor, diagnostic peaks) δ_C 139.3, 135.95 (d, *J* = 3.1 Hz), 118.6, 114.5 (d, *J* = 21.3 Hz), 78.3, 66.00, 55.2; **^{19}F NMR** (376 MHz, $CDCl_3$) (major) δ_F -115.0-115.3 (m); **^{19}F NMR** (376 MHz, $CDCl_3$) (minor) δ_F -114.9-115.0 (m); **HRMS** (ESI/TOF) *m/z*: $[M + Na]^+$ Calcd for $C_{17}H_{17}FNaO_2$ 295.1105; Found 295.1107.

Methyl 4-(1-hydroxy-2-(hydroxymethyl)-2-phenylbut-3-en-1-yl)benzoate (4.3i)

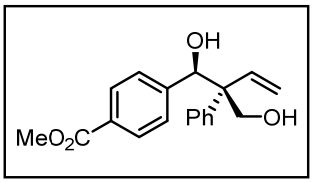

Yellowish oil (Method A, 20.2 mg, 65% yield, 85:15 *dr*); **IR** (neat): ν = 3400, 2951, 1706, 1611, 1436, 1277, 1108, 1008, 1053, 1017, 729, 699 cm^{-1}; **^{1}H NMR** (400 MHz, $CDCl_3$) (major) δ_H 7.89-7.81 (m, 2H), 7.36-7.19 (m, 5H), 7.16-7.11 (m, 2H), 6.25 (dd, *J* = 18.0, 11.2 Hz, 1H), 5.46 (dd, *J* = 11.2, 1.0 Hz, 1H), 5.39 (s, 1H), 5.20 (dd, *J* = 18.0, 1.0 Hz, 1H), 4.02 (d, *J* = 11.2 Hz, 1H), 3.88 (s, 3H), 3.81 (d, *J* = 11.2 Hz, 1H), 3.11 (br s, 1H), 2.08 (br s, 1H); **^{1}H NMR** (400 MHz, $CDCl_3$) (minor, diagnostic peaks) δ_H 5.94 (dd, *J* = 17.8, 11.1 Hz, 1H), 5.42 (dd, *J* = 11.1, 1.0 Hz, 1H), 5.34 (s, 1H), 5.14 (dd, *J* = 17.8, 1.0 Hz, 1H), 4.09 (d, *J* = 11.5 Hz, 1H); **^{13}C NMR** (101 MHz, $CDCl_3$) (major) δ_C 167.2, 145.7, 140.4, 139.1, 129.4, 128.8, 128.5, 128.4, 128.0, 127.4, 118.0, 77.7, 65.9, 54.9, 52.2; **^{13}C NMR** (101 MHz, $CDCl_3$) (minor, diagnostic peaks) δ_C 167.1, 145.5, 139.8, 138.9, 118.7, 78.5, 66.1, 55.1; **HRMS** (ESI/TOF) *m/z*: $[M + Na]^+$ Calcd for $C_{19}H_{20}NaO_4$ 335.1254; Found 335.1260.

2-Phenyl-1-(4-(trifluoromethyl)phenyl)-2-vinylpropane-1,3-diol (4.3j)

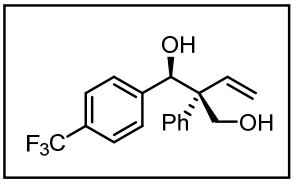

Yellowish oil (Method A, 27.2 mg, 84% yield, 80:20 *dr*); **IR** (neat): ν = 3379, 3061, 2898, 1620, 1323, 1163, 1113, 1066, 1016, 909, 850, 731, 699 cm^{-1}; **^{1}H NMR** (500 MHz, $CDCl_3$) (major) δ_H 7.42 (d, *J* = 8.1 Hz, 2H), 7.32-7.25 (m, 2H), 7.25-7.21 (m, 3H), 7.16 (d, *J* = 8.1 Hz, 2H), 6.21 (dd, *J* = 18.1, 11.3 Hz, 1H), 5.44 (dd, *J* = 11.3, 1.0 Hz, 1H), 5.37 (s, 1H), 5.16 (dd, *J* = 18.1, 0.9 Hz, 1H), 3.96 (d, *J* = 11.3 Hz, 1H), 3.76 (d, *J* = 11.2 Hz, 1H), 2.38 (br s, 2H); **^{1}H NMR** (500 MHz, $CDCl_3$) (minor, diagnostic peaks) δ_H 7.12 (d, *J* = 8.1 Hz, 2H), 5.90 (dd, *J* = 17.8, 11.1 Hz, 1H), 5.32 (s, 1H), 5.13 (dd, *J* = 10.4, 0.9 Hz, 1H), 4.06 (d, *J* = 11.5 Hz, 1H), 3.96 (d, *J* = 11.8 Hz, 1H); **^{13}C NMR** (126 MHz, $CDCl_3$) (major) δ_C 144.4, 140.3, 138.8, 129.8 (q, *J* = 32.3 Hz), 128.8, 128.7, 128.5, 128.4, 127.5, 124.4 (q, *J* = 4.0 Hz), 118.2, 77.4, 66.0, 55.0; **^{13}C NMR** (126 MHz, $CDCl_3$) (minor, diagnostic peaks) δ_C 144.3, 139.6, 118.9, 78.3, 66.2, 55.1; **^{19}F NMR** (471 MHz, $CDCl_3$) (major) δ_F -62.55; **^{19}F NMR** (471 MHz, $CDCl_3$) (minor) δ_F -62.57; **HRMS** (ESI/TOF) *m/z*: $[M + Na]^+$ Calcd for $C_{18}H_{17}F_3NaO_2$ 345.1073; Found 345.1090.

1-(3-(Benzyloxy)phenyl)-2-phenyl-2-vinylpropane-1,3-diol (4.3k)

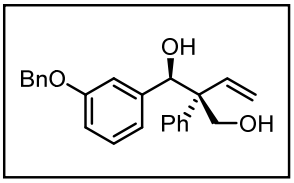

Yellowish oil (Method A, 32.3 mg, 90% yield, 91:9 *dr*); **IR** (neat): ν = 3380, 3063, 3033, 2883, 0266, 1494, 1446, 1252, 1025, 907, 727, 696 cm^{-1}; **^{1}H NMR** (400 MHz, $CDCl_3$) (major) δ_H 7.42-7.37 (m, 4H), 7.35-7.31 (m, 2H), 7.31-7.25 (m, 4H), 7.13 (t, *J* = 7.9 Hz, 1H), 6.85 (ddd, *J* = 8.2, 2.6, 1.0 Hz, 1H), 6.75-6.68 (m, 1H), 6.68-6.61 (m, 1H), 6.26 (dd, *J* = 18.0, 11.2 Hz, 1H), 5.46 (dd, *J* = 11.2, 1.1 Hz, 1H), 5.28 (s, 1H), 5.23 (dd, *J* = 18.0, 1.1 Hz, 1H), 4.90 (s, 2H), 4.04 (d, *J* = 11.1 Hz, 1H), 3.83 (d, *J* = 11.1 Hz, 1H), 2.16 (br s, 2H); **^{1}H NMR** (400 MHz, $CDCl_3$) (minor, diagnostic peaks) δ_H 5.96 (dd, *J* = 17.8, 11.1 Hz, 1H), 5.39 (dd, *J* = 11.1, 1.1 Hz, 1H), 5.12 (dd, *J* = 17.8, 1.2 Hz, 1H), 4.06 (d, *J* = 11.5 Hz, 1H, partially overlaps), 4.01 (d, *J* = 11.5 Hz, 1H, partially overlaps); **^{13}C NMR** (101 MHz, $CDCl_3$) (major) δ_C 158.1, 142.0, 140.9, 139.4, 137.23, 128.7, 128.6, 128.6, 128.4, 128.0, 127.6, 127.1, 120.6, 117.8, 114.7, 114.3, 78.1, 69.9, 65.9, 55.0; **^{13}C NMR** (101 MHz, $CDCl_3$) (minor, diagnostic peaks) δ_C 158.2, 141.9, 140.2, 139.5, 137.18, 120.7, 118.4, 114.8, 78.9, 70.1, 55.2; **HRMS** (ESI/TOF) *m/z*: $[M + Na]^+$ Calcd for $C_{24}H_{24}NaO_3$ 383.1618; Found 383.1625.

2-Phenyl-1-(*m*-tolyl)-2-vinylpropane-1,3-diol (4.3l)

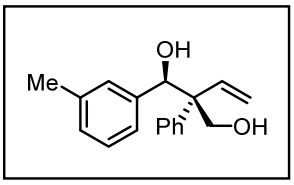

Yellowish oil (Method A, 20.2 mg, 75% yield, 89:11 *dr*); **IR** (neat): ν = 3361, 3058, 3025, 2921, 1493, 1445, 1051, 908, 728, 698 cm^{-1}; **^{1}H NMR** (400 MHz, $CDCl_3$) (major) δ_H 7.36-7.22 (m, 5H), 7.10 (t, *J* = 7.5 Hz, 1H), 7.06-7.00 (m, 1H), 6.91-6.83 (m, 2H), 6.29 (dd, *J* = 18.0, 11.2 Hz, 1H), 5.48 (dd, *J* = 11.2, 1.1 Hz, 1H), 5.28 (s, 1H), 5.23 (dd, *J* = 18.0, 1.1 Hz, 1H), 4.04 (d, *J* = 11.1 Hz, 1H), 3.84 (d, *J* = 11.2 Hz, 1H), 2.26 (s, 3H), 2.17 (br s, 2H, overlaps); **^{1}H NMR** (400 MHz, $CDCl_3$) (minor, diagnostic peaks) δ_H 5.96 (dd, *J* = 17.8, 11.1 Hz, 1H), 5.39 (dd, *J* = 11.1, 1.2 Hz, 1H), 5.10 (dd, *J* = 17.8, 1.1 Hz, 1H), 2.27 (s, 3H, partially overlaps); **^{13}C NMR** (101 MHz, $CDCl_3$) (major) δ_C 140.8, 140.2, 139.4, 137.1, 128.7, 128.6, 128.4, 128.3, 127.5, 127.1, 125.1, 117.8, 78.1, 66.0, 55.1, 21.5; **^{13}C NMR** (101 MHz, $CDCl_3$) (minor, diagnostic peaks) δ_C 140.13, 140.06, 139.7, 137.2, 118.3, 79.1, 65.8, 55.2, 21.6; **HRMS** (ESI/TOF) *m/z*: $[M + Na]^+$ Calcd for $C_{18}H_{20}NaO_2$ 291.1356; Found 291.1358.

1-(3-Chlorophenyl)-2-phenyl-2-vinylpropane-1,3-diol (4.3m)

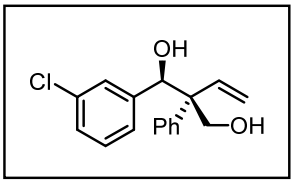

Yellowish oil (Method A, 22.1 mg, 77% yield, 83:17 *dr*); **IR** (neat): ν = 3356, 3061, 2896, 1596, 1573, 1429, 1194, 1050, 907, 729, 697 cm^{-1}; **^{1}H NMR** (400 MHz, $CDCl_3$) (major) δ_H 7.36-7.30 (m, 2H), 7.30-7.24 (m, 3H), 7.22-7.17 (m, 1H), 7.13 (t, *J* = 7.8 Hz, 1H), 7.09 (br t, *J* = 1.9 Hz, 1H), 6.94 (br d, *J* = 7.7 Hz, 1H), 6.25 (dd, *J* = 18.0, 11.3 Hz, 1H), 5.49 (dd, *J* = 11.3, 1.0 Hz, 1H), 5.31 (s, 1H), 5.21 (dd, *J* = 18.0, 1.0 Hz, 1H), 4.01 (d, *J* = 11.3 Hz, 1H), 3.82 (d, *J* = 11.2 Hz, 1H), 2.92 (br s, 1H), 1.90 (br s, 1H); **^{1}H NMR** (400 MHz, $CDCl_3$) (minor, diagnostic peaks) δ_H 7.13 (t, *J* = 7.7 Hz, 1H, partially overlaps), 7.05 (br t, *J* = 2.0 Hz, 1H), 6.91 (br d, *J* = 7.7 Hz, 1H, partially overlaps), 5.95 (dd, *J* = 17.9, 11.1 Hz, 1H), 5.45 (dd, *J* = 11.2, 1.0 Hz, 1H), 5.26 (s, 1H), 5.15 (dd, *J* = 17.8, 1.0 Hz, 1H), 4.09 (d, *J* = 11.5 Hz, 1H); **^{13}C NMR** (101 MHz, $CDCl_3$) (major) δ_C 142.5, 140.4, 138.9, 133.6, 128.7, 128.6, 128.5, 128.1, 127.8, 127.4, 126.2, 118.1, 77.4 (overlaps), 65.9, 55.0; **^{13}C NMR** (101 MHz, $CDCl_3$) (minor, diagnostic peaks) δ_C 142.4, 139.8, 139.0, 133.7, 118.7, 78.4, 66.1, 55.1; **HRMS** (ESI/TOF) *m/z*: $[M + Na]^+$ Calcd for $C_{17}H_{17}ClNaO_2$ 311.0809; Found 311.0809.

1-(2-Methoxyphenyl)-2-phenyl-2-vinylpropane-1,3-diol (4.3n)

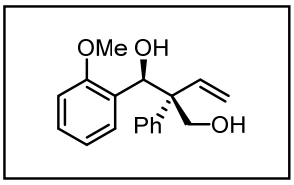

Yellowish oil (Method A, 25.6 mg, 90% yield, 84:16 *dr*); **IR** (neat): ν = 3401, 2939, 2837, 1600, 1491, 1462, 1440, 1240, 1050, 1028, 908, 754, 727, 698 cm^{-1}; **^{1}H NMR** (400 MHz, $CDCl_3$) (major) δ_H 7.44-7.38 (m, 2H), 7.35-7.28 (m, 3H), 7.28-7.22 (m, 2H), 6.95 (td, *J* = 7.5, 1.1 Hz, 1H), 6.81 (dd, *J* = 8.3, 1.1 Hz, 1H), 6.29 (dd, *J* = 18.1, 11.3 Hz, 1H), 5.76 (s, 1H), 5.43 (dd, *J* = 11.3, 1.2 Hz, 1H), 5.10 (dd, *J* = 18.1, 1.2 Hz, 1H), 3.89 (d, *J* = 11.6 Hz, 1H), 3.83 (d, *J* = 11.6 Hz, 1H), 3.66 (s, 3H), 2.72 (br s, 1H), 2.46 (br s, 1H); **^{1}H NMR** (400 MHz, $CDCl_3$) (minor, diagnostic peaks) δ_H 6.11 (dd, *J* = 17.8, 11.1 Hz, 1H), 5.62 (s, 1H), 5.39 (dd, *J* = 11.1, 1.2 Hz, 1H), 5.17 (dd, *J* = 17.8, 1.2 Hz, 1H); **^{13}C NMR** (101 MHz, $CDCl_3$) (major) δ_C 156.7, 141.2, 139.0, 129.9, 128.9, 128.8, 128.1, 126.9, 120.6, 117.6, 110.35, 71.7, 66.5, 56.2, 55.5; **^{13}C NMR** (101 MHz, $CDCl_3$) (minor, diagnostic peaks) δ_C 156.9, 140.8, 120.5, 117.4, 110.44, 65.6, 56.0; **HRMS** (ESI/TOF) *m/z*: $[M + Na]^+$ Calcd for $C_{18}H_{20}NaO_3$ 307.1305; Found 307.1300.

2-Phenyl-1-(*o*-tolyl)-2-vinylpropane-1,3-diol (4.3o)

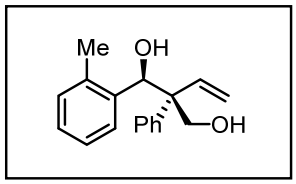

Yellowish oil (Method A, 21.6 mg, 80% yield, 94:6 *dr*); **IR** (neat): ν = 3242, 3056, 3021, 2968, 2926, 1491, 1469, 1444, 1041, 1015, 925, 748, 693 cm^{-1}; **^{1}H NMR** (500 MHz, $CDCl_3$) (major) δ_H 7.44-7.37 (m, 1H), 7.25-7.19 (m, 3H), 7.21-7.18 (m, 1H), 7.18-7.12 (m, 3H), 6.98 (br d, *J* = 7.5 Hz, 1H), 6.31 (dd, *J* = 18.1, 11.3 Hz, 1H), 5.60 (dd, *J* = 11.3, 1.0 Hz, 1H), 5.47 (s, 1H), 5.46 (dd, *J* = 18.1, 1.0 Hz, 1H, partially overlaps), 4.35 (d, *J* = 11.4 Hz, 1H), 3.87 (d, *J* = 11.4 Hz, 1H), 2.34 (br s, 2H), 1.80 (s, 3H); **^{1}H NMR** (500 MHz, $CDCl_3$) (minor, diagnostic peaks) δ_H 5.95 (dd, *J* = 17.7, 11.0 Hz, 1H), 5.51 (s, 1H), 5.27 (dd, *J* = 11.0, 1.2 Hz, 1H), 4.90 (dd, *J* = 17.6, 1.2 Hz, 1H), 4.24 (d, *J* = 11.6 Hz, 1H), 4.02 (d, *J* = 11.7 Hz, 1H); **^{13}C NMR** (126 MHz, $CDCl_3$) (major) δ_C 140.3, 140.1, 138.7, 136.9, 130.1, 128.7, 128.20, 128.19, 127.7, 127.3, 125.6, 117.8, 74.2, 65.6, 55.3, 19.3; **^{13}C NMR** (126 MHz, $CDCl_3$) (minor, diagnostic peaks) δ_C 139.6, 118.7, 75.2, 65.4, 55.9, 19.9; **HRMS** (ESI/TOF) *m/z*: $[M + Na]^+$ Calcd for $C_{18}H_{20}NaO_2$ 291.1356; Found 291.1357.

1-(3,5-Dimethylphenyl)-2-phenyl-2-vinylpropane-1,3-diol (4.3p)

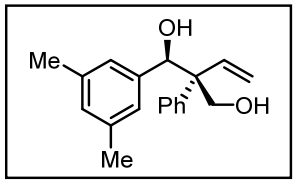

Yellowish oil (Method A, 23.0 mg, 81% yield, 89:11 *dr*); **IR** (neat): ν = 3198, 3019, 2918, 2862, 1602, 1445, 1067, 1042, 1016, 909, 853, 754, 731, 697 cm^{-1}; **^{1}H NMR** (400 MHz, $CDCl_3$) (major) δ_H 7.35-7.22 (m, 5H), 6.90-6.80 (m, 1H), 6.69-6.62 (m, 2H), 6.29 (dd, *J* = 18.0, 11.2 Hz, 1H), 5.49 (dd, *J* = 11.3, 1.1 Hz, 1H), 5.26 (dd, *J* = 18.0, 1.1 Hz, 1H, partially overlaps), 5.22 (s, 1H, overlaps), 4.05 (d, *J* = 11.2 Hz, 1H), 3.85 (d, *J* = 11.1 Hz, 1H), 2.22 (s, 6H), 2.18 (br s, 1H, overlaps); **^{1}H NMR** (400 MHz, $CDCl_3$) (minor, diagnostic peaks) δ_H 5.96 (dd, *J* = 17.8, 11.1 Hz, 1H), 5.39 (dd, *J* = 11.1, 1.2 Hz, 1H), 5.20 (s, 1H), 5.09 (dd, *J* = 17.8, 1.1 Hz, 1H), 2.23 (s, 6H, partially overlaps); **^{13}C NMR** (101 MHz, $CDCl_3$) (major) δ_C 140.9, 140.1, 139.5, 137.0, 129.3, 128.7, 128.3, 127.1, 125.8, 117.7, 78.2, 66.0, 55.2, 21.4; **^{13}C NMR** (101 MHz, $CDCl_3$) (minor, diagnostic peaks) δ_C 139.8, 137.1, 118.3, 79.2, 65.7; **HRMS** (ESI/TOF) *m/z*: $[M + Na]^+$ Calcd for $C_{19}H_{22}NaO_2$ 305.1512; Found 305.1502.

1-(3,4-Dimethoxyphenyl)-2-phenyl-2-vinylpropane-1,3-diol (4.3q)

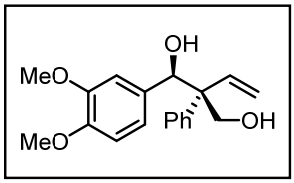

Yellowish oil (Method A, 25.5 mg, 81% yield, 95:5 *dr*); **IR** (neat): ν = 3414, 3002, 2936, 2836, 1514, 1464, 1256, 1234, 1139, 1025, 909, 727, 699 cm^{-1}; **^{1}H NMR** (500 MHz, $CDCl_3$) (major) δ_H 7.31-7.26 (m, 2H), 7.26-7.21 (m, 3H), 6.75 (dd, *J* = 8.3, 1.9 Hz, 1H), 6.72 (d, *J* = 8.3 Hz, 1H), 6.33 (d, *J* = 1.8 Hz, 1H), 6.27 (dd, *J* = 18.0, 11.3 Hz, 1H), 5.47 (dd, *J* = 11.2, 1.1 Hz, 1H), 5.26 (dd, *J* = 18.1, 1.1 Hz, 1H), 5.22 (s, 1H), 4.11 (d, *J* = 11.1 Hz, 1H), 3.86 (d, *J* = 11.1 Hz, 1H), 3.83 (s, 3H), 3.59 (s, 3H), 2.84 (br s, 1H), 2.17 (br s, 1H); **^{1}H NMR** (500 MHz, $CDCl_3$) (minor, diagnostic peaks) δ_H 6.03 (dd, *J* = 17.9, 11.1 Hz, 1H), 3.58 (s, 3H, partially overlaps); **^{13}C NMR** (126 MHz, $CDCl_3$) (major) δ_C 148.5, 148.0, 141.0, 139.8, 132.9, 128.7, 128.3, 127.0, 120.0, 117.6, 111.4, 110.2, 78.2, 65.8, 55.9, 55.7, 55.0; **^{13}C NMR** (126 MHz, $CDCl_3$) (minor, diagnostic peaks) δ_C 139.7, 120.2, 118.5, 111.2, 78.5, 66.1; **HRMS** (ESI/TOF) *m/z*: [M + Na]+ Calcd for $C_{19}H_{22}NaO_4$ 337.1410; Found 337.1404.

1-(3,4-Dichlorophenyl)-2-phenyl-2-vinylpropane-1,3-diol (4.3r)

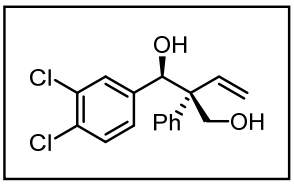

Yellowish oil (Method A, 27.8 mg, 86% yield, 79:21 *dr*); **IR** (neat): ν = 3357, 3087, 3060, 2895, 1468, 1392, 1053, 1029, 908, 730, 699 cm^{-1}; **^{1}H NMR** (500 MHz, $CDCl_3$) (major) δ_H 7.35-7.28 (m, 2H), 7.25-7.21 (m, 3H), 7.15 (d, *J* = 2.1 Hz, 1H), 6.85 (dd, *J* = 8.3, 2.1 Hz, 1H), 6.20 (dd, *J* = 18.0, 11.2 Hz, 1H), 5.47 (dd, *J* = 11.1, 0.9 Hz, 1H), 5.28 (s, 1H), 5.19 (dd, *J* = 18.0, 0.8 Hz, 1H), 3.97 (d, *J* = 11.2 Hz, 1H), 3.78 (d, *J* = 11.2 Hz, 1H), 3.14 (br s, 1H), 1.90 (br s, 1H); **^{1}H NMR** (500 MHz, $CDCl_3$) (minor, diagnostic peaks) δ_H 7.09 (d, *J* = 2.1 Hz, 1H), 6.80 (dd, *J* = 8.3, 2.1 Hz, 1H), 5.93 (dd, *J* = 17.9, 11.2 Hz, 1H), 5.46 (dd, *J* = 11.1, 0.7 Hz, 1H, partially overlaps), 5.22 (s, 1H), 5.17 (dd, *J* = 17.9, 0.9 Hz, 1H, partially overlaps), 4.08 (d, *J* = 11.5 Hz, 1H); **^{13}C NMR** (126 MHz, $CDCl_3$) (major) δ_C 140.7, 140.2, 138.7, 131.7, 131.5, 130.0, 129.4, 128.7, 128.4, 127.5, 127.4, 118.2, 76.8, 65.9, 54.9; **^{13}C NMR** (126 MHz, $CDCl_3$) (minor, diagnostic peaks) δ_C 138.6, 119.0, 77.8, 66.3, 55.0; **HRMS** (ESI/TOF) *m/z*: $[M + Na]^+$ Calcd for $C_{17}H_{16}Cl_2NaO_2$ 345.0420; Found 345.0430.

1-(4-Hydroxy-3-methoxyphenyl)-2-phenyl-2-vinylpropane-1,3-diol (4.3s)

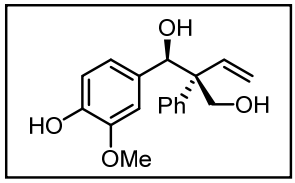

Yellowish solid (Method B, 21.7 mg, 72% yield, 97:3 *dr*); **IR** (neat): ν = 3337, 3057, 2940, 2884, 1601, 1515, 1432, 1270, 1235, 1151, 1054, 1030, 910, 737, 696 cm^{-1}; **^{1}H NMR** (500 MHz, $CDCl_3$) (major) δ_H 7.32-7.21 (m, 5H), 6.76 (d, J = 8.1 Hz, 1H), 6.68 (dd, J = 8.2, 2.0 Hz, 1H), 6.34 (d, J = 2.0 Hz, 1H), 6.27 (dd, J = 18.0, 11.2 Hz, 1H), 5.62 (br s, 1H), 5.47 (dd, J = 11.3, 1.1 Hz, 1H), 5.26 (dd, J = 18.0, 1.1 Hz, 1H), 5.21 (s, 1H), 4.10 (d, J = 11.1 Hz, 1H), 3.86 (d, J = 11.1 Hz, 1H), 3.61 (s, 3H), 2.80 (br s, 1H), 2.06 (br s, 1H); **^{1}H NMR** (500 MHz, $CDCl_3$) (minor, diagnostic peaks) δ_H 6.03 (dd, J = 17.9, 11.1 Hz, 1H); **^{13}C NMR** (126 MHz, $CDCl_3$) (major) δ_C 145.7, 145.1, 141.0, 139.8, 132.2, 128.7, 128.3, 127.0, 120.8, 117.6, 113.5, 110.8, 78.2, 65.8, 55.8, 55.1; **^{13}C NMR** (126 MHz, $CDCl_3$) (minor, diagnostic peaks) δ_C 145.4, 78.6, 65.5; **HRMS** (ESI/TOF) m/z: $[M + Na]^+$ Calcd for $C_{18}H_{20}NaO_4$ 323.1254; Found 323.1246.

1-(Furan-2-yl)-2-phenyl-2-vinylpropane-1,3-diol (4.3t)

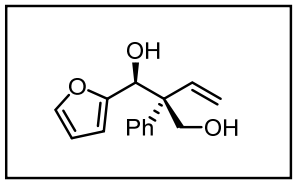

Yellowish oil (Method A, 21.7 mg, 89% yield, 88:12 *dr*); **IR** (neat): ν = 3385, 3088, 3056, 2891, 1497, 1446, 1147, 1052, 1008, 910, 729, 698 cm^{-1}; **^{1}H NMR** (500 MHz, $CDCl_3$) (major) δ_H 7.35-7.28 (m, 5H), 7.27-7.22 (m, 1H), 6.26 (dd, J = 3.2, 1.8 Hz, 1H, partially overlaps), 6.21 (dd, J = 18.0, 11.2 Hz, 1H, partially overlaps), 6.01 (dt, J = 3.3, 0.7 Hz, 1H), 5.49 (dd, J = 11.2, 1.1 Hz, 1H), 5.31 (s, 1H), 5.27 (dd, J = 18.0, 1.1 Hz, 1H), 4.21 (d, J = 11.3 Hz, 1H), 3.93 (d, J = 11.2 Hz, 1H), 2.90 (br s, 1H), 2.02 (br s, 1H); **^{1}H NMR** (500 MHz, $CDCl_3$) (minor, diagnostic peaks) δ_H 6.07 (dt, J = 3.3, 0.6 Hz, 1H, overlaps), 6.07 (dd, J = 17.9, 11.1 Hz, 1H, partially overlaps), 5.43 (dd, J = 11.2, 1.1 Hz, 1H), 5.34 (s, 1H), 5.16 (dd, J = 17.9, 1.1 Hz, 1H), 4.17 (d, J = 11.5 Hz, 1H), 4.08 (d, J = 11.5 Hz, 1H); **^{13}C NMR** (126 MHz, $CDCl_3$) (major) δ_C 154.1, 141.7, 140.36, 139.3, 128.5, 128.3, 127.2, 118.1, 110.3, 108.3, 72.3, 66.6, 55.2; **^{13}C NMR** (126 MHz, $CDCl_3$) (minor, diagnostic peaks) δ_C 153.9, 141.8, 140.41, 138.6, 118.5, 108.5, 72.7, 66.9, 55.0; **HRMS** (ESI/TOF) m/z: $[M + Na]^+$ Calcd for $C_{15}H_{16}NaO_3$ 267.0992; Found 267.0998.

tert-Butyl 3-(1-hydroxy-2-(hydroxymethyl)-2-phenylbut-3-en-1-yl)-1*H*-indole-1-carboxylate (4.3u)

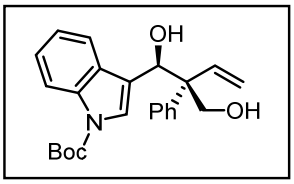

Yellowish oil (Method A, 36.2 mg, 92% yield, 96:4 *dr*); **IR** (neat): ν = 3400, 3053, 2979, 2933, 1730, 1451, 1368, 1254, 1152, 1082, 736, 700 cm^{-1}; **^{1}H NMR** (400 MHz, $CDCl_3$) (major) δ_H 8.09 (d, J = 8.4 Hz, 1H), 7.45-7.36 (m, 3H), 7.34-7.28 (m, 2H), 7.28-7.21 (m, 2H), 7.18 (br s, 1H), 7.16-7.07 (m, 1H), 6.29 (dd, J = 18.0, 11.3 Hz, 1H), 5.61 (s, 1H), 5.49 (dd, J = 11.3, 1.0 Hz, 1H), 5.29 (dd, J = 18.1, 1.0 Hz, 1H), 4.19 (d, J = 11.2 Hz, 1H), 3.95 (d, J = 11.2 Hz, 1H), 2.63 (br s, 1H), 1.95 (br s, 1H), 1.62 (s, 9H); **^{1}H NMR** (400 MHz, $CDCl_3$) (minor, diagnostic peaks) δ_H 8.16 (d, J = 8.5 Hz, 1H, partially overlaps), 6.12 (dd, J = 17.8, 11.1 Hz, 1H), 5.44 (dd, J = 11.1, 0.9 Hz, 1H, partially overlaps), 5.20 (dd, J = 17.8, 1.1 Hz, 1H), 1.64 (s, 9H); **^{13}C NMR** (101 MHz, $CDCl_3$) (major) δ_C 149.7, 140.7, 139.4, 134.9, 130.0, 128.8, 128.4, 127.3, 124.9, 124.3, 122.6, 120.4, 119.8, 117.8, 115.1, 83.8, 71.5, 66.3, 55.4, 28.3; **^{13}C NMR** (101 MHz, $CDCl_3$) (minor, diagnostic peaks) δ_C 115.5, 71.4; **HRMS** (ESI/TOF) *m/z*: $[M + Na]^+$ Calcd for $C_{24}H_{27}NNaO_4$ 416.1832; Found 416.1828.

1-(6-Methoxynaphthalen-2-yl)-2-phenyl-2-vinylpropane-1,3-diol (4.3v)

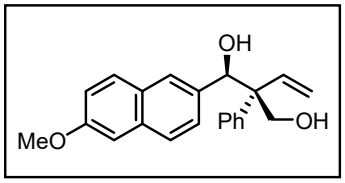

Yellowish foam (Method A, 30.8 mg, 92% yield, 96:4 *dr*); **IR** (neat): ν = 3387, 3059, 2938, 1606, 1483, 1264, 1031, 905, 726, 699 cm^{-1}; **^{1}H NMR** (500 MHz, $CDCl_3$) (major) δ_H 7.61 (d, J = 9.0 Hz, 1H), 7.54 (d, J = 8.6 Hz, 1H), 7.48 (s, 1H), 7.34-7.22 (m, 5H), 7.17-7.06 (m, 3H), 6.32 (dd, J = 18.0, 11.3 Hz, 1H), 5.47 (dd, J = 11.2, 1.1 Hz, 1H), 5.43 (s, 1H), 5.21 (dd, J = 18.0, 1.1 Hz, 1H), 4.06 (d, J = 11.2 Hz, 1H), 3.91 (s, 3H), 3.85 (d, J = 11.1 Hz, 1H), 2.96 (br s, 1H), 2.07 (br s, 1H); **^{1}H NMR** (500 MHz, $CDCl_3$) (minor, diagnostic peaks) δ_H 5.99 (dd, J = 17.8, 11.1 Hz, 1H), 5.40 (s, 1H, partially overlaps), 5.40 (dd, J = 11.0, 0.9 Hz, 1H), 5.11 (dd, J = 17.8, 1.0 Hz, 1H); **^{13}C NMR** (126 MHz, $CDCl_3$) (major) δ_C 157.8, 140.8, 139.4, 135.6, 134.1, 129.7, 128.6, 128.4, 128.3, 127.1, 126.8, 126.6, 125.8, 118.9, 117.8, 105.6, 78.2, 66.1, 55.4, 55.2; **^{13}C NMR** (126 MHz, $CDCl_3$) (minor, diagnostic peaks) δ_C 140.2, 139.6, 135.5, 79.1; **HRMS** (ESI/TOF) *m/z*: $[M + Na]^+$ Calcd for $C_{22}H_{22}NaO_3$ 357.1461; Found 357.1468.

2,5-Diphenyl-2-vinylpentane-1,3-diol (4.3w)

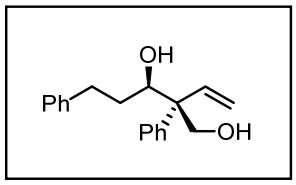

Yellowish oil (Method A, 14.7 mg, 52% yield, 82:18 *dr*); **IR** (neat): ν = 3385, 3084, 3060, 3025, 2927, 1495, 1446, 1046, 921, 698 cm^{-1}; **^{1}H NMR** (500 MHz, $CDCl_3$) (major) δ_H 7.37-7.32 (m, 4H), 7.28-7.23 (m, 4H), 7.15-7.12 (m, 2H), 6.12 (dd, *J* = 18.0, 11.3 Hz, 1H), 5.44 (dd, *J* = 11.3, 1.0 Hz, 1H), 5.17 (dd, *J* = 18.0, 1.0 Hz, 1H), 4.18 (d, *J* = 11.1 Hz, 1H), 4.12 (dd, *J* = 10.5, 1.7 Hz, 1H), 3.97 (d, *J* = 11.1 Hz, 1H), 2.89 (ddd, *J* = 14.2, 9.5, 4.9 Hz, 1H), 2.63 (ddd, *J* = 13.7, 9.1, 7.4 Hz, 1H), 1.89 (br s, 2H), 1.76 (dddd, *J* = 14.1, 9.3, 7.4, 1.7 Hz, 1H), 1.60-1.50 (m, 1H); **^{1}H NMR** (500 MHz, $CDCl_3$) (minor, diagnostic peaks) δ_H 6.02 (dd, *J* = 18.0, 11.3 Hz, 1H), 5.49 (dd, *J* = 11.3, 1.1 Hz, 1H), 5.29 (dd, *J* = 18.0, 1.1 Hz, 1H), 4.23 (dd, *J* = 10.5, 1.7 Hz, 1H), 4.09 (d, *J* = 11.4 Hz, 1H), 4.04 (d, *J* = 11.3 Hz, 1H), 1.65 (dddd, *J* = 14.0, 10.5, 9.0, 4.9 Hz, 1H); **^{13}C NMR** (126 MHz, $CDCl_3$) (major) δ_C 142.1, 140.7, 140.4, 128.67, 128.63, 128.5, 128.3, 127.13, 126.00, 117.3, 74.7, 66.2, 54.7, 34.3, 33.1; **^{13}C NMR** (126 MHz, $CDCl_3$) (minor, diagnostic peaks) δ_C 142.0, 141.6, 138.3, 128.75, 128.0, 127.08, 126.04, 118.6, 75.4, 67.6, 54.6, 34.5, 33.0; **HRMS** (ESI/TOF) *m/z*: $[M + Na]^+$ Calcd for $C_{19}H_{22}NaO_2$ 305.1512; Found 305.1510.

4-Methyl-2-phenyl-2-vinylpentane-1,3-diol (4.3x)

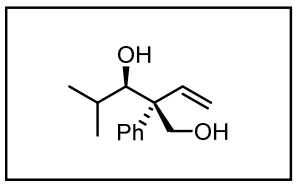

Yellowish oil (Method C, 9.5 mg, 43% yield, 95:5 *dr*); **IR** (neat): ν = 3384, 3087, 3059, 2959, 2874, 1733, 1634, 1600, 1495, 1467, 1446, 1254, 1047, 1002, 920, 700 cm^{-1}; **^{1}H NMR** (400 MHz, $CDCl_3$) (major) δ_H 7.44-7.37 (m, 2H), 7.37-7.31 (m, 2H), 7.29-7.22 (m, 1H), 6.23 (dd, *J* = 18.0, 11.3 Hz, 1H), 5.46 (dd, *J* = 11.3, 1.1 Hz, 1H), 5.27 (dd, *J* = 18.0, 1.1 Hz, 1H), 4.28 (d, *J* = 11.1 Hz, 1H), 4.00 (d, *J* = 11.1 Hz, 1H, overlaps), 3.98 (d, *J* = 3.1 Hz, 1H, overlaps), 2.02 (br s, 2H), 1.80 (heptd, *J* = 6.8, 3.1 Hz, 1H), 0.90 (d, *J* = 6.9 Hz, 3H), 0.67 (d, *J* = 6.7 Hz, 3H); **^{1}H NMR** (400 MHz, $CDCl_3$) (minor, diagnostic peaks) δ_H 5.51 (dd, *J* = 11.3, 1.1 Hz, 1H ,partially overlaps), 5.33 (dd, *J* = 18.0, 1.1 Hz, 1H, partially overlaps), 0.87 (d, *J* = 7.3 Hz, 3H, partially overlaps); **^{13}C NMR** (101 MHz, $CDCl_3$) (major) δ_C 141.3, 141.2, 128.6, 128.2, 127.0, 116.9, 79.4, 66.3, 55.0, 29.5, 23.2, 17.1; **^{13}C NMR** (101 MHz, $CDCl_3$) (minor, diagnostic peaks) δ_C 140.8, 128.7, 128.0, 79.9; **HRMS** (ESI/TOF) *m/z*: $[M + Na]^+$ Calcd for $C_{14}H_{20}NaO_2$ 243.1356; Found 243.1351.

1,2-Bis(4-methoxyphenyl)-2-vinylpropane-1,3-diol (4.3y)

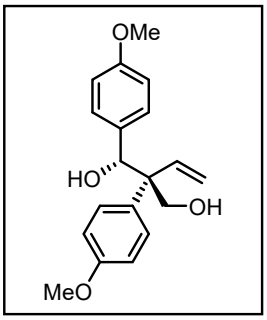

Yellowish oil (Method A, 21.3 mg, 68% yield, 94:6 *dr*); **IR** (neat): ν = 3414, 3001, 2935, 2836, 1609, 1510, 1244, 1175, 1031, 909, 831, 728 cm^{-1}; **^{1}H NMR** (400 MHz, $CDCl_3$) (major) δ_H 7.24-7.16 (m, 2H), 7.06-6.98 (m, 2H), 6.88-6.80 (m, 2H), 6.79-6.72 (m, 2H), 6.24 (dd, *J* = 18.0, 11.2 Hz, 1H), 5.45 (dd, *J* = 11.2, 1.1 Hz, 1H), 5.24 (s, 1H), 5.20 (dd, *J* = 18.0, 1.1 Hz, 1H), 3.99 (d, *J* = 11.1 Hz, 1H), 3.81 (app s, 1H, overlaps), 3.80 (s, 3H), 3.78 (s, 3H), 2.53 (br s, 1H), 1.89 (br s, 1H); **^{1}H NMR** (400 MHz, $CDCl_3$) (minor, diagnostic peaks) δ_H 5.95 (dd, *J* = 17.8, 11.0 Hz, 1H), 5.39 (dd, *J* = 11.0, 1.1 Hz, 1H), 5.20 (s, 1H), 5.13 (dd, *J* = 17.8, 1.1 Hz, 1H); **^{13}C NMR** (101 MHz, $CDCl_3$) (major) δ_C 159.1, 158.6, 139.6, 132.51, 132.46, 129.8, 129.1, 117.5, 113.8, 113.0, 77.7, 66.2, 55.4, 55.3, 54.7; **^{13}C NMR** (101 MHz, $CDCl_3$) (minor, diagnostic peaks) δ_C 130.2, 128.5, 118.2, 113.6, 113.1; **HRMS** (ESI/TOF) *m/z*: $[M + Na]^+$ Calcd for $C_{19}H_{22}NaO_4$ 337.1410; Found 337.1411.

2-(4-(*tert*-Butyl)phenyl)-1-(4-methoxyphenyl)-2-vinylpropane-1,3-diol (4.3z)

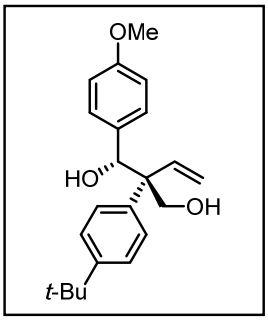

Yellowish oil (Method A, 26.1 mg, 77% yield, 95:5 *dr*); **IR** (neat): ν = 3378, 2961, 2904, 2836, 1611, 1511, 1463, 1245, 1175, 1034, 909, 833, 729 cm^{-1}; **^{1}H NMR** (400 MHz, $CDCl_3$) (major) δ_H 7.38-7.28 (m, 2H), 7.28-7.19 (m, 2H), 7.10-6.98 (m, 2H), 6.80-6.70 (m, 2H), 6.26 (dd, *J* = 18.1, 11.3 Hz, 1H), 5.44 (d, *J* = 11.2 Hz, 1H), 5.31 (s, 1H), 5.17 (d, *J* = 18.0 Hz, 1H), 3.93 (d, *J* = 11.2 Hz, 1H), 3.78 (s, 3H), 3.76 (app s, 1H, overlaps), 2.37 (br s, 1H), 1.84 (br s, 1H), 1.32 (s, 9H); **^{1}H NMR** (400 MHz, $CDCl_3$) (minor, diagnostic peaks) δ_H 5.92 (dd, *J* = 17.8, 11.0 Hz, 1H), 5.35 (d, *J* = 11.1 Hz, 1H), 5.24 (s, 1H), 5.08 (d, *J* = 17.8 Hz, 1H); **^{13}C NMR** (101 MHz, $CDCl_3$) (major) δ_C 159.1, 150.0, 139.2, 137.6, 132.5, 129.2, 128.2, 125.4, 117.5, 112.9, 77.3, 66.3, 55.3, 55.0, 34.5, 31.5; **^{13}C NMR** (101 MHz, $CDCl_3$) (minor, diagnostic peaks) δ_C 139.9, 128.6, 125.2, 118.0, 113.0, 78.7, 65.7, 54.9; **HRMS** (ESI/TOF) *m/z*: $[M + Na]^+$ Calcd for $C_{22}H_{28}NaO_3$ 363.1931; Found 363.1932.

1-(4-Methoxyphenyl)-2-(*p*-tolyl)-2-vinylpropane-1,3-diol (4.3aa)

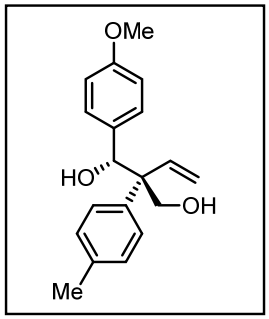

Yellowish oil (Method A, 17.8 mg, 60% yield, 97:3 *dr*); **IR** (neat): ν = 3388, 2934, 2836, 1611, 1510, 1244, 1175, 1032, 909, 835, 813, 729 cm^{-1}; **^{1}H NMR** (500 MHz, $CDCl_3$) (major) δ_H 7.21-7.16 (m, 2H), 7.14-7.09 (m, 2H), 7.07-7.01 (m, 2H), 6.79-6.73 (m, 2H), 6.25 (dd, *J* = 18.1, 11.3 Hz, 1H), 5.44 (dd, *J* = 11.3, 1.1 Hz, 1H), 5.27 (s, 1H), 5.18 (dd, *J* = 18.0, 1.1 Hz, 1H), 3.96 (d, *J* = 11.1 Hz, 1H), 3.80 (app s, 1H, overlaps), 3.78 (s, 3H), 2.62 (br s, 1H), 2.33 (s, 3H), 1.90 (br s, 1H); **^{1}H NMR** (500 MHz, $CDCl_3$) (minor, diagnostic peaks) δ_H 7.30-7.27 (m, 2H), 6.91-6.87 (m, 2H), 5.96-5.88 (m, 1H), 5.37 (dd, *J* = 11.1, 1.1 Hz, 1H), 5.23 (s, 1H), 5.10 (dd, *J* = 17.8, 1.1 Hz, 1H), 3.99 (d, *J* = 5.7 Hz, 1H), 2.35 (s, 3H); **^{13}C NMR** (126 MHz, $CDCl_3$) (major) δ_C 159.2, 139.4, 137.7, 136.8, 132.5, 129.19, 129.17, 128.5, 117.5, 113.0, 77.6, 66.2, 55.3, 55.0, 21.1; **^{13}C NMR** (126 MHz, $CDCl_3$) (minor, diagnostic peaks) δ_C 139.9, 129.0, 128.9, 128.8; **HRMS** (ESI/TOF) *m/z*: $[M + Na]^+$ Calcd for $C_{19}H_{22}NaO_3$ 321.1461; Found 321.1457.

2-([1,1'-Biphenyl]-4-yl)-1-(4-methoxyphenyl)-2-vinylpropane-1,3-diol (4.3ab)

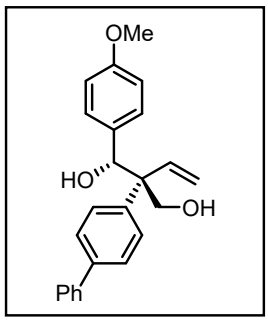

Yellowish oil (Method A, 33.5 mg, 93% yield, 95:5 *dr*); **IR** (neat): ν = 3455, 3030, 2921, 2877, 1605, 1505, 1487, 1323, 1168, 1046, 1005, 926, 837, 827, 772, 759, 729, 696 cm^{-1}; **^{1}H NMR** (400 MHz, $CDCl_3$) (major) δ_H 7.63-7.58 (m, 2H), 7.58-7.52 (m, 2H), 7.49-7.42 (m, 2H), 7.41-7.33 (m, 3H), 7.10-7.04 (m, 2H), 6.80-6.74 (m, 2H), 6.30 (dd, *J* = 18.0, 11.3 Hz, 1H), 5.49 (dd, *J* = 11.3, 1.1 Hz, 1H), 5.33 (s, 1H), 5.23 (dd, *J* = 18.1, 1.1 Hz, 1H), 4.04 (d, *J* = 11.1 Hz, 1H), 3.86 (d, *J* = 11.1 Hz, 1H), 3.78 (s, 3H), 2.61 (br s, 1H), 1.95 (br s, 1H); **^{1}H NMR** (400 MHz, $CDCl_3$) (minor, diagnostic peaks) δ_H 5.99 (dd, *J* = 17.7, 11.1 Hz, 1H), 5.41 (dd, *J* = 11.1, 1.1 Hz, 1H), 5.28 (s, 1H), 5.14 (dd, *J* = 17.8, 1.0 Hz, 1H); **^{13}C NMR** (101 MHz, $CDCl_3$) (major) δ_C 159.2, 140.7, 139.9, 139.8, 139.3, 132.4, 129.2, 129.1, 128.9, 127.5, 127.1, 127.0, 117.8, 113.0, 77.6, 66.2, 55.3, 55.1; **^{13}C NMR** (101 MHz, $CDCl_3$) (minor, diagnostic peaks) δ_C 129.5, 128.8, 126.8, 118.3, 113.1, 78.7, 65.2, 55.4; **HRMS** (ESI/TOF) *m/z*: $[M + Na]^+$ Calcd for $C_{24}H_{24}NaO_3$ 383.1618; Found 383.1627.

2-(4-Chlorophenyl)-1-(4-methoxyphenyl)-2-vinylpropane-1,3-diol (4.3ac)

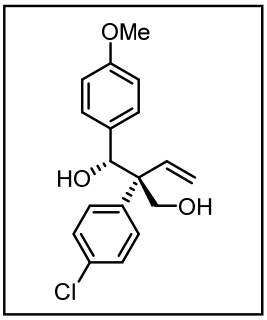

Yellowish oil (Method A, 25.0 mg, 78% yield, 94:6 *dr*); **IR** (neat): ν = 3385. 2935, 2837, 1611, 1511, 1492, 1245, 1176, 1032, 1012, 907, 833, 728 cm^{-1}; **^{1}H NMR** (400 MHz, $CDCl_3$) (major) δ_H 7.27-7.23 (m, 2H), 7.22-7.17 (m, 2H), 7.01-6.94 (m, 2H), 6.77-6.71 (m, 2H), 6.20 (dd, *J* = 18.0, 11.2 Hz, 1H), 5.46 (dd, *J* = 11.2, 1.0 Hz, 1H), 5.20 (s, 1H), 5.18 (app d, *J* = 1.0 Hz, 1H, overlaps), 4.01 (d, *J* = 11.1 Hz, 1H), 3.79 (d, *J* = 11.2 Hz, 1H), 3.77 (s, 3H), 2.05 (br s, 2H); **^{1}H NMR** (400 MHz, $CDCl_3$) (minor, diagnostic peaks) δ_H 5.93 (dd, *J* = 17.8, 11.1 Hz, 1H), 5.38 (dd, *J* = 11.1, 1.0 Hz, 1H), 5.17 (s, 1H), 5.05 (dd, *J* = 17.8, 1.0 Hz, 1H); **^{13}C NMR** (101 MHz, $CDCl_3$) (major) δ_C 159.3, 139.4, 139.2, 132.9, 132.2, 130.3, 129.1, 128.3, 118.0, 113.1, 77.6, 66.0, 55.3, 54.9; **^{13}C NMR** (101 MHz, $CDCl_3$) (minor, diagnostic peaks) δ_C 139.6, 130.7, 128.2, 118.6, 113.2, 78.5, 65.7; **HRMS** (ESI/TOF) *m/z*: $[M + Na]^+$ Calcd for $C_{18}H_{19}ClNaO_3$ 341.0915; Found 341.0910.

1-(4-Methoxyphenyl)-2-(4-(methylsulfonyl)phenyl)-2-vinylpropane-1,3-diol (4.3ad)

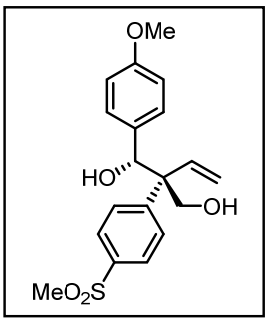

Yellowish foam (Method A, 33.1 mg, 91% yield, 85:15 *dr*); **IR** (neat): ν = 3514, 2911, 2834, 1609, 1588, 1510, 1295, 1227, 1242, 1143, 1030, 905, 838, 779, 726 cm^{-1}; **^{1}H NMR** (400 MHz, $CDCl_3$) (major) δ_H 7.94-7.77 (m, 2H), 7.63-7.47 (m, 2H), 7.06-6.96 (m, 2H), 6.82-6.70 (m, 2H), 6.22 (dd, *J* = 18.0, 11.2 Hz, 1H), 5.48 (dd, *J* = 11.2, 0.9 Hz, 1H), 5.29 (s, 1H), 5.14 (dd, *J* = 18.1, 0.9 Hz, 1H), 4.02 (d, *J* = 11.1 Hz, 1H), 3.86 (d, *J* = 11.1 Hz, 1H), 3.77 (s, 3H), 3.03 (s, 3H), 2.67 (br s, 1H), 2.10 (br s, 1H); **^{1}H NMR** (400 MHz, $CDCl_3$) (minor, diagnostic peaks) δ_H 5.92 (dd, *J* = 17.8, 11.1 Hz, 1H), 5.36 (dd, *J* = 11.1, 0.9 Hz, 1H), 5.22 (s, 1H), 4.95 (dd, *J* = 17.8, 0.9 Hz, 1H), 3.78 (s, 3H), 3.04 (s, 3H); **^{13}C NMR** (101 MHz, $CDCl_3$) (major) δ_C 159.4, 148.0, 138.81, 138.5, 132.0, 130.1, 129.1, 126.9, 118.5, 113.2, 77.19 (overlaps), 66.0, 55.6, 55.3, 44.6; **^{13}C NMR** (101 MHz, $CDCl_3$) (minor, diagnostic peaks) δ_C 159.5, 147.4, 139.3, 138.75, 118.8, 113.3, 78.6, 65.3, 55.5; **HRMS** (ESI/TOF) *m/z*: $[M + Na]^+$ Calcd for $C_{19}H_{22}NaO_5S$ 385.1080; Found 385.1081.

1-(4-Methoxyphenyl)-2-(*m*-tolyl)-2-vinylpropane-1,3-diol (4.3ae)

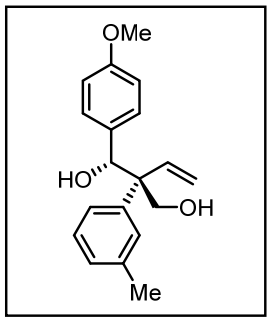

Yellowish oil (Method A, 24.2 mg, 81% yield, 97:3 *dr*); **IR** (neat): ν = 3392, 2934, 2836, 1609, 1511, 1245, 1175, 1031, 909, 835, 729, 705 cm^{-1}; **^{1}H NMR** (500 MHz, $CDCl_3$) (major) δ_H 7.24-7.17 (m, 1H), 7.13-7.08 (m, 2H), 7.08-7.05 (m, 1H), 7.05-7.02 (m, 2H), 6.79-6.73 (m, 2H), 6.26 (dd, *J* = 18.1, 11.3 Hz, 1H), 5.45 (dd, *J* = 11.3, 1.1 Hz, 1H), 5.28 (s, 1H), 5.18 (dd, *J* = 18.1, 1.1 Hz, 1H), 3.94 (d, *J* = 11.1 Hz, 1H), 3.78 (d, *J* = 11.2 Hz, 1H, partially overlaps), 3.78 (s, 3H), 2.53 (br s, 1H), 2.33 (s, 3H), 1.95 (br s, 1H); **^{1}H NMR** (500 MHz, $CDCl_3$) (minor, diagnostic peaks) δ_H 5.93 (dd, *J* = 17.8, 11.1 Hz, 1H), 5.36 (dd, *J* = 11.1, 1.1 Hz, 1H), 5.24 (s, 1H), 5.10 (dd, *J* = 17.8, 1.2 Hz, 1H), 2.34 (s, 3H, partially overlaps); **^{13}C NMR** (126 MHz, $CDCl_3$) (major) δ_C 159.1, 140.8, 139.3, 138.0, 132.5, 129.3, 129.1, 128.3, 127.9, 125.6, 117.5, 113.0, 77.5, 66.2, 55.3, 55.2, 21.8; **^{13}C NMR** (126 MHz, $CDCl_3$) (minor, diagnostic peaks) δ_C 139.7, 118.1, 78.6, 65.8; **HRMS** (ESI/TOF) *m/z*: $[M + Na]^+$ Calcd for $C_{19}H_{22}NaO_3$ 321.1461; Found 321.1466.

1-(4-Methoxyphenyl)-2-(3-(trifluoromethyl)phenyl)-2-vinylpropane-1,3-diol (4.3af)

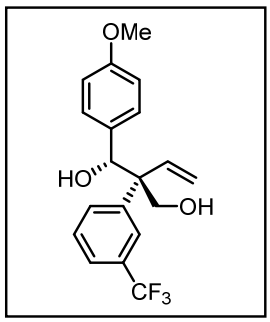

Yellowish oil (Method A, 25.8 mg, 73% yield, 94:6 *dr*); **IR** (neat): ν = 3406, 2938, 2839, 1611, 1512, 1327, 1246, 1164, 1121, 1077, 1033, 908, 836, 731, 703 cm^{-1}; **^{1}H NMR** (400 MHz, $CDCl_3$) (major) δ_H 7.56-7.45 (m, 3H), 7.45-7.36 (m, 1H), 7.00-6.92 (m, 2H), 6.79-6.70 (m, 2H), 6.23 (dd, *J* = 18.1, 11.3 Hz, 1H), 5.51 (dd, *J* = 11.2, 0.9 Hz, 1H), 5.26 (s, 1H), 5.20 (dd, *J* = 18.1, 0.9 Hz, 1H), 4.07 (d, *J* = 11.2 Hz, 1H), 3.86 (d, *J* = 11.2 Hz, 1H), 3.77 (s, 3H), 2.62 (br s, 1H), 2.05 (br s, 1H); **^{1}H NMR** (400 MHz, $CDCl_3$) (minor, diagnostic peaks) δ_H 5.99 (dd, *J* = 17.8, 11.1 Hz, 1H), 5.41 (dd, *J* = 11.1, 0.9 Hz, 1H), 5.21 (s, 1H), 5.05 (dd, *J* = 17.8, 1.0 Hz, 1H); **^{13}C NMR** (101 MHz, $CDCl_3$) (major) δ_C 159.4, 142.1, 138.9, 132.29, 132.28, 132.1, 130.4 (q, *J* = 31.9 Hz), 129.0, 128.5, 125.9 (q, *J* = 3.9 Hz), 123.8 (q, *J* = 3.8 Hz), 118.5, 113.2, 77.5, 66.0, 55.4, 55.3; **^{13}C NMR** (101 MHz, $CDCl_3$) (minor, diagnostic peaks) δ_C 139.4, 118.9, 78.5; **^{19}F NMR** (376 MHz, $CDCl_3$) (major) δ_F -62.57; **^{19}F NMR** (376 MHz, $CDCl_3$) (minor) δ_F -62.53; **HRMS** (ESI/TOF) *m/z*: $[M + Na]^+$ Calcd for $C_{19}H_{19}F_3NaO_3$ 375.1178; Found 375.1177.

2-(3-(Methoxymethoxy)phenyl)-1-(4-methoxyphenyl)-2-vinylpropane-1,3-diol (4.3ag)

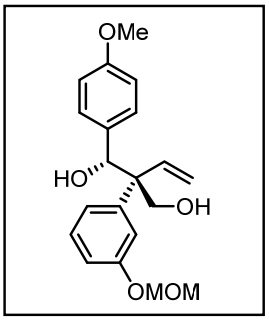

Yellowish oil (Method A, reaction time = 17 h, 27.3 mg, 79% yield, 95:5 *dr*); **IR** (neat): ν = 3423, 2955, 2902, 2836, 1608, 1582, 1511, 1243, 1175, 1150, 1009, 994, 909, 836, 728, 701 cm^{-1}; **^{1}H NMR** (400 MHz, $CDCl_3$) (major) δ_H 7.30-7.17 (m, 1H), 7.08-6.97 (m, 2H), 7.00-6.90 (m, 3H), 6.79-6.71 (m, 2H), 6.25 (dd, *J* = 18.0, 11.3 Hz, 1H), 5.45 (dd, *J* = 11.2, 1.0 Hz, 1H), 5.27 (s, 1H), 5.20 (dd, *J* = 18.0, 1.0 Hz, 1H), 5.12 (s, 2H), 3.98 (d, *J* = 11.2 Hz, 1H), 3.78 (d, *J* = 15.3 Hz, 1H, partially overlaps), 3.77 (s, 3H), 3.45 (s, 3H), 2.61 (br s, 1H), 2.00 (br s, 1H); **^{1}H NMR** (400 MHz, $CDCl_3$) (minor, diagnostic peaks) δ_H 5.93 (dd, *J* = 17.9, 11.0 Hz, 1H), 5.37 (d, *J* = 11.2 Hz, 1H); **^{13}C NMR** (101 MHz, $CDCl_3$) (major) δ_C 159.1, 157.3, 142.7, 139.1, 132.4, 129.4, 129.1, 122.1, 117.7, 117.3, 114.6, 113.0, 94.6, 77.5, 66.1, 56.1, 55.3, 55.2; **^{13}C NMR** (101 MHz, $CDCl_3$) (minor, diagnostic peaks) δ_C 139.4, 122.5, 113.1, 78.7; **HRMS** (ESI/TOF) *m/z*: $[M + Na]^+$ Calcd for $C_{20}H_{24}NaO_5$ 367.1516; Found 367.1521.

2-(3-Hydroxyphenyl)-1-(4-methoxyphenyl)-2-vinylpropane-1,3-diol (4.3ah)

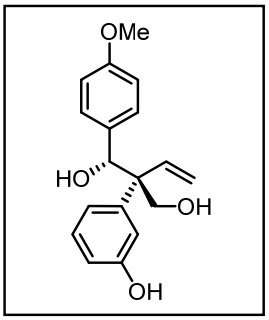

Yellowish oil (Method B, 23.9 mg, 80% yield, 95:5 *dr*); **IR** (neat): ν = 3350, 2936, 2838, 1610, 1585, 1511, 1444, 1244, 1176, 1031, 906, 837, 726 cm^{-1}; **^{1}H NMR** (400 MHz, $CDCl_3$) (major) δ_H 7.12 (t, *J* = 7.9 Hz, 1H), 7.05-6.94 (m, 2H), 6.81-6.66 (m, 5H), 6.51 (br s, 1H), 6.16 (dd, *J* = 18.0, 11.3 Hz, 1H), 5.38 (dd, *J* = 11.2, 1.0 Hz, 1H), 5.18 (s, 1H), 5.10 (dd, *J* = 18.0, 1.1 Hz, 1H), 3.85 (d, *J* = 11.2 Hz, 1H), 3.74 (s, 3H), 3.70 (d, *J* = 11.2 Hz, 1H), 2.95 (br s, 1H), 2.35 (br s, 1H); **^{1}H NMR** (400 MHz, $CDCl_3$) (minor, diagnostic peaks) δ_H 5.77 (dd, *J* = 17.6, 11.1 Hz, 1H); **^{13}C NMR** (101 MHz, $CDCl_3$) (major) δ_C 159.1, 156.0, 142.6, 138.9, 132.2, 129.6, 129.2, 120.6, 117.7, 115.8, 114.3, 113.0, 77.48 (completely overlaps), 66.1, 55.3, 55.0; **^{13}C NMR** (101 MHz, $CDCl_3$) (minor, diagnostic peaks) δ_C 128.5, 128.3, 113.8, 113.7, 77.9, 55.4; **HRMS** (ESI/TOF) *m/z*: $[M - H]^-$ Calcd for $C_{18}H_{19}O_4$ 299.1289; Found 299.1298.

1-(4-Methoxyphenyl)-2-(*o*-tolyl)-2-vinylpropane-1,3-diol (4.3ai)

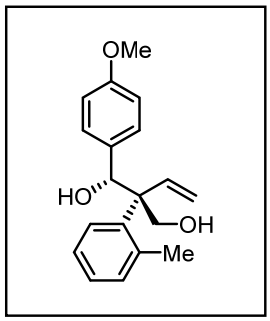

Yellowish oil (Method C, 13.3 mg, 45% yield, 98:2 *dr*); **IR** (neat): ν = 3395, 2954, 2836, 1609, 1510, 1246, 1176, 1031, 909, 829, 727 cm^{-1}; **^{1}H NMR** (400 MHz, $CDCl_3$) (major) δ_H 7.17-7.09 (m, 2H), 7.06-6.96 (m, 1H), 6.91-6.78 (m, 3H), 6.72-6.65 (m, 2H), 6.62 (dd, *J* = 18.0, 11.0 Hz, 1H, partially overlaps), 5.46 (dd, *J* = 11.0, 1.3 Hz, 1H), 5.43 (s, 1H), 5.07 (dd, *J* = 18.0, 1.3 Hz, 1H), 4.22 (d, *J* = 10.9 Hz, 1H), 3.81 (dd, *J* = 10.8, 0.6 Hz, 1H), 3.75 (s, 3H), 3.21 (br s, 1H), 2.40 (s, 3H), 2.17 (br s, 1H); **^{1}H NMR** (400 MHz, $CDCl_3$) (minor, diagnostic peaks) δ_H 6.27 (dd, *J* = 18.1, 11.2 Hz, 1H); **^{13}C NMR** (101 MHz, $CDCl_3$) (major) δ_C 158.9, 140.9, 139.5, 137.3, 133.0, 132.9, 128.6, 128.5, 127.1, 125.7, 117.5, 112.9, 76.5, 66.3, 55.3, 54.8, 24.2; **^{13}C NMR** (101 MHz, $CDCl_3$) (minor, diagnostic peaks) δ_C none detected; **HRMS** (ESI/TOF) *m/z*: $[M + Na]^+$ Calcd for $C_{19}H_{22}NaO_3$ 321.1467; Found 321.1462.

2-(3,5-Dimethylphenyl)-1-(4-methoxyphenyl)-2-vinylpropane-1,3-diol (4.3aj)

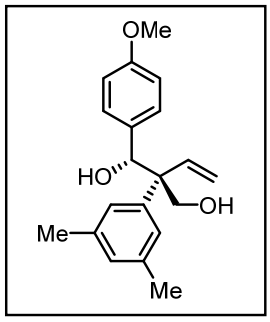

Yellowish oil (Method A, 24.3 mg, 74% yield, 94:6 *dr*); **IR** (neat): ν = 3376, 2915, 2837, 1608, 1511, 1463, 1442, 1245, 1175, 1032, 908, 837, 728 cm^{-1}; **^{1}H NMR** (400 MHz, $CDCl_3$) (major) δ_H 7.12-7.00 (m, 2H), 6.94 (s, 2H), 6.90 (s, 1H), 6.82-6.73 (m, 2H), 6.26 (dd, *J* = 18.0, 11.3 Hz, 1H), 5.43 (dd, *J* = 11.2, 1.2 Hz, 1H), 5.29 (s, 1H), 5.15 (dd, *J* = 18.1, 1.2 Hz, 1H), 3.88 (d, *J* = 11.1 Hz, 1H), 3.79 (s, 3H), 3.76 (d, *J* = 11.2 Hz, 1H, partially overlaps), 2.47 (br s, 1H), 2.30 (s, 6H), 1.76 (br s, 1H); **^{1}H NMR** (400 MHz, $CDCl_3$) (minor, diagnostic peaks) δ_H 5.90 (dd, *J* = 17.7, 11.0 Hz, 1H), 5.36 (d, *J* = 11.1 Hz, 1H), 5.24 (s, 1H), 2.20 (s, 3H); **^{13}C NMR** (101 MHz, $CDCl_3$) (major) δ_C 159.1, 140.7, 139.0, 138.0, 132.4, 129.2, 128.9, 126.3, 117.4, 112.9, 77.3, 66.3, 55.34, 55.32, 21.7; **^{13}C NMR** (101 MHz, $CDCl_3$) (minor, diagnostic peaks) δ_C 140.0, 139.8, 137.7, 132.4, 118.0, 78.6, 65.7; **HRMS** (ESI/TOF) *m/z*: $[M + Na]^+$ Calcd for $C_{20}H_{24}NaO_3$ 335.1618; Found 335.1624.

1-(4-Methoxyphenyl)-2-(thiophen-3-yl)-2-vinylpropane-1,3-diol (4.3ak)

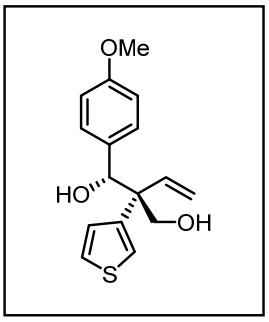

Yellowish oil (Method A, 19.8 mg, 68% yield, 89:11 *dr*); **IR** (neat): ν = 3390, 3105, 2934, 2836, 1610, 1510, 1244, 1175, 1031, 910, 834, 784, 730 cm^{-1}; **^{1}H NMR** (400 MHz, $CDCl_3$) (major) δ_H 7.29 (dd, *J* = 5.1, 2.9 Hz, 1H), 7.04 (dd, *J* = 3.0, 1.4 Hz, 1H), 7.02-6.97 (m, 3H), 6.81-6.72 (m, 2H), 6.19 (dd, *J* = 17.9, 11.2 Hz, 1H), 5.41 (dd, *J* = 11.2, 1.1 Hz, 1H), 5.22 (dd, *J* = 18.0, 1.1 Hz, 1H), 5.14 (s, 1H), 4.01 (d, *J* = 11.1 Hz, 1H), 3.81 (d, *J* = 11.2 Hz, 1H), 3.78 (s, 3H), 2.65 (br s, 1H), 2.06 (br s, 1H); **^{1}H NMR** (400 MHz, $CDCl_3$) (minor, diagnostic peaks) δ_H 7.12 (dd, *J* = 3.0, 1.4 Hz, 1H), 5.96 (dd, *J* = 17.7, 11.0 Hz, 1H), 5.35 (dd, *J* = 11.0, 1.2 Hz, 1H), 5.11 (s, 1H, partially overlaps), 5.10 (dd, *J* = 17.7, 1.2 Hz, 1H), 3.78 (s, 3H, overlaps); **^{13}C NMR** (101 MHz, $CDCl_3$) (major) δ_C 159.2, 141.6, 139.1, 132.3, 129.0, 128.0, 125.3, 123.3, 117.4, 113.09, 78.1, 66.3, 55.3, 53.9; **^{13}C NMR** (101 MHz, $CDCl_3$) (minor, diagnostic peaks) δ_C 141.1, 139.3, 128.5, 128.2, 125.0, 123.5, 118.1, 113.14, 79.1, 66.6, 54.0; **HRMS** (ESI/TOF) *m/z*: $[M + Na]^+$ Calcd for $C_{16}H_{18}NaO_3S$ 313.0869; Found 313.0870.

2-(Benzofuran-2-yl)-1-(4-methoxyphenyl)-2-vinylpropane-1,3-diol (4.3al)

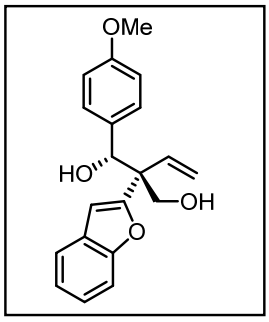

Yellowish oil (Method A, 21.2 mg, 65% yield, 83:17 *dr*); **IR** (neat): ν = 3397, 2934, 2837, 1611, 1512, 1454, 1246, 1175, 1031, 907, 833, 728 cm^{-1}; **^{1}H NMR** (500 MHz, $CDCl_3$) (major) δ_H 7.54-7.46 (m, 2H), 7.31-7.27 (m, 1H), 7.26-7.19 (m, 2H), 7.15-7.09 (m, 2H), 6.80-6.72 (m, 2H), 6.56 (d, *J* = 0.9 Hz, 1H), 6.22 (dd, *J* = 17.9, 11.1 Hz, 1H), 5.45 (dd, *J* = 11.1, 0.9 Hz, 1H), 5.35 (s, 1H), 5.25 (dd, *J* = 17.9, 0.9 Hz, 1H), 4.05 (d, *J* = 11.2 Hz, 1H), 3.90 (d, *J* = 11.2 Hz, 1H), 3.76 (s, 3H), 2.27 (br s, 2H); **^{1}H NMR** (500 MHz, $CDCl_3$) (minor, diagnostic peaks) δ_H 6.63 (d, *J* = 0.9 Hz, 1H), 5.82 (dd, *J* = 17.7, 11.0 Hz, 1H), 5.14 (dd, *J* = 17.7, 1.0 Hz, 1H), 3.77 (s, 3H, overlaps); **^{13}C NMR** (126 MHz, $CDCl_3$) (major) δ_C 159.5, 158.1, 154.7, 136.1, 132.0, 128.8, 128.4, 124.3, 123.12, 121.2, 118.7, 113.5, 111.4, 106.2, 77.2, 65.3, 55.4, 54.1; **^{13}C NMR** (126 MHz, $CDCl_3$) (minor, diagnostic peaks) δ_C 136.2, 124.2, 123.08, 118.9, 106.5, 78.0; **HRMS** (ESI/TOF) *m/z*: $[M + Na]^+$ Calcd for $C_{20}H_{20}NaO_4$ 347.1254; Found 347.1245.

1-(4-Methoxyphenyl)-2-(naphthalen-2-yl)-2-vinylpropane-1,3-diol (4.3am)

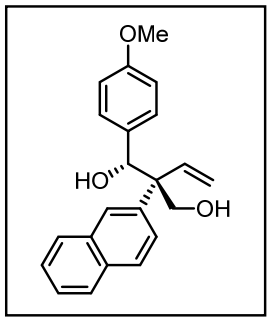

Yellowish oil (Method A, 24.9 mg, 74% yield, 94:6 *dr*); **IR** (neat): ν = 3395, 3058, 2934, 2889, 2836, 1610, 1510, 1245, 1176, 1032, 906, 836, 816, 727 cm^{-1}; **^{1}H NMR** (400 MHz, $CDCl_3$) (major) δ_H 7.87-7.70 (m, 4H), 7.52-7.39 (m, 3H), 7.09-6.99 (m, 2H), 6.78-6.68 (m, 2H), 6.35 (dd, *J* = 18.0, 11.2 Hz, 1H), 5.51 (dd, *J* = 11.2, 1.1 Hz, 1H), 5.41 (s, 1H), 5.22 (dd, *J* = 18.1, 1.2 Hz, 1H), 4.09 (d, *J* = 11.2 Hz, 1H), 3.91 (d, *J* = 11.2 Hz, 1H), 3.76 (s, 3H), 2.57 (br s, 1H), 1.99 (br s, 1H); **^{1}H NMR** (400 MHz, $CDCl_3$) (minor, diagnostic peaks) δ_H 6.01 (dd, *J* = 17.7, 10.9 Hz, 1H), 5.35 (s, 1H), 5.09 (d, *J* = 17.8 Hz, 1H); **^{13}C NMR** (101 MHz, $CDCl_3$) (major) δ_C 159.2, 139.3, 138.3, 133.3, 132.4, 132.4, 129.1, 128.3, 127.9, 127.9, 127.5, 126.6, 126.2 (2C), 118.1, 113.0, 77.45 (overlaps), 66.3, 55.5, 55.3; **^{13}C NMR** (101 MHz, $CDCl_3$) (minor, diagnostic peaks) δ_C 139.7, 118.6, 113.2, 78.7, 65.9; **HRMS** (ESI/TOF) *m/z*: $[M + Na]^+$ Calcd for $C_{22}H_{22}NaO_3$ 357.1461; Found 357.1448.

1-(4-Methoxyphenyl)-2-phenethyl-2-vinylpropane-1,3-diol (4.3aw)

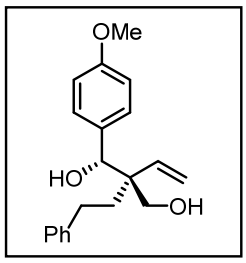

Yellowish oil (Method A, 24.9 mg, 28% yield, 83:17 *dr*); **IR** (neat): ν = 3349, 3026, 3001, 2993, 2836, 1611, 1511, 1455, 1246, 1176, 1030, 1006, 909, 836, 726, 699 cm^{-1}; **^{1}H NMR** (400 MHz, $CDCl_3$) (major) δ_H 7.31-7.22 (m, 4H), 7.22-7.13 (m, 3H), 6.89-6.81 (m, 2H), 5.70 (dd, *J* = 18.0, 11.3 Hz, 1H), 5.26 (dd, *J* = 11.3, 1.1 Hz, 1H), 4.98 (dd, *J* = 18.0, 1.1 Hz, 1H), 4.76 (s, 1H), 3.95 (d, *J* = 11.1 Hz, 1H), 3.80 (s, 3H), 3.69 (d, *J* = 11.1 Hz, 1H), 2.68 (br s, 2H), 2.69-2.53 (m, 2H), 2.04 (ddd, *J* = 17.6, 11.2, 6.5 Hz, 1H), 1.66 (ddd, *J* = 13.8, 11.6, 5.3 Hz, 1H); **^{1}H NMR** (400 MHz, $CDCl_3$) (minor, diagnostic peaks) δ_H 5.71 (dd, *J* = 18.1, 11.3 Hz, 1H, overlaps), 5.33 (dd, *J* = 11.3, 1.0 Hz, 1H), 5.16 (dd, *J* = 18.0, 1.1 Hz, 1H), 4.80 (s, 1H); **^{13}C NMR** (101 MHz, $CDCl_3$) (major) δ_C 159.3, 143.0, 138.8, 132.9, 129.1, 128.5, 128.5, 125.9, 116.5, 113.3, 79.7, 64.8, 55.4, 48.7, 34.7, 30.3; **^{13}C NMR** (101 MHz, $CDCl_3$) (minor, diagnostic peaks) δ_C none detected; **HRMS** (ESI/TOF) *m/z*: $[M + Na]^+$ Calcd for $C_{20}H_{24}NaO_3$ 335.1618; Found 335.1612.

1-(4-Methoxyphenyl)-2-methyl-2-vinylpropane-1,3-diol (4.3ay)

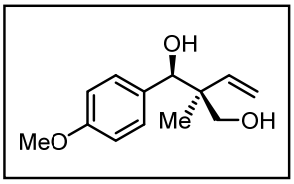

Yellowish oil (Method A, 16.9 mg, 76% yield, 83:17 *dr*); **IR** (neat): ν = 3370, 3081, 2935, 2837, 1726, 1611, 1511, 1244, 1175, 1031, 911, 832, 729 cm^{-1}; **^{1}H NMR** (400 MHz, $CDCl_3$) (major) δ_H 7.27-7.18 (m, 2H), 6.87-6.80 (m, 2H), 6.06 (dd, J = 17.7, 11.0 Hz, 1H), 5.23 (dd, J = 11.0, 1.3 Hz, 1H), 5.05 (dd, J = 17.7, 1.3 Hz, 1H), 4.67 (s, 1H), 3.79 (s, 3H), 3.62 (d, J = 10.7 Hz, 1H), 3.55 (d, J = 10.7 Hz, 1H), 2.62 (br s, 2H), 0.91 (s, 3H); **^{1}H NMR** (400 MHz, $CDCl_3$) (minor, diagnostic peaks) δ_H 5.88 (dd, J = 17.7, 11.0 Hz, 1H), 5.15 (dd, J = 11.0, 1.2 Hz, 1H), 5.07 (dd, J = 17.6, 1.2 Hz, 1H), 4.73 (s, 1H), 0.94 (s, 3H); **^{13}C NMR** (101 MHz, $CDCl_3$) (major) δ_C 159.3, 139.9, 133.2, 129.0, 116.3, 113.2, 79.7, 70.0, 55.4, 46.7, 17.8; **^{13}C NMR** (101 MHz, $CDCl_3$) (minor, diagnostic peaks) δ_C 141.6, 128.8, 80.3, 69.4, 46.4, 16.8; **HRMS** (ESI/TOF) *m/z*: $[M + Na]^+$ Calcd for $C_{13}H_{18}NaO_3$ 245.1148; Found 245.1154.

4.5.5 General Procedure for the Synthesis of Homoallylic Alcohols

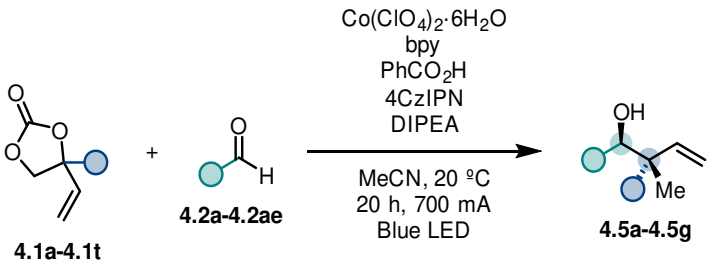

SCHEME 4.22. General synthesis of homoallylic alcohols.

Method: $Co(ClO_4)_2 \cdot 6H_2O$ (10 µmol, 3.7 mg), 2,2'-bipyridine (20 µmol, 3.2 mg), $PhCO_2H$ (20 µmol, 2.4 mg) and 4CzIPN (2 µmol, 1.6 mg) were weighed in a flat-bottom Schlenk flask. The solids were dissolved in MeCN (1 mL), and DIPEA (26.1 µL, 0.15 mmol), VCC **4.1a-4.1t** (0.1 mmol), and aldehyde **4.2a-4.2ae** (0.15 mmol) were added, affording an orange solution. The flask was sealed with a Teflon cap and the mixture was freeze-pump-thawed 3 times and stirred under N_2 at room temperature for 5–20 minutes after which it was irradiated for 20 hours at 20 °C using a single high-power blue LED (λ_{em} = 445 nm, 700 mA, 1.2 µeinstein s^{-1}) from the bottom. After the reaction, the mixture was evaporated to dryness and the residue was purified by column chromatography (SiO_2, EtOAc/hexanes) to afford homoallylic alcohol products **4.5a-4.5g**.

2-Methyl-1,2-diphenylbut-3-en-1-ol (4.5a)

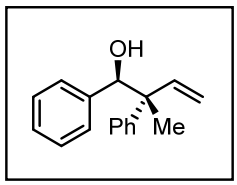

Yellowish oil (17.9 mg, 75% yield, 97:3 *dr*, 96:4 *rr*); **IR** (neat): ν = 3564, 3451, 3085, 3059, 3029, 2980, 2881, 1494, 1445, 1189, 1039, 1023, 916, 725, 697 cm^{-1}; **^{1}H NMR** (400 MHz, $CDCl_3$) (major) δ_H 7.42-7.36 (m, 2H), 7.36-7.29 (m, 2H), 7.27-7.19 (m, 4H), 7.15-7.08 (m, 2H), 6.57 (dd, J = 17.7, 10.9 Hz, 1H), 5.33 (dd, J = 10.9, 1.2 Hz, 1H), 5.11 (dd, J = 17.6, 1.2 Hz, 1H), 5.08 (s, 1H), 2.07 (br s, 1H), 1.30 (s, 3H); **^{1}H NMR** (400 MHz, $CDCl_3$) (minor diastereomer, diagnostic peaks) δ_H 6.26 (dd, J = 17.4, 10.8 Hz, 1H), 5.17 (dd, J = 10.9, 1.1 Hz, 1H), 5.03 (s, 1H), 5.00 (dd, J = 17.6, 1.1 Hz, 1H); **^{1}H NMR** (400 MHz, $CDCl_3$) (regioisomers, diagnostic peaks) δ_H 5.41 (d, J = 1.0 Hz, 1H), 5.23 (t, J = 1.2 Hz, 1H), 4.71 (d, J = 3.7 Hz, 1H), 4.63 (d, J = 8.6 Hz, 1H, minor regioisomer), 3.19-3.12 (m, 1H), 1.10 (d, J = 7.0 Hz, 3H); **^{13}C NMR** (101 MHz, $CDCl_3$) (major) δ_C 145.1, 142.2, 140.2, 128.4, 128.1, 127.6, 127.4, 127.3, 126.7, 115.7, 80.4, 50.4, 20.7; **HRMS** (ESI/TOF) *m/z*: $[M + Na]^+$ Calcd for $C_{17}H_{18}NaO$ 261.1250; Found 261.1258.

1-(4-Methoxyphenyl)-2-methyl-2-phenylbut-3-en-1-ol (4.5b)

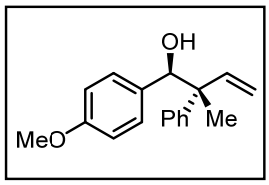

Yellowish oil (17.1 mg, 64% yield, 98:2 *dr*, 98:2 *rr*); **IR** (neat): ν = 3473, 3084, 3057, 2978, 2934, 2836, 1610, 1511, 1444, 1245, 1174, 1030, 917, 831, 699 cm^{-1}; **^{1}H NMR** (500 MHz, $CDCl_3$) (major) δ_H 7.40-7.35 (m, 2H), 7.35-7.29 (m, 2H), 7.25-7.21 (m, 1H), 7.06-7.01 (m, 2H), 6.78-6.72 (m, 2H), 6.56 (dd, J = 17.7, 10.9 Hz, 1H), 5.33 (dd, J = 10.9, 1.2 Hz, 1H), 5.11 (dd, J = 17.7, 1.3 Hz, 1H), 5.03 (s, 1H), 3.77 (s, 3H), 2.02 (br s, 1H), 1.28 (s, 3H); **^{1}H NMR** (500 MHz, $CDCl_3$) (minor diastereomer, diagnostic peaks) δ_H 6.25 (dd, J = 17.5, 10.8 Hz, 1H); **^{1}H NMR** (500 MHz, $CDCl_3$) (regioisomers, diagnostic peaks) δ_H 3.16-3.09 (m, 1H); **^{13}C NMR** (126 MHz, $CDCl_3$) (major) δ_C 159.0, 145.3, 142.3, 132.3, 129.1, 128.4, 127.4, 126.6, 115.7, 112.8, 80.1, 55.3, 50.5, 20.8; **HRMS** (ESI/TOF) *m/z*: $[M + Na]^+$ Calcd for $C_{18}H_{20}NaO_2$ 291.1356; Found 291.1359.

2-Methyl-2-(naphthalen-2-yl)-1-phenylbut-3-en-1-ol (4.5c)

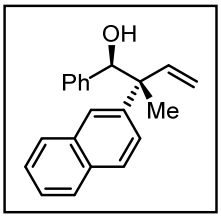

Yellowish oil (20.9 mg, 72% yield, 97:3 *dr*, 97:3 *rr*); **IR** (neat): ν = 3569, 3453, 3058, 3030, 2980, 2885, 1631, 1598, 1453, 1374, 1186, 1039, 1024, 907, 815, 725, 700 cm^{-1}; **^{1}H NMR** (500 MHz, $CDCl_3$) (major) δ_H 7.87-7.81 (m, 2H), 7.81-7.77 (m, 2H), 7.60 (dd, *J* = 8.7, 2.0 Hz, 1H), 7.51-7.45 (m, 2H), 7.25-7.19 (m, 3H), 7.19-7.13 (m, 2H), 6.67 (dd, *J* = 17.7, 11.0 Hz, 1H), 5.39 (dd, *J* = 10.9, 1.2 Hz, 1H), 5.22 (s, 1H), 5.15 (dd, *J* = 17.7, 1.2 Hz, 1H), 2.06 (br s, 1H), 1.40 (s, 3H); **^{1}H NMR** (500 MHz, $CDCl_3$) (minor diastereomer, diagnostic peaks) δ_H 6.34 (dd, *J* = 17.5, 10.9 Hz, 1H), 5.15 (s, 1H), 5.03 (dd, *J* = 17.5, 1.1 Hz, 1H); **^{1}H NMR** (500 MHz, $CDCl_3$) (regioisomers, diagnostic peaks) δ_H 4.76 (d, *J* = 3.7 Hz, 1H), 4.70 (d, *J* = 8.5 Hz, 1H), 3.32-3.26 (m, 1H); **^{13}C NMR** (126 MHz, $CDCl_3$) (major) δ_C 142.6, 142.0, 140.2, 133.4, 132.2, 128.2, 128.1, 128.0, 127.6, 127.5, 127.4, 126.4, 126.1, 125.9, 125.6, 116.1, 80.2, 50.6, 21.1; **HRMS** (ESI/TOF) *m/z*: $[M + Na]^+$ Calcd for $C_{21}H_{20}NaO$ 311.1406; Found 311.1399.

2-(3,5-Dimethylphenyl)-2-methyl-1-phenylbut-3-en-1-ol (4.5d)

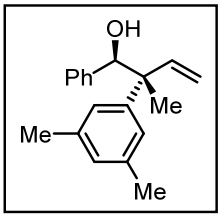

Yellowish oil (18.2 mg, 68% yield, 97:3 *dr*, 98:2 *rr*); **IR** (neat): ν = 3553, 3458, 3030, 2979, 2916, 1601, 1452, 1185, 1039, 1025, 911, 847, 719, 700 cm^{-1}; **^{1}H NMR** (500 MHz, $CDCl_3$) (major) δ_H 7.26-7.22 (m, 3H), 7.21-7.16 (m, 2H), 7.03-6.99 (m, 2H), 6.91-6.88 (m, 1H), 6.58 (dd, *J* = 17.7, 11.0 Hz, 1H), 5.31 (dd, *J* = 11.0, 1.3 Hz, 1H), 5.06 (s, 1H), 5.04 (dd, *J* = 17.7, 1.3 Hz, 1H, partially overlaps), 2.32 (s, 6H), 1.97 (br s, 1H), 1.25 (s, 3H); **^{1}H NMR** (500 MHz, $CDCl_3$) (minor diastereomer, diagnostic peaks) δ_H 6.93-6.91 (m, 1H), 6.23 (dd, *J* = 17.4, 10.9 Hz, 1H), 5.11 (dd, *J* = 10.8, 1.2 Hz, 1H), 4.94 (dd, *J* = 17.5, 1.2 Hz, 1H); **^{1}H NMR** (500 MHz, $CDCl_3$) (regioisomers, diagnostic peaks) δ_H 4.71 (d, *J* = 3.5 Hz, 1H), 3.17-3.09 (m, 1H).; **^{13}C NMR** (126 MHz, $CDCl_3$) (major) δ_C 145.2, 141.8, 140.2, 137.9, 128.4, 128.2, 127.5, 127.3, 125.1, 115.6, 80.6, 50.3, 21.7, 21.5; **HRMS** (ESI/TOF) *m/z*: $[M + Na]^+$ Calcd for $C_{19}H_{22}NaO$ 289.1563; Found 289.1561.

2-Methyl-2-(4-(methylsulfonyl)phenyl)-1-phenylbut-3-en-1-ol (4.5e)

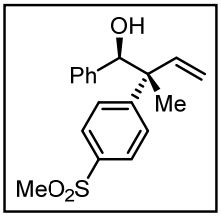

White solid (14.5 mg, 46% yield, 90:10 *dr*, 84:16 *rr*); **IR** (neat): ν = 3491, 2978, 2925, 2870, 1592, 1295, 1146, 1093, 1047, 955, 921, 778, 700 cm^{-1}; **^{1}H NMR** (500 MHz, $CDCl_3$) (major) δ_H 7.88-7.83 (m, 2H), 7.61-7.56 (m, 2H), 7.25-7.17 (m, 3H), 7.14-7.08 (m, 2H), 6.52 (dd, *J* = 17.7, 10.9 Hz, 1H), 5.38 (dd, *J* = 11.0, 1.0 Hz, 1H), 5.11 (dd, *J* = 17.6, 1.0 Hz, 1H), 5.07 (s, 1H), 3.04 (s, 3H), 2.12 (br s, 1H), 1.32 (s, 3H); **^{1}H NMR** (500 MHz, $CDCl_3$) (minor diastereomer, diagnostic peaks) δ_H 6.27 (dd, *J* = 17.5, 10.9 Hz, 1H), 5.22 (dd, *J* = 10.9, 0.9 Hz, 1H); **^{1}H NMR** (500 MHz, $CDCl_3$) (regioisomers, diagnostic peaks) δ_H 4.63 (d, *J* = 4.8 Hz, 1H), 4.60 (d, *J* = 8.2 Hz, 1H); **^{13}C NMR** (101 MHz, $CDCl_3$) (major) δ_C 152.2, 141.1, 140.0, 138.5, 128.7, 128.1, 128.0, 127.7, 127.2, 116.8, 80.2, 50.6, 44.7, 21.5; **HRMS** (ESI/TOF) *m/z*: $[M + Na]^+$ Calcd for $C_{18}H_{20}NaO_3S$ 339.1025; Found 339.1029.

2-(4-Methoxyphenyl)-2-methyl-1-phenylbut-3-en-1-ol (4.5f)

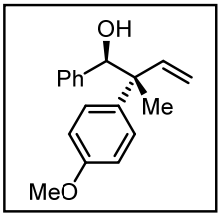

Yellowish oil (6.6 mg, 25% yield, 96:4 *dr*, >99:1 *rr*); **IR** (neat): ν = 3466, 3061, 3031, 2976, 2934, 2835, 1608, 1510, 1453, 1293, 1248, 1182, 1027, 911, 829, 727, 700 cm^{-1}; **^{1}H NMR** (400 MHz, $CDCl_3$) (major) δ_H 7.31-7.26 (m, 2H), 7.23-7.18 (m, 3H), 7.13-7.07 (m, 2H), 6.90-6.82 (m, 2H), 6.52 (dd, *J* = 17.6, 10.9 Hz, 1H), 5.30 (dd, *J* = 10.9, 1.2 Hz, 1H), 5.09 (dd, *J* = 17.7, 1.2 Hz, 1H), 5.02 (s, 1H), 3.81 (s, 3H), 1.27 (s, 3H); **^{1}H NMR** (400 MHz, $CDCl_3$) (minor diastereomer, diagnostic peaks) δ_H 6.23 (dd, *J* = 17.5, 10.9 Hz, 1H), 5.14 (dd, *J* = 10.9, 1.2 Hz, 1H), 4.97 (s, 1H), 3.82 (s, 3H), 1.36 (s, 3H); **^{13}C NMR** (101 MHz, $CDCl_3$) (major) δ_C 158.2, 142.5, 140.2, 137.0, 128.5, 128.1, 127.5, 127.3, 115.5, 113.7, 80.5, 55.4, 49.8, 20.8; **HRMS** (ESI/TOF) *m/z*: $[M + Na]^+$ Calcd for $C_{18}H_{20}NaO_2$ 291.1356; Found 291.1358.

2-([1,1'-Biphenyl]-4-yl)-2-methyl-1-phenylbut-3-en-1-ol (4.5g)

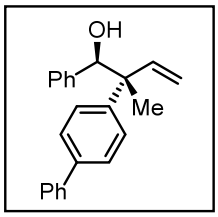

Yellowish solid (23.8 mg, 76% yield, 96:4 *dr*, 97:3 *rr*); **IR** (neat): ν = 3558, 3028, 2978, 2879, 1483, 1020, 926, 906, 732, 720, 696 cm^{-1}; **^{1}H NMR** (500 MHz, $CDCl_3$) (major) δ_H 7.66-7.60 (m, 2H), 7.60-7.55 (m, 2H), 7.49-7.43 (m, 4H), 7.39-7.34 (m, 1H), 7.26-7.21 (m, 3H), 7.20-7.13 (m, 2H), 6.61 (dd, *J* = 17.7, 10.9 Hz, 1H), 5.37 (dd, *J* = 10.9, 1.2 Hz, 1H), 5.14 (dd, *J* = 17.7, 1.2 Hz, 1H), 5.12 (s, 1H), 2.10 (br s, 1H), 1.34 (s, 3H); **^{1}H NMR** (500 MHz, $CDCl_3$) (minor diastereomer, diagnostic peaks) δ_H 6.31 (dd, *J* = 17.4, 10.9 Hz, 1H), 5.20 (dd, *J* = 10.8, 1.1 Hz, 1H); **^{1}H NMR** (500 MHz, $CDCl_3$) (regioisomers, diagnostic peaks) δ_H 4.77 (d, *J* = 3.7 Hz, 1H), 4.68 (d, *J* = 8.5 Hz, 1H), 3.24-3.18 (m, 1H); **^{13}C NMR** (126 MHz, $CDCl_3$) (major) δ_C 144.3, 142.0, 140.8, 140.2, 139.4, 128.9, 128.1, 127.8, 127.6, 127.41, 127.37, 127.15, 127.05, 115.9, 80.4, 50.2, 21.0; **HRMS** (ESI/TOF) *m/z*: $[M + Na]^+$ Calcd for $C_{23}H_{22}NaO$ 337.1563; Found 337.1563.

4.5.6 Stern-Volmer Plots

Stern-Volmer analysis was performed by fluorimetry and time-correlated single-photon counting. For the fluorometric analysis, samples containing a solution of 4CzIPN in THF (1.6 mg in 100 mL, to obtain an absorbance of 0.1 at 450 nm over a path length of 1 cm) were deoxygenated by purging argon through the cuvette sealed by a septum. The emission spectrum was measured by excitation at 450 nm. Then, aliquots of quencher compound (*i.e.*, HE, $[Co(DPEPhos)Cl_2]$, **4.1a** or **4.2a**) dissolved in the same 4CzIPN solution were added, thus maintaining the absorbance of the solution while increasing the concentration of quencher. The emission spectrum was measured for several concentrations of quencher until over 50% of the fluorescence was quenched. The emission intensity at 550 nm without quencher divided by the emission intensity with quencher was then plotted as a function of the concentration of quencher to obtain the Stern-Volmer plot. For TCSPC, the same procedure was followed, but instead of fluorimetry, the measured TCSPC decay was fitted to a biexponential to obtain the decay-constants of the prompt fluorescence and the thermally activated delayed fluorescence. The lifetime of either the PF or TADF without quencher divided by the lifetime in the presence of quencher was plotted as a function of quencher to obtain the Stern-Volmer plot, according to the following formula.

$$\frac{\tau_0}{\tau} = 1 + \tau_0 k_q [Q]$$

By extrapolation using the rate constants and catalytic concentrations of quenchers HE and [Co(DPEPhos)Cl$_2$], we calculated the quantum yield of quenching of the prompt fluorescence by HE to be 90% at the start of the reaction. The UV-vis spectrum of each sample was measured before and after fluorimetry or TCSPC measurements to ensure no decomposition took place during the measurement and ensure a stable absorbance.

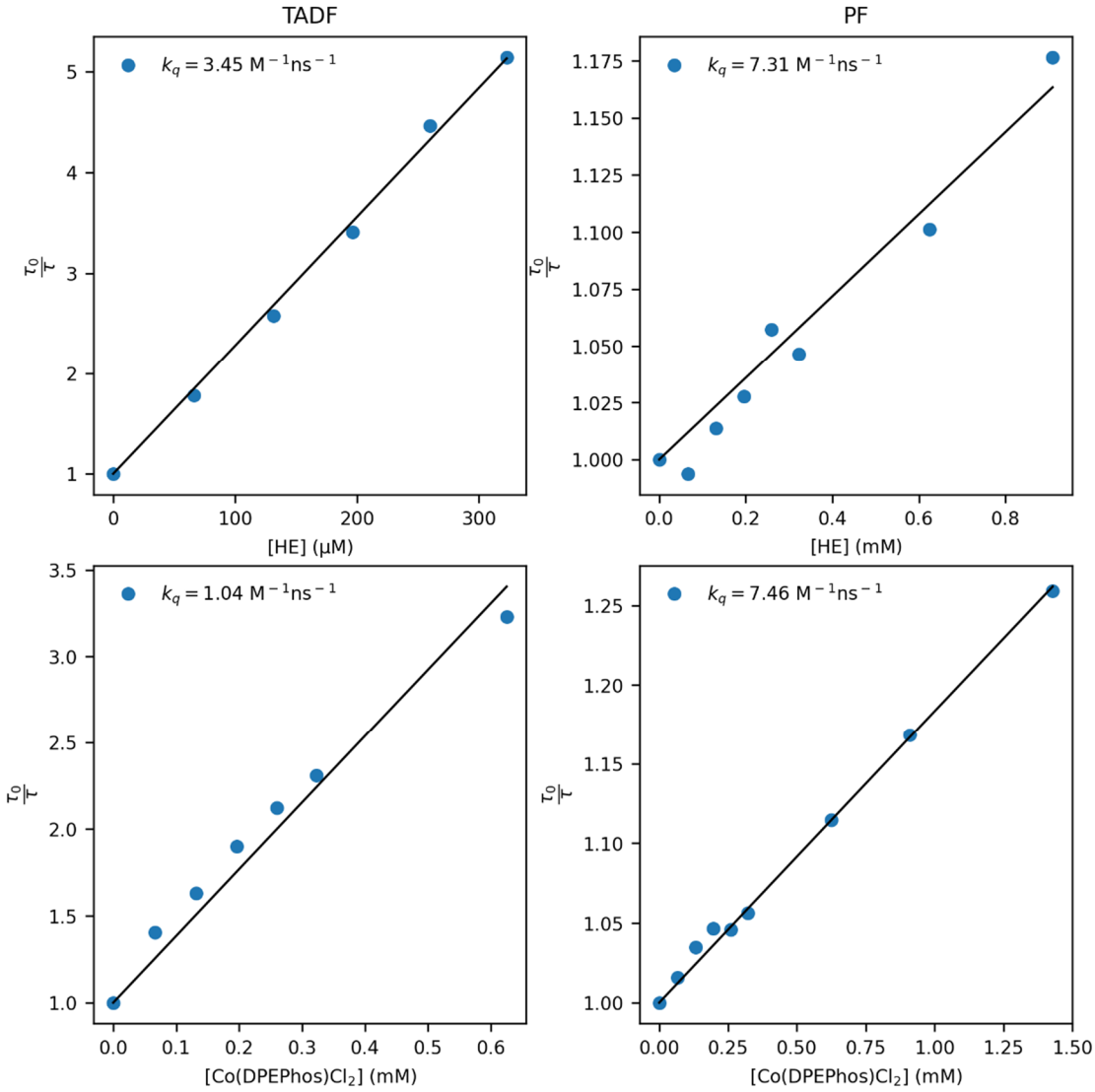

FIGURE 4.6. Stern-Volmer plots for the quenching of the Thermally Activated Delayed Fluorescence Decay (TADF) and Prompt Fluorescence decay (PF) states of 4CzIPN by HE (top) or [Co(DPEPhos)Cl$_2$] (bottom).

4.5.7 Quantum Yield Determination

Following the general procedure, 4CzIPN (2 μmol, 1.6 mg), $CoCl_2 \cdot 6H_2O$ (10 μmol, 2.4 mg), DPEPhos (10 μmol, 5.4 mg), K_3PO_4 (0.15 mmol, 31.8 mg) and Hantzsch ester (0.15 mmol, 38.0 mg) were weighed in a flat-bottom Schlenk flask. The solids were dissolved in THF (1 mL) and Ph-VCC **4.1a** (0.1 mmol) and benzaldehyde **4.2a** (0.15 mmol) were added, affording a green suspension. The flask was sealed with a Teflon cap and the mixture was freeze-pump-thawed 3 times and stirred under N_2 at room temperature for 5–20 minutes after which it was irradiated for the indicated time at 20 °C using a single high-power blue LED (λ_{em} = 445 nm, 700 mA, 1.2 μeinstein s^{-1}) from the bottom. After the reaction, the mixture was directly filtered through basic Al_2O_3 (3 cm, Ø = 0.5 cm) eluting with CH_2Cl_2/MeOH (9:1, 5 mL). The filtrate was evaporated to dryness and the residue was dissolved in $CDCl_3$ and analyzed by ^1H NMR using mesitylene as internal standard to measure the yield of **4.3a**. The procedure was repeated for 9 independent reactions quenched at different times.

The overall quantum yield was determined to be 1.82% from the regression line of the following plot:

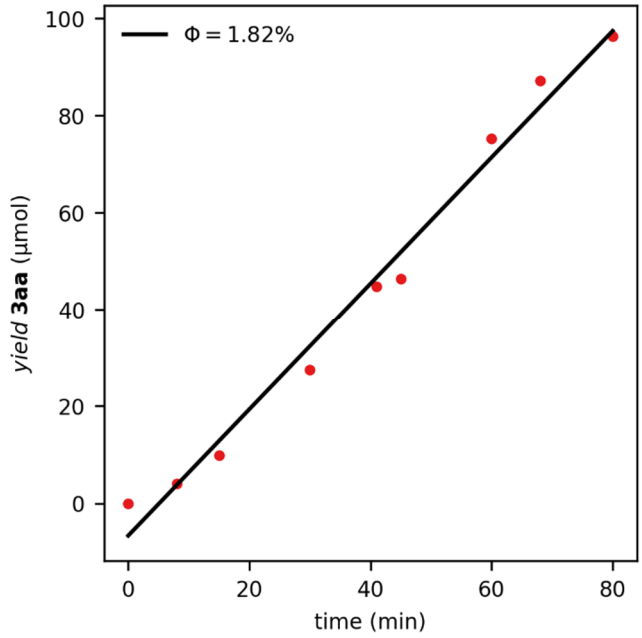

FIGURE 4.7. Overall quantum yield determination. The red dots indicate the yield of **4.3a** from different reactions quenched at different times.

4.5.8 Determination of the Relative Configuration in 1,3-Diol

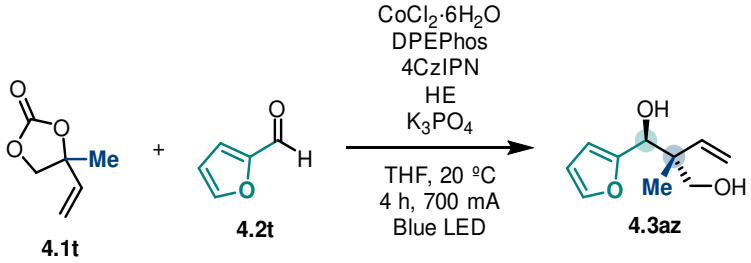

SCHEME 4.23. Synthesis of 1,3-diol **4.3az**.

4CzIPN (2 μmol, 1.6 mg), $CoCl_2 \cdot 6H_2O$ (10 μmol, 2.4 mg), DPEPhos (10 μmol, 5.4 mg), K_3PO_4 (0.15 mmol, 31.8 mg) and Hantzsch ester (0.15 mmol, 38.0 mg) were weighed in a flat-bottom Schlenk flask. The solids were dissolved in THF (1 mL), and 4-methyl-4-vinyl-1,3-dioxolan-2-one **4.1t** (0.1 mmol) and furfural **4.2t** (0.15 mmol) were added. The flask was sealed with a Teflon cap and the mixture was freeze-pump-thawed 3 times and stirred under N_2 at room temperature for 5–20 minutes after which it was irradiated for 4 hours at 20 °C using a single high-power blue LED (λ_{em} = 445 nm, 700 mA, 1.2 μeinstein s^{-1}) from the bottom. After the reaction, the mixture was aerated and evaporated to dryness. The residue was dissolved in CH_2Cl_2 and passed through basic Al_2O_3 (3 cm, Ø = 0.5 cm) eluting with CH_2Cl_2 (10 mL), and subsequently CH_2Cl_2/MeOH (9:1, 5 mL). The second fraction was evaporated to dryness and was analyzed by ^{1}H NMR ($CDCl_3$, 400 MHz).

^{1}H NMR of crude **4.3az** (**FIGURE 4.8**) indicates that the major isomer is the *anti*-1,3-diol, as compared to previous characterization data.[207] Therefore, we concluded that the major diastereomer in product **4.3az** is also *anti*-configured.

[207] See Krische, M. J. *et al. J. Am. Chem. Soc.* **2014** (*ref.* 176b) on page 138.

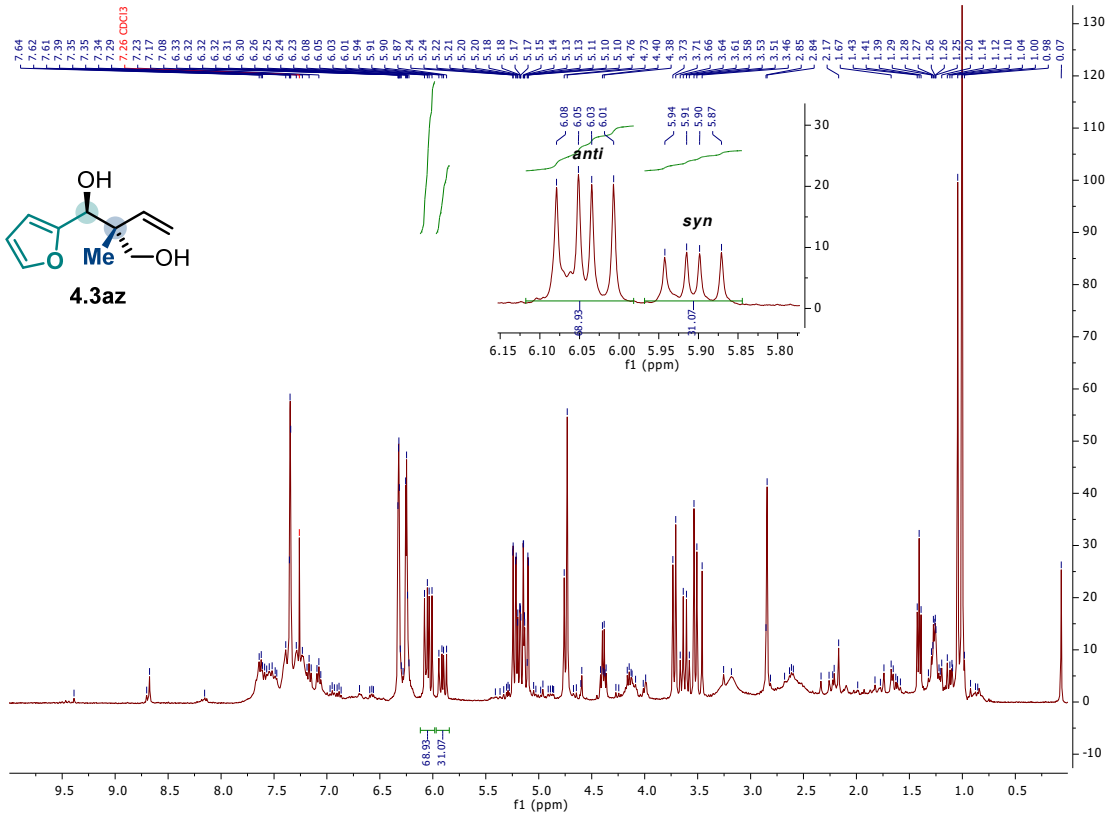

FIGURE 4.8. ^{1}H NMR of crude 1,3-diol 4.3az

4.5.9 GC-MS analysis

Analysis by GC-MS shows that the reaction mixture for the benchmark reaction contained 1,3-diene **4.AP** after irradiation for 2 h (**FIGURE 4.9**, t_R = 3.75 min). This was further confirmed by comparison with an authentic sample of 1,3-diene **4.AP**, and also by comparison of their EI-MS spectra (**FIGURE 4.10**). The additional peak at t_R = 5.55 min corresponds to the homo-Diels-Alder adduct of **4.AP**, which is likely formed by the high temperatures inside the GC.

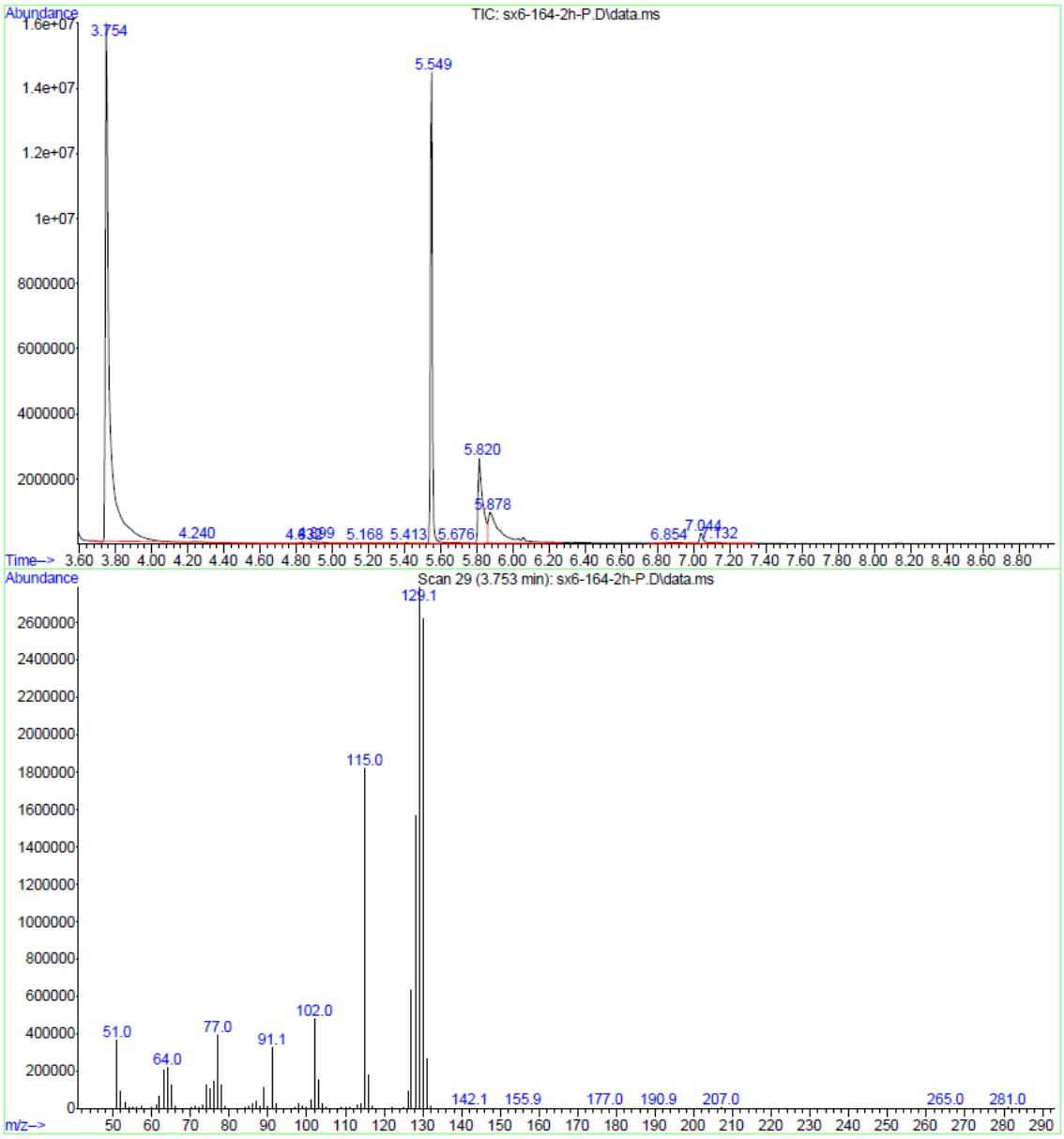

FIGURE 4.9. GC chromatogram and EI-MS spectrum for a sample of the reaction mixture stirred for 2 h.

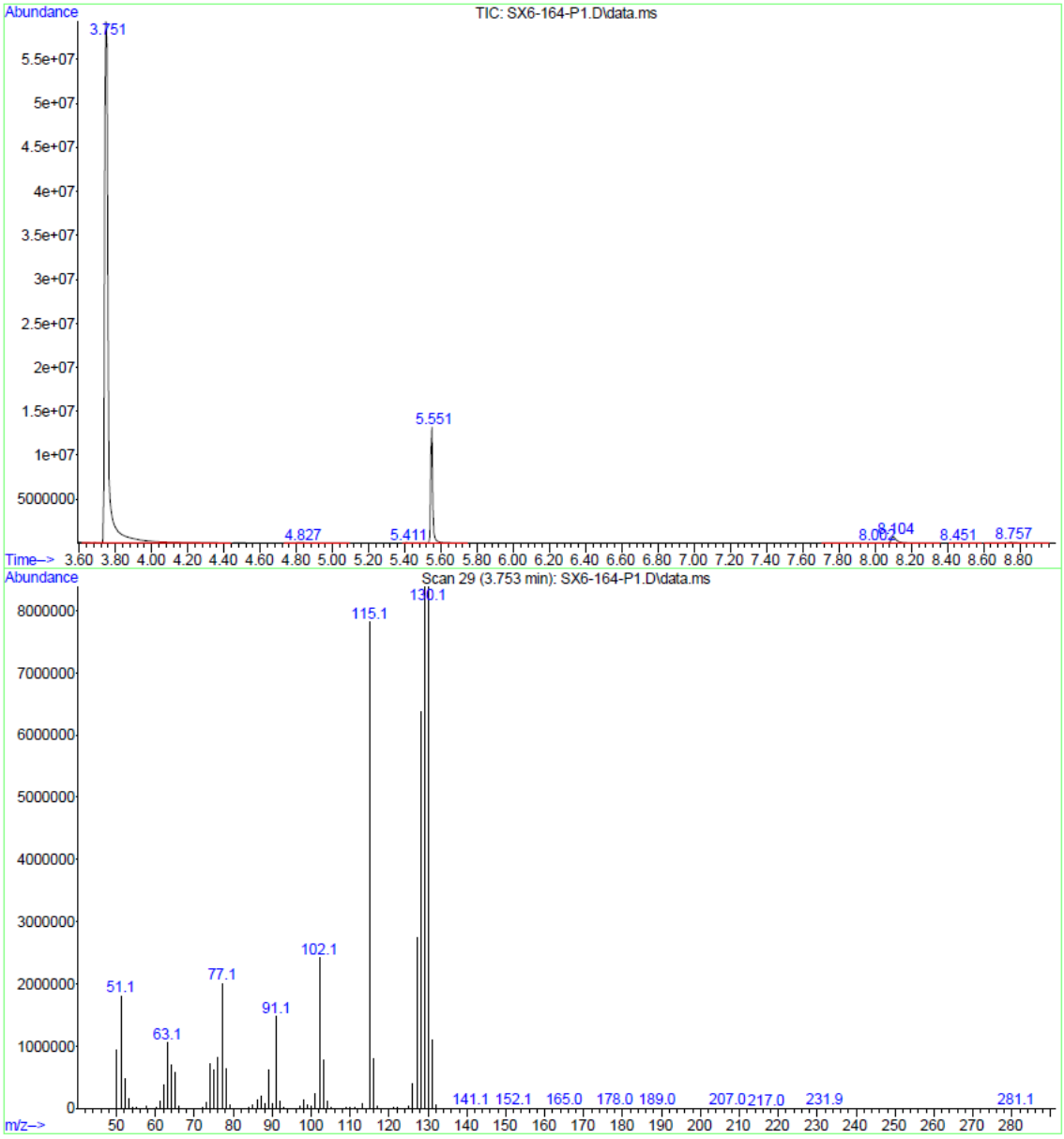

FIGURE 4.10. GC chromatogram and EI-MS spectrum for an authentic sample of pure 1,3-diene **4.AP**.

4.5.10 Crystallographic Studies

The experimental procedure for measuring single crystals of compounds **4.3s** and **4.5g** by X-ray diffraction is detailed in chapter 2. Single crystals of compound **4.3s** and **4.5g** suitable for X-ray diffraction were obtained by vapor diffusion of pentane into a solution of each respective product in CH_2Cl_2.

TABLE 4.12. Crystal data and structure refinement for **4.3s** (CCDC-2067791).

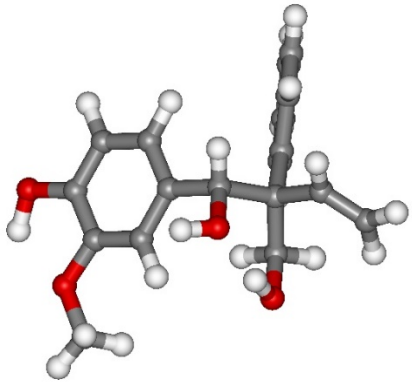

Empirical formula	$C_{18}H_{20}O_4$	
Formula weight	300.34	
Temperature	100(2) K	
Wavelength	0.71073 Å	
Crystal system	orthorhombic	
Space group	$Pna2_1$	
Unit cell dimensions	a = 11.9332(2) Å	α = 90°
	b = 8.6809(2) Å	β = 90°
	c = 29.5082(6) Å	γ = 90°
Volume	3056.78(11) Å^3	
Z	8	
Density (calculated)	1.305 mg·m^{-3}	
Absorption coefficient	0.091 mm^{-1}	
F(000)	1280	
Crystal size	0.200 × 0.200 × 0.150 mm^3	
Theta range for data collection	2.446 to 32.001°.	
Index ranges	-17 <= h <= 17, -12 <= k <= 12, -43 <= l <= 43	
Reflections collected	46208	
Independent reflections	10055[R(int) = 0.0202]	
Completeness to theta =32.011°	97.3%	
Absorption correction	Multi-scan	
Max. and min. transmission	1.00 and 0.71	
Refinement method	Full-matrix least-squares on F^2	
Data / restraints / parameters	10055/ 1/ 415	
Goodness-of-fit on F^2	1.045	
Final R indices [I>2σ(I)]	R_1 = 0.0398, wR_2 = 0.1147	
R indices (all data)	R_1 = 0.0423, wR_2 = 0.1168	
Largest diff. peak and hole	0.421 and -0.263 e·Å^{-3}	

TABLE 4.13. Crystal data and structure refinement for **4.5g**.[208]

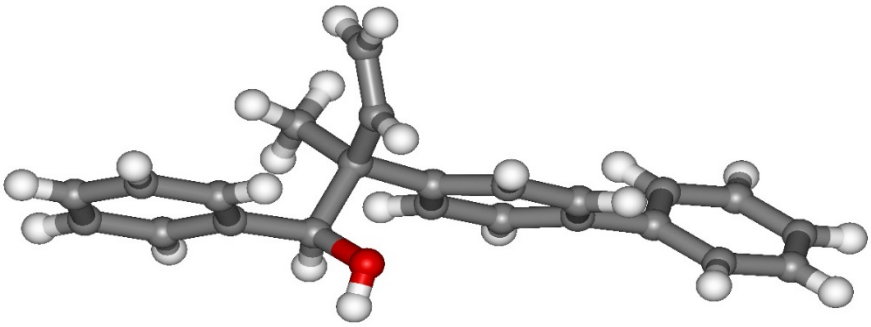

Empirical formula	$C_{23}H_{22}O$	
Formula weight	314.40	
Temperature	100(2) K	
Wavelength	0.71073 Å	
Crystal system	monoclinic	
Space group	$P2_1/c$	
Unit cell dimensions	a = 6.1078(7) Å	α = 90°
	b = 23.368(3) Å	β = 100.277(2)°
	c = 12.0794(13) Å	γ = 90°
Volume	1696.4(3) Å^3	
Z	4	
Density (calculated)	1.231 mg·m^{-3}	
Absorption coefficient	0.073 mm^{-1}	
F(000)	672	
Crystal size	0.300 × 0.300 × 0.200 mm^3	
Theta range for data collection	1.743 to 32.595°.	
Index ranges	-9 <= h <= 9, -35 <= k <= 35, -18 <= l <= 18	
Reflections collected	41051	
Independent reflections	6050[R(int) = 0.0393]	
Completeness to theta =32.595°	97.7%	
Absorption correction	Multi-scan	
Max. and min. transmission	0.74 and 0.69	
Refinement method	Full-matrix least-squares on F^2	
Data / restraints / parameters	6050/ 0/ 219	
Goodness-of-fit on F^2	1.094	
Final R indices [I>2σ(I)]	R_1 = 0.0723, wR_2 = 0.1923	
R indices (all data)	R_1 = 0.0821, wR_2 = 0.1983	
Largest diff. peak and hole	0.875 and -0.438 e·Å^{-3}	

[208] Please note that this structure still requires full refinement and should be regarded as preliminary.

UNIVERSITAT ROVIRA I VIRGILI
STEREOSELECTIVE TRANSFORMATIONS OF VINYL CYCLIC CARBONATES AND APPLICATIONS IN NATURAL PRODUCT SYNTHESIS
Àlex Cristòfol Martínez

UNIVERSITAT ROVIRA I VIRGILI
STEREOSELECTIVE TRANSFORMATIONS OF VINYL CYCLIC CARBONATES AND APPLICATIONS IN NATURAL PRODUCT SYNTHESIS
Àlex Cristòfol Martínez

General Conclusions

Our main objective in this doctoral thesis was the development of novel catalytic and stereoselective transformations using vinyl cyclic carbonates, with a focus on forging new carbon-carbon bonds, which could prospectively then be applied to the synthesis of more complex molecules, such as natural products. In this sense and considering the state-of-the-art at the beginning of this doctoral thesis, we have successfully introduced novel carbon-carbon bond-forming reactions to transform vinyl cyclic carbonates into useful advanced intermediates and succeeded in applying those methods towards the synthesis of complex alkaloids.

In chapter 2, we introduced nitroalkanes as suitable carbon pronucleophiles in palladium-catalyzed allylic substitution reaction using vinyl cyclic carbonates as allylic surrogates. Importantly, this transformation featured exceptional levels of diastereoselectivity, as well as attractive functional group tolerance. Comparing to previous research reported by our group and others, our method effectively expanded the repertoire of suitable pronucleophiles and showed potential to be applied to the synthesis of other complex molecular scaffolds.

In chapter 3, we explored synthetic routes towards the synthesis of biologically active indolizidine and quinolizidine alkaloids, which relied on our developed stereoselective allylation of nitroalkanes with vinyl cyclic carbonates. Importantly, we have demonstrated that cyclic carbonates can also play an active role in multistep synthesis, as compared to the ubiquitous role of cyclic carbonates as protecting group.

In chapter 4, we introduced novel cobalt/organophotoredox dual catalytic methods to effectively enable the generation of nucleophilic allyl species from vinyl cyclic carbonates, which were effectively coupled to suitable aldehyde electrophiles. These methods effectively produced compounds featuring an acyclic quaternary carbon stereocenter with high levels of diastereocontrol without relying on precious transition metals. Compared to the previous state-of-the-art, we significantly expanded the knowledge in the generation of nucleophilic allyl species from vinyl cyclic carbonates, which, up to the point of developing this chemistry, remained scarce.

Overall, we believe that the results described in this doctoral thesis have contributed to further shape the future of vinyl cyclic carbonates as versatile intermediates in the formation of challenging carbon-carbon bonds, and how to apply these methods to synthesize more complex natural products. We foresee that our findings and developments will be useful to the chemical community to continue developing not only other valuable allylation protocols, but expanding these transformations with propargylation or allenylation reactions, with a special focus on using more environmentally friendly and cheaper 3d transition metals.

UNIVERSITAT ROVIRA I VIRGILI
STEREOSELECTIVE TRANSFORMATIONS OF VINYL CYCLIC CARBONATES AND APPLICATIONS IN NATURAL PRODUCT SYNTHESIS
Àlex Cristòfol Martínez

Science may set limits to knowledge, but should not set limits to imagination.

— Bertrand Russell

APPENDIX A

CHEMICAL STRUCTURES OF SELECTED COMPOUNDS

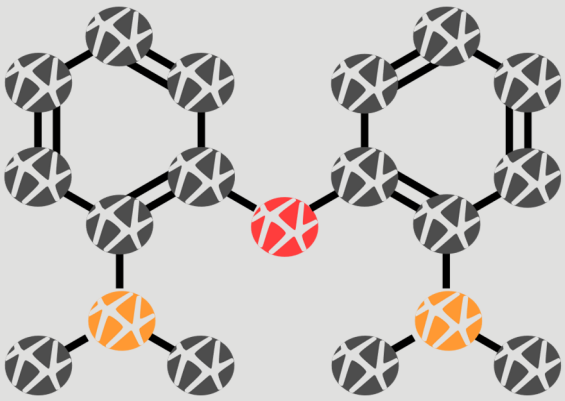

Bite angles of common diphosphine ligands were collected from:

Dierkes, P.; van Leeuwen, P. W. N. M. *J. Chem. Soc., Dalton Trans.*, **1999**, 1519-1530

Phosphine Ligands (Bite Angle)

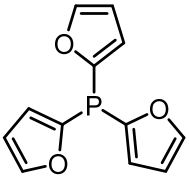

TFP

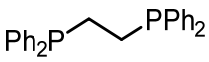

dppe (85º)

dppp (91º)

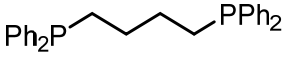

dppb (98º)

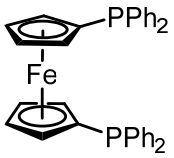

dppf (96º)

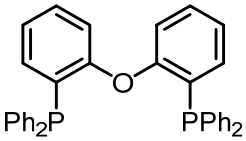

DPEPhos (103º)

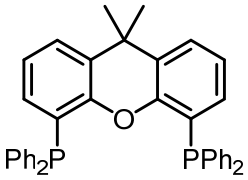

XantPhos (107º)

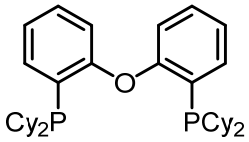

L1

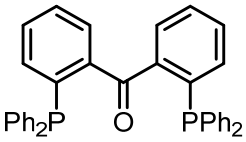

L2

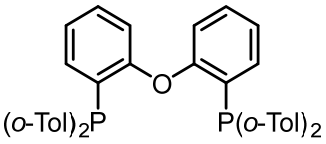

L3

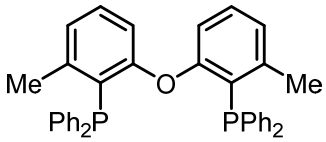

L4

N,N-Ligands		
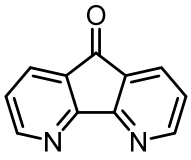 **DAF**	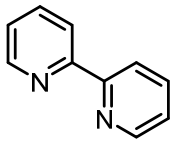 **bpy**	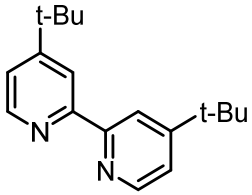 **dtbbpy**
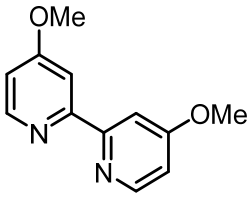 **4,4'-OMe-bpy**	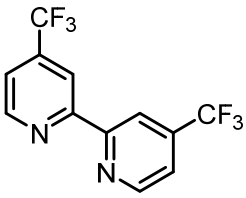 **4,4'-CF_3-bpy**	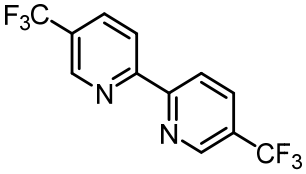 **5,5'-CF_3-bpy**
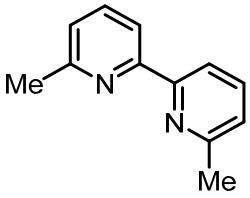 **6,6'-Me-bpy**	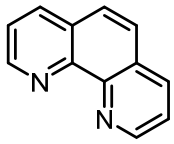 **phen**	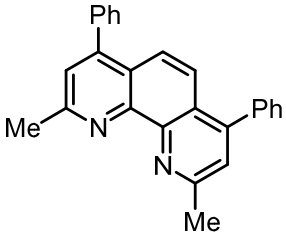 **batho**
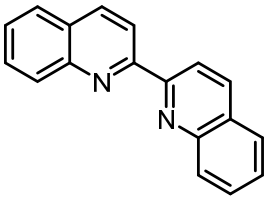 **L5**	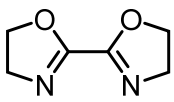 **L6**	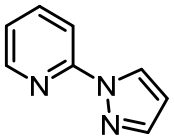 **L7**
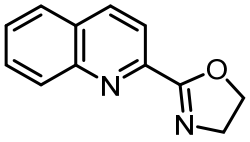 **L8**	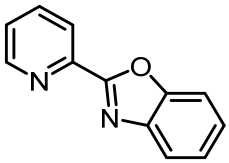 **L9**	

Organic Bases

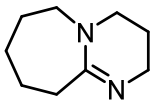

DBU

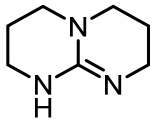

TBD

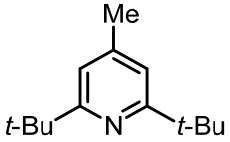

DTBMP

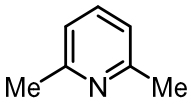

2,6-lutidine

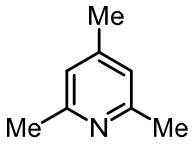

2,4,6-collidine

Other Organic Compounds

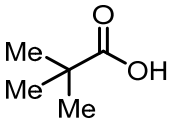

PivOH

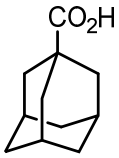

1-AdCO$_2$H

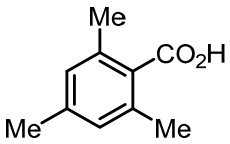

MesCO$_2$H

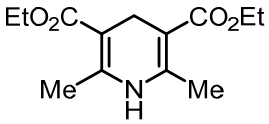

HE

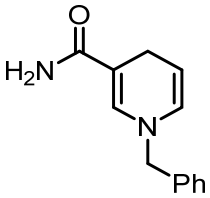

BNAH

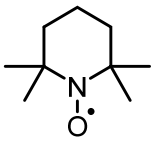

TEMPO

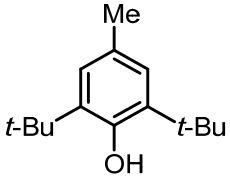

BHT

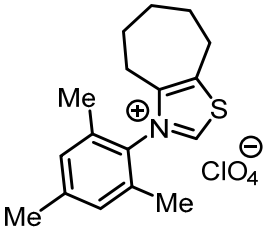

NHC precatalyst

Photocatalysts

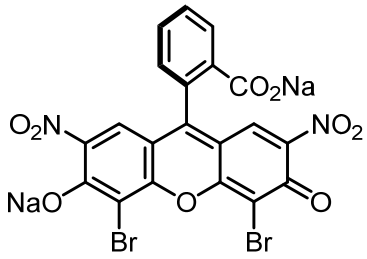

Eosin B

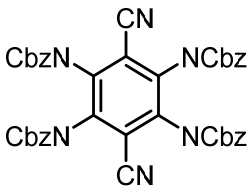

4CzTPN

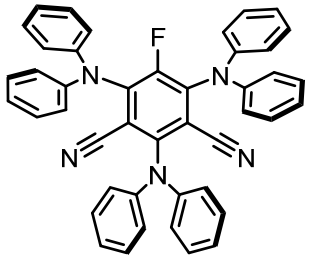

3DPAFIPN

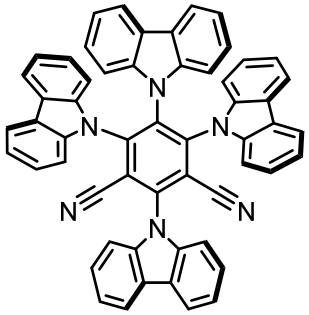

4CzIPN

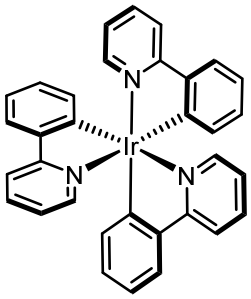

Ir(ppy)$_3$

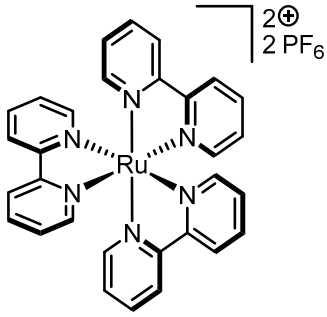

Ru(bpy)$_3$(PF$_6$)$_2$

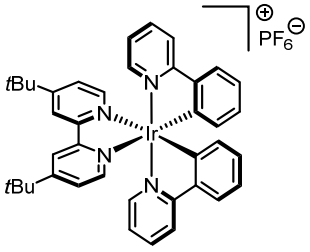

[Ir(dtbbpy)(ppy)$_2$](PF$_6$)

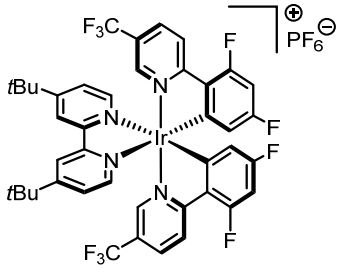

[Ir(dF,CF$_3$ppy)$_2$(dtbbpy)](PF$_6$)

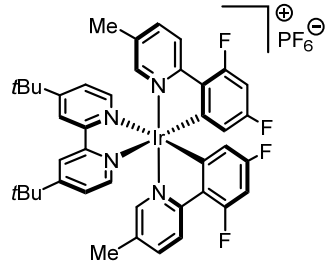

[Ir(dF,Meppy)$_2$(dtbbpy)](PF$_6$)

UNIVERSITAT ROVIRA I VIRGILI
STEREOSELECTIVE TRANSFORMATIONS OF VINYL CYCLIC CARBONATES AND APPLICATIONS IN NATURAL PRODUCT SYNTHESIS
Àlex Cristòfol Martínez

UNIVERSITAT ROVIRA I VIRGILI
STEREOSELECTIVE TRANSFORMATIONS OF VINYL CYCLIC CARBONATES AND APPLICATIONS IN NATURAL PRODUCT SYNTHESIS
Àlex Cristòfol Martínez

UNIVERSITAT
ROVIRA i VIRGILI